KINETICS AND THERMOCHEMISTRY OF

HOMOGENEOUS GAS REACTIONS OF ORGANIC CYANIDES

BY

RICHARD D. GODDARD, B.E. (CHEM)

DEPARTMENT OF CHEMICAL ENGINEERING
UNIVERSITY OF ADELAIDE

PH.D THESIS
JUNE, 1976

RESUBMITTED
FEBRUARY, 1978

Table of Contents Continued......

Table of Contents Continued......

A B S T R A C T

Fundamental knowledge on the kinetics and thermochemistry of decomposition of organic cyanides is very limited. A research program described herein was undertaken to investigate the gas-phase pyrolysis of three small ring cyanides and four alkyl cyanides. From these studies the C-C bond fission and HCN elimination pathways of decomposition were compared, and heats of formation of cyanoalkyl radicals and the effect of the cyano group on bond dissociation energies were obtained.

The unimolecular decomposition of cyclobutyl cyanide was followed over the temperature range 833-1203K using the technique of very low-pressure pyrolysis (VLPP). The reaction yields ethylene and vinyl cyanide as the only products. If A_∞ is based on the high-pressure study of this compound, then the unimolecular rate constants are consistent with $\log k_\infty = 15.0 - (57.0 \pm 1.0)/\Theta$, where k has the units $\sec^{-1}$, and $\Theta = 2.303$ RT kcal/mole. Adjusting A_∞ relative to the more recent VLPP of cyclobutane, yields $\log k_\infty = 15.9 - (59.1 \pm 1.0)/\Theta$. Comparison of these kinetics with that for methylcyclobutane yields a value of 5.1 ± 1kcal/mole for the cyano stabilization energy. The high-pressure stirred-flow pyrolysis of trans-1,2-dicyano-cyclobutane yields vinyl cyanide as the only product over the temperature range 571-661K. The rate constants are given by $\log k = 15.3-50.9/\Theta$, which yields 5.25 kcal/mole per cyano group as the stabilization energy. Both the cyclobutyl cyanide and dicyanide studies show that the previous studies by Sarner and coworkers were affected by secondary, probably heterogeneous reactions. Cyclopentyl cyanide was followed by both VLPP and at high pressure conditions in the stirred-flow system over the range 905-1143K. Decomposition proceeded via two pathways to yield in similar concentrations vinyl cyanide + propylene and cyanopropene + ethylene, as well as via the minor pathway of HCN elimination. The kinetics obtained from both reactor systems were in

excellent agreement. The Arrhenius expressions are $\log k = (16.0 \pm 0.3) -$ $(80 \pm 1.5)/\Theta$ (for vinyl cyanide formation), and $\log k = 15.9 - 80/\Theta$ (for the formation of cyanopropene + ethylene). These data are consistent with a biradical mechanism. HCN elimination accounts for ca. 25% of the overall decomposition, and the expression obtained from the VLPP analysis is $\log k = (13.2 \pm 0.3) - (69.3 \pm 2)/\Theta$.

The pyrolyses of isopropyl cyanide, n-propyl cyanide, and tert-butyl cyanide were investigated in the VLPP system over approximately the same temperature range of 1050-1250K, and were found to decompose via the competitive pathways of C-C fission and HCN elimination. Taking into account the mutual interaction of the pathways in the fall-off region, Arrhenius expressions consistent with the unimolecular rate constants were obtained. The C_2-C_3 fission rate constants in isopropyl cyanide, n-propyl cyanide, and tert-butyl cyanide are in accord with $\log k_\infty = (15.7 \pm 0.3) - (79.0 \pm 2.0)/\Theta$, $\log k_\infty = (15.4 \pm 0.3) - (76.7 \pm 1.7)/\Theta$, and $\log k_\infty = (15.8 \pm 0.3) - (74.9 \pm 1.6)/\Theta$ respectively. The C_2-C_3 fission pathway accounted for >90% of the overall decomposition, with HCN elimination accounting for the remainder of isopropyl cyanide and of tert-butyl cyanide disappearance; the results being in accord with $\log k_\infty = (13.9 \pm 0.3) - (76.2 \pm 2.0)/\Theta$, and $\log k_\infty = (14.1 \pm 0.3) - (74.1 \pm 1.6)/\Theta$ respectively. C_3-C_4 fission accounted for the remainder of n-propyl cyanide decomposition. The activation energies for C-C fission in these alkyl cyanides leads to $DH^0_{298}[CH_3CH(CN)-CH_3] =$ 78.8 ± 2.0, $DH^0_{298}[C_2H_5-CH_2CN] = 76.9 \pm 1.7$, $DH^0_{298}[(CH_3)_2 C(CN) - CH_3] =$ 74.7 ± 1.6, and $\Delta H^0_{f,298}[CH_3\dot{C}HCN, g] = 50.1 \pm 2.3$, $\Delta H^0_{f,298}[\dot{C}H_2CN, g] = 58.5 \pm 2.2$, $\Delta H^0_{f,298}[(CH_3)_2 \dot{C}CN, g] = 39.8 \pm 2.0$, all in kcal/mole. The stabilization energies of the α-cyanoethyl, cyanomethyl, and α-cyanoisopropyl radicals are found to be 5.1 ± 2.5, 5.1 ± 2.3, and 5.5 ± 2.0 kcal/mole respectively.

The values of the cyano stabilization energy obtained from the small ring cyanide and the alkyl cyanide studies show excellent agreement. It is found that the cyano group consistently decreased the adjacent bond strength

by 5.1 ± 1.8 kcal/mole, with no variation in α-methyl substitution being observed. Revised values of the group contributions of $[\dot{C}\text{-}(H)_2(CN)]$, $[\dot{C}\text{-}(H)(C)(CN)]$, and $[\dot{C}\text{-}(C)_2(CN)]$ to the heat of formation of free radicals are calculated. HCN elimination activation energies obtained from the studies were found to be in substantial agreement with the theoretical semi-ion pair models of Benson-Haugen and of Tschuikow-Roux and coworkers.

Using the estimated $\Delta H^0_{f,298}[\dot{C}H_2CN]$, the high-pressure Arrhenius expression for ethyl cyanide pyrolysis via C-C fission was predicted to be $\log k \simeq 15.4 - 81/\Theta$. Experiments in the stirred-flow system were found to support the parameters. HCN elimination is not an observable pathway for primary cyanide decomposition relative to C-C fission, over the temperature range investigated. Stirred-flow experiments carried out on isopropyl cyanide and ethyl cyanide under similar conditions to the studies of Hunt, Kerr and Trotman-Dickenson, and Dastoor and Emovon, lead to the conclusion that free radical chain processes make a significant contribution to HCN elimination despite the presence of chain inhibitors.

DECLARATION

    To the Author's knowledge and belief, the material in this thesis, except where due reference is made or common knowledge is assumed, is original.

    No part of this work has been submitted for any other award or degree in any University.

R.D. Goddard.

ACKNOWLEDGEMENTS

CHAPTER 1.

INTRODUCTION

The conversion of one substance to another, by means of a chemical reaction forms an important part of many industrial processes. Successful design of chemical reactors requires an understanding of chemical kinetics coupled with knowledge of such physical processes as mass and energy transport. The achievement of higher conversions with lower costs and better plant utilization, requires a fundamental knowledge of the kinetics and thermochemistry of the reactions. Although many of the reactions involved in industry are carried out in reactor systems with catalysts, a primary prerequisite in design is a knowledge of the chemical thermodynamics which can be obtained from homogeneous studies. For example, if a homogeneous investigation indicates that an equilibrium is reached, then this is the same extent to which the reaction will proceed in a heterogeneous system, independent of the catalyst used.

Industrially, acrylonitrile (or vinyl cyanide) is a very useful compound, being very important in the polymer field and also being employed in cyanoethylation procedures. Polyacrylonitrile (PAN) is finding an important and rapidly expanding future in the manufacture of carbon fibres. The PAN fibres are subjected to an oxidizing pretreatment below $300^{\circ}C$, the shrinkage of the fibres being prevented by clamping so that preorientation in the direction of the fibre axis is provided for the graphite crystallites to be formed. This is then followed by a carbonization step at $1000^{\circ}C$, and then by further heating in an inert atmosphere between $1600 - 2800^{\circ}C$, dependent on the tensile strength and modulus properties required. This is the British process based on the work of Shindo and of Watt [1], and it produces a superior fibre compared to the American (Union Carbide) process [2] which begins with cellulose fibres (rayon). Synthetic resins reinforced with polycrystalline

inorganic fibres are expected to find a spectrum of applications similar in breadth to that existing at present for glass-fibre reinforced plastics. Applications include lighter and stronger civil structures, corrosion resistant structural components in shipbuilding, and corrosion resistant pressure vessels, tanks and reactors in chemical reactor engineering. Although extensive research into the formation of carbon fibres from PAN has been carried out, the chemistry of the conversion process is not fully understood.

Approximately 70% of the world's acrylonitrile production of 3 million tonnes is used in the production of acrylic fibres, which are manufactured into soft, woolen-like fabrics. Acrylonitrile - butadiene - stryene (ABS) copolymers are extensively used for the production of high tensile and impact strength plastic goods, and also in ABS/SAN type resins. Almost 20% of the world's demand of acrylonitrile is accounted for in these copolymers. Nitrile rubbers are no longer used as extensively as they were twenty years ago, and account for about 5%. In addition, there is a world-wide trend towards the manufacture of nylon via the acrylonitrile route - acrylonitrile to adiponitrile to hexamethylenediamine plus adipic acid to yield nylon 66. It is forecast [3] that acrylonitrile demand may grow 16% annually in spite of the growing ammonia shortage and the increasing usage of propylene for polypropylene. Due to the higher priced raw materials, acrylonitrile (and hence its products) will cost more during the remainder of this decade. Thus additional processes for manufacturing acrylonitrile are desired, and hence studies of the pyrolysis of organic cyanides should provide useful data.

Recently Hall and coworkers [4] of E.I. du Pont de Nemours and Company have reported on studies of the polymerization of substituted small strained carbocyclic rings, and they found that monomers containing bridgehead cyano or ester substituents polymerize readily. These species undergo free-radical or anionic homopolymerization to form high molecular

weight polymers, containing 1,3 cyclobutane links in the chain. This new class of reactive monomers constitutes a new area of polymer chemistry for the future. To determine the thermodynamics of their polymerization requires knowledge of the thermochemistry of cyanides, which at present is limited.

The aim of this research project is to study the kinetics and thermochemistry of thermal gas-phase reactions of several organic cyanides using laboratory reactors. From a fundamental viewpoint, the kinetic parameters of reactions such as carbon-carbon bond fission and hydrogen cyanide elimination should be of importance in the determination of bond energies, the thermochemical properties of free radicals and the formulation of reaction rate theories. These data should also assist in the interpretation of the kinetics and mechanisms of the pyrolysis of nitrile polymers.

Before outlining the investigations that were carried out, an exposition of chemical kinetics and the relevant reaction schemes and rate theories is justified.

1.1   Reaction Kinetics

Chemical kinetics are concerned with the rates of reactions, and how the rates are influenced by changes in the physical conditions. In particular we are interested in the effects of changes to the concentration, temperature and pressure of the chemical species involved in the reaction. From studies of the effect of these factors on the reaction, a detailed mechanism can be postulated; such as whether the reaction proceeds via a single step or a sequence of steps.

The rate of reaction is normally expressed in terms of the concentration of products and reactants with respect to time. If the rate is directly proportional to a single concentration, $R = kC$, the reaction is referred to as first-order. Similarly if the rate is proportional to the product of concentrations, $R = kC^2$ or $R = kC_A C_B$ then it is a second-order reaction. The order of the reaction should not be confused with molecularity which is defined as the number of molecules entering into an elementary step.

The constant k in the above equations is known as the rate constant for the reaction. If the reaction is affected by wall or surface effects then secondary reactions are involved and they will each have a different k value. For an elementary process the dependency of k on temperature T follows the Arrhenius equation [5]

$$k = Ae^{-E/RT}$$

where A is the frequency factor, with the same units as k, E is the activation energy, generally with the units of kcal/mole*, and R is the universal gas constant.

---

* Throughout this research, 1 kcal = 4.184 kJ

If we consider the reversible reaction, $aA + bB + \ldots \underset{-1}{\overset{1}{\rightleftharpoons}} pP + qQ + \ldots$ then the relationship between the Arrhenius parameters and thermo-chemical quantities is described [5] by

equilibrium constant, $\quad K = \dfrac{k_1}{k_{-1}} = \left(\dfrac{A_1}{A_{-1}}\right) e^{\dfrac{-(E_1 - E_{-1})}{RT}}$ (2)

$$\Delta G^O = - RT \ln K \tag{3}$$

also $\quad \Delta G^O = \Delta H^O - T\Delta S^O$ (4)

$\therefore \quad K = e^{\left(\dfrac{\Delta S^O}{R} - \dfrac{\Delta H^O}{RT}\right)}$ (5)

equating (2) and (5), gives

$$\Delta S^O = 2.303 \, R \, \log\left(\dfrac{A_1}{A_{-1}}\right) \tag{6}$$

and $\quad \Delta H^O = E_1 - E_{-1}$ (7)

Although the great majority of reaction rate constants are expressible by the simple Arrhenius equation, a small group of them are not. For these cases, such as termolecular recombinations of atoms or atoms with diatomic molecules, a modified Arrhenius equation [5] is used in which a temperature variation for the A - factor is introduced

$$k = A' \, T^n \, e^{-E'/RT} \tag{8}$$

When the data is analysed in the form of the Arrhenius equation, the relation between the parameters is

$$A = A' \, (e \, T)^n \tag{9}$$

$$E = E' + n \, RT \tag{10}$$

Explaining his postulated equation, Arrhenius [6] suggested that during the course of reaction the reactant molecules become activated by collisions with one another, and that there is an equilibrium existing between normal (ground state) and activated molecules. The energy of activation represents the energy that molecules must acquire in order to be capable of

undergoing reaction. Having acquired this energy of activation the molecules are referred to as activated. Schematically it can be represented as
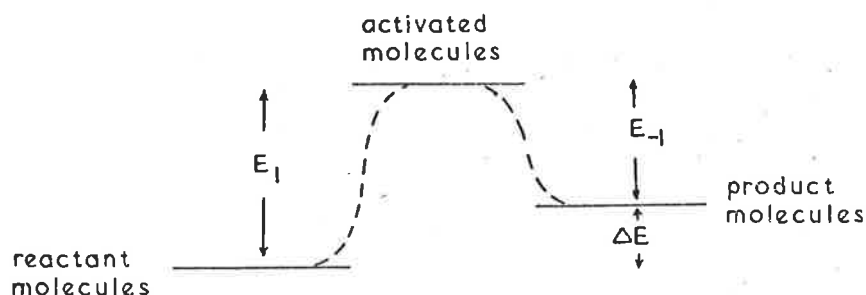
1.1.1 Chain Reactions

Many organic decompositions obey simple kinetic laws and may mistakenly be considered to be elementary processes. However they often involve bond fission reactions which yield free radicals capable of initiating a chain reaction. The presence of certain atoms and free radicals in a reaction system makes it necessary to write down all the elementary reactions that can be expected to occur. If two of these reactions involve the attack of the reactant molecule then these are called chain-propagating steps. When such a feature exists in a mechanism the process is referred to as a chain reaction. Chain reactions consist of three kinds of elementary steps : initiation, propagation, and termination.

In 1934, Rice and Herzfeld [7] showed how complex mechanisms for decomposition reactions can lead to simple overall kinetic behaviour. As an example consider the case of a reaction showing overall first-order kinetics

$$M \xrightarrow{1} 2\ R_1 \qquad \text{initation step}$$
$$R_1 + M \xrightarrow{2} R_1 H + R_2$$
$$R_2 \xrightarrow{3} P + R_1 \qquad \text{propagation step}$$
$$R_1 + R_2 \xrightarrow{4} M_2 \qquad \text{termination step}$$

$$M \rightarrow R_1H + P \qquad \text{observed overall step}$$
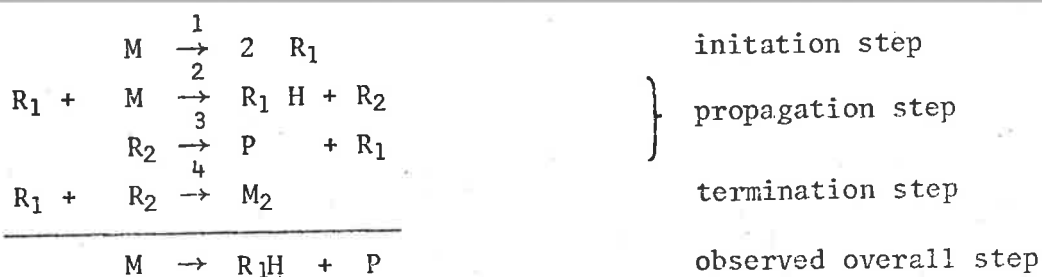
Rather than trying to solve the time-dependent differential equations for formation of the R_1 and R_2 radicals, making use of the steady-state treatment will give a satisfactory approximate solution. The rate of formation of the product R_1H is then

$$\frac{d[R_1H]}{dt} = k_2 [R_1][M] = \left[\frac{k_1 k_2 k_3}{k_4}\right]^{\frac{1}{2}} [M]$$

i.e. the reaction is of first-order.

Rewriting the rate expression in terms of the Arrhenius parameters,

$$\text{Rate} = \left[\frac{A_1 e^{-E_1/RT} \; A_2 e^{-E_2/RT} \; A_3 e^{-E_3/RT}}{A_4 e^{-E_4/RT}}\right]^{\frac{1}{2}} [M]$$

Therefore $A \text{ overall} = \left[\frac{A_1 A_2 A_3}{A_4}\right]^{\frac{1}{2}}$

$E \text{ overall} = \frac{1}{2}(E_1 + E_2 + E_3 - E_4)$

Since E_1 is usually very much larger than either E_2 and E_3, the overall activation energy is observed to be appreciably smaller than E_1.

Time dependent solutions of the differential equations can be obtained nowadays with the use of computer programs. Expanded models of more reaction steps can be solved and the results sometimes shown discrepanies with solutions obtained using the steady-state assumption [8]. It should be noted that Arrhenius parameters obtained via the steady-state treatment should only be considered as approximate and not necessarily as accurate values.

The overall reaction order depends on the manner in which the chains are initiated and terminated. Goldfinger, Letort and Niclause [9] have shown that two types of radicals can be distinguished : radicals involved in bimolecular propagating steps referred to as β radicals, and radicals which undergo unimolecular reactions in the propagation steps, known as μ radicals. The termination step involves the combination of radicals (with or without a third body, designated M) so as to break the propagation. The results of Goldfinger and coworkers' general kinetic scheme are summarized in Table 1.1 , and

TABLE 1.1 Overall Orders of Reaction for Various Types of Initiation and Termination Reactions

First-order initiation		Second-order initiation		Overall order
Simple termination	Third body termination	Simple termination	Third body termination	
		$\beta\beta$		2
$\beta\beta$		$\beta\mu$	$\beta\beta M$	$3/2$
$\beta\mu$	$\beta\beta M$	$\mu\mu$	$\beta\mu M$	1
$\mu\mu$	$\beta\mu M$		$\mu\mu M$	$1/2$
	$\mu\mu M$			0

are of great value in deciding the probable reaction mechanisms, since they avoid the necessity of working out the steady-state equations in each case. The table has been constructed for the cases of simple chain processes and is of little value for more complicated systems.

1.2   Theories of Elementary Reactions

To enable experimental rates to be predicted requires the derivation of a theory based on some physical assumptions of how a reaction proceeds.   In 1918 Lewis [10] formulated an explanation of the magnitude of the frequency factor of the Arrhenius equation by identifying it with the collision number of molecules which were treated as hard spheres.   The calculation of the frequency of collisions on this basis gives only satisfactory agreement with experiment for atoms and simple molecules, but as the complexity of the reactant molecules increases so does the deviation between predicted and experimental values.   Moreover, unimolecular decompositions are difficult to explain by collision theory. For reactions between more complicated molecules a more detailed treatment was required.

1.2.1   Transition-State Theory*

In the 1930's Eyring, Polanyi and their coworkers [11] used quantum mechanics to formulate the theory that for a reaction to occur the reacting atoms or molecules must approach one another and pass over a free-energy barrier.   The molecular species at the top of such a barrier are referred to as a transition-state complex, and the rate of reaction is controlled by the rate by which these complexes travel over the top of the barrier.   The complex is assumed to possess vibrational and rotational energy as well as translational energy, and the activated complex is assumed to be in thermodynamic equilibrium with the reactants. Essentially the complex possesses the required energy of activation but before decomposition can occur the energy, to break a bond for example, must be specifically located in that bond.

---

* The Transition-State Theory is also known under the title of Theory of

Absolute Reaction Rates.

Consider two reactant molecules A and B reacting together to form a product; i.e. the following reaction scheme --

$$A + B \rightleftharpoons (A\ B)^* \rightleftharpoons (A\ B)^{\neq} \rightleftharpoons \text{Products}$$

excited   transition
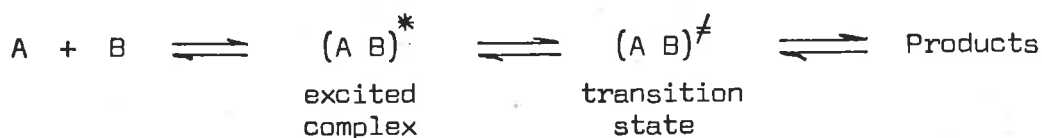
complex   state

where the complex is an excited combination of A and B, and the transition state is essentially a rearrangement of $(AB)^*$ closely resembling the products. The rate of reaction equals the rate of passage over the barrier multiplied by the concentration of transition-state molecules

$$R = k_{AB}^{\neq} \left[(A\ B)^{\neq} \right] \tag{11}$$

$$= k_{AB}^{\neq}\ K_{AB}^{\neq}\ [A][B] \tag{12}$$

since $A + B \rightleftharpoons (A\ B)^{\neq}$, the equilibrium

constant $\quad K_{AB}^{\neq} = \dfrac{[(AB)^{\neq}]}{[A][B]}$

Therefore $\quad k_{AB} = k_{AB}^{\neq}\ K_{AB}^{\neq}$

$$= \nu\ K_{AB}^{\neq} \tag{13}$$

where ν is the frequency of motion through the transition-state region. Taking the value of this vibration factor in the limit as ν tends to zero, then as shown by Glasstone, Laidler and Eyring [12]

$$K_{AB}^{\neq} = \left[\frac{kT}{h\nu} \right]\ K^{\neq} \tag{14}$$

where $K^{\neq}$ is the equilibrium constant referring to the remaining degrees of vibration freedom.

$$\therefore\ k_{AB} = \frac{kT}{h}\ K^{\neq} \tag{15}$$

k is Boltzmann's constant, and h is Planck's constant.

Relating the equilibrium constant to the standard free energy change for the formation of the transition-state

$$K^{\neq} = e^{-\Delta G^{\neq}/RT} = e^{(\Delta S^{\neq}/R)\ -\ (\Delta H^{\neq}/RT)} \tag{16}$$

Therefore $\quad k_{AB}^{\neq} = \dfrac{kT}{h}\ e^{\Delta S^{\neq}/R}\ e^{-\Delta H^{\neq}/RT} \tag{17}$

For unimolecular reactions, there is no mole change as the activated complex is formed, and the activation energy

$$E = \Delta H^{\neq} + RT \tag{18}$$

$$\therefore \quad A = \frac{ekT}{h} \; e^{\Delta S^{\neq}/R} \tag{19}$$

To predict these parameters requires sufficient detailed knowledge of the transition-state to enable the enthalpy and entropy of activation to be calculated.

1.3 Unimolecular Reactions

The transition-state theory provides an acceptable explanation of the first-order rate of unimolecular reactions. A unimolecular reaction is one in which the reacting molecules gain energy from collisions and then forms an activated complex from a single reactant molecule. From experimental evidence, unimolecular reactions follow the Arrhenius relationship and are first-order at high pressures, but as the pressure decreases the rate becomes second-order. Lindemann [13] showed in 1922 that activation by collision resulted in first-order kinetics at high pressures, and second-order kinetics at low pressures. The theory of Lindemann is the basis of modern theories of unimolecular reactions, with important modifications to it being made by Hinshelwood [14] later by Rice, Ramsperger and Kassel [15] , and more recently by Marcus [16]. What follows is a treatment of the theory of Lindemann and Hinshelwood, followed by a discussion of the modifications of Rice, Ramsperger, Kassel and Marcus.

1.3.1 Lindemann-Hinshelwood Theory

Consider the reaction scheme

$$A + M \underset{-1}{\overset{1}{\rightleftharpoons}} A^* + M$$

$$A^* \overset{2}{\rightarrow} P$$
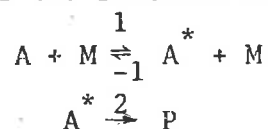
Application of the steady-state treatment gives

$$\frac{d[A^*]}{dt} = k_1 [A] [M] - k_{-1} [A^*] [M] - k_2 [A^*] = 0$$

$$\therefore [A^*] = \frac{k_1 [A] [M]}{k_{-1}[M] + k_2} \tag{20}$$

The reaction rate, $R = k_2 [A^*]$

$$\therefore \frac{d[P]}{dt} = \frac{k_1 k_2 [A] [M]}{k_{-1}[M] + k_2} \tag{21}$$

At sufficiently high pressures, the rate of activation of molecules is practically equal to their rate of deactivation, since the rate of product

formation is slow compared to deactivation by collision; i.e.

$k_{-1}[M] \gg k_2$

$$\therefore R = \frac{k_1 k_2}{k_{-1}} [A] \equiv k_\infty [A] \tag{22}$$

and the reaction is thus of first-order. The unimolecular rate constant k_{uni} will be a function of ω, the frequency of collision of the average molecule with a second body. The frequency of collision at low pressures is not sufficient to maintain an equilibrium distribution of energy in the reacting molecules, and thus the measured rate is less than k_∞, the constant rate for ω tending to infinity. That is since $k_{-1}[M] \ll k_2$,

$$R = k_1 [A] [M] \quad \text{which is proportional to } \omega \tag{23}$$

and the reaction is of second-order. This area where the reaction changes from first to second order is normally referred to as the "fall-off" region.

Lindemann's theory gave a satisfactory qualitative explanation of unimolecular reactions, but when it was compared with experimental results, deviations were apparent. First-order behaviour was exhibited to lower concentrations than that predicted by the theory. This is illustrated below

$$k_{uni} = \frac{1}{[A]} \frac{dP}{dt} = \frac{k_\infty [M]}{[M] + k_2/k_{-1}} \tag{24}$$
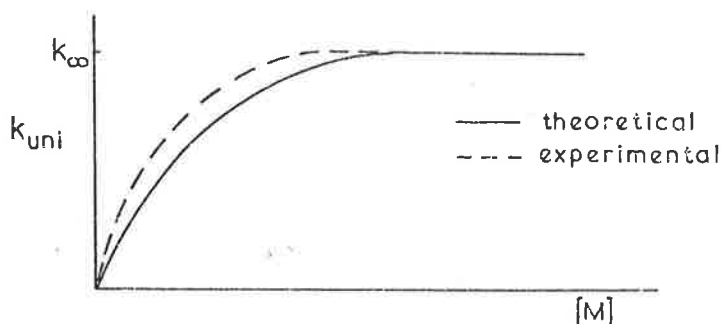
Plotting by another procedure, the plot of $^1/k_{uni}$ against the reciprocal of the concentration, should from theory give a straight line with the slope of $^1/k_1$

$$\frac{1}{k_{uni}} = \frac{k_{-1}}{k_1 k_2} + \frac{1}{k_1 [M]} \tag{25}$$
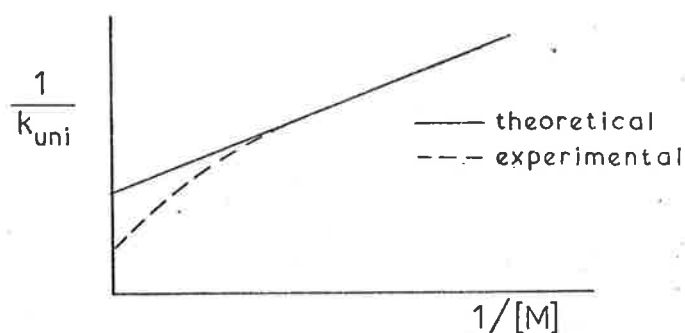
The value of k_∞ can be obtained from experiment , and according to collision theory k_1 should equal $Z_1 e^{-E'/RT}$. Since the rates fall off at a higher pressure than is actually observed, k_1 must be in error. Hinshelwood [14] pointed out that Lindemann assumed the molecules to be hard spheres with only one degree of freedom, when in fact they would normally have more. Hence a molecule having more than one degree of freedom would have a greater probability of acquiring the energy E', since this energy is distributed among all the degrees of freedom [5]. The expression for k_1 that applies to the case of s classical oscillators (or degrees of freedom) is

$$k_1 = \frac{Z_{AM}}{(s-1)!} \left(\frac{E'}{RT}\right)^{s-1} e^{-E'/RT} \qquad (26)$$

This combined theory however did not completely satisfy the observed experimental rates in the fall-off region. The failure of the Lindemann - Hinshelwood expression was that the probability of reaction was considered to be independent of the excess of energy beyond that required for activation.

1.3.2 Rice-Ramsperger-Kassel (RRK) Theory

The RRK theory [15] of unimolecular reactions uses the basic Lindemann-Hinshelwood mechanism of collisional energization and de-energization, but considers the more realistic approach that the rate of conversion of an energized molecule to products is a function of its energy content.

Rewriting the reaction scheme

$$A + M \underset{-1}{\overset{1}{\rightleftharpoons}} A^* + M$$

$$A^* \overset{2}{\rightarrow} P$$
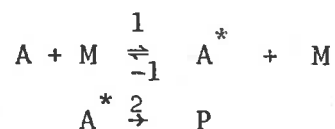
The Lindemann-Hinshelwood theory gives

$$k_{uni} = \frac{k_1 k_2 / k_{-1}}{1 + k_2/k_{-1}[M]} \qquad (24) \text{ rearranged}$$

with

$$k_1 = \frac{Z_{AM}}{(s-1)!} \left(\frac{E'}{RT}\right)^{s-1} e^{-E'/RT} \qquad (26)$$

$$k_{-1} \simeq Z_{AM}$$

For a reaction to occur the energized molecule must become an activated complex; occurring when a critical amount of energy E_o concentrates in one particular mode of vibration. On every vibration it is supposed that there is a complete reshuffling of the quanta of energy between the normal modes, so that for any energized molecule with $E > E_o$, there is a finite probability that E_o will be found in the relevant part of the molecule. RRK theory assumes that the rate constant for conversion of the energized molecule to products is proportional to this probability.

$$\text{Probability} \equiv \left(\frac{E - E_o}{E}\right)^{s-1} \qquad (27)$$

$$\therefore \quad k_2 (E) = A \left(\frac{E - E_o}{E}\right)^{s-1} \qquad (28)$$

where A is the proportionality constant at this stage. Integrating (26) with respect to E

$$\frac{k_1}{k_{-1}} \equiv \int_{E_o}^{\infty} \frac{\delta k_1}{k_{-1}} = \int_{E_o}^{\infty} \frac{1}{(s-1)!} \left(\frac{E}{RT}\right)^{s-1} e^{-E/RT} \left(\frac{dE}{RT}\right) \qquad (29)$$

Combining (31), (35) and (36) gives

$$k_{uni} = \int_{E_o}^{\infty} \frac{\dfrac{1}{(s-1)!} \left(\dfrac{E}{RT}\right)^{s-1} \dfrac{e^{-E/RT}}{RT} A \left(\dfrac{E-E_o}{E}\right)^{s-1}}{1 + \dfrac{A}{k_{-1}[M]} \left(\dfrac{E - E_o}{E}\right)^{s-1}} \, dE \qquad (30)$$

Letting $x = \left(\dfrac{E - E_o}{RT}\right)$ and $B = \dfrac{E_o}{RT}$

$$\frac{k_{uni}}{k_\infty} = \frac{1}{(s-1)!} \int_0^\infty \frac{x^{s-1} \, e^{-x} \, dx}{1 + \dfrac{A}{k_{-1}[M]} \left(\dfrac{x}{x+B}\right)^{s-1}} \tag{31}$$

where the R.H.S. is known as the Kassel Integral.

Equation (37) can also be written

$$k_{uni} = \int \frac{P(E) \, k_2(E)}{1 + \dfrac{k_2(E)}{\omega}} \, dE \tag{32}$$

where $P(E)$ is the energy distribution function, given by

$$P(E) = \frac{1}{\Gamma(s)} \left(\frac{E}{RT}\right)^{s-1} \frac{e^{-E/RT}}{RT} \tag{33}$$

and $\quad \omega = k_{-1}[M] \tag{34}$

which is the collision frequency for de-energization

Thus knowing A, E, s and ω it is possible to predict k_{uni} from k_∞, or vice versa.

The quantum version of Kassel's theory is very similar to the classical theory outlined above. It assumes, in its simplest form, that there are s identical oscillators in the molecule, all having the same frequency. A description of the theory is presented by Robinson and Holbrook [17], and it is a more accurate treatment than the classical version.

1.3.3 Rice-Ramsperger-Kassel-Marcus (RRKM) Theory

Marcus [16] has developed a quantum-mechanical formulation of the RRK theory, which results in the most realistic and successful of current theory. Although the theory was described over twenty-five years ago, the practical application of the treatment has been slow due to the complexity of the calculational procedures. Computer assess has eased this and permitted kineticists to apply the formulation to their experimental results.

An accumulation of literature has been written on RRKM theory, and for a clear, well documented presentation the recent texts by Robinson and Holbrook [17] and Forst [19] are recommended to the reader for a full treatment of the mechanics of computation. An outline of the development of RRKM expressions is given below.

The reaction scheme used in RRKM theory is

$$A + M \xrightarrow[k_{-1}]{\delta k_1 (E^* \to E^* + \delta E^*)} A^*_{(E^* \to E^* + \delta E^*)} + M \quad (35)$$

$$A^*_{(E^*)} \xrightarrow{k_2(E^*)} A^{\neq} \xrightarrow{k^{\neq}} \text{Products} \quad (36)$$
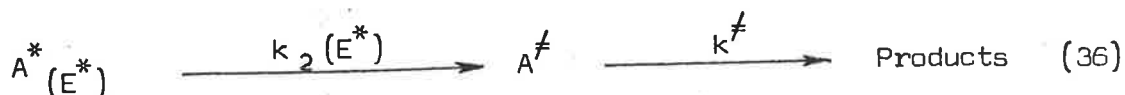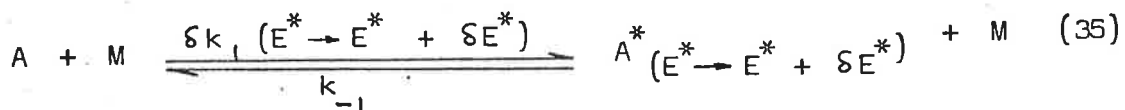
where A^* is the energized molecule

and $A^{\neq}$ is the activated complex.

There are essentially two new principles involved in the RRKM treatment. Firstly the energization rate constant k_1 is evaluated as a function of energy by a quantum-statistical-mechanical treatment instead of the classical treatment used in the RRK and Slater theories.

$$k_{uni} = -\frac{1}{[A]}\frac{d[A]}{dt} = \int_{E^*=E_0}^{\infty} \frac{k_2(E^*) \, dk_1 \, (E^* \to E^* + dE^*) \, / \, k_{-1}}{1 + k_2(E^*) \, / \, k_{-1} \, [M]} \quad (37)$$

The de-energization rate constant k_{-1} is considered as in RRK theory to be independent of energy. Secondly the application of Transition State Theory (or Absolute Rate Theory) [18] to the calculation of $k_2(E^*)$. For this purpose a distinction has been made between the energized molecule A^* and activated complex $A^{\neq}$. The energized molecule is basically an A molecule having enough energy to react, but not in the correct distributions to undergo conversions to products. The activated complex is a species recognizable as being intermediate between reactant and products, characterized by a configuration corresponding to the top of an energy barrier between reactants and products.

RRKM theory uses statistical mechanics for calculating the equilibrium concentrations of A^* and $A^{\neq}$, and evaluates the number of ways of distributing a given amount of energy between the degrees of freedom of a molecule. Fixed energy, such as the translational energy of the molecule which cannot be redistributed, has no effect on the rate of molecular reactions. However some energy of the molecule is considered free to move around the molecule, and subject to rapid redistributions; the vibrational (E_v) and 'active' rotational (E_r) energies contribute to this non-fixed energy.

The quantity $\delta k_1 {}_{(E^* \to E^* + \delta E^*)} / k_{-1}$ is the equilibrium constant for reaction (42) and is given by statistical mechanics as the partition function ratio $Q (A^*_{(E^* \to E^* + \delta E^*)}) / Q_{-1}$. If δE is small, the exponential terms in $Q = \sum g_i \exp(-E_i /kT)$ all become $\exp(-E^*/kT)$; where g_i is the number of quantum states of the energy level E_i.

Defining $N^*(E^*)$ as the number of quantum states per unit range of energy at energies close to E^*, then

$$Q (A^*_{(E^* \to E^* + \delta E^*)}) = \left[\sum_{E^* \to E^* + \delta E^*} g_i \right] \exp(-E^*/kT) \qquad (38)$$

$$= N^*(E^*) \delta E^* \qquad \exp(-E^*/kT) \qquad (39)$$

Thus

$$\frac{\delta k_1 (E^* \to E^* + \delta E^*)}{k_{-1}} = \frac{N^*(E^*) \exp(-E^*/kT)}{Q_{-1}} \delta E^* \qquad (40)$$

To find an expression for the rate constant $k_2(E^*)$ of reaction (36), steady-state treatment to $A^{\neq}$ gives $k_2 [A^*] = k^{\neq} [A^{\neq}]$ and hence

$$k_2 (E^*) = \frac{1}{2} k^{\neq} \left[\frac{[A^{\neq}]}{[A^*]} \right]_{equilibrium} \qquad (41)$$

The non-fixed energy of activated complex $A^{\neq}$ from energized molecule A^* of energy E^* is $E^{\neq}$, and is made up of energy of vibration and rotation $(E^{\neq}_{vr})$ and energy associated with the translational motion of $A^{\neq}$ in the reaction coordinate X .

---

* For description of statistical mechanics and partition function Q, Appendix 2 of reference [17] is recommended.

Energy level of reacting molecule

$$E^* = E^*_{vr} = E^*_v + E^*_r$$

$$E^\dagger = E^\dagger_{vr} + x = E^\dagger_v + E^\dagger_r + x$$
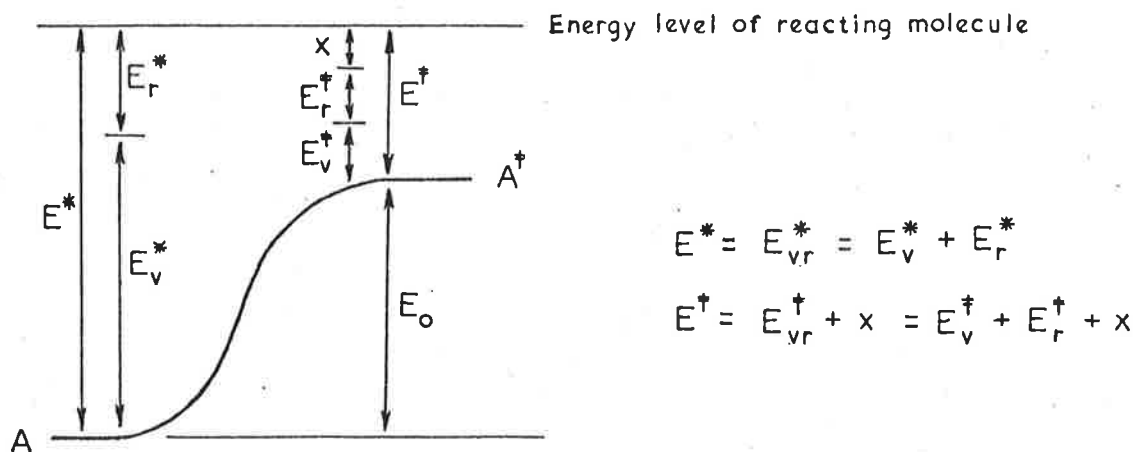
(Note: adiabatic and inactive degrees of freedom excluded from above schematic sketch.)

Thus reaction (36) can be written as

$$A^*_{(E^*)} \xrightarrow{\ k_2(E^{\neq}_{vr,x})\ } A^{\neq}_{(E^{\neq}_{vr,x})} \xrightarrow{\ k^{\neq}(x)\ } \text{Products} \qquad (42)$$

and (41) as

$$k_2(E^*) = \sum_{E^{\neq}_{vr} = 0}^{E^{\neq}} \frac{1}{2}\, k^{\neq}(x) \left[\frac{\left[A^{\neq}(E^{\neq}_{vr,x}) \right]}{\left[A^*(E^*) \right]} \right]_{eqm} \qquad (43)$$

Evaluating $k^{\neq}(x)$ and $([A^{\neq}]/[A^*])_{eqm}$ (for details, reference 17, pg 71-73), the resultant equation obtained is

$$k_2(E^*) = \sum_{E^{\neq}_{vr} = 0}^{E^{\neq}} \frac{1}{2} \left(\frac{2x}{\mu \delta^2} \right)^{\frac{1}{2}} \frac{P(E^{\neq}_{vr})(2\mu\delta^2/h^2 x)^{\frac{1}{2}}}{N^*(E^*)} \qquad (44)$$

$$= \frac{1}{h\, N^*(E^*)} \sum_{E^{\neq}_{vr} = 0}^{E^{\neq}} P(E^{\neq}_{vr}) \qquad (45)$$

where $P(E^{\neq}_{vr})$ is the number of vibrational-rotational quantum states of $A^{\neq}$ with vibrational-rotational non-fixed energy equal to $E^{\neq}_{vr}$, and h is Planck's constant.

The above expression has been developed from consideration of the 'active' non-adiabatic rotational energy. However adiabatic rotations (those that stay in the same quantum state during the change from energized molecule to activated complex) do suffer an energy change because of the different moments of inertia of A^* and $A^{\neq}$, releasing energy into other degrees of freedom thereby affecting the rate constant $k_2(E^*)$. For the high pressure limiting case, it is found [17] that the correct k_∞ is obtained if the expression (45) for $k_2(E^*)$ is multiplied by $Q_1^{\neq} / Q_1$, where $Q = Q(A)$ is the partition function for the adiabatic rotations. A second modification to (45) involves the inclusion of a statistical factor $L^{\neq}$ which takes account of the possibility that a reaction can proceed by different paths which are kinetically equivalent. The equation for $k(E^*)$ generally used in RRKM calculations is thus

$$k(E^*) = L^{\neq} \frac{Q^{\neq}}{Q} \frac{1}{h N^*(E^*)} P(E_{vr}^{\neq}) \tag{46}$$

Substituting equations (40) and (46) into (37) gives the RRKM expressions for k_{uni}

$$k_{uni} = \frac{L^{\neq} Q_1^{\neq}}{h Q_1 Q_{-1}} \int_{E^* = E_0}^{\infty} \frac{[P(E_{vr}^{\neq})] \exp(-E^*/kT) \, dE^*}{1 + k_2(E^*)/k_{-1}[M]} \tag{47}$$

and since $E^* = E_0 + E^{\neq}$ and $dE^* = dE^*$

$$k_{uni} = \frac{L^{\neq} Q_1^{\neq} \exp(-E_0/kT)}{h Q_1 Q_{-1}} \int_{E^{\neq} = 0}^{\infty} \frac{[P(E_{vr}^{\neq})] \exp(-E^{\neq}/kT) \, dE^{\neq}}{1 + k_2(E_0 + E^{\neq})/k_{-1}[M]} \tag{48}$$

The high pressure limit is obtained by putting $[M] \rightarrow \infty$, and evaluating the summation over all possible values of $E_{vr}^{\neq}$, resulting in the expression

$$k_{\infty} = L^{\neq} \frac{kT}{h} \frac{Q_1^{\neq} Q_{-1}^{\neq}}{Q_1 Q_{-1}} \exp(-E_0/kT) \tag{49}$$

Substituting equation (49) into expressions (50) and (51),

$$E_{\infty} = kT^2 \, d \ln k_{\infty}/dT \tag{50}$$

$$\ln A_{\infty} = \ln k_{\infty} + E_{\infty}/kT \tag{51}$$

as defined by Slater's Theory [17], we obtain

$$E_{\infty}(RRKM) = E_0 + kT + kT^2 \, d \, (\ln Q_1^{\neq} Q_{-1}^{\neq} / Q_1 Q_{-1}) \, dT \tag{52}$$

$$\ln A_{\infty}(RRKM) = \ln (L^{\neq} e \, kT/h) + d(T \ln Q_1^{\neq} Q_{-1}^{\neq} / Q_1 Q_{-1}) \, dT \tag{53}$$

$$= \ln (L^{\neq} e \, kT/h) + \Delta S^{\neq} / R \tag{54}$$

Application of RRKM calculations to the postulated model depends significantly on an assessment of the distribution of vibrational-rotational quantum states at various energy levels. From these assignments, the entropy of activation $\Delta S^{\neq}$ can be obtained and also A_{∞}. The appropriate critical energy E_0 for a given model can then be calculated by comparison with the experimental E_{∞}. If the model is chosen to give the experimental A-factor, the RRKM formulation will automatically predict the experimental values of k_{∞} and its temperature dependence. Details of such procedures are described in Chapter 3.

1.4 Semi-Ion Pair Theory

The unimolecular decomposition of substituted alkanes often involves the elimination of the substituents either as a hydride or substituent molecule. The proposed mechanism for this is via a transition state involving a four-centre structure. Maccoll and coworker [20] showed that, for the kinetic data of the alkyl halides, while little correlation existed between the activation energy for elimination and the homolytic bond dissociation energies $D (R - X)$, there was a clear correlation with the heterolytic bond dissociation energies $D (R^+ X^-)$. For the elimination of other groups the term "degree of heterolysis" [20b] was introduced. In 1963, a semi-ion pair transition state was postulated by Benson and Bose [21], and on this basis Benson and Haugen [22] extended the treatment to calculate activation energies in good agreement with experiment for several elimination systems. It is not proposed to make any detailed comparison between this concept and the formulations of Maccoll.

The basic premise of the semi-ion pair model is that the transition state is represented by a quadrupole formed from two semi-ion pairs, and is partially ionic in character. One semi-ion pair is the polarized olefin, the other is the polarized bond of the diatomic adduct. The activation energy for addition is regarded as a composite of the electrostatic polarisation energies required to generate a formal charge separation in each of the reacting bonds, the short range intermolecular repulsion, and the electrostatic energies regained by the mutual interaction of these polarized bonds. The polar energy that resides in the ground-state of the reactants is subtracted. For the following four centre transition state complex
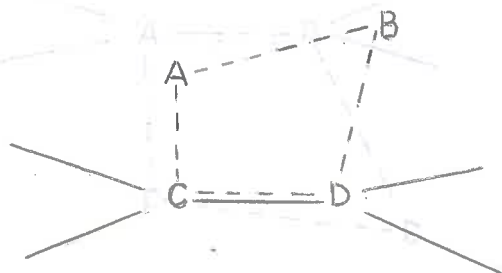
the total energy of generation of the semi-ion quadrupole is

$$E = \frac{e^2 q^2}{2} \left[\frac{\left(r_{AB}^{\neq}\right)^2}{\alpha_{\ell, AB}^{\neq}} + \frac{\left(r_{CD}^{\neq}\right)^2}{\alpha_{\ell, CD}^{\neq}} - \frac{3}{2} \frac{(r_{AB}^{\neq})(r_{CD}^{\neq})}{r_e^3} \right] - \frac{\varepsilon^2}{2} \frac{\mu_{AB}^2}{\alpha_{\ell, AB}^o} \tag{55}$$

where

q is the formal charge across the bond in the transition state,

$r^{\neq}$ is the length of the bond in the transition state,

$\alpha_{\ell}^{\neq}$ is the effective longitudinal polarizability,

α_{ℓ}^o is the ground state longitudinal polarizability,

μ is the ground state bond dipole,

e^2 and ε^2 are conversion factors,

and r_e is the equilibrium distance between the dipole centres, estimated from

$$r_e \simeq \frac{1}{2} \left[r_{AC}^{\neq} \sqrt{1 - \frac{1}{4} \left(\frac{r_{AB}^{\neq} - r_{CD}^{\neq}}{r_{AC}^{\neq}} \right)^2} + r_{BD}^{\neq} \sqrt{1 - \frac{1}{4} \left(\frac{r_{AB}^{\neq} - r_{CD}^{\neq}}{r_{BD}^{\neq}} \right)^2} \right] \tag{56}$$

The first term of equation (55) is the polarization energy of the AB bond, the second the polarization energy of the CD bond, the third is the equilibrium electrostatic energy of the dipoles and the final term is the ground-state electrostatic energy. Agreement between theoretical calculations and experimental data is very good (within ± 2 kcal/mole) for compounds whose activation energies are known with some degree of certainty [22].

Recently Tschuikow-Roux, Maltman and Jung [23] have developed a modification to the semi-ion pair theory, which combines the basic concepts of the Benson-Haugen model with the bond-energy-bond-order concepts of Johnston [24]. The energy contributions to the activation process depend only on the ground-state properties of reactants and products. Their model is reported to have similar agreement as the Benson-Haugen model.

1.5 Review of Previous Work on Cyanides

Despite the apparent need for information about the effects of a cyano group on the reaction kinetics and thermochemistry of organic cyanides, few observations have been reported on this important substituent group, and much of it is subject to uncertainties.

1.5.1 Reaction Kinetics

Although industrial catalytic decomposition of long-chain nitriles have been investigated to some degree [25], few studies have been reported on the homogeneous kinetics and mechanisms of the pyrolysis of shorter chain organic cyanides. Rabinovitch and Winkler [26] in 1942 carried out an investigation on the pyrolyses of methyl and ethyl cyanides to obtain information about the nature of the reactions involved and the products formed. This was carried out using a silica plug-flow reactor over two flow rates and two temperatures, 948 and 1138 K. They found in the case of methyl cyanide that hydrogen cyanide was a primary product, along with hydrogen, methane and carbon. Secondary reactions were suspected. Ethyl cyanide decomposition was found to be very complex with product analyses yielding hydrogen, methane, ethane, ethylene, hydrogen cyanide, methyl cyanide, vinyl cyanide and carbon, plus some high boiling materials. Secondary and chain reactions were suggested to account for the variety of products.

The pyrolysis of methyl cyanide was investigated more recently by Asmus and Houser [27] over the temperature range 1153 - 1233 K in an atmospheric pressure stirred-flow reactor using helium as the carrier gas. Gas chromatographic analysis revealed the major volatile products to be methane and hydrogen cyanide, plus small amounts of ethylene and vinyl cyanide. They also observed a brown, non-volatile polymeric residue deposited along the exit lines, which from analysis was believed to be of a cyano-substituted

ethylenic type. A fractional reaction order greater than one was found, which was interpreted as mixed first-and second-order kinetics. Their Arrhenius plots gave the following expressions

$$\log (k_1, \sec^{-1}) = 11.8 - (72.0 \pm 4.0)/\theta$$

for the first-order reaction, and

$$\log (k_2, 1 \text{ mole}^{-1} \sec^{-1}) = 20.5 - (120.0 \pm 6.0)/\theta$$

for the second-order reaction; where $\theta \equiv 2.303$ RT kcal/mole.

Ethyl, tert-butyl, and cumyl cyanides have been investigated by Hunt, Kerr, and Trotman-Dickenson [28] in a plug-flow reactor, using the aniline-carrier technique developed by Swarc [29], and were found to exhibit first-order kinetics. In the case of ethyl cyanide over the temperature range 959-1038 K, Hunt and coworkers found products relating to the elimination of both hydrogen and hydrogen cyanide, as well as the bond fission reaction yielding methane and methyl cyanide. However their kinetic parameters are suspect. The Arrhenius A-factor ($10^{15 \cdot 0}$ $\sec^{-1}$) for hydrogen cyanide elimination is too high for this type of reaction [30], and the kinetics of the fission reaction give a relatively low value for the recombination rate constant [31]. The formation of hydrogen was observed in all aniline-carrier studies and cannot be explained in terms of a molecular elimination. It has been suggested by Benson and O'Neal [31] that the products from both hydrogen and hydrogen cyanide eliminations arise from free radical induced decomposition. Tert-butyl cyanide was followed over the range 875-925 K and Hunt and coworkers found that bond fission was predominant; some hydrogen was observed. The Arrhenius expression for the fission reaction was reported as $\log (k, \sec^{-1}) = (15.16 \pm 0.34) - (70.2 \pm 1.4)/\theta$ which yields a value of 10.6 kcal/mole for the resonance stabilization of the cyanoisopropyl radical. For the case of cumyl cyanide pyrolysis, followed over the range 793-897 K, methane was produced as well as some hydrogen.

The A-factor ($10^{12.3}$ sec^{-1}) obtained from a least-mean squares treatment of the results is much lower than that expected from analogous reactions, and Hunt and coworkers suggested that the methane formation could arise from a four-centre molecular elimination reaction rather than the bond fission reaction yielding methyl radicals. This would, however, involve pentavalent carbon in the transition-state, and thus is not considered probable [30].

Recently Dastoor and Emovon [32] reported their observations on the pyrolyses of ethyl, isopropyl, and tert-butyl cyanides using a flow system over the temperature range 803-943 K. They found hydrogen cyanide elimination as the mode of decomposition, and the reactions appeared to be homogeneous and molecular with no indication of carbon-carbon bond fission. The reaction was followed titrimetrically with silver nitrate, with confirmation of any other products via gas chromatography. A four centre reaction similar to hydrogen halide elimination from alkyl halides was suggested by Dastoor and Emovon; but although the reported A-factor ($10^{13.1}$ sec^{-1}) for isopropyl and tert-butyl cyanides are lower than expected [30]. (It is worth noting that in a similar study of the pyrolysis of alkyl fluorides [33], Dastoor and Emovan again obtained low A-factors). As well, the activation energies for the series ethyl, isopropyl, tert-butyl cyanides do not show any trend with α-methyl substitution. It is surprising that Dastoor and Emovan did not observe any bond fission reaction for tert-butyl cyanide, while Hunt and coworkers found only this reaction over the same temperature range. Free radical chain processes could possibly be a contribution to the rate of formation of hydrogen cyanide. Dastoor and Emovon did report runs with and without toluene (in the ratio of ca. 1:1 with the reactant) as a chain inhibitor to confirm the absence of free radicals, but as suggested by Swarc [29], the inhibitor should exist in

bulk such as in a carrier-gas system, to be certain of scavenging all the radicals. In addition, at the temperatures at which the cyanides were investigated the chain inhibitor itself begins to decompose to produce more radicals [31].

Small ring nitriles have been the subject of a few recent investigations since small ring compound reactions are normally well behaved kinetically, and they give strong indications as to the effect of substituent groups. Their decompositions can also be followed at lower temperatures than the alkyl cyanides, thus avoiding higher temperature complications. Luckraft and Robinson [34] followed the isomerization of cyclopropyl cyanide in the gas-phase over 660-760 K and 2-89 torr within a batch reactor. Product analysis was carried out by gas chromatography, and the reactions were found to be first-order, homogeneous and unaffected by the presence of radical chain inhibitors. Cyclopropyl cyanide isomerized to give cis- and trans-crotonitrile, and allyl cyanide, with a trace of methyl vinyl cyanide. The overall rate constants were given by

$$\log (k, \sec^{-1}) = (14.58 \pm 0.08) - (57.9 \pm 0.3)/\theta$$

and on the basis of a biradical mechanism, a cyano stabilization energy of 7.2 kcal/mole may be calculated.

Kinetic data for the gas-phase pyrolysis of five cyano-substituted cyclobutanes have been reported by Sarner and coworkers [35] . Gas chromatographic analysis of the products formed showed then to be entirely analogous to those found in reactions of the parent hydrocarbons. Two sets of runs were carried out for the pyrolysis of cyclobutyl cyanide over the temperature range 726-792 K, and the activation energies obtained were identical (56.6 kcal/mole) for the two kinetic runs, but differed by a factor of ca. 2.5 in A-factors and rate constants. A third set of approximate measurements was mentioned by the authors which gave values intermediate between the above sets of data, but with an indication of a lower activation energy. The average rate equation for the two sets of data was

$$\log (k, \text{sec}^{-1}) = (15.3 \pm 1.2) - (56.7 \pm 4.1)/\theta$$

which leads to a resonance stabilization of ca. 6 kcal/mole by the cyano group relative to a hydrogen atom. Their study of trans- 1,2-dicyanocyclobutane showed that it decomposed to vinyl cyanide over the range 593-683 K, but the reported A-factor of $10^{12.4}$ sec^{-1} seems low when compared to analogous reactions. In addition, their determination of 10-11 kcal/mole per cyano group for the cyano stabilization energy seems high with that obtained from their cyclobutyl cyanide results. The formation of the trans isomer complicates the reaction of cis-1,2-dicyanocyclobutane, but indications were that the same rate equation governing the decomposition of the trans isomer also fitted the data for the cis isomer. The decomposition of 3-methylene-1-cyanocyclobutane also proceeded via a biradical mechanism to produce vinyl cyanide and allene. Once again the A-factor and activation energy reported seem low when compared with methylenecyclobutane. Although the reactor used in their studies has been described as free from surface effects [36], this tendency of A and E to be lower than expected is indicative of some contribution from a heterogeneous process. The decompositions of cyanobicyclobutane and cyanocyclobutene were observed by Sarner and coworkers to occur via a concerted mechanism and, as expected, the cyanogroup offered no additional stabilization energy in the concerted reaction path.

Very recently, Bellus and Rist [37], in a study of the mechanisms of pyrolysis of substituted bicyclo-[2.2.0]-hexanes, reported on the pyrolysis of 1,4 - dicyanobicyclo-[2.2.0]-hexane. NMR measurements over the temperature range 293 -323 K yielded the following rate expression

$$\log (k, \text{sec}^{-1}) = (11.6 \pm 1.0) - (21.7 \pm 1.4)/\theta$$

The activation energy when compared with that for the pyrolysis of bicyclo - [2.2.0]-hexane gave 7.3 kcal/mole as the stabilization energy per cyano group. It should be noted that the stabilization energies derived above

for small ring compound pyrolyses are quoted relative to H.

The isomerization of two cyanides have been investigated and reported, and from these the resonance energy for the effect of the cyano group can be determined. Kistiakowsky and Smith [38] in 1936 observed the kinetics of the cis-trans isomerization of β-cyanostyrene over the temperature range 581-651 K. Analysis was be means of a refractometer, and it was found that at pressures of 15-40 torr a surface reaction was evident, whilst at higher pressures (150-450 torr) it did not interfere with the homogeneous reaction. The high pressure rate data was reported to be given by $\log(k, sec^{-1}) = (11.6 \pm 0.4) - (46.0 \pm 1.0)/\theta$ yielding Arrhenius parameters that are lower than expected from other isomerizations. However, using a regression program on their data gave $\log k = (12.3 \pm 0.3) - (48.2 \pm 0.9)/\theta$ which seems more acceptable. From the activation energy a cyanostabilization energy for the biradical was calculated to be ca. 10 kcal/mole.

The cis-trans isomerization of crotonitrile was reported by Butler and McAlpine [39], who also studied the equilibrium. Rate constants were measured over the range 673-833 K and 0.7 to 20 torr. Gas chromatography analysisrevealed a unimolecular, first-order reversible reaction with $\log k = (11.0 \pm 1.0) - (51.3 \pm 3.7)/\theta$. Surface polymerization yielded a tarry deposit at the higher temperatures. Their Arrhenius parameters are relatively low, but performing a simple regression calculation on their data resulted in $\log k = (12.1 \pm 0.2) - (55.0 \pm 0.6)/\theta$, which is appreciably different from that reported above. Taking this activation energy, a resonance of ca. 10 kcal is calculated for the effect of the cyano group on the radical. Very recently the shock tube cis-trans isomerization of crotonitrile has been examined by Marley and Jeffers [40] over the range 1060-1280 K, using the relative rate technique. Chromatographic analysis of the product mixture resulted in the following rate expression

$$\log (k, \sec^{-1}) = (13.2 \pm 0.3) - (58.0 \pm 2.0)/\theta$$

Extrapolation of their results passes very close to the rate constants of Butler and McAlpine. Comparison of the activation energy with that for the isomerization of 2-butene [31] implies a resonance stabilization of ca. 8 kcal/mole. Note that this calculation assumes that the energy for rotation from cis to trans position in the biradical is the same for both compounds [41].

1.5.2 Thermochemistry

Although the thermochemistry of hydrocarbons and the associated free radicals is known to a good degree of certainty, the data concerning cyano-substituted hydrocarbons and their related free radicals are particularly sparse. In 1969, Benson and coworkers [42] tabulated the thermochemistry of several studies cyanides, and compared them with the group additivity predictions. Unfortunately much of the data was the sole source used for determining a particular group value, and there were few reliable values for ΔH_f^o. Recently, Hall and Baldt [43] determined the enthalpies of formation of several alkyl and cycloalkyl cyanides using a rotating bomb calorimeter. They reported that replacement of H by CN in an organic molecule made $\Delta H_{f,298}^o$ more positive by 24 kcal/mole, but this value is incorrect; analysis of their results shows that it is ca.30 kcal/mole.

Free radical species as reactive intermediates are involved in a vast majority of gas-phase reactions, and their thermochemistry is most accurately obtained from kinetic studies. The thermochemistry of free radicals has been discussed recently by O'Neal and Benson [44] and data on the α-cyanoethyl, and cyanoisopropyl radicals were included.However the enthalpies of formation of these free radicals were based upon the studies of Hunt and coworkers [28] and as explained earlier this work needs re-examining. The group additivity values derived for the above three cyanoalkyl radicals were based upon resonance stabilizations of approximately 11-13 kcal/mole, which are high compared with the more recent values of 6-7.3 kcal/mole [34,35,37].

1.6   The Present Investigation

The overriding aspect of much of the previous work on gas-phase pyrolysis of organic cyanides is the suspicion that chain processes occurred and heterogeneous reactions were present.   Despite the assurances that the reactions showed no changes when checked with chain inhibitors and extended surface reactors, analysis of the Arrhenius parameters suggest otherwise.   Enough knowledge of transition-state theory coupled with an understanding of molecular basis of entropy now exists to put fairly rigid constraints on the values of the Arrhenius A-factor for most elementary reactions [30, 31, 45, 46].   Very often investigators lose sight of the meaning of Arrhenius parameters;   simply plotting the logarithm of their experimental rate constants versus the reciprocal of temperatures in their limited range, and with a least-means-squares treatment obtain the intercept and slope, i.e. values of the A-factor and activation energy.   A slight change in slope of the best-fit line (while still being within their error limits of the data) can often result in a change to the obtained A-factor of a factor of ten, and by two or three kcal/mole in the activation energy.   It is important to realize that the theoretical calculational procedure requires the estimation of molecular parameters of the transition-state complex, and as such is no substitute for highly reliable data.   Conversely, however, the calculations render obsolete all but the most precise experimental data.

From the preceeding discussion it is apparent that a critical re-examination of the alkyl cyanides is required to determine the competitiveness of carbon-carbon

bond fission and hydrogen cyanide elimination. From these studies thermochemical data on cyanoalkyl radicals can be determined, as well as C-C and C-H bond dissociation energies in these cyanides. Reliable thermochemical knowledge on free radicals is very necessary for the formulation of possible reaction mechanism for a chemical reaction.

An excellent technique for following unimolecular reactions, and ensuring that secondary reactions are eliminated is very low-pressure pyrolysis (VLPP) [47]. This technique gives direct quantitative information on the reaction occuring, and since the collisions are predominately gaswall rather than gas-gas, due to the low pressures, secondary reactions are virtually eliminated. A description of the technique is given in Chapter 2. Dr. K.D. King of the Chemical Engineering Department of the University of Adelaide has recently constructed such a system [48], and has permitted parts of this investigation to be carried out using it. Two conventional reactor systems were designed and constructed to enable studies to be made of cyanides whose reactivity and physical properties hindered their study by the VLPP technique. A stirred-flow reactor, and a batch reactor connected to a vacuum line, were built in the laboratory. A gas chromatograph was used for analysis.

Since most small-ring compound reactions are kinetically straight forward and normally free from radical processes and surface effects, it was decided to study the decomposition of cyclobutyl cyanide first. The rate expression obtained would then be able to be compared with the two differing sets of data reported by Sarner and coworkers [35]. The investigation was carried out in the VLPP system, and the results were hoped to be informative on the pyrolysis of cyclobutane [49] carried out in a similar system, but which had given inconclusive results. A follow-up investigation of the decomposition of cyclopropyl cyanide using VLPP was attemped as well, but proved impractical, since the mass spectra of the cyanide and its products

did not have any unique peaks with which to monitor the pyrolysis.

After familiarizing myself with the VLPP system by following the above biradical decomposition, the pyrolyses of a series of alkyl cyanides were carried out. The kinetics of the decompositions of ethyl cyanide, isopropyl cyanide, n-propyl cyanide, and tert-butyl cyanide were examined; n-propyl cyanide not having been studied previously. Carbon-carbon bond fission and hydrogen cyanide elimination were the probable reaction pathways, and the study of the series was hoped to clarify the conflicting observations of Hunt and coworkers [28] and of Dastoor and Emovon [32] , and to determine to what extent secondary reactions were involved in their work. In addition, information concerning the cyanomethyl, α-cyanoethyl, and α-cyanoisopropyl free radicals would be obtained. Most of this work involved the VLPP technique, supplemented by the stirred-flow system which could follow more closely the experimental conditions used in previous investigations. The upper temperature limitation of the VLPP apparatus necessitated the kinetics of the ethyl cyanide decomposition to be studied in the flow system only. Due to the distinct possibility of secondary reactions occuring at the temperatures of this investigation, the use of an efficient chain inhibitor was required. The large yields of hydrogen, observed by Hunt and coworkers during the pyrolysis of ethyl cyanide, was also examined.

These investigations of the alkyl cyanides revealed that hydrogen cyanide elimination was a minor reaction pathway accounting for less than 10% of the overall decomposition. To enable the elimination reaction to be followed more closely, and obtain more information on its kinetic parameters, entailed the investigation of cyano compounds in which the carbon-carbon bonds adjacent to the CN group are stronger relative to those in the alkyl cyanides. Cycloalkyl cyanides such as cyclopentyl cyanide or cyclohexyl cyanide seemed suitable, and could be followed with little difficulty in the static and flow systems.

The effect of more than one cyano group on the bond strength of the adjacent carbon-carbon bond would be of value in checking against the stabilization energy obtained from mono-substituted cyano compounds. Since the investigation of Sarner and coworkers [34] on trans -1,2-dicyanocyclobutane required a re-examination, this compound was selected to observe the effect of two adjacent cyano groups. The resultant biradical should be doubly stabilized since conjunction with both cyano groups is possible at the point of ring breaking. Studies of decompositions of divinylcyclobutane and 1,2- dimethallylcyclobutane [50] show that the biradical was stabilized in an additive fashion. Bellus and Rist [37] have studied the pyrolysis of 1,4- dicyanobicyclo[2.2.0] hexane, and found it to give a stabilization energy per cyano group in good agreement with those obtained from cyclopropyl cyanide [34] and cyclobutyl cyanide [35].

CHAPTER 2.

EXPERIMENTAL TECHNIQUES

The investigations were conducted using three reactor systems in order to obtain results over a wide range of conditions. These systems were

(1)   Very low-pressure pyrolysis technique, which involves a high temperature, steady-state, stirred-flow reactor operating at the molecular level. Reactions were monitored by means of a quadrupole mass spectrometer.

(2)   Conventional carrier-gas flow reactor, operating at atmospheric pressure using a Vycor reaction vessel connected to a gas saturator. Product analysis was by means of gas chromatography.

(3)   Conventional static (batch) reactor, which used a Vycor reaction vessel connected to a Pyrex high-vacuum line. The course of the reactions could be followed by gas chromatography and pressure measurements via a pressure transducer.

Each system had its purposes and limitations of range, and some compounds, due to their reactivity and physical properties, were only able to be studied in one of the reactors.

Before describing each reactor system and the procedures of product analysis, the preparation and purification of the materials used in this study are discussed.

2.1 Preparation and Purification of Materials

Most reactants, and compounds required for characterization of products, were obtained commercially, in the highest purity available.

The following procedure described for one of the reactant compounds was carried out for all the commercially obtained materials. A few millilitres of cyclobutyl cyanide (from P.C.R. Inc.) were thoroughly degassed using liquid nitrogen and a high-vacuum line, before being pumped on at $< 5 \times 10^{-3}$ torr * for at least five minutes. Vacuum distillation bulb-to-bulb was then carried out a few times. Product purity was checked by either mass spectrometry or gas chromatography. This was performed each time the material was required. The following materials were treated similarly : isopropyl cyanide, n-propyl cyanide, tert-butyl cyanide, vinyl cyanide, allyl cyanide, crotonitrile, cyclopentene (all from Koch - Light), methyl cyanide (Ajax, Univar), methyl vinyl cyanide (Eastman) ethyl cyanide (K & K Laboratories), cyclopentyl cyanide (Fluka).

Hydrocarbon gases were obtained from Matheson and were of C.P. grade. Ethane, ethylene, propylene and isobutene were degassed before use, whilst methane was used directly. The gases were used only for identification and calibration purposes. Argon (from C.I.G. high purity dry) was required as the internal standard for monitoring the VLPP reactions, and it was used directly.

trans - 1, 2-Dicyanocyclobutane

The dicyanide is commerically available as a mixture of cis and trans isomers, and a small amount of the material was obtained from Aldrich. Information concerning its physical properties was obtained from patents [51], which were helpful in determining the boiling points of the isomers. They resolve that under a vacuum of a few torr the boiling range of the

---

* Throughout this research, 1 torr $\equiv 133.322$ N m^{-2} in S.I. units.

dicyanide is between 100-150°C, with the trans isomer boiling point being approximately 30 C less than that of the cis isomer. With such a difference in boiling points, it was expected that the mixture could be separated into its isomers with a good degree of purity by using a vacuum distillation column.

Vacuum distillation was carried out in a semi-micro apparatus consisting of a 50 ml. still, a jacketed fractionating column, an air condensor, and 5 ml. bottles for collection of the fractions. The still was heated by an oil bath, the temperature of which was monitored by a thermometer, and the temperature at the top of the column also being followed by thermometer. About 10 ml. of the dicyanide were added, and at atmospheric pressure, the mixture was observed to melt at 40-50 $^\circ$C. The apparatus was evacuated via a cold trap by a rotary pump, and the pressure within the equipment was maintained at ca. 0.5 torr. At this pressure the still was heated slowly until the top temperature rose suddenly and steadied. The first fraction was collected at a bath temperature of 125°C and a top temperature of 87°C. After sampling 2-3 mls, a second fraction was taken until the temperature dropped (indicating the end of the trans isomer). Heat was increased to the still until the top temperature rose sharply and steadied. The condensate was initially collected in the second fraction bottle, before the third bottle was used the fraction. Conditions for this fraction were a bath temperature of 155°C and a top temperature of 110°C. Distillation was continued until only a small amount of material was left in the still.

Gas chromatography was used to determine the purity of the fractions. Using a 10% w/w Apiezon L column at 130°C with hydrogen flame ionization detection, the first fraction was found to be better than 99% pure in trans-1,2-dicyanocyclobutane. The second fraction was a mixture of the two isomers, whilst the third fraction consisted of about 98% cis 1,2-dicyanocyclobutane. For this investigation, only the thermal decomposition

of the trans isomer was studied. The vacuum distilled fraction of the trans-dicyanide was degassed and further distilled bulb-to-bulb in vacuo a few times, until gas chromatography analysis indicated a pure sample.

Hydrogen cyanide

Hydrogen cyanide was prepared in a closed semi-micro apparatus within a fume cupboard. To 20 ml. of a 2.5 M aqueous solution of potassium cyanide, 2.5 M sulphuric acid was added dropwise. The solution was kept warmed to about $35^{o}C$, enabling the hydrogen cyanide produced to vaporize and condense in a water cooled condensor. Droplets of the compound were collected at $0^{o}C$. After degassing and distillation bulb-to-bulb in vacuo, the purity was checked. Both mass spectrometry and gas chromatography showed it to be pure with no trace of water or any other contaminants. The hydrogen cyanide was used to prepare calibration mixtures for the systems in which cyclopentyl cyanide and ethyl cyanide decompositions were followed.

Cyclopentadiene

One of the products required to be followed in the thermal decomposition of cyclopentyl cyanide was cyclopentadiene, which is prepared from the dimer. Dicyclopentadiene (Koch-Light) was cracked and fractionated in a semi-micro apparatus at atmospheric pressure. The column was packed with glass helixes, and the still heated by an oil bath to a temperature of ca. $180^{o}C$. At this temperature the cyclopentadiene came over at a top temperature of $40-45^{o}C$. The monomer was then degassed and distilled bulb-to-bulb on the vacuum line. Mass spectrometry and gas chromatography confirmed its purity. It was stored under vacuum at $-78^{o}C$ until required.

2.2 Very Low-Pressure Pyrolysis (VLPP) Technique

One of the greatest difficulties encountered in the experimental study of kinetic systems is that of secondary reactions. In the mid 1960's Spokes and Benson [52] constructed a system which gave direct, quantitative information on gas-phase reactions operating at the molecular level. The principle behind the scheme was to flow a reactive gas at very low-pressures into a heated Knudsen cell where it would decompose unimolecularly, and then the products and reactant would flow molecularly through an exit hole to a mass spectrometer where they would be analysed directly. Due to the low pressures the collisions between species are predominantly gas-wall rather than gas-gas, and thereby no secondary reactions occur. The question of heterogeneous reactions may occur to the reader. However, heterogeneous reactions are usually slow reactions requiring a molecule or radical to reside on an active surface site for chemical rearrangement. Reevaporation, with a very high A-factor and low activation energy, is a much faster competing reaction for the absorbed molecule than chemical rearrangement, which has a low A-factor and moderate activation energy. In addition, as the temperature is increased, the residence time of the species on the surface decreases.

The applicability of this technique to the study of unimolecular reactions has been well substantiated [47]. The rate constant data obtained lie in the fall-off region, and in conjunction with RRK(M) theory, can yield high-pressure activation energies, if a reasonable transition-state model can be made to estimate the activation entropy. VLPP is a useful method for obtaining heats of formation of free radicals formed in a unimolecular bond homolysis, as well as activation energies for concerted processes.

2.2.1 Description

The apparatus was constructed by Dr. K.D. King of the Chemical Engineering Department of the University of Adelaide [48]. A brief description is given here. The design was based on that known as VLPP-I at Stanford Research Institute, Menlo Park, California [47,52,53]. The reactor was of similar design to the "triple-aperture reactor" [53] depicted in Figure 2.1, and was made of Vycor and had a reactor volume of 161 mls. It was heated electrically and housed in a cylindrical furnace made of Incoloy DS; the temperature of which could be controlled by a Eurotherm PID/SCR controller to better than 1 K.

The reactant flow rates were measured by observing the pressure drop per unit time from a calibrated volume through precision-bore capillaries using a Celesco P7D differential pressure transducer. Product and reactant gases effuse from the reactor into the ionization chamber of a quadrupole mass spectrometer. The analyser head of an EAI Quad 1110A mass spectrometer was flange mounted inside a 152 mm i.d. by 279 mm long cylindrical stainless steel vacuum chamber, such that it is in direct alignment with the exit beam of molecules. The pressure within the chamber was monitored by an AEI VC20 Ion Gauge. A 102 mm i.d. stainless steel elbow connects the chamber to the vacuum pumping system, where a 650 litres/sec diffusion pump backed by a 10 cubic metres/hour single-stage rotary pump evacuated the chamber through a liquid nitrogen cold trap. The base chamber pressures was ca. 2×10^{-7} torr without trapping and ca. 6×10^{-8} torr with liquid nitrogen trapping. The highest pressure during kinetic runs did not rise above ca. 10^{-5} torr at the highest reactant flow rates. The mass spectra were monitored with the Quad control console oscilloscope and recorded with a Gould Brush 500 X-Y recorder. Two views of the VLPP system are presented in Plates 1 and 2.

THIS SECTION IS REMOVABLE
THROUGH JOINT

1 mm APERTURE PLATE MANIPULATOR

3.3 mm
APERTURE
PLATE
MANIPULATOR

GAS INLET TUBE

3.3 mm
APERTURE PLATE

APERTURE PLATES MAY BE
INDEPENDENTLY MOVED
TO COVER 1 cm HOLE PLATE

1 cm HOLE

1 mm APERTURE PLATE
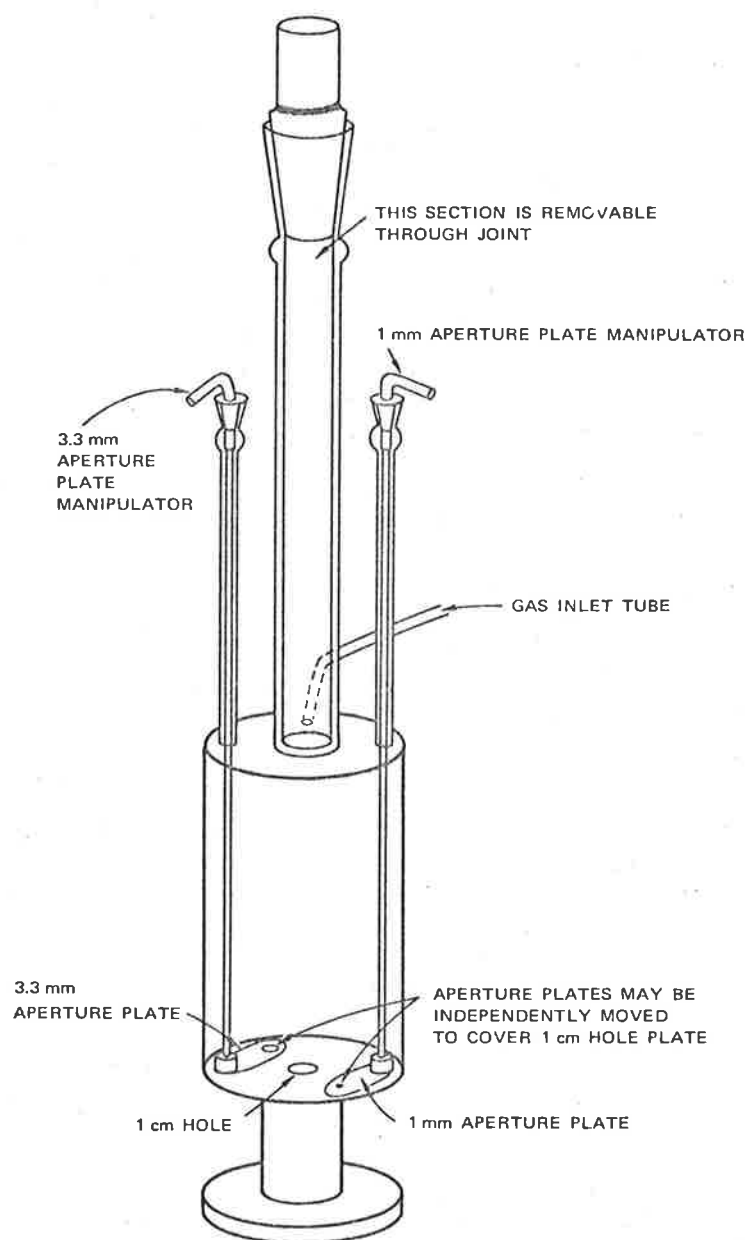
Figure 2.1   The triple-aperture reactor.

PLATE 1.   View of VLPP System.

The vacuum line precision-bore capillaries are
shown at the left. The triple-aperture reactor
and furnace are mounted on top of the stainless
steel vacuum chamber. Quad control console,
ionization gauge meter, and X-Y recorder are shown
to the right.

PLATE 1.   View of VLPP System.
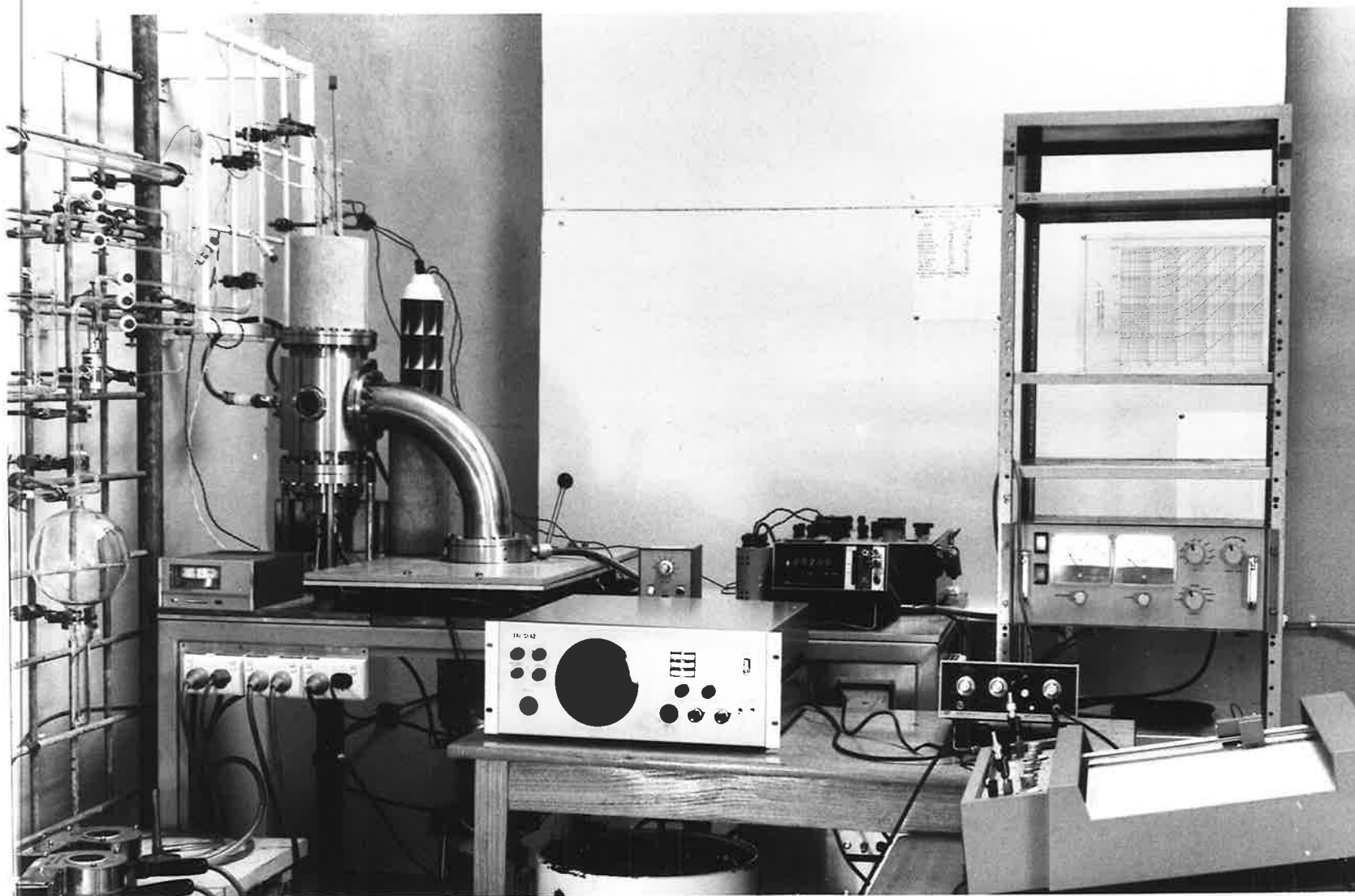
PLATE 2   View of VLPP reactor and analyser

The triple-aperture reactor is housed in a
cylindrical furnace on top of the vacuum
chamber, while the mass spectrometer head is
mounted from below in alignment with the exit
beam of molecules.

PLATE 2   View of VLPP reactor and analyser
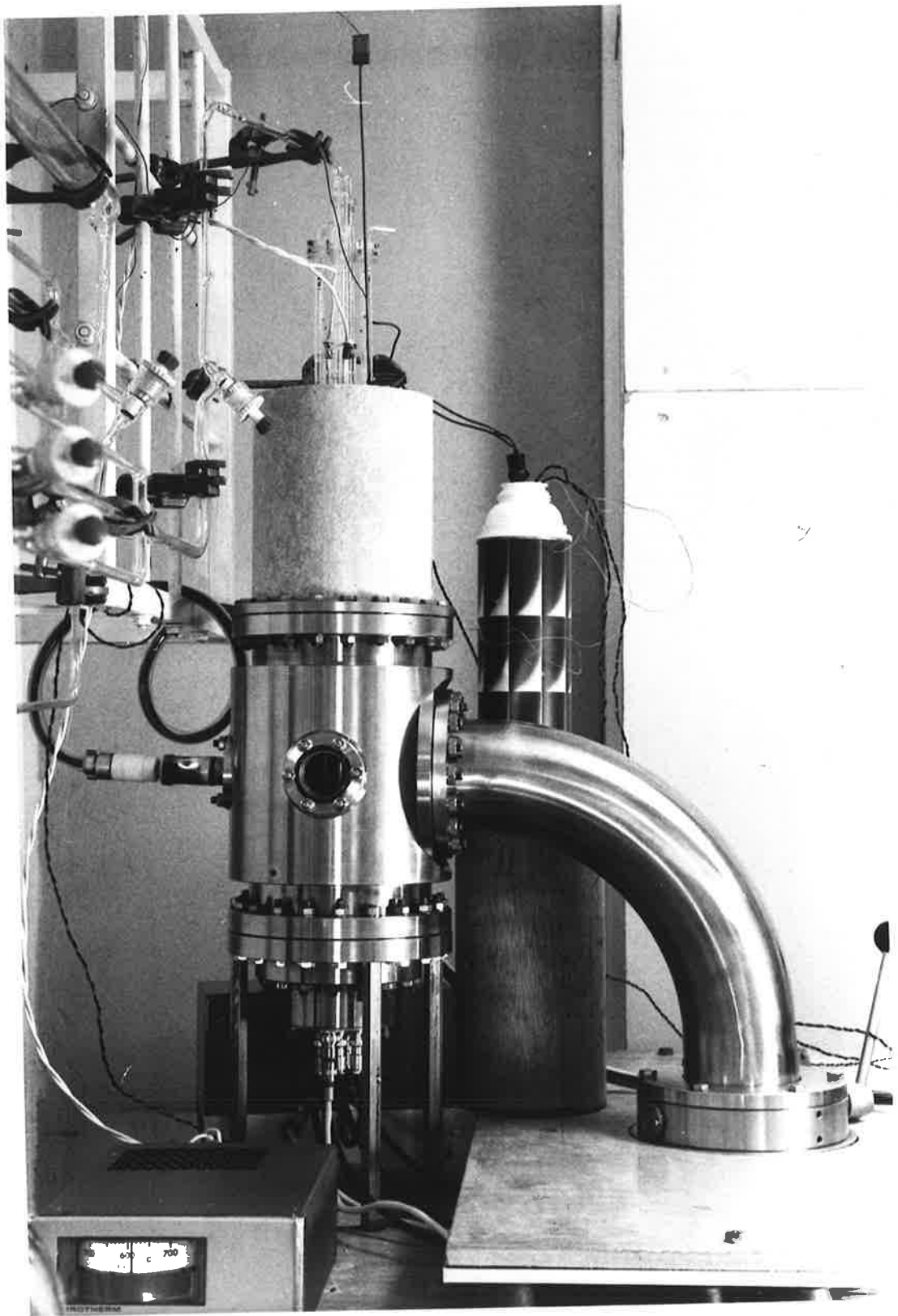
The conditions in VLPP correspond closely to those in a stirred flow reactor [52]. The pathways for a reactant molecule A can be represented by

$$A \underset{k_{ea}}{\overset{k_{uni}}{\rightarrow}} \quad \begin{array}{l} \text{products } (pP + qQ) \\ \text{escape through aperture} \end{array}$$
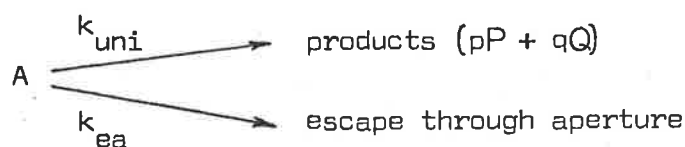
in the absence of any secondary reactions.

Thus
$$[A]_{ss} = \frac{N_A}{(k_{ea} + k_{uni}) V} \tag{1}$$

where $[A]_{ss}$ is the steady-state concentration of A in the reactor of volume V,

and N_A is the steady-state flow rate.

However, it should be noted that k_{ea} depends on the average molecular speed, and this is the important difference between the stirred flow reactor equations for high and for very low pressure.

From kinetic theory, the rate constant for escape from the reactor is given by [52]

$$k_{ea} = \frac{\bar{c} A_{he}}{4V} \quad \text{sec}^{-1} \tag{2}$$

where V is the reactor volume, in cm^3,

$\bar{c}$ is the mean molecular speed, in cm/sec, and is given by kinetic theory as

$$\bar{c} = \sqrt{\frac{8RT}{\pi M}} = 1.46 \times 10^4 \sqrt{\frac{T}{M}}, \tag{3}$$

and A_{he} is the effective area of the hole, in cm^2; calculated from $A_{he} = A_h C_h$ where A_h is the aperture area and C_h is the Clausing factor for the shape of the hole.*

Thus
$$k_{ea} = 3.65 \times 10^3 \frac{A_{he}}{V} \sqrt{\frac{T}{M}} \tag{4}$$

The escape rate constants* for the VLPP system [48] used in this research are shown in Table 2.1.

_____

* The Clausing factors and escape rate constants were calculated by Dr K.D. King in the same manner as outlined in reference [53].

Table 2.1 Apertures and Escape Rate Constants.

Hole diameter, cm	$A_h \times 10^3$, cm^2	C_h	$A_{he} \times 10^3$, cm^2	k_{ea}, sec^{-1}
0.108	9.18	0.935	8.58	$0.194 \sqrt{T/M}$
0.327	83.8	0.937	78.5	$1.75 \sqrt{T/M}$
1.00	785	0.87	683	$12.9 \sqrt{T/M}$

The average number of collisions with the walls, Z_w, made by a molecule during its residence in the cell is given by the ratio of the reactor wall area A_v and the escape aperture area A_h. In this system the reactor collision numbers were 19,550, 2,140, and 246 for the 1.1 mm, 3.3mm and 1.0mm apertures respectively. The frequency ω of collision of the average molecule with the reactor walls is given by

$$\omega = Z_w k_{ea} = \frac{\bar{c} A_v}{4V} \qquad (5)$$

Thus $\omega = 3.8 \times 10^3 \sqrt{T/M}$ based on a reactor surface area of 167.7 cm^2 and a volume of 161 cm^3.

For the irreversible unimolecular reaction

$$A \longrightarrow pP + qQ$$

the typical stable product P has a steady-state concentration given by

$$[P]_{ss} = \frac{p \, k_{uni} \, [A]_{ss}}{k_{eP}} \qquad (6)$$

Thus $\qquad k_{uni} = k_{ea} \dfrac{k_{eP} \, [P]_{ss}}{p \, k_{ea} \, [A]_{ss}} \qquad (7)$

$$\equiv k_{ea} \left(\frac{f}{1-f}\right) \qquad (8)$$

where f is the fraction of unimolecular decomposition.

Alternatively, equation (8) can be written as

$$k_{uni} = k_{ea} \left(\frac{I_A^o - I_A}{I_A}\right) \qquad (9)$$

where I_A is the intensity of the reactant peak at temperature T, and $I_A{}^o$ is the intensity of the same peak at a temperature below which no decomposition occurs.

In terms of product formation, $\quad k_{uni} = k_{ea} \; \alpha \; \dfrac{I_P}{p I_A}$ (10)

where α is the calibration factor determined by measuring I_P/I_A

for known mixtures of P and A.

2.2.2 Experimental Procedure

Before kinetic runs could be carried out in the VLPP system, a gas mixture of the reactant and internal standard was prepared on the vacuum line accompanying the system, and then stored in one of the storage bulbs. When the pressure in the ionization chamber was ca. 6×10^{-8} torr, the background mass spectra was recorded. The reservoir of reactant and internal standard was then opened to the VLPP aparatus via one of the precision-bore capillaries. Flow rates through the reactor were able to be selected from ca. 3×10^{14} to ca. 2×10^{16} molecules/sec; the highest pressure in the mass spectrometer chamber being less than 10^{-5} torr. After allowing at least twenty minutes for the reactor to come to thermal equilibrium the selected mass spectral range was recorded on the X-Y recorder, and the reactor temperature measured. The background contribution to the peaks used to monitor the reaction were then subtracted. When using the 1.1 mm aperture and the 3.3 mm aperture at low decompositions, the reactant to internal standard ratio at zero decomposition was checked by recording the mass spectra with the 10 mm aperture setting. At the end of a series of runs for the day, the reactant - internal standard reservoir was turned off, and the base pressure in the system and the background spectra were checked.

The kinetic data obtained from this VLPP apparatus has been confirmed by the investigation of two reactions (one molecular and one radical) [48] which had been investigated previously in the VLPP systems at Stanford Research Institute. These reactions were the molecular elimination of hydrogen iodide from isopropyl iodide [47,53] and oxygen-oxygen bond fission in di-t-butyl peroxide [54] . The Arrhenius parameters of these reactions are very different, and required the VLPP system to be tested over a wide temperature range. The results showed excellent agreement with the other studies, and clearly indicated that the system in Adelaide yields accurate and reliable kinetic data.

2.3 Stirred-Flow Reactor System

Due to the inherent uncertainties regarding the temperature and flow conditions within a tubular flow reactor [55], it was decided that a stirred-flow reactor would be a more versatile system to operate. Composition throughout this form of reactor is uniform due to the stirring which also helps attain uniform temperature conditions. In addition the effluent gases flowing from the reactor vessel have the same steady-state composition as the contents of the vessel. Reactions can also be followed to higher conversions than tubular flow reactors which operate at low conversions and pressures.

The theoretical basis is as follows:
consider the unimolecular reaction scheme, $A \rightarrow pP + qQ$, then for an ideal continuously stirred reactor at steady-state operation

$$R = -\frac{dc}{dt} = \frac{U}{V}\left([A]^O - [A]\right) \tag{11}$$

$$\therefore \quad \frac{V}{U[A]^O} = \frac{[A]^O - [A]}{[A]^O R} \equiv \frac{x}{R} \tag{12}$$

where U is the volumetric flow rate through the reactor,

V is the volume of the reaction vessel,

and x is the fraction of decomposition.

$$\text{Thus} \quad k = \frac{R}{[A]} = \frac{U}{V}\left(\frac{[A]^O - [A]}{[A]}\right) \tag{13}$$

In the case where a carrier gas is used to transport the diluted concentration of reactant through the reactor, then changes in the molar flow rate of the streams are insignificant. Thus the flow rate through the apparatus is only dependent on the temperature. The measured volumetric flow rate must be corrected to the reactor temperature, and this is achieved by multiplying by the ratio $T_{reactor}/T_{flowmeter}$.

2.3.1 Description and Procedure

The flow system apparatus is presented diagrammatically in Figure 2.2, and shown in Plate 3. It was constructed by incorporating the general techniques of Herndon [56] and the stirred-flow reactor design of Mulcahy and Williams [57]. A similar system [58] was used for gas kinetic studies at University College, London, and was found to yield rate constants in good agreement with those obtained by both static and flow methods.

The nitrogen carrier gas with reactant vapour was injected radially into a spherical Vycor reaction vessel from a small perforated sphere at the centre. The reaction volume within the furnace was measured to be 179.3 mls. Housed in a well of the vessel, a chromel/alumel theromcouple, calibrated against a platinum/platinum - 13 rhodium thermocouple, was used to measure the reaction temperature, being considered accurate to within $\pm$ 0.5K. Before installing the reaction vessel, experiments were carried out to obtain the mixing requirements within the vessel by diffusion and forced convection. The diffusion mechanism was checked by passing nitrogen through the reactor and then introducing nitrogen dioxide; a minimum flow rate for mixing by diffusion was determined. Forced convection was observed by adding dyestuff to water flowing through the vessel. On the basis of dynamic similarity (or equivalence of Reynolds' numbers) the temperature dependence of the mixing modes was examined, and a minimum flow rate of $\sim$ 20 mls/sec through the reactor was found to satisfy good mixing criteria up to 700°C, while 25 mls/sec was required for 700-850°C. The surface to volume ratio of 0.9 for this reactor vessel was able to be raised by the addition of lengths of silica tubing, 10 mm by 2 mm i.d. (0.6 mm wall thickness). The addition of 170 such lengths resulted in a reaction volume of 171.0 mls with a threefold increase in the surface to volume ratio.
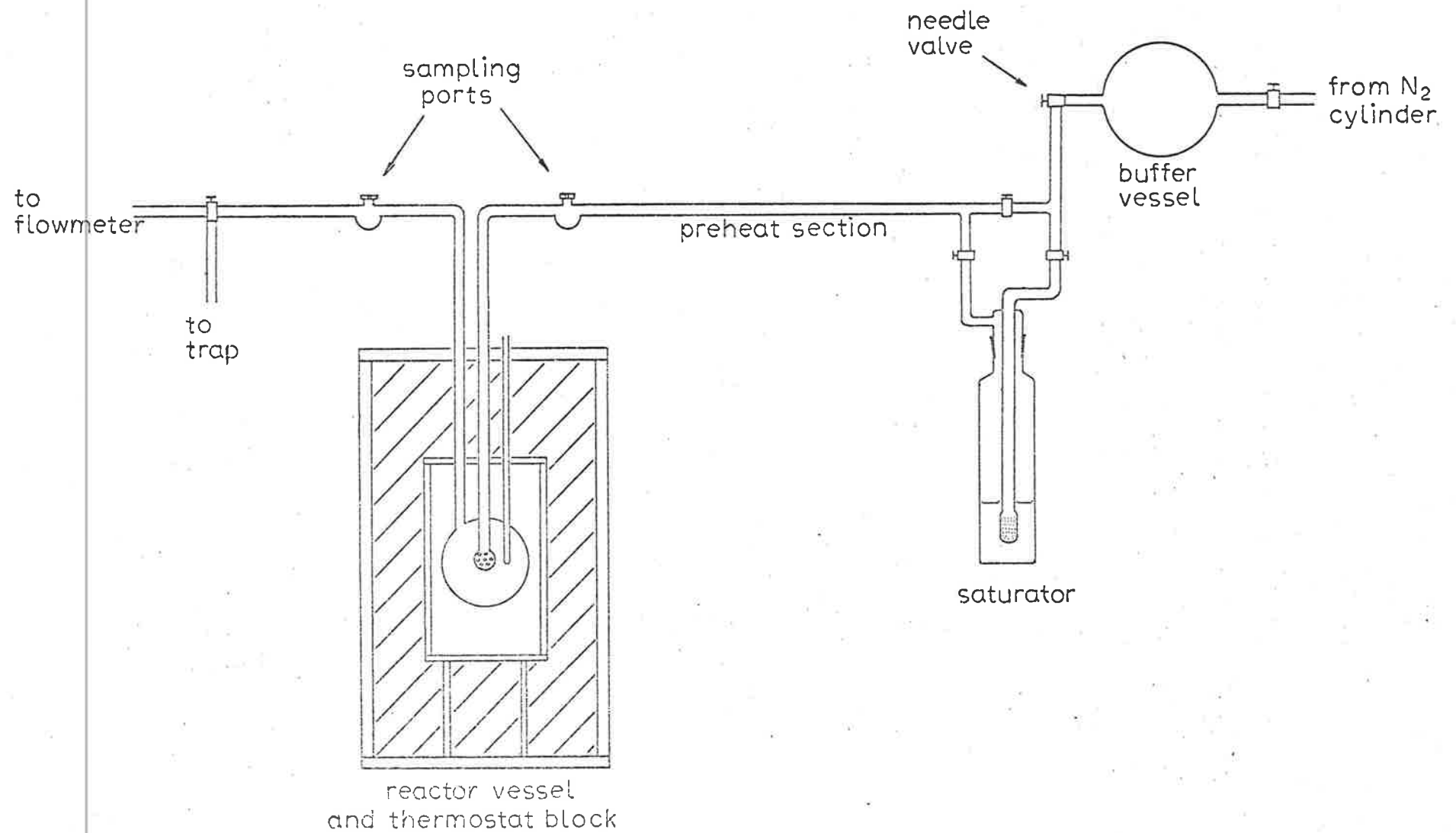
Figure 2.2   The stirred-flow reactor system.

48.

PLATE 3   View of stirred-flow reactor system
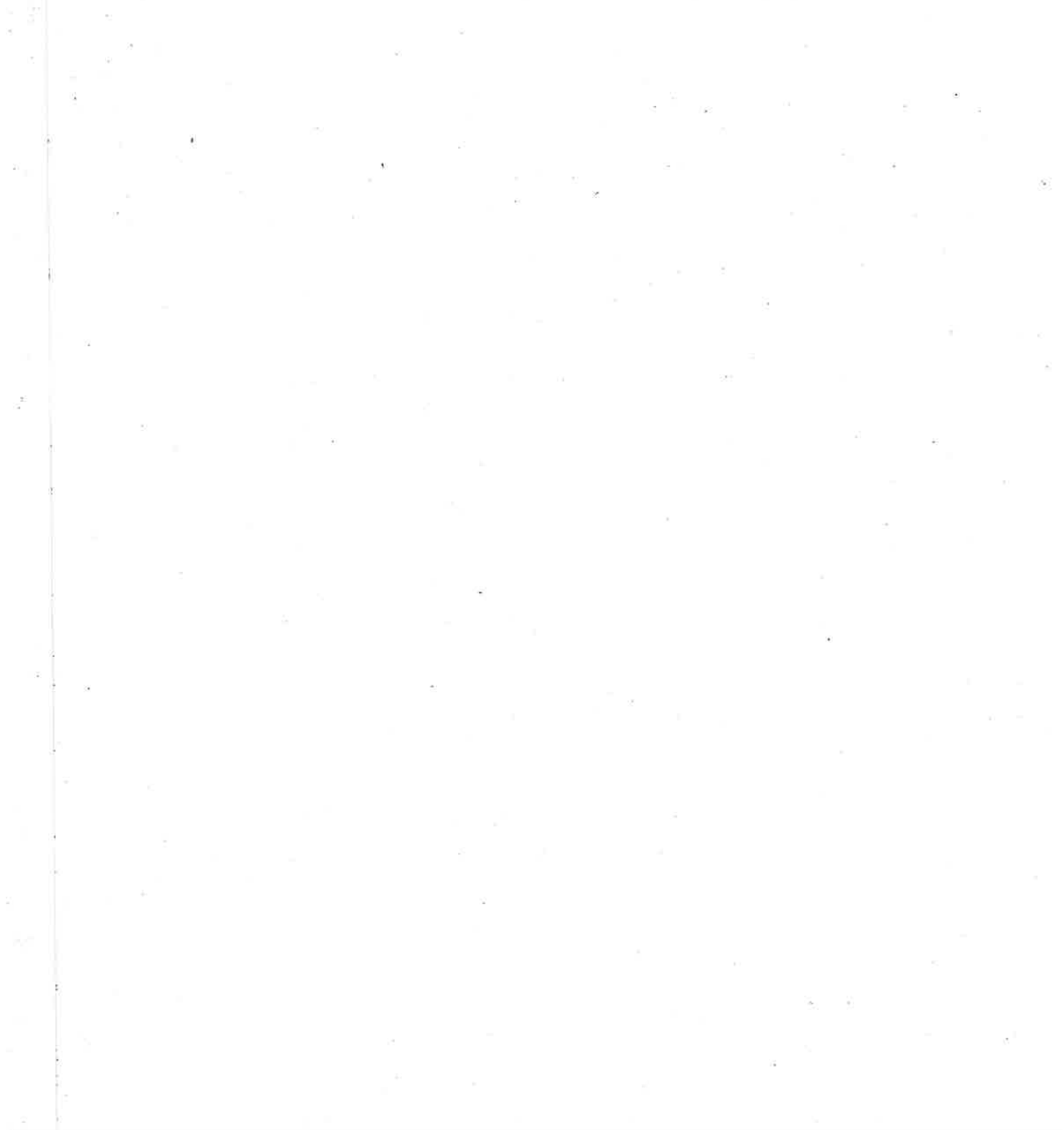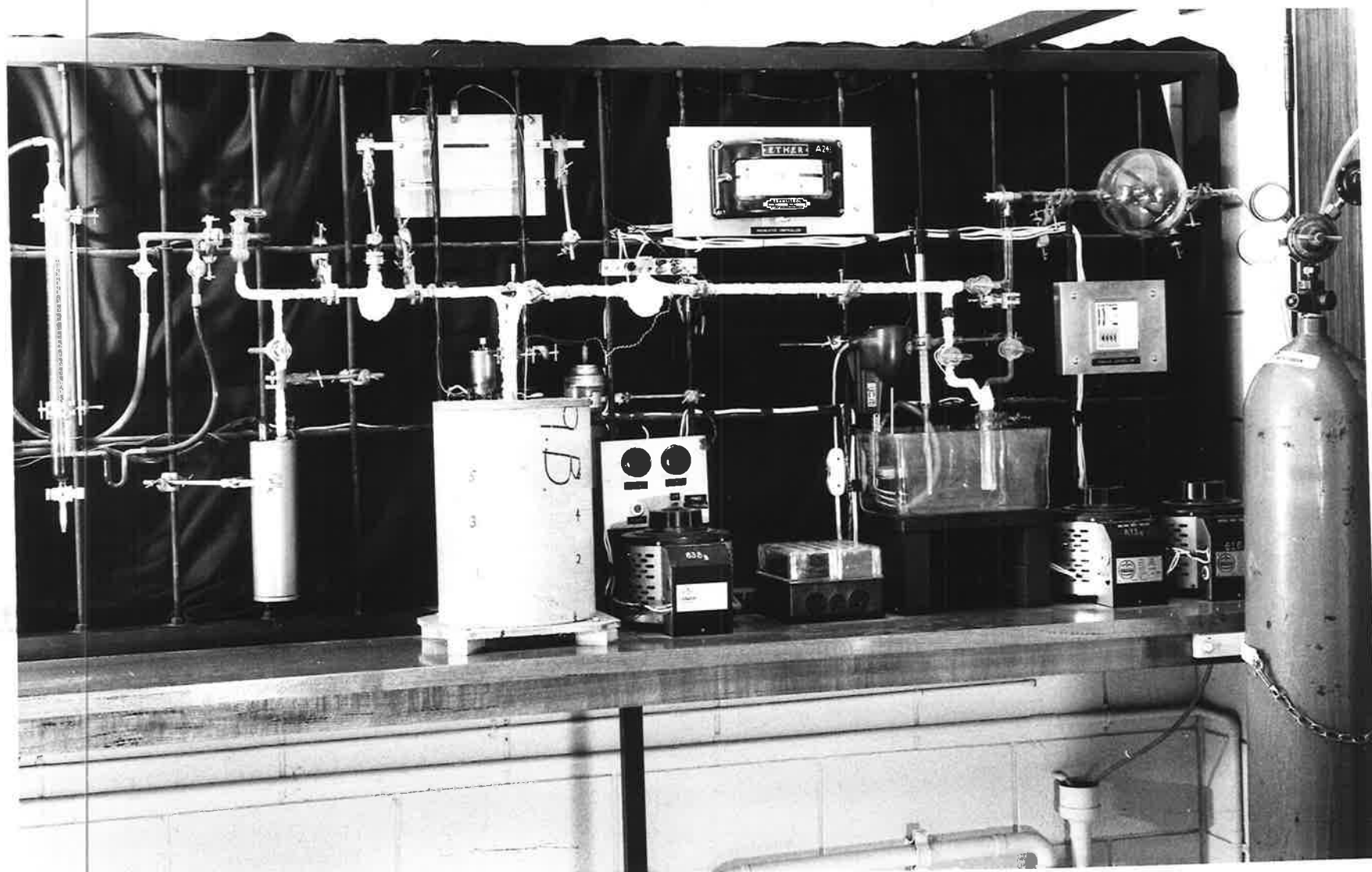
The reaction vessel was located within a vertical electric furnace 230 mm long by 90 mm internal diameter (6 mm thickness), made of 321 stainless steel, which was wound with 80/20 nichrome resistance wire. The wiring had three sections whose heat input were adjusted by varying the resistances that shunted the wiring, to give a uniform temperature gradient along the furnace. Six chromel/alumel thermocouples were located in the walls of the furnace, to check on the temperature uniformity and one was used for control by a Eurotherm controller, type 017. The temperatures of the six thermocouples varied by no more than ± 2 K at 973 K, and the variation within the vessel would be much less. The furnace was housed with a 340 mm long by 255 mm diameter asbestos pipe with vermiculite being used as the insulation medium.

Nitrogen (C.I.G., high purity dry) was regulated by valves and a two litre buffer vessel followed by an Edwards OS1D needle valve, which controlled the flow rate through the system. The carrier gas stream could then be bubbled through liquid reactant in a saturator, which used a sintered glass distributor to obtain a large gas-reactant surface contact. The saturator (or vaporiser) was warmed by placing it in a water bath, controlled by an on-off detector, to enable the vapour pressure of the reactant to be raised if necessary. The reactant-saturated nitrogen was then passed through a 1145 mm by 10 mm diameter length Pyrex preheater which could raise the temperature of the gas to approximately $300^{\circ}C$ before entering the furnace. A sampler consisting of a B14 joint with septum cap holder was located immediately before the reactor. From the reactor, the effluent gas stream passed through another sampling part (the exit line being warmed to about $80^{\circ}C$ to prevent condensation) and then to either trapping, soap-bubble flow-meter or exit. Product analysis of the inlet and effluent streams was by gas chromatography.

2.3.2 Product Analysis

Analysis samples of between 100 to 500µℓ were taken from the sampling ports, and injected into a dual column Shimadzu Gas Chromatograph GC-4A PTF. The chromatograph had provision for programming the column temperature, and detection was by means of thermal conductivity or hydrogen flame ionization.

Nitrogen was used as the column carrier gas with a flow rate of normally 60 mls/min. The peaks were recorded by a Shimadzu R-101 X-T recorder, which as a Disc integrator attached.

A number of different column packings were prepared by the slurry method to coat a solid support of Gas-Chrom Z of size 60-80 mesh. Moderately polar column packings of 10% w/w diethylene glycol adiapate and 10% w/w dinonyl phthalate were prepared, as well as non-polar packings of 10% w/w squalane and 10% w/w apiezon L (all from Allied Science). Stainless-steel columns of 3 metres by 3 mm internal diameter were individually packed and conditioned. A Porapak Q + R column * was also available for checking the formation of low boilers.

---

* The author is grateful to Mr. I.S. Crawford for the loan of this column.

2.4 Batch Reactor System

Batch (or static) reactor systems are widely used for kinetic studies of gaseous reactions. This is because a known concentration of reactant can be placed within the isothermal volume and the change in its concentration with time can be followed accurately. The batch reactor has a much larger temperature range than some flow systems, in that the residence time within the reactor can be extended from minutes to hours.

2.4.1 Description

The apparatus is presented diagrammatically in Figure 2.3 and shown in Plate 4. The techniques of Maccoll [59] and Swinbourne [60] were incorporated in the construction of the system.

Reactions were carried out in a Vycor reactor vessel of 391 mls capacity, and surface-to-volume ratio of 0.94 cm^{-1}, housed within an aluminium alloy thermostat. The reactor was connected to a high-vacuum system, and could also be connected to a Celesco P7D differential pressure transducer head with a resultant dead-space of 6.7 mls. A chromel/alumel thermocouple, calibrated against a platinum/platinum-13 rhodium thermocouple, was inserted in the thermowell of the vessel, and this was used to measure the reactor temperature. The thermocouple was considered accurate to within ± 0.5 K. An extended surface reactor made from Pyrex, with similar dimensions to the Vycor vessel but packed with thin Pyrex tubes was also constructed. It has a reactor volume of 277 mls, and a surface-to-volume ratio of approximately 13.5 cm^{-1}. The thermostat was constructed of an aluminium alloy A2011 in the form of a cylinder 115 mm diameter by 305 mm length, with a cylindrical recess of 80 mm diameter by 275 mm depth to accomodate the reactor vessel. A cap of similar material fitted on top.

to
pirani
guage

to
vacuum
pumps

transducer
head

manometers

gas manifold

storage
vessels

reactor vessel
and thermostat block
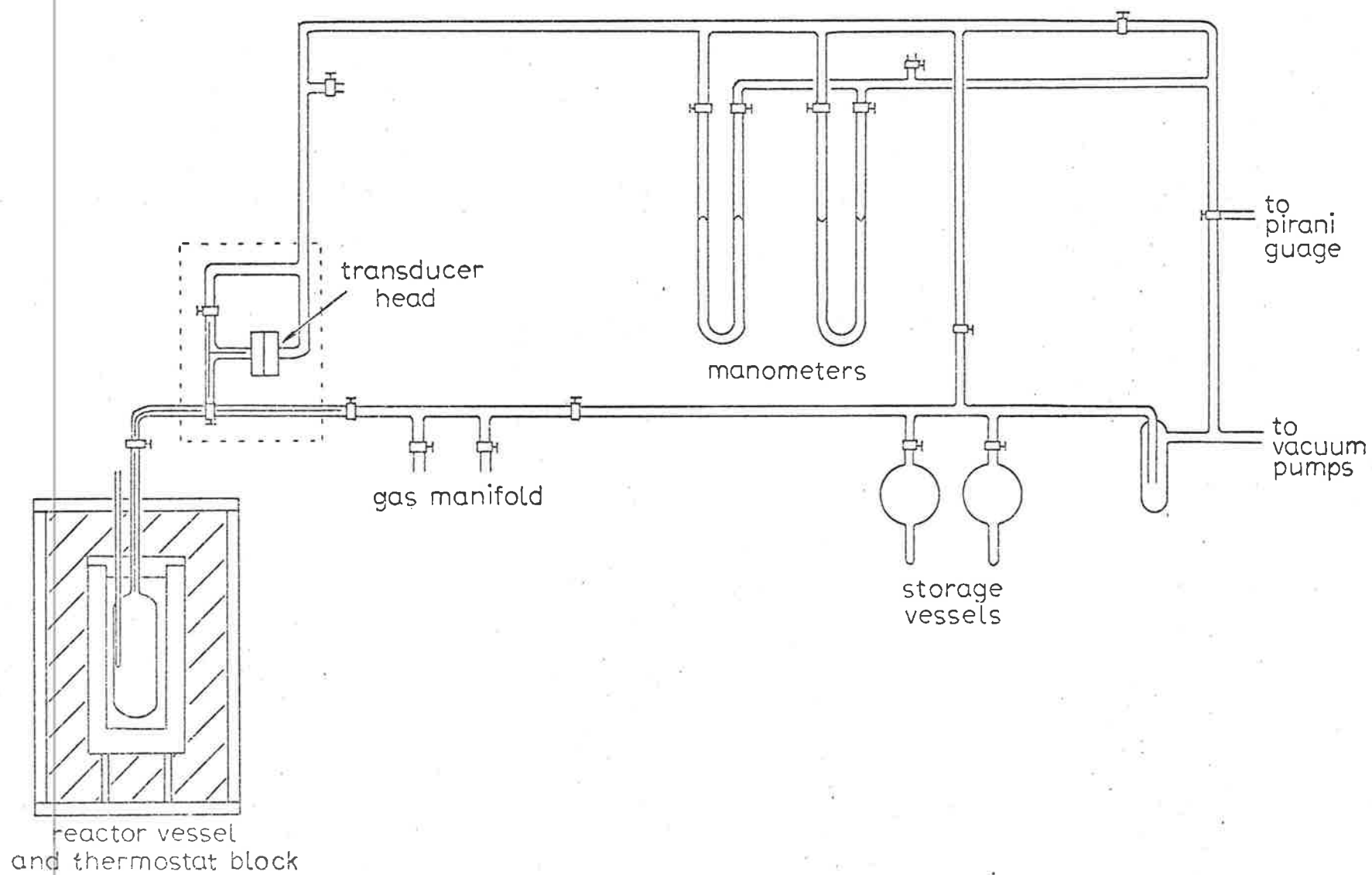
Figure 2.3   The batch reactor system and vacuum line.

53.

PLATE 4.   View of batch reactor system.
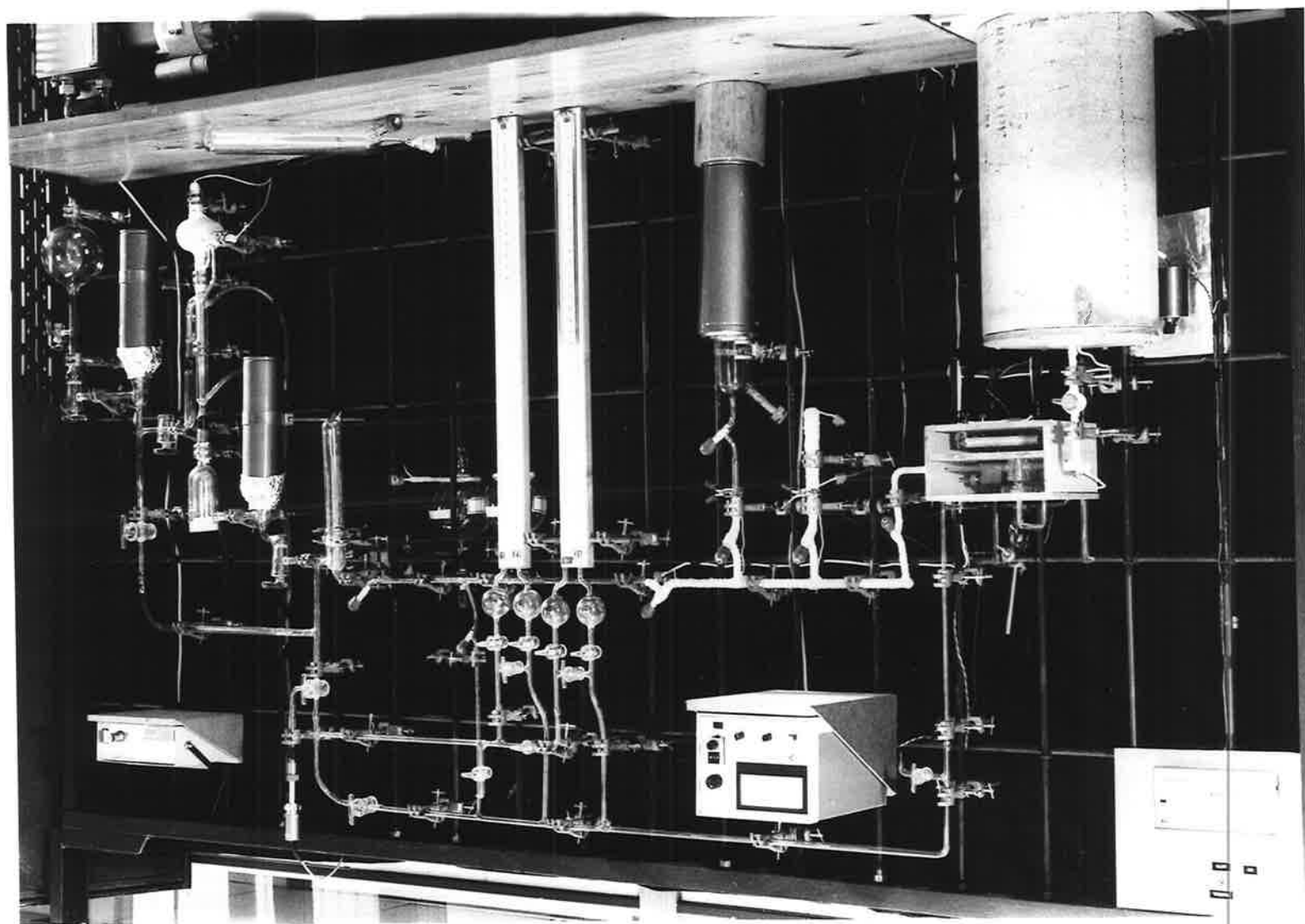
Heating was provided by means of 80/20 nichrome resistance wire wound around the outside of the thermostat block. To ensure uniform control of the temperature along the thermostat, three windings were used, with the top and bottom windings wound more closely spaced at the ends to reduce the effects of end heat loss. The resistance wires were wound onto asbestos paper and covered with alumdum cement, and are connected to the main via a variable transformer. The thermostat has six chromel/alumel thermocouples located along its length to check the uniformity of the temperature. They can each be connected via a switch to a Eurotherm indicator controller, type 070, which is connected in line with the load around the thermostat. A temperature distribution study about the thermostat and within the reaction vessel over the range 200-350°C showed it to be uniform with a gradient of less than 0.5°C.

The vacuum system backing the reaction vessel contains a manifold for the addition and removal of materials, two manometers (mercury and di-n-butyl phthalate) and large storage bulbs. The apparatus could be evacuated to about 2×10^{-4} torr by means of a two-stage mercury diffusion pump backed by a twin single-stage rotary oil pump. A Sadla-Vac pirani gauge was used to monitor the pressure. All vacuum lines of the apparatus that are used for handling condensible materials were wound with resistance wire, and the transducer head was located within a "hot box". These vacuum lines and the hot box were normally maintained at about 80°C.

2.4.2 Experimental Procedure

To carry out a kinetic run, the reactor system was completely evacuated, and the transducer zeroed. Air was admitted to one side of the diaphagm to a pressure approximately equal to that anticipated as the initial pressure of the reactant in the reactor vessel. The degassed compound was then distilled quickly into the reactor until the transducer reading was zeroed,

and then a stopwatch was started. The pyrolysis could be followed by
monitoring the pressure change with time, if a molar change is involved.
At the end of a run, the reaction mixture was trapped with liquid nitrogen
in a large sample collection vessel of approximately 1200 mls. These
vessels had a septum cap holder incorporated in their design. After
bringing the contents of the vessel to atmospheric pressure, by bleeding
in high-purity nitrogen via a rubber bladder, samples of the reaction
mixture were injected into the gas chromatograph for analysis. The product
analysis by gas chromatography has been described in section 2.3.2.

CHAPTER 3.

RESULTS

In this chapter, each compound investigated during the research program is dealt with in turn. Each section on a particular cyanide describes the techniques used, the results of the experimental runs, and the derivation of kinetic parameters. The experimental data and calibration plots used to calculate the percentages of decomposition and rate constants summarized in this chapter, are collated in the Appendix. Discussion of these results is contained in Chapter 4. However, certain parameters derived in this chapter for some of the cyanides studied in the early stages of the research program were used to anticipate modes of decomposition and their kinetic parameters for the later studied compounds. Mention is made in the chapter when such an estimation was used.

3.1   Cyclobutyl Cyanide

It was decided to use the VLPP technique to obtain more accurate data for the decomposition of cyclobutyl cyanide, in order to clarify the two differing sets of data reported by Sarner and coworkers [35]. Although Arrhenius expressions were not reported, a least-squares treatment of their results gives

$$\log (k, sec^{-1}) = (15.4\pm0.2) - (56.6\pm0.7)/\Theta \qquad and$$

$$\log (k, sec^{-1}) = (15.0\pm0.3) - (56.6\pm0.9)/\Theta$$

for the first and second sets of data respectively. For the two sets combined

$$\log (k, sec^{-1}) = (15.3\pm1.2) - (56.7\pm4.1)/\Theta$$

this being the equation quoted by Sarner and coworkers without error limits.

Ethylene and vinyl cyanide (VCN) were found to be the only products. The reaction was followed quantitatively by monitoring the disappearance of cyclobutyl cyanide (c-BuCN) at the mass spectral peak $m/e = 54$ amu, and the formation of vinyl cyanide at peak $m/e = 53$ amu. Argon ($m/e=40$ amu) was used as an internal standard. By preparing known mixtures of vinyl cyanide and cyclobutyl cyanide on the vacuum line, and allowing this to effuse into the ionization chamber, the mass spectral peak sensitivities were calibrated. Five mixtures were prepared and it was found from a linear regression program that

$$[VCN]/[c\text{-}BuCN] = (I_{53}/I_{54} - 0.1007)/0.4911$$

This relationship was then included in a computer program[*] written to calculate the unimolecular rate constants from the temperature of the reactor, the aperture size, and the peak intensities of argon, vinyl cyanide and cyclobutyl cyanide.

---

[*] Refer to Appendix A.3, page 210.

TABLE 3.1   VLPP RESULTS FOR CYCLOBUTYL CYANIDE

(Z = 19,550, flow rate = 5.6 x 10^{14} molecules/sec)

		% decomposition		
Run[a]	Temp K	c-BuCN decay	VCN formation	k_{uni}[b] sec^{-1}
CB 81	832.8	12.0	9.4	0.084
82	844.2	16.4	13.0	0.123
83	854.2	20.1	17.3	0.159
84	863.7	23.9	22.0	0.199
92	863.7	25.3	22.9	0.21
85	873.3	30.1	27.7	0.27
87	882.7	35.8	33.2	0.36
88	893.0	42.8	39.9	0.48
93	902.8	51.1	47.4	0.68
89	904.1	48.5	46.1	0.61
94	912.9	57.9	54.3	0.90
95	932.3	63.3	59.5	1.13
96	933.2	68.0	65.3	1.40
97	941.5	71.8	69.1	1.68
98	953.3	76.9	74.5	2.22
99	964.2	80.7	78.5	2.79
100	972.9	83.5	81.4	3.41
101	983.8	86.4	84.5	4.30

[a] Flow rate = 3 x 10^{15} molecules/sec for Runs CB 81-89.

[b] Cyclobutyl cyanide disappearance.

TABLE 3.2 VLPP Results for Cyclobutyl Cyanide
(Z = 2,140, Flow rate = 8-9 x 10^{14} molecules/sec)

| Run [a] | Temp K | % decomposition | | k_{uni} sec^{-1} [b] |
		c-BuCN decay	VCN formation	
CB 45	902.8	9.9	10.4	0.66
31A	922.9	17.5	18.1	1.28
46	923.6	16.8	17.3	1.22
32	933.1	19.8	19.1	1.50
47	942.1	23.1	25.3	1.83
33	952.6	28.9	27.1	2.49
48	962.9	32.9	35.5	3.02
34	970.6	41.4	40.2	4.4
54	972.3	40.1	39.4	4.2
103A	982.4	54.3	50.2	7.4
55	984.0	45.8	45.3	5.3
104	991.9	56.6	52.0	8.2
35	993.6	53.8	51.3	7.3
56	1002.5	56.2	54.8	8.1
105	1003.5	62.4	57.9	10.5
36	1012.6	62.3	60.3	10.5
106	1014.1	67.1	62.4	12.9
57	1024.5	67.9	64.7	13.5
37	1032.6	71.2	68.7	15.8
107	1037.5	75.1	71.6	19.3
58	1043.5	75.4	72.0	19.6
38	1053.0	77.8	75.6	22.6
108	1059.0	80.6	77.8	26.9
39	1073.1	83.2	81.4	32.3
40	1093.2	87.2	85.7	44.8

[a] Flow rate = 3.3 x 10^{14} molecules/sec for Runs CB 54-58,
and 4.7 x 10^{14} molecules/sec for Runs CB103A-108

[b] Cyclobutyl cyanide disappearance.

TABLE 3.3 VLPP Results for Cyclobutyl Cyanide
(Z = 246, flow rate = 1.2×10^{15} molecules/sec)

| Run [a] | Temp K | % decomposition | | k_{uni} sec^{-1} [b] |
		c-BuCN decay	VCN formation	
CB 8	962.4	10.4	9.9	5.2
9	982.7	13.9	13.9	7.3
10	1002.0	18.0	20.1	10.0
11	1021.9	28.2	26.4	18.0
12	1042.7	34.4	34.3	24.2
13	1063.0	42.7	41.3	34.9
14	1081.4	48.9	48.7	45.1
17	1081.4	49.8	48.9	46.8
18	1103.4	56.7	57.0	62.4
19	1121.9	62.7	63.0	80.8
20	1143.1	69.9	69.9	113
21	1163.4	75.3	75.0	149
22	1183.9	79.8	79.6	195
23	1202.9	83.1	83.1	244

[a]
Flow rate = 5.7×10^{14} molecules/sec for Runs CB 8-14

[b]
Cyclobutyl cyanide disappearance.

The results of the pyrolysis of cyclobutyl cyanide are summarised in Tables 3.1 to 3.3. Percentage of decomposition calculated from reactant disappearance or product formation agreed to better than 5% in most cases. The rate constants were found to be independent of the aperture size and the reactant flow rates, which is indicative of a unimolecular first-order irreversible process [47].

Unimolecular rate constants are a function of the collision frequency ω, and will be in the fall-off region under VLPP conditions. The Rice, Ramsperger, Kassel (RRK) and Marcus (RRKM) unimolecular reaction rate theories provide a means for converting k_{uni} to k_∞ (and vice versa), and thereby obtain the Arrhenius high pressure parameters A_∞ and E_∞. Other studies of low pressure effects are carried out by measuring the apparent first-order rate constant at a fixed temperature but successively lower pressures. In the VLPP technique, the frequency of wall collisions is fixed by the dimensions of the vessel, and the rate constants are investigated over a range of temperatures.

Accordingly, if one of the high pressure parameters is known, then the value of the other may be determined from a fit of k_{uni} versus T to a computed curve. In general, A-factors for unimolecular processes can be estimated with considerable accuracy if the process is unambiguous [30, 31, 45], thus allowing E_∞ to be determined from the fit. This is normally the procedure adopted in VLPP studies.

The RRKM calculations were carried out with the assistance of a computer program.*

As outlined in Chapter 1, section 1.3.3, the essential requirement for applying the RRKM formulations is the assignment of the internal vibrational and rotational modes for the reacting molecule and transition-state complex. In addition the moments of inertia products of the species

---

* The computer program was supplied originally by Professor B.S. Rabinovitch of the University of Washington. It has been modified and adapted to the University of Adelaide's CDC 6400 computer by Dr K.D. King. The program and its listing did not form part of this research program, and is only outlined above. Details of similar programs are available on request from various reliable sources (see Appendix 3, reference [17]).

are required. By adjusting some of the low frequency vibration
assignments, while still maintaining a reasonable physical picture of the
molecule, the value of A_∞ can be altered to give the experimental value,
or if this is unavailable or unreliable to the value predicted from
theoretical considerations. The Arrhenius parameters and not the exact
details of the transition-state model are important in determining the
degree of fall-off [17].

Substituent groups that are attached to the tetramethylene biradical
can cause resonance to be set up with the unpaired electrons, stabilizing
the biradical and lowering the A-factor and activation energy relative to
the values for the pyrolysis of cyclobutane. This occurs when the
substituent group contains π-bond electrons, such as in the case of
isopropenylcyclobutane, where we have

The A-factor is found to be lower than that for cyclobutane by about
a power of ten, due to the loss of the hindered rotation of the vinyl
group in the stiffened resonance stabilized biradical [61]. A biradical
mechanism has been assumed for cyclobutyl cyanide pyrolysis. Because of
the cylindrical symmetry of the $C \equiv N$ triple bond there are no such rotational
constraints in the biradical, but resonance stabilization should cause
changes in the low frequency $C - C - (CN)$ and $C - C \equiv N$ bends. Benson [45],
in his book "Thermochemical Kinetics", has outlined methods for the
estimation of rate parameters, and if these are applied to the determination
of the transition-state frequencies for the above bends, then it is found

that the cyano group lowers the cyclobutane A-factor by ca. $10^{0.6} sec^{-1}$ overall or $10^{0.3} sec^{-1}$ per reaction path. Luckraft and Robinson [34] found the cyano group lowered the cyclopropane A-factor by $10^{0.4} sec^{-1}$ per path in the case of cyclopropyl cyanide. Thus from the observed A-factor of $10^{15.6} sec^{-1}$ [61] for cyclobutane, resonance considerations favour the lower A-factor ($10^{15.0} sec^{-1}$) found by Sarner and coworkers.

Although a complete vibrational assignment for cyclobutyl cyanide has not been reported in the literature, Blackwell and coworkers [62] have determined the ring puckering vibration and the $C - C \equiv N$ bends. On the basis of the frequency assignments for cyclobutane [63] and isopropyl cyanide [64], the other frequencies for the cyclobutyl cyanide molecule were estimated. The frequencies are listed with the molecular parameters used for the RRKM calculations in Table 3.4, and are averaged and rounded. The moments of inertia were calculated using the bond lengths and angles given by Durig, Carriera and Lafferty [65], and the collision diameter was assumed to be approximated by that for n-propyl cyanide (5.5 Å, [66]). From the group additivity tables [42] the molecular entropy was predicted to be $S^0_{300} = 77.9$ cal $K^{-1} mole^{-1}$, and the entropy calculated from the above parameters was made to agree with this value by slightly adjusting some of the low-valued frequencies. Based upon the following transition-state structure
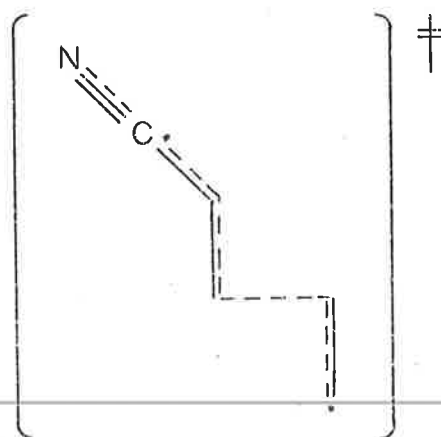
the changes in molecular frequencies were estimated by the methods of Benson [45], and by analogy with the transition-state complexes of

TABLE 3.4 Molecular Parameters for Cyclobutyl Cyanide Pyrolysis

	Molecule	Complex	
Frequencies (cm^{-1}) and degeneracies	2900 (7)	2900 (7)	
	2250 (1)	2250 (1)	
	1450 (3)	1450 (3)	
	1300 (5)	1300 (5)	
	1150 (3)	1150 (3)	
	940 (3)	1000 (2)	
	700 (5)	950 (1)	
	600 (1)	830 (1)	
	425 (1)	700 (3)	
	300 (1)	400 (1)	
	230 (1)	200 (3)	139 (3)[b]
	175 (1)	170 (1)	105 (1)
	120 (1)	90 (2)	70 (2)
$I_A \cdot I_B \cdot I_C$, $(g\ cm^2)^3 \times 10^{113}$	1.27	4.37	
Sigma[a]	1.0	1.0	
Collision diameter, Å	5.5		
S^0_{300} , cal K^{-1} mol^{-1}	77.9	85.3	89.3

[a]
    Sigma = σ/n , where σ is the symmetry number for external
                rotation, and n is the number of optical isomers.

[b]
    Denotes alterations made to give $A_\infty = 10^{15.9}\ sec^{-1}$ (see text).

cyclobutane [49] and isopropenylcyclobutane [61]. The breaking C — C

bond in the biradical was lengthened by 1Å in accordance with the procedure

of Rabinovitch and coworkers [69].

The molecular parameters shown in Table 3.4 were used in the RRKM

calculations, and yields an A-factor of $10^{15.0}$ sec^{-1} at 700 K. The RRKM

computed curve is found to fit the experimentally obtained unimolecular

rate constants when E_∞(700 K) = 57.0 kcal/mole, as shown in Figure 3.1.

The spread in experimental data was small and an error limit of $\pm$ 1 kcal/mole

was found to cover the scatter, thereby giving the Arrhenius equation for

the pyrolysis of cyclobutyl cyanide as

$$\log k_\infty \ (700 \ K) \ = \ 15.0 \ - \ (57.0 \ \pm \ 1.0) \ / \ \theta$$

(The parameters have been quoted for 700 K in order to obtain a comparison

with the high-pressure data for cyclobutyl cyanide and cyclobutane).

The above A-factor was derived from resonance considerations which were

found to lower the analogous cyclobutane A-factor by $10^{0.6}$ sec^{-1}.

However, a VLPP of cyclobutane [49] has reported Arrhenius parameters of

$A_\infty = 10^{16.5}$ sec^{-1} and $E_\infty = 65.5$ kcal/mole. Maintaining the difference

between the two compounds at $10^{0.3}$ sec^{-1} per reaction path implies an

A-factor of $10^{15.9}$ sec^{-1} for cyclobutyl cyanide pyrolysis. After suitable

alterations were made to the low-valued frequencies of the complex (see

Table 3.4) to give this value, an RRKM calculation yields $E_\infty = 59.1$ kcal/

mole. This has been included on Figure 3.1.

Extending this per reaction path difference to trans - 1,2 -

dicyanocyclobutane, then an A-factor for the dicyanide of $10^{1.2}$ sec^{-1}

lower than that for cyclobutane was predicted.
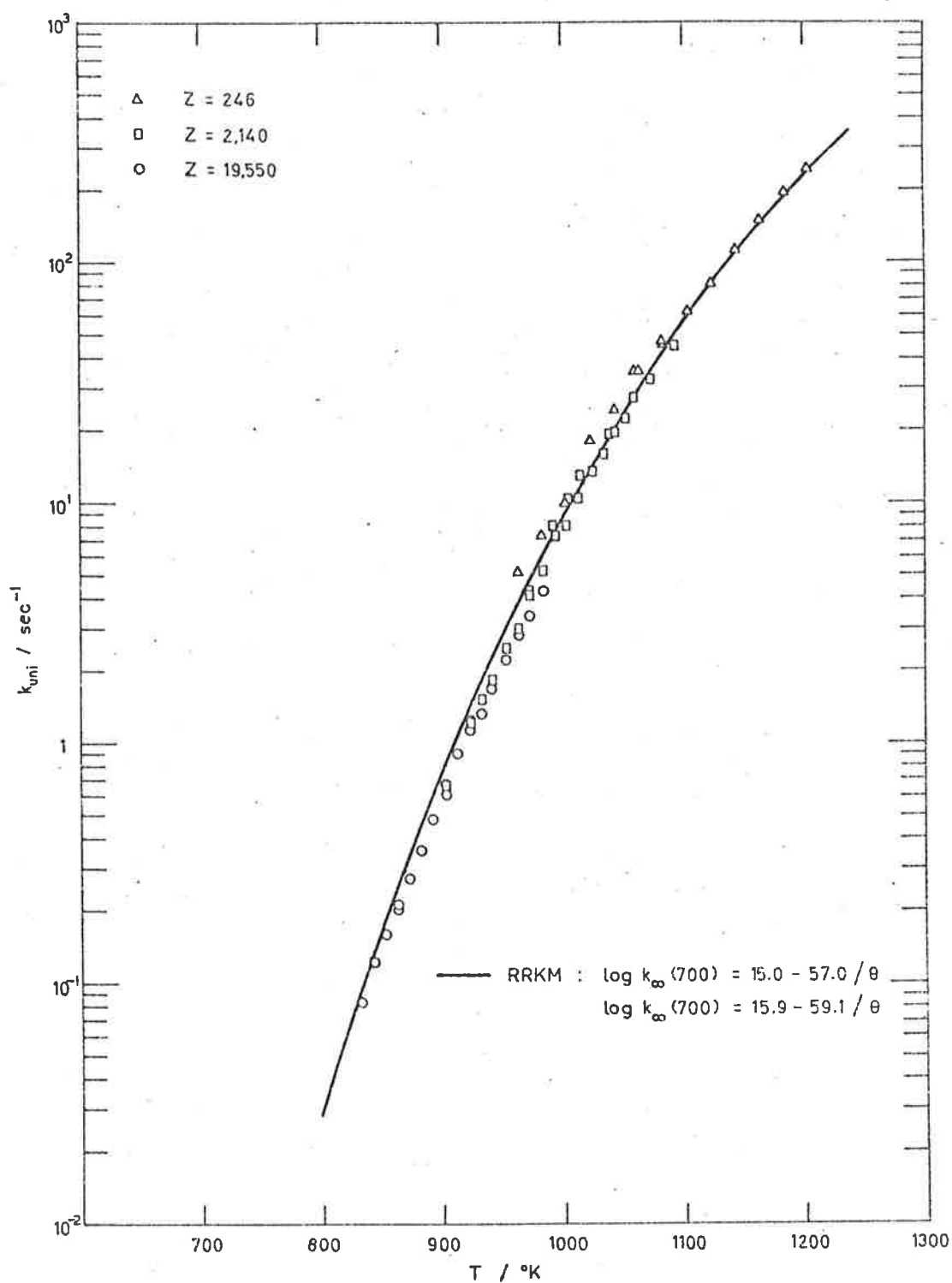
Figure 3.1 k_{uni} as a function of T for the decomposition
of cyclobutyl cyanide.

3.2 trans - 1,2 - Dicyanocyclobutane

Trans - 1,2-dicyanocyclobutane was expected to decompose via a biradical mechanism producing two molecules of vinyl cyanide

The compound was separated from a mixture of the isomers, and purified as outlined in Chapter 2. Its purity was checked by gas chromatography (GLC) and the isomer was found to contain no impurities. Its vapour pressure was low (less than reported by Hall and Baldt [43]) and this was a major obstacle to overcome when transferring gaseous samples to and from the reactor. Since the chromatograph used for product analysis was not on-line, care had to be exercised when transferring a sample from the reactor to the column to ensure that no reactant material condensed on the surfaces of the sampling vessels or syringe.

Initial experiments were carried out within the batch reactor, described in Chapter 2. Whilst maintaining the vacuum lines and hot box at 90°C to avoid condensation, the trans isomer was distilled quickly into the reactor vessel. The pressure obtained within the reactor was only ca.0.5 torr and following the reaction by pressure measurements proved fruitless. On transferring the reaction mixture to a sampling vessel and pressurising to atmospheric with nitrogen, gas chromatography revealed that most of the reactant was condensing on the walls of the vessel. Although the vessel was kept heated, there was no assurity that the syringe sample was a correct measure. In addition, RRK calculations showed that at 0.5 torr the reaction was in the fall-off region[*]. To avoid this problem and to assist in overcoming the condensation problem when sampling, the reaction was

carried out in the presence of an added gas which doubled as a solvent for the reactant and product when sampled. Benzene was selected since its chromatographic peak did not interfere with those of the reaction mixture. Immediately after adding the reactant, benzene vapour was added to a pressure of approximately 25 torr[*] in the reactor. At the completion of a run, the reaction mixture was trapped into an additional 0.2 mls of benzene. The complete mixture was then vaporised and pressurised to atmospheric with nitrogen. Chromatographic analysis proved to be more successful by this method.

The gas chromatograph flame ionization detector (FID) was calibrated for the relative sensitivities of the dicyanide and vinyl cyanide (VCN) by preparing known liquid mixtures of the two. The samples were injected on to an apiezon L column and the resultant calibration plot is shown in the Appendix. A regression treatment gives

peak area ratio, $trans\text{-}1,2\text{-}C_4H_6(CN)_2/VCN$

$$= 1.33 \quad \frac{[trans\text{-}1,2\text{-}C_4H_6(CN)_2]}{[VCN]}$$

In a few experiments with the batch reactor system, the decomposition was analysed at three reaction temperatures over times of 15 to 60 minutes. The results had some scatter attached to them, and the potential error of condensation was still of an uncertain nature. At temperatures of 573, 600 and 623 K the average rate constants obtained were $2.5 \times 10^{-5} \, sec^{-1}$, $1.2 \times 10^{-3} \, sec^{-1}$ and $5 \times 10^{-3} \, sec^{-1}$ respectively. These values are less than those of Sarner and coworkers [35], and seemed to be closer to the kinetic

---

* Using $k \sim 10^{15.0-51/\theta}$ (estimated from trans-1,2-dimethyl-cyclobutane [61], with E corrected for stabilization by the cyano group [34,37,48, see discussion]) and the tables of the Kassel integral [67]: at 600K, S = 19.5, B = 42.8 and D = 8.3. 6.6 and 6.3 at pressures of 0.5, 25 and 50 torr respectively, giving k_{uni}/k_{∞} = 0.80, 0.98 and 0.99 for these pressures.

parameters expected from the study of cyclobutyl cyanide.

It was decided that due to its direct sampling facilities, the stirred-flow system would be more suitable to follow the decomposition. To ensure a measurable flow of reactant the saturator water bath was maintained at 70°C, and the GLC syringe was kept warmed to minimize condensation when sampling. The temperatures, flow rates and peak areas obtained from the experimental runs are tabulated in the Appendix, and the results are summarized in Table 3.5. The reproducibility of the rate constants obtained is good suggesting that the problem of reactant condensation had been minimized.

The reaction was followed over the temperature range of 571-699 K with residence times of 5.1 to 12.8 seconds. At temperatures above 665 K the rate constants showed an upward trend away from the values predicted by the results at lower temperatures, but showed no discernable correlation with reactant flow rate. The possibility of an alternative pathway for decomposition, namely the fission of the adjacent carbon-carbon bond as well as of the bond between the cyano groups was considered. However, examination of the chromatograph records showed no peaks which could be attributed to ethylene or dicyanoethylene, and the predicted parameters[*] for this alternative reaction $(A \sim 10^{15.0}\,sec^{-1}, E \sim 57\text{-}58$ kcal/mole) show it to be too slow to be observed. The possibility of condensation seems a more likely cause. At low decompositions a small discrepancy in the reactant concentration due to condensation, will cause the error in the [VCN]/[trans-1,2-$C_4H_6(CN)_2$] ratio to be insignificant but at higher conversions ($\sim 60\%$ or more) the error is magnified causing the ratio to be larger than the true value. Thus it was decided to restrict analysis of the rate

* Estimated from decomposition of cyclobutyl cyanide

TABLE 3.5   Stirred-flow Reactor Results for trans-1,2-Dicyanocyclobutane

Run	Temp K	Flow rate U, mls/sec	U/V sec^{-1}	k x 10^3 sec^{-1}
DI 27	570.7	14.02	0.0782	0.055
51	570.7	14.11	0.0787	0.071
28	570.8	14.02	0.0782	0.060
52	570.8	14.04	0.0783	0.067
53	570.8	13.98	0.0780	0.070
29	579.6	14.28	0.0796	0.11
30	590.8	14.20	0.0792	0.13
54	588.9	14.62	0.0815	0.24
55	589.0	14.43	0.0805	0.22
31	589.4	14.50	0.0808	0.16
33	590.3	14.41	0.0803	0.23
56	590.6	14.61	0.0815	0.22
32	590.7	14.46	0.0806	0.23
34	599.7	14.68	0.0819	0.75
37	600.3	14.75	0.0823	0.69
36	600.4	14.74	0.0822	0.54
35	600.8	14.77	0.0824	0.65
57	608.6	14.91	0.0831	0.79
38	609.1	15.06	0.0840	1.29
58	609.6	14.90	0.0831	1.09
41	609.7	26.97	0.1504	0.84
42	610.0	15.51	0.0865	1.26
40	610.3	21.30	0.1188	0.84
39	610.3	14.99	0.0836	1.27
59	610.9	15.01	0.0837	1.05
6	613.8	15.09	0.0842	1.46
8	615.2	21.44	0.1196	1.66
7	615.6	15.20	0.0848	1.51
43	618.6	15.97	0.0891	2.50
44	619.6	21.79	0.1215	2.45
45	620.1	27.46	0.1532	2.89
60	627.9	15.51	0.0865	4.18

TABLE 3.5 Continued......

Run	Temp K	Flow rate U, mls/sec	U/V sec^{-1}	k x 10^3 sec^{-1}
DI 47	628.3	15.85	0.0884	5.25
48	628.9	22.11	0.1233	6.00
11	629.2	22.09	0.1232	3.83
61	629.4	15.64	0.0872	5.64
49	629.5	27.98	0.1561	6.22
10	629.7	15.59	0.0869	3.63
9	629.9	15.64	0.0872	3.60
64	630.0	14.41	0.0803	4.96
63	630.6	27.57	0.1538	3.32
62	630.9	21.94	0.1224	3.35
65	638.6	23.15	0.1291	5.69
66	639.2	16.90	0.0943	7.94
67	639.6	28.88	0.1611	6.88
12	643.6	16.00	0.0892	14.0
13	644.8	15.99	0.0892	14.5
14	645.6	22.62	0.1261	15.4
68	648.2	31.33	0.1747	9.9
69	648.9	26.32	0.1468	12.8
70	649.6	22.18	0.1237	15.4
71	649.9	17.78	0.0992	21.1
72	659.3	22.63	0.1262	40.4
17	659.7	28.88	0.1611	26.7
74	659.7	28.41	0.1584	35.0
73	659.8	15.53	0.0866	29.8
14	660.3	23.30	0.1300	32.2
15	660.5	16.34	0.0911	36.0

constants to the temperature range 571-661K, in which the decompositions are <50%. The data points are plotted in Figure 3.2. A few experiments were carried out in the extended surface flow reactor, described in Chapter 2, and the results obtained are also shown in the figure. These experiments were conducted over a similar range of flow rates, and it was found that the rate constants are unaffected by a threefold increase in the surface-to-volume ratio of the reaction vessel. Analysis of the experimental rate data obtained in this study reveal the reaction to be first-order and homogeneous with rate constants given by

$$\log k = (16.0 \pm 0.3) - (52.9 \pm 0.8)/\Theta$$

where the error limits are standard deviations.

In the pyrolysis of cyclobutyl cyanide it was estimated that the cyano group lowers the cyclobutane A-factor by $10^{0.3}$ sec^{-1} per reaction path. On this basis and considering reaction path degeneracy, then the A-factor for trans-1,2-dicyanocyclobutane is lower by $10^{1.2}$ sec^{-1} overall than that for cyclobutane. Thus an A-factor of $10^{14.4}$ sec^{-1} is estimated from the value given for cyclobutane pyrolysis [61] from the work of Walters and Coworkers, or taking the recent work on the VLPP of cyclobutane [49] as correct, then A = $10^{15.3}$ sec^{-1}. In either case, the observed A-factor of $10^{16.0}$ sec^{-1} seems high but tends to support the results of the VLPP study. This will be discussed further in Chapter 4.
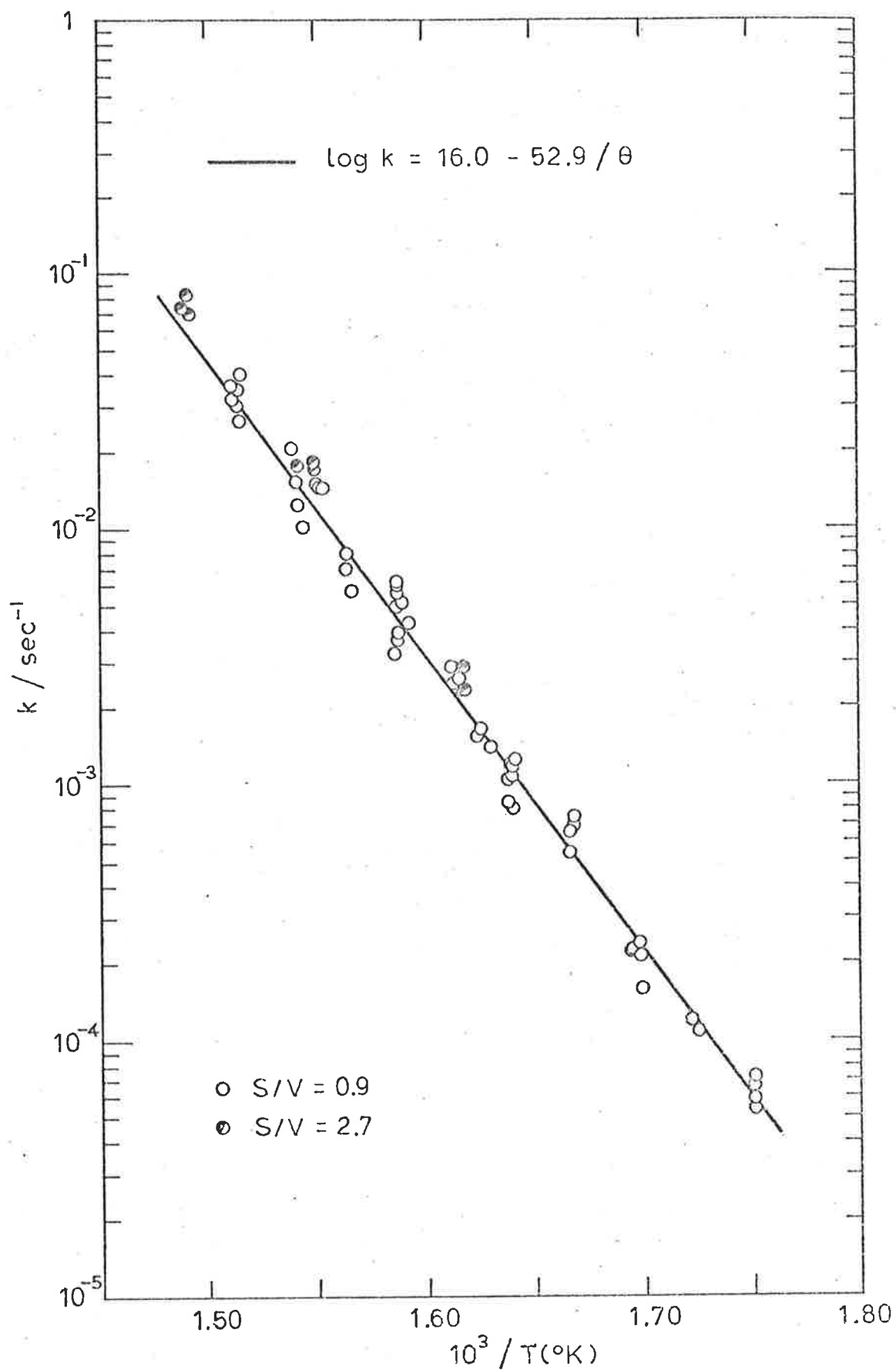
Figure 3.2   Arrhenius plot for the decomposition of
trans-1,2-dicyanocyclobutane.

3.3 Isopropyl Cyanide

From previous studies, the expected reactions for the decomposition of isopropyl cyanide are

$$CH_3CH(CN)CH_3 \rightarrow CH_3\dot{C}HCN + \dot{C}H_3 \tag{1}$$

and $$CH_3CH(CN)CH_3 \rightarrow C_3H_6 + HCN \tag{2}$$
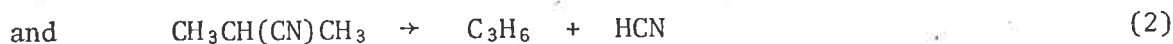
followed by decomposition of the α-cyanoethyl radical

$$CH_3\dot{C}HCN \rightarrow CH_2CHCN + H \tag{3}$$
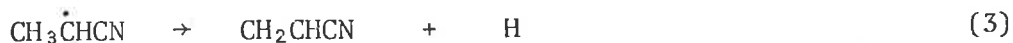
The kinetic parameters of reaction (3) should be similar to those for the analogous isopropyl radical decomposition [30], but with E corrected for stabilization by the cyano group (~ 6 kcal/mole) [34, 35, *], and A corrected for reaction path degeneracy. Thus

$$\log (k_3, sec^{-1}) \simeq 14.0 - 47.3/\theta$$

Using the tables of the Kassel integral computed by Emanuel [67], RRK calculations [†] showed that under the VLPP conditions all of the α-cyanoethyl radicals should decompose before escaping from the reactor. The product mass spectrum was consistent with these expectations.

The disappearance of isopropyl cyanide (i-PrCN) was followed by monitoring the peak at m/e=68 amu, whilst the bond fission product of vinyl cyanide (VCN) was monitored at m/e = 53 amu, and propylene as a measure of HCN elimination at m/e = 41 amu. Argon, used as an internal standard, was monitored at m/e = 20 (Ar^{++}) rather than the Ar^+ peak at m/e = 40 amu because of interference from other species. To obtain the ratio [product]/[reactant],

---

* See discussion on cyclobutyl cyanide pyrolysis [48] (Chapter 4).

[†] At 1075K, $S \simeq (C_p - 4R)/R = 12$, $B \simeq E/RT = 22.1$, and $D \simeq \log A - \log \omega = 9.8$ giving $k_{uni} = 25$ sec^{-1} which is larger than the escape rate constant, k_{ea} (1.1 mm) = 0.77 sec^{-1}; at 1250K, $S = 12$, $B = 19.0$ and $D = 9.8$ giving $k_{uni} = 189$ sec^{-1} compared to k_{ea} (3.3 mm) = 6.9 sec^{-1}.

the VLPP system was calibrated by measuring the mass spectral peak
intensity ratio for known mixtures of product and reactant. These calibration
plots have been included in the Appendix; the resultant relationships
were found to be

$$[VCN]/[i\text{-}PrCN] = (I_{53}/I_{54} - 0.316)/1.930$$

$$[Propylene]/[i\text{-}PrCN] = (I_{41}/I_{68} - 1.35)/3.048$$

The experimental data obtained over the temperature range 1074-
1253K are tabulated in the Appendix, and the calculated VLPP rate constants
are presented in Tables 3.6 and 3.7. Only the 1.1mm and 3.3mm apertures
were used, since no decomposition was observed for the 10mm aperture
over the experimental temperature range. It can be seen that under VLPP
conditions, C-C bond fission was the major reaction; the formation of
propylene accounted for only ~ 10% of the overall decomposition. Although
the percentage decomposition based on propylene is small, it should be
noted that it is the directly measured ratio. [propylene]/[i-PrCN], which
determines k_{uni}, The material balance between the products and reactant
was noticed to be not quite in agreement, but the discrepancy was small and
showed no significant trend. The results were checked by monitoring the
reactions at mass numbers different to those quoted above; isopropyl cyanide
was monitored at 42 amu, vinyl cyanide at 26 amu, and propylene at 39 amu.
These intensities and the respective calibration plots have been included
in the Appendix, and the results were found to agree within experimental
error with Tables 3.6 and 3.7. Inspection of the reactor during maintenance
to the apparatus revealed that a light carbonaceous coating had formed on
the walls, and this probably accounted for the isopropyl cyanide material
balance discrepancy . Heterogeneous decomposition was considered, but over
the period of several months that this investigation was carried out,

TABLE 3.6   VLPP Results for Isopropyl Cyanide

(Z = 19,550, flow rate = 9.1 x 10^{14} molecules/sec)

		% decomposition			k_{uni}, sec^{-1}	
Run[a]	Temp K	i-PrCN decay	Product formation VCN	C_3H_6	VCN	C_3H_6
IP 179	1074.3	5.2	4.3	(0.4)[b]	0.034	
189	1082.8	7.9	5.8	(1.9)	0.049	
190	1093.5	10.3	7.8	(2.7)	0.067	
161	1101.7	9.7	7.0	-	0.058	
180	1104.8	10.8	8.0	(1.0)	0.068	
188	1106.9	10.4	9.6	(1.5)	0.084	
128A	1111.5	12.2	9.4	(0.9)	0.082	
162	1117.4	14.1	9.9	(0.4)	0.086	
151	1123.3	16.0	11.7	(1.5)	0.105	
129	1132.4	19.0	14.9	(1.4)	0.140	
152	1145.4	24.0	18.5	2.3	0.185	0.022
181	1148.7	24.9	18.9	2.9	0.191	0.029
130	1155.5	28.8	22.8	2.8	0.243	0.030
153	1164.0	31.9	25.4	2.6	0.28	0.029
131	1172.3	36.4	29.3	3.2	0.35	0.038
154	1185.7	41.3	33.9	3.2	0.43	0.042
132	1191.6	44.8	37.0	3.9	0.50	0.053
155	1203.7	50.5	41.3	3.9	0.61	0.058
133	1210.9	54.3	45.8	4.4	0.75	0.072
156	1224.5	59.2	49.9	4.3	0.89	0.078
134	1232.2	63.3	54.4	4.9	1.10	0.099
157	1243.0	66.3	56.5	5.1	1.21	0.109
135	1251.0	69.4	60.5	5.2	1.46	0.126

a
   Flow rate = 1 x 10^{15} molecules/sec for Runs IP 179-190;
   7.5 x 10^{14} molecules/sec for Runs IP 161-2 ; and
   5.2 x 10^{14} molecules/sec for Runs IP 151-7.

b
Bracketed data not used in calculation of rate constants.

TABLE 3.7   VLPP Results for Isopropyl Cyanide

(Z = 2,140,   flow rate = 1.2×10^{15} molecules/sec)

| Run[a] | Temp K | % decomposition | | | k_{uni}, sec^{-1} |
| | | i-Pr-CN decay | Product formation | | |
			VCN	C_3H_6	VCN
IP 146	1198.7	10.2	6.3	(0.5)[b]	0.49
140	1202.7	10.5	6.6	(0.5)	0.52
166	1206.4	9.9	6.7	(0.1)	0.52
145	1220.5	13.8	8.9	(1.4)	0.73
141	1221.7	13.4	9.4	(1.0)	0.77
167	1222.7	14.3	10.2	(0.4)	0.84
142	1241.5	18.0	12.9	(1.1)	1.11
168	1251.3	19.5	14.3	(0.8)	1.26
144	1252.5	22.9	15.2	(4.4)	1.41
143	1253.4	20.7	15.1	(1.3)	1.34

a
Flow rate = 5.4×10^{15} molecules/sec for Runs IP 144-6;
and 7.1×10^{14} molecules/sec for Runs IP 166-8.

b
Bracketed data not used in calculation of rate constants.

reproducibility was good irrespective of whether the reactor was conditioned or not. Hence it was concluded that the formation of carbon must occur independently of the homogeneous reactions (1)-(3).

The A-factor for C-C bond fission in isopropyl cyanide was determined by considering the reverse radical recombination reaction, thermochemistry, and the A-factors for analogous reactions. Radical recombination rate constants have been derived by Benson and O'Neal [31], from an analysis of the bulk of unimolecular bond fission reactions carried out to 1970. and they recommend for the combination of stabilized radical plus radical $\log (k_r, M^{-1} sec^{-1}) = 8.4 \pm 0.5$. This should be a reasonable estimate for the combination $CH_3CHCN + CH_3$. To calculate the A-factor for the foreward reaction, from the rate constant of the reverse reaction and thermochemistry requires an estimate of E_{-1} which for most radical combinations is close to zero at 300K if not at higher temperatures. Thus combining $k_{-1} = 8.4 = A_{-1}$ at 300K with $\log (A_1 sec^{-1}/A_{-1}, M^{-1} sec^{-1}) = 6.96$ (from the thermochemical data tabulated in Table 4.2 of Chapter 4), yields $\log (A_1, sec^{-1}) = 15.4$, which is reasonable when compared with analogous reactions [31].

A transition-state model was set up to represent the reactions, and from the parameters a value for the A-factor could be obtained. As explained earlier, bond fissions resulting in the formation of resonance-stabilized radicals have lower A-factors than their saturated counterparts [31, 68], which is due to the resonance stiffening of hindered rotations. Although there are no rotational constraints in the cases of alkyl cyanides (and alkynes) because of the cylindrical symmetry of the triple bond, resonance in the $C-C\equiv N$ (and $C-C\equiv CH$) bends should cause an increase in these low frequency modes with a resultant lowering of the A-factor relative to alkanes. Rabinovitch and Setser [69a], and Johnson and Coworkers [69b] have

described a transition-state model for C-C bond fission and have
applied it to the decomposition of alkanes. The usual transition-state
model outlined by them is the assignment of the C-C stretch in the
breaking bond as the reaction co-ordinate, the lengthening of that bond
by 1Å with the barrier to internal rotation about it being reduced to
zero, and the weakening of the four bending frequencies which are destined
to become external rotations of the product radicals. Tsang [68b] has
found that the formation of ethyl radicals from alkanes has an A-factor
of $10^{16.2}$ sec $^{-1}$ per reaction path at 1100 K. Application of the above
model to these reactions revealed that the four bending frequencies are
lowered to ca. 30% of their molecular values to obtain this A-factor.
The alkyne analog of isopropyl cyanide is 3-methyl-1-butyne, but the only
detailed study of C-C fission in an alkyne is the shock-tube work of
Tsang [70] on 4-methyl-1-pentyne. He obtained $A_{\infty} = 10^{15.56}$ sec $^{-1}$
at 1100 K which is $\sim 10^{0.6}$ sec $^{-1}$ per path lower than for alkanes.
Extension of the above model to the calculations for 4-methyl-1-pentyne
showed that the two $C-C \equiv CH$ bending frequencies have to be increased to
ca. 140% of their molecular values to give agreement with the experimental
A-factor. This may be regarded as a consequence of the development of
resonance in the transition-state.

The above transition-state model of Rabinovitch and Setser [69a]
and Johnson and coworkers [69b] with the resonance modifications is
postulated as the model to represent C-C bond fission in organic cyanides.

Frequency assignments for the isopropyl cyanide molecule were
taken from the work of Klaboe [64a] and Durig and coworkers [64b], and are
listed in Table 3.8A. Using the bond lengths and angles tabulated by
Sutton [71] with the atomic masses, the product of the moments of inertia
of the molecule is calculated to be 6.23×10^{-114} $(g \ cm^2)^3$. This value
is in agreement with the value found by Durig and Li [72]. From the
vibrational assignment, the molecular entropy can be calculated directly by
methods of statistical thermodynamics. The calculational
procedure is straight forward and described in standard

TABLE 3.8A   Frequency Assignments for Isopropyl Cyanide Fission
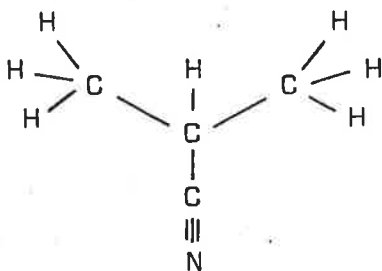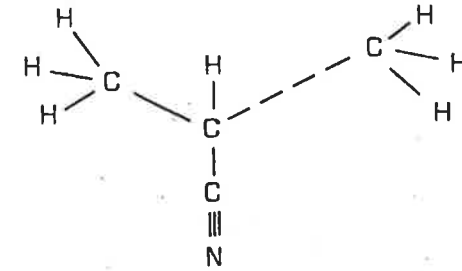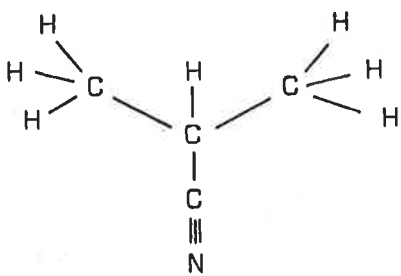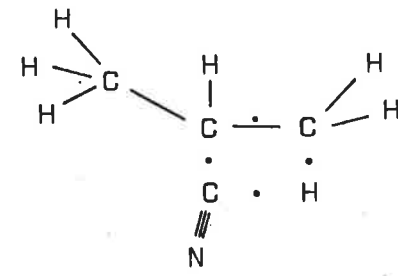
Molecule				C-C Fission Complex			

Mode	Bond	Degen.	Freq.(cm^{-1})	Mode	Bond	Degen.	Freq.(cm^{-1})
Stretch	C-H	7	2950	Stretch	C-H	7	2950
	C-C	2	769		C---C		r.c.
			1104		C-C	1	1104
	C-CN	1	738		C-CN	1	738
	C≡N	1	2255		C≡N	1	2255
Bend	H-C-H	6	1440	Bend	H-C-H	6	1440
	C-C-C	1	510		C-C---C	1	153
	C-C-(CN)	2	355		C---C-(CN)	1	107
			490		C-C-(CN)	1	490
	H-C-(CN)	2	1296		H-C-(CN)	2	1296
			1326				1326
	C-C≡N	2	175		C-C≡N	2	243
			220				308
Rock	-CH$_3$	2	916	Rock	---CH$_3$	2	275
			1068				320
	-CH$_3$	2	932		-CH$_3$	2	932
			1175				1175
Torsion	CH$_3$ ⇀	2	220	Torsion	CH$_3$ ⇀	1	220
			220		CH$_3$ ⇀		free rotation

TABLE 3.8B   Frequency Assignments for Isopropyl Cyanide Pyrolysis

Molecule				HCN Elimination Complex			
Mode	Bond	Degen.	Freq.(cm^{-1})	Mode	Bond	Degen.	Freq.(cm^{-1})
Stretch	C–H	7	2950	Stretch	C–H	6	2950
					C·H	1	2200
	C–C	2	769		C÷C	1	1300
			1104		C–C	1	1104
	C–CN	1	738		C·CN		r.c.
	C≡N	1	2255		C≡N	1	2255
Bend	H–C–H	6	1440	Bend	H–C–H	6	1440
	C–C–C	1	510		C–C÷C	1	510
	C–C–(CN)	2	355		C÷C·(CN)	1	355
			490		C–C·(CN)	1	353
	H–C–(CN)	2	1296		H–C·(CN)	1	933
			1326		H–C–(CN)	1	1326
	C–C≡N	2	175		C·C≡N	2	126
			220				158
Rock	–CH$_3$	2	916	Rock	–CH$_2$·H	2	660
			1068				770
	–CH$_3$	2	932		–CH$_3$	2	932
			1175				1175
Torsion	CH$_3$ ⇀	2	220	Torsion	CH$_2$ ÷	1	400
			220		CH$_3$ ⇀	1	220

texts [45, 46]. A molecular entropy of the isopropyl cyanide molecule at 300 K of 76.2 cal K^{-1} mole $^{-1}$ is obtained which agrees with the value predicted from group additivity tables [42].

The complete vibrational assignment for the C-C bond fission transition-state complex is shown in Table 3.8A. As described in the above postulated model, the C-C stretch (769 cm^{-1}) was taken as the reaction co-ordinate. The four bending frequencies involving the breaking bond were reduced to 30% of their molecular values. These frequencies were two methyl rocks (916, 1068 cm^{-1}), one C-C-C bend (510 cm^{-1}), and one C-C-(CN) bend (355 cm^{-1}). In addition the two C-C≡N bends (175, 220 cm^{-1}) were increased to 140% of their molecular values due to resonance. One of the two torsional frequencies (220 cm^{-1}) of the molecule is treated as a free rotation about the breaking bond, and its moment is calculated to be 5.34×10^{-40} g cm^2. Using the same bond lengths and angles as for the molecule except that the breaking C-C bond was lengthened by 1$\overset{\circ}{A}$, the product of moments of inertia for the transition-state model is calculated to be 15.6×10^{-114} (g cm^2)^3.

RRKM calculations were made using these molecular assignments and it is found that the postulated model gives A_∞ (300 K) = $10^{15.3}$ sec^{-1} for C-C fission in isopropyl cyanide. This agrees very well with the value estimated from the reverse reaction and thermochemistry. At 1100 K, the model yields A_∞ (1100 K) = $10^{15.4}$ sec^{-1} per path or $10^{15.7}$ sec^{-1} overall.

A four-centre transition-state model was assumed for the HCN elimination reaction from isopropyl cyanide. The frequencies of the normal and partial bond bending and stretching were assigned by following the procedures outlined by O'Neal and Benson [30, 45], and the assignments are shown in Table 3.8B. The six transition-state frequencies involved in the four-centre model were reduced to ca. 72% of their molecular values, in accord with other estimates [30, 45]. Frequencies involving the cyano group which are not listed by O'Neal and Benson are as follows

$\overset{C}{\underset{C}{\diagup}}\diagdown(CN)$ 490 cm^{-1} $\overset{C}{\underset{C}{\diagup}}\cdot(CN)$ 353 cm^{-1}

$\overset{C}{\underset{H}{\diagup}}\diagdown(CN)$ 1296 cm^{-1} $\overset{C}{\underset{H}{\diagup}}\cdot(CN)$ 933 cm^{-1}

$\overset{C}{\underset{C}{\diagup}}\diagup\!\!\!\!\equiv N$ 175, 220 cm^{-1} $\overset{\cdot C}{\underset{C}{}}\!\!\equiv N$ 126, 158 cm^{-1}

The moments of inertia of the complex were calculated using distances and angles determined according to the method of Benson and Haugen [22]. Using these molecular parameters for the postulated HCN elimination model, RRKM calculations yield a value (including reaction path degeneracy) for A_∞(1100 K) of $10^{13.9}$ sec^{-1}. At 600 K, the A-factor obtained is $10^{13.7}$ sec^{-1} which is similar to the experimental and theorectical values for HX eliminations from isopropyl halides [30, 73].

RRKM calculations were carried out on the molecular parameters for C–C bond fission and HCN elimination shown summarized in Table 3.8C. The frequencies have been grouped and rounded.

For isopropyl cyanide decomposition, we have the situation of competing unimolecular paths in the fall-off region, where energized molecules are depleted by all reaction paths and each path feels the effect of the drain on energized molecules of the other paths. The usual unimolecular rate theory expression for k_{uni} has to be modified to take into account this mutual interaction among reaction paths. The RRK theory expression has been modified previously [53] for the scheme of two competitive reaction paths, and the resultant procedure was called the RRK/2 method[*]. The rate data for the pyrolysis of isopropyl cyanide were analysed with the RRK/2 formulations and the results are shown in Figure 3.3 together with the computed lines found by applying RRK and RRKM theory on the same input information.

It was found that the minor reaction pathway of HCN elimination

---

[*] Refer to Appendix A.4, page 214.

TABLE 3.8C   Molecular Parameters for Isopropyl Cyanide Pyrolysis

	Molecule	Complex (C-C)	Complex (-HCN)
Frequencies (cm^{-1})	2950 (7)	2950 (7)	2950 (6)
and degeneracies	2255 (1)	2255 (1)	2230 (2)
	1440 (6)	1440 (6)	1440 (6)
	1310 (2)	1310 (2)	1310 (2)
	1110 (3)	1140 (2)	1140 (2)
	925 (2)	932 (1)	933 (2)
	754 (2)	738 (1)	770 (1)
	500 (2)	490 (1)	660 (1)
	355 (1)	300 (3)	510 (1)
	220 (3)	243 (1)	369 (3)
	175 (1)	220 (1)	220 (1)
		153 (1)	158 (1)
		107 (1)	126 (1)
$I_A \cdot I_B \cdot I_C$ $(g\ cm^2)^3 \times 10^{114}$	6.23	15.6	15.9
I_r, $g\ cm^2 \times 10^{40}$	-	5.34[a]	-
Sigma	1.0	0.5	1.0
Collision Diameter, Å	5.5[c]		
S^0_{300}, cal K^{-1} mole^{-1}	76.2	85.6	77.8

[a]
  Using symmetry ≡ "foldness" of barrier = 3.

[b]
  Sigma = σ/n, where σ is the symmetry number for external rotation and n is the number of optical isomers.

[c]
  Assumed equal to that for n-propyl cyanide [51]
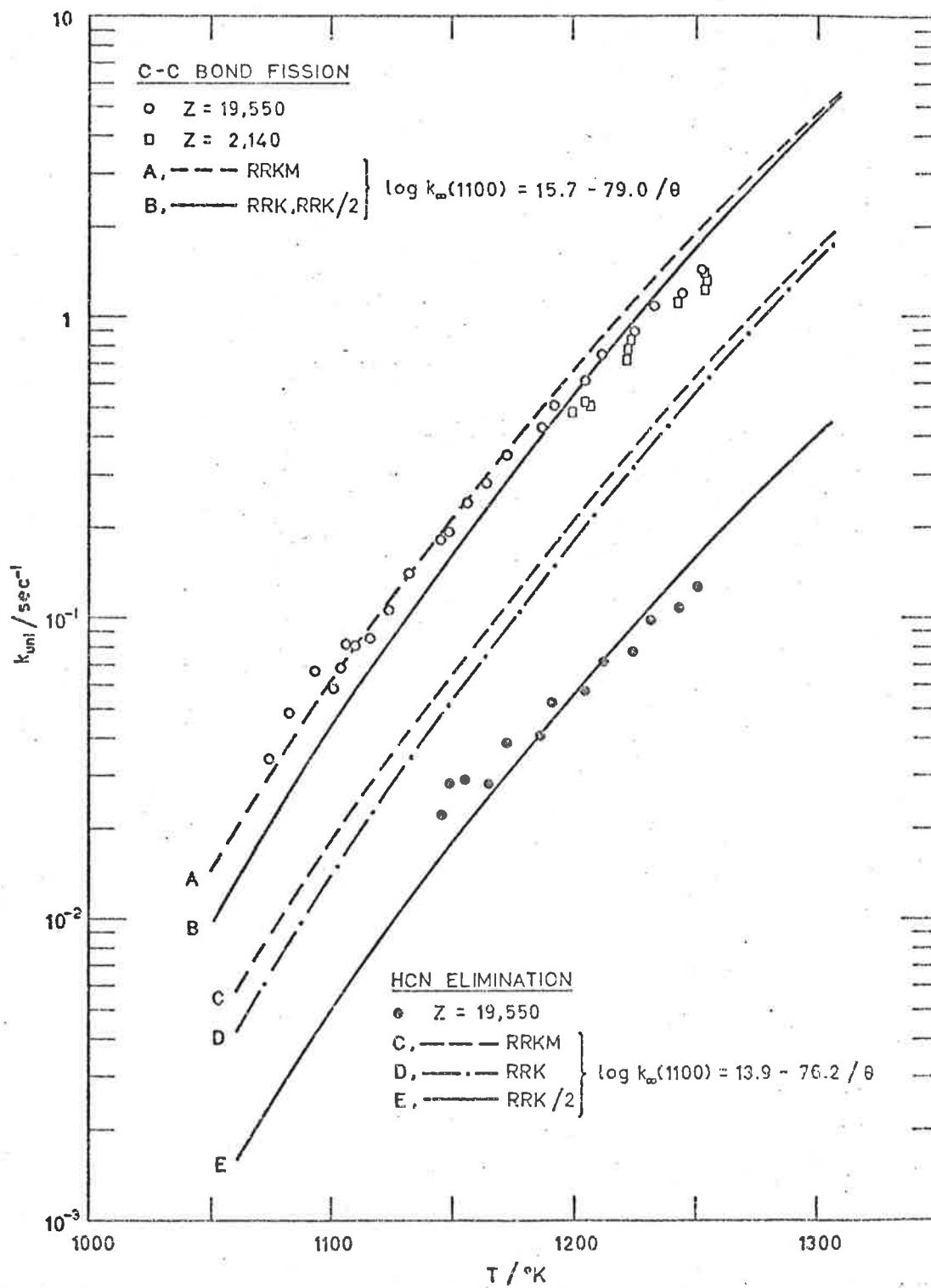
Figure 3.3 k_{uni} as a function of T for the decomposition of isopropyl cyanide.

had little effect on the major process of C-C bond fission, as emphasised
by the virtually identical calculations of the RRK and RRK/2 theories for
the fission reaction. As expected [*] the RRKM calculations are little
different; thus enabling RRK(M) theory to determine the activation energy
for reaction (1), while the RRK/2 method was used to find the activation
energy for reaction (2). It was found that interaction of the competitive
paths in the energy-dependent region caused the rate constants for the
elimination reaction to be lower by a factor of ~3 than the values
predicted on the basis of no interaction (RRK, RRKM)[**].

The Arrhenius A-factors estimated from transition-state models
have been shown [30,61] to be reliable to about $10^{\pm 0.3}$ in A. It
was found that changes of this size in A_∞ required changes in E_∞ of ca.
± 1kcal/mole to refit the data for both reactions. The spread in measured
rate constants were found to be covered by a further error limit of
± 1 kcal/mole. Therefore the high-pressure Arrhenius expressions which satisfy
the unimolecular rate constants are

$$\log k_1 (1100K) = (15.7 \pm 0.3) - (79.0 \pm 2.0)/\theta$$

and $\quad \log k_2 (1100K) = (13.9 \pm 0.3) - (76.2 \pm 2.0)/\theta$

where k is in sec^{-1}

In order to clarify the observation of Dastoor and Emovon [33]
that HCN elimination was the only reaction pathway in the pyrolysis of
isopropyl cyanide, with no indication of bond fission, an experimental
investigation both in the absence and presence of toluene was carried out
in the stirred-flow reactor. Initial chromatographic analysis showed that
methane, propylene, hydrogen cyanide, ethyl cyanide and vinyl cyanide were the

---

[*] It has been shown that RRK (using $s = C_{vib}(T)/R$) and RRKM
theory give substantially the same result for fall-off calculations
for thermally activated systems [74].

[**] Recently, a computer program for treating two competitive paths in the
fall-off region using RRKM theory has been developed by B.J. Gaynor, K.D. King
and R.G. Gilbert. This RRKM/2 method gives results that differ from the
RRK/2 values by only ca. ± 0.2 kcal/mole in activation energy.

major products. On the addition of a chain inhibitor, namely toluene, the yield of propylene decreased markedly. This observation is in sharp disagreement with Dastoor and Emovon, who state that when toluene was added "in equal volume" as the reactant, the elimination of hydrogen cyanide was unaffected. Indications are that a large amount of toluene is required to prevent any chain processes from occurring. In two series of experiments carried out at 903 and 927K, the yield of propylene was determined for toluene/isopropyl cyanide ratios up to ~20; the results being summarised in Table 3.9. Over this range of inhibitor the rate was observed to decline by a factor of ca. 50, and it was not clear that a minimum value had been reached. Obviously the amount of toluene used by Dastoor and Emovon was not adequate to inhibit the chain processes, although it is surprising that they did not observe any changes at all with and without the addition of toluene.

Using a toluene to reactant ratio of ca. 6, an investigation[*] of the decomposition of isopropyl cyanide was followed over the temperature range 872-974K, and the experimental results are given in Table 3.10. Both vinyl cyanide and ethyl cyanide (EtCN) were observed to be formed in greater quantities than propylene, and the vinyl cyanide/ethyl cyanide ratio was found to be a function of both the relative concentration of toluene and the temperature. This probably results from the competition between reactions (4) and (5) in the following scheme
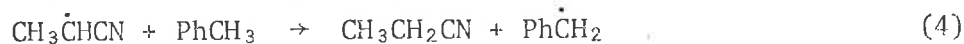
$$CH_3CH(CN)CH_3 \rightarrow CH_3CH = CH_2 + HCN \tag{1}$$
$$CH_3CH(CN)CH_3 \rightarrow CH_3\dot{C}HCN + \dot{C}H_3 \tag{2}$$
$$\dot{C}H_3 + PhCH_3 \rightarrow CH_4 + Ph\dot{C}H_2 \tag{3}$$
$$CH_3\dot{C}HCN + PhCH_3 \rightarrow CH_3CH_2CN + Ph\dot{C}H_2 \tag{4}$$
$$CH_3\dot{C}HCN \rightarrow CH_2 = CHCN + H \tag{5}$$
$$H + PhCH_3 \rightarrow H_2 + Ph\dot{C}H_2 \tag{6}$$
$$Ph\dot{C}H_2 + Ph\dot{C}H_2 \rightarrow PhCH_2CH_2Ph \tag{7}$$

TABLE 3.9   Effect of Inhibitor on Propylene Formation from

Decomposition of Isopropyl Cyanide at High-pressure

$\dfrac{\text{Toluene}}{\text{i-PrCN}}$	$\dfrac{[\text{Propylene}]}{[\text{i-PrCN}]} \times 10^2$	$\dfrac{\text{Toluene}}{\text{i-PrCN}}$	$\dfrac{[\text{Propylene}]}{[\text{i-PrCN}]} \times 10^2$
$T = 903$ K $\quad U \simeq 29$ mls/sec		$T = 927$ K $\quad U \simeq 43.5$ mls/sec	
0	21.7	0	5.7
0.6	4.0	0.1	4.7
1.7	2.7	0.4	3.9
2.5	2.4	1.1	2.7
3.2	1.8	1.6	1.9
5.8	0.54	2.3	1.2
7.6	0.85	3.9	0.62
16	0.45	5.1	0.79
22	0.43	5.9	0.70
>22	propylene not detected	>6	propylene not detectable

TABLE 3.10   Experimental Results for Stirred-Flow Pyrolysis of
Isopropyl Cyanide

Temp K	Flow rate mls/sec	U/V sec^{-1}	[Product] / [Reactant] $\times$ 10^2		
			$\dfrac{[C_3H_6]}{[i\text{-}PrCN]}$	$\dfrac{[EtCN]}{[i\text{-}PrCN]}$	$\dfrac{[VCN]}{[i\text{-}PrCN]}$
851.2	38.76	0.2162	0.077	0.52	
851.2	38.76	0.2162	0.074	0.36	
851.6	38.78	0.2163	0.073	0.41	
871.9	39.43	0.2199	0.21	0.88	0.29
871.9	39.43	0.2199	0.20	0.93	0.27
871.9	39.43	0.2199	0.21	0.77	0.21
890.2	47.71	0.2661	0.39	1.51	0.58
891.2	47.76	0.2664	0.39	1.56	0.63
891.5	56.66	0.3160	0.30	1.23	0.57
891.5	56.66	0.3160	0.31	1.17	0.51
892.0	40.21	0.2242	0.52	2.10	1.06
892.2	40.22	0.2243	0.54	2.16	1.03
911.9	58.61	0.3269	0.73	3.0	1.74
912.1	58.62	0.3270	0.69	3.0	1.69
912.3	48.65	0.2713	0.88	3.1	2.2
912.3	47.40	0.2644	0.96	3.6	2.3
912.5	39.92	0.2227	1.16	4.3	3.0
913.1	39.32	0.2193	1.38	4.7	3.3
932.4	59.19	0.3301	1.45	5.6	4.0
932.4	59.19	0.3301	1.61	6.0	4.9
932.6	49.39	0.2755	1.95	7.9	5.8
932.6	49.39	0.2755	1.83	7.5	4.0
932.6	41.16	0.2296	2.31	9.9	7.0
932.8	41.17	0.2296	2.22	9.3	6.7

The product to reactant concentration ratios obtained in
Table 3.10, were determined from calibration plots of mixtures of propylene,
ethyl cyanide and vinyl cyanide with isopropyl cyanide prepared on a
vacuum line and analysed using the 10% w/w dinonyl phthalate column with
hydrogen flame ionization detection.   The following calibration relationships
were obtained

[Propylene]/[i-PrCN] = 1.303 x peak area ratio of C_3H_6/i-PrCN

[EtCN]/[i-PrCN] = 1.585 x peak area ratio of EtCN/i-PrCN

[VCN]/[i-PrCN] = 1.575 x peak area ratio of VCN/i-Pr^{CN}.

3.4   n - Propyl Cyanide

From the VLPP study of isopropyl cyanide, the unimolecular decomposition was found to proceed via C-C bond fission, while HCN elimination accounted for less than 10% of the overall decomposition. Since $DH^0[C_2H_5-C_2H_5] < DH^0[(CH_3)_2 CH - CH_3]$ [45] and, in addition, from a comparison of the alkyl halide decompositions [73], HCN elimination from a primary alkyl cyanide is expected to be slower than from a secondary cyanide, then n-propyl cyanide was anticipated to decompose almost entirely via C_2-C_3 bond fission

$$CH_3CH_2CH_2CN \longrightarrow CH_3\dot{C}H_2 + \dot{C}H_2CN \qquad (1)$$

The competing HCN elimination

$$CH_3CH_2CH_2CN \longrightarrow C_3H_6 + HCN \qquad (2)$$

should be too slow to observe.   The ethyl radical formed as a result of reaction (1) will decompose to ethylene and an H atom

$$CH_3\dot{C}H_2 \longrightarrow C_2H_4 + H \qquad (3)$$

and RRK calculations* showed that under the VLPP conditions the radicals should decompose completely before leaving the reactor.

The disappearance of n-propyl cyanide (n-PrCN) was monitored by measuring the mass spectral peak $m/e = 29$ amu, using argon ($m/e = 20$ amu) as an internal standard.   Ethylene formation was followed at $m/e = 26$ amu. Reasonable agreement between the disappearance of n-propyl cyanide and the formation of ethylene was obtained, but evidence indicated that C_2-C_3 fission was not the sole pathway for decomposition.   The formation of vinyl cyanide (VCN), monitored at $m/e = 53$ amu, was observed but accounted for less than 10% of the overall decomposition.

---

* Using the rate constant expression, $k_3 = 10^{13.5-40.7/\theta}$ [31] and the tables of the Kassel integral [67], then at 1100K, S = 9.6 B = 18.6 and D = 9.1 giving $k_{uni} = 79.2 sec^{-1}$, which is much larger than the escape rate constants of k_{ea} (1.1 mm) = 1.2 sec^{-1} and K_{ea} (3.3 mm) = 11.2 sec^{-1}

Its formation may be attributed to C_3-C_4 bond fission

$$CH_3CH_2CH_2CN \longrightarrow \dot{C}H_3 + \dot{C}H_2CH_2CN \qquad\qquad (4)$$

$$\dot{C}H_2CH_2CN \longrightarrow C_2H_3CN + H \qquad\qquad (5)$$
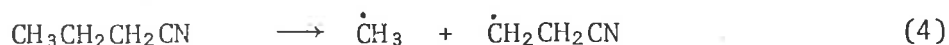
which was further supported by yields of methane via CH_3 formation (monitored at m/e = 15 amu).* The mass spectrometer was calibrated by measuring the peak intensity ratio for known mixtures of product and reactant, and the relationships were found to be

$$[Ethylene]/[n\text{-PrCN}] = (I_{26}/I_{29} - 0.177)/0.5109$$

$$[VCN]/[n\text{-PrCN}] = (I_{53}/I_{29} - 0.008)/0.2928$$

Corrections to m/e = 26 amu were made for the contributions of other products. The formation of ethylene + methyl cyanide was also followed at m/e = 14 amu, and the results were in agreement with ethylene formation at m/e = 26 amu.

The results of this investigation are presented in Tables 3.11 and 3.12. Only the 1.1mm and 3.3mm apertures were used over the temperature range 1090-1251K. From the tables it can be seen that the rate constants are independent of the aperture size and flow rates (in the range where the gas-gas collision frequency is smaller than the gas-wall collision frequency), indicating that the reactions are unimolecular first-order irreversible processes [47]. As a check on the HCN elimination reaction a careful search for propylene was carried out. Using its characteristic mass spectral peak at m/e = 42 amu as a marker (n-propyl cyanide was found to be the only other species in the reaction mixture to contribute to this mass number) a yield of propylene of ~0.9% at 1251 K was determined. This gives an estimated upper limit of ~0.025 sec^{-1} for the unimolecular rate constant.

---

* Some of the $\dot{C}H_3$ should reach the mass spectrometer as CH_4 due to collisions with the walls of the vacuum chamber.

TABLE 3.11   VLPP Results for n-Propyl Cyanide

($Z = 19,550$,   flow rate = $1-2 \times 10^{15}$ molecules/sec)

Run [a]	Temp K	% decomposition [b]				k_{uni} sec^{-1}	
			Product formation				
		n-PrCN decay	C_2H_4	VCN	Propylene (I_{42}/I_{29})	C_2H_4	VCN
NP 98	1089.8	9.1	6.9	1.2	0.053	0.058	0.010
109	1092.7	9.7	9.5	1.0	0.052	0.082	0.009
66	1102.5	14.2	14.6	–	0.058	0.13	–
99	1111.4	14.6	13.2	2.4	0.052	0.12	0.022
67	1124.8	21.2	23.3	–	0.057	0.24	–
100	1131.0	19.9	18.3	3.7	0.053	0.18	0.037
110	1132.0	20.5	19.3	–	0.053	0.19	–
68	1143.0	28.6	30.2	–	0.058	0.34	–
101	1151.7	29.7	26.2	5.1	0.056	0.30	0.059
69	1160.5	34.4	36.3	–	0.057	0.45	–
102	1171.0	36.0	33.0	6.0	0.054	0.43	0.078
111	1172.1	37.3	35.1	–	0.049	0.46	–
70	1184.0	46.1	49.0	–	0.058	0.77	–
103	1193.7	46.9	43.5	6.0	0.054	0.70	0.107
71	1203.3	54.3	58.5	–	0.066	1.14	–
104	1210.7	54.2	50.7	7.2	0.060	0.98	0.14
72	1223.2	62.9	66.4	–	0.063	1.61	–
73	1231.0	66.6	69.2	–	0.059	1.84	–
105	1231.8	63.5	59.4	7.1	0.065	1.46	0.17
74	1242.6	70.4	73.5	–	0.068	2.28	–
106	1250.7	70.6	66.3	6.6	0.065	2.02	0.20

[a] Flow rate = 7.1×10^{14} molecules/sec for Runs NP 109-111.

[b] In the experimental runs where VCN was not measured, the C_2H_4 formation is slightly larger than the total disappearance of n-propyl cyanide; this is because m/e = 26 was not corrected for contribution from VCN.

TABLE 3.12   VLPP Results for n-Propyl Cyanide

(Z = 2,140,   flow rate = 6.1×10^{14} molecules/sec)

| Run [a] | Temp K | % decomposition [b] | | k_{uni} sec^{-1} [c] |
		n-PrCN decay	C_2H_4 formation	
NP 87	1171.1	5.8	7.2	0.51
113	1172.5	5.1	6.5	0.45
82	1190.6	10.5	11.3	0.89
88	1190.9	7.5	6.7	0.57
114	1192.4	9.2	8.1	0.69
90	1211.1	-	13.5	1.11
89	1211.4	12.1	14.0	1.11
91	1211.7	15.4	13.6	1.26
115	1212.7	12.4	11.8	1.01
83	1213.8	15.1	15.6	1.33
84	1232.7	18.5	20.3	1.78
116	1235.6	17.7	16.6	1.54
85	1247.6	24.1	25.1	2.43
117	1248.7	21.4	20.3	1.97

[a] Flow rate = 1.7×10^{15} molecules/sec for Runs NP 82-85; 3.2×10^{15} molecules/sec for Runs NP 87-89; 8.4×10^{15} molecules/sec for Run NP 90; and 5.2×10^{15} molecules/sec for Run NP 91.

[b] VCN formation was too small to be of quantitative significance.

[c] Average.

Frequency assignments for the n-propyl cyanide molecule and activated complex model were based on the work of Fujiyama [75], and the frequencies for other alkyl cyanides [64, 76] and analogus hydrocarbons [77]. Using normal bond lengths and angles for alkyl cyanides [71], the moments of inertia were calculated, and the rotational constants were found to be in agreement with those reported by Hirota [78]. The collision diameter was taken from Chan and coworkers [66]. The calculated molecular entropy of 77.8 cal K^{-1} mole^{-1} at 300K agrees with the value predicted from group additivity [42]. The frequency assignments and molecular parameters are shown in Table 3.13.

The transition-state model for C_2-C_3 bond fission was constructed according to the procedure outlined for isopropyl cyanide. It was estimated that $A_{1,\infty}(1100K) = 10^{15.4}$ sec^{-1}, which is the same as the value (per reaction path) for isopropyl cyanide. The formation of vinyl cyanide via C_3-C_4 fission should have the same A-factor as that for the analogous fission in alkanes, since the strength of this C-C bond was not expected to be influenced by the cyano group. Applying the transition-state model for C-C fission [69] to the formation of the methyl radical from alkanes revealed that the four critical bending frequencies must be reduced to ca. 22% of their molecular values to give A_∞ (1100K) = $10^{16.2}$ sec^{-1}, the value recommended by Tsang [68b]. The same A-factor was obtained when this model was applied to the pyrolysis of n-propyl cyanide. The parameters for C_3-C_4 fission are shown in Table 3.13.

The unimolecular rate constants obtained were compared with the computed curves of the RRK/2 method and are shown in Figure 3.4. The lines corresponding to RRK and RRKM theories are also included to demonstrate the effect of interaction between the two pathways. The three curves for C_2-C_3

TABLE 3.13 Molecular Parameters for n-Propyl Cyanide Pyrolysis

	Molecule	Complex (C_2-C_3)	Complex (C_3-C_4)
Frequencies (cm^{-1}) and degeneracies	2950 (7)	2950 (7)	2950 (7)
	2255 (1)	2255 (1)	2255 (1)
	1445 (5)	1445 (5)	1445 (5)
	1290 (2)	1290 (2)	1290 (2)
	1140 (4)	1140 (4)	1150 (2)
	925 (1)	925 (1)	750 (3)
	750 (1)	738 (1)	490 (1)
	490 (1)	525 (1)	378 (1)
	404 (2)	314 (1)	253 (1)
	220 (2)	220 (3)	215 (2)
	100 (1)	147 (1)	165 (1)
		129 (1)	98 (2)
I_A, I_B, I_C $(g\ cm^2)^3 \times 10^{114}$	5.04	15.1	9.7
I_r, $(g\ cm^2) \times 10^{40}$	-	16.7[a]	4.71[a]
Sigma[b]	0.333[c]	1.0	0.333
Collision diameter, Å	5.5		
S_{300}^0 , cal K^{-1} $mole^{-1}$	77.8	86.4	88.4

[a] Using internal symmetry ≡ "foldness" of the rotor.

[b] Sigma = σ/n, where σ is the symmetry number for external rotation and n is the number of optical isomers.

[c] Accounts for the entropy of mixing of trans and gauche forms.
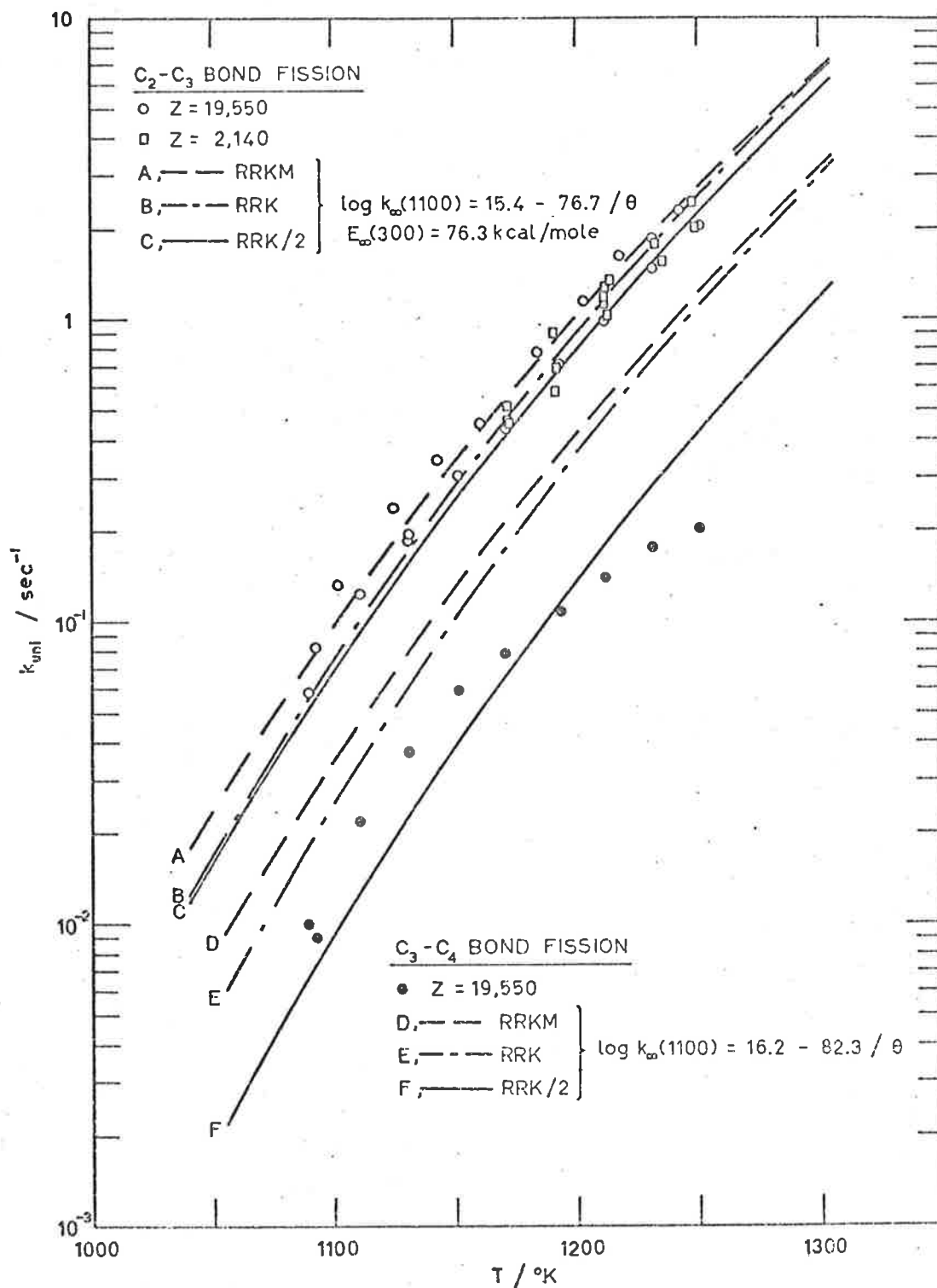
Figure 3.4 k_{uni} as a function of T for the decomposition
of n-propyl cyanide.

fission gave essentially the same result since decomposition proceeded almost entirely via this pathway. Competitive path interaction resulted in the unimolecular rate constants for vinyl cyanide formation to be below the values predicted by RRK and RRKM theories by a factor of ~3. Applying an uncertainty in A_1 of $10^{\pm 0.3}$ sec^{-1} required a change in E_1 of ca. ± 1 kcal/mole to refit the data, and the scatter of the measured rate constants was found to allow for further errors of ca. ± 0.7 kcal/mole. Thus the rate data for C_2-C_3 fission in n-propyl cyanide are given by the high-pressure Arrhenius expression

$$\log\ k_{1_\infty}\ (1100K) = (15.4 \pm 0.3) - (76.7 \pm 1.7)/\theta$$

while the rate constants for C_3-C_4 fission are reasonably consistent with

$$\log k_{3_\infty}\ (1100K) = 16.2 - 82.3/\theta$$

where k is in sec^{-1}. This latter expression is in good agreement with the parameters for methyl rupture from n-butane, corrected for reaction path degeneracy [68b].

Following the procedure outlined for isopropyl cyanide, the transition-state model for HCN elimination from n-propyl cyanide gave an estimated A-factor of $10^{13.4}$ sec^{-1}. Application of this A-factor to the observation of ≤ 0.9% yield of propylene gives a lower limit of ≥76.5 kcal/ mole for the activation energy. This calculation was carried out using a theoretical scheme where the interaction among three reaction pathways (C_2-C_3 fission, C_3-C_4 fission, and HCN elimination) in the fall-off region was taken into account. The scheme was derived by extending the RRK theory along the lines outlined for the RRK/2 method [53].

The derivation of this procedure, appropriately called the RRK/3 method, is discussed in the Appendix. The rate constants given by this method for the C_2-C_3 and C_3-C_4 fissions were virtually the same as the

RRK/2 method since these reactions dominate the decomposition relative to HCN elimination.

3.5   tert-Butyl Cyanide

The VLPP studies on isopropyl cyanide and n-propyl cyanide have shown that they decompose mainly via C-C fission of the bond adjacent to the cyano group; HCN elimination is a minor reaction. Thus it was expected that tert-butyl cyanide should also decompose in a similar manner. From a comparison of the alkyl halides [73], the HCN elimination should be more competitive than it was for the primary and secondary compounds. The kinetic parameters obtained from the pyrolysis of tert-butyl cyanide should enable the heat of formation and the stabilization energy of the α-cyanoisopropyl radical to be calculated.

Decomposition reactions expected are

$$(CH_3)_3 \, CCN \longrightarrow (CH_3)_2 \, \overset{\bullet}{C}CN + \overset{\bullet}{C}H_3 \tag{1}$$

$$(CH_3)_3 \, CCN \longrightarrow (CH_3)_2 \, CCH_2 + HCN \tag{2}$$
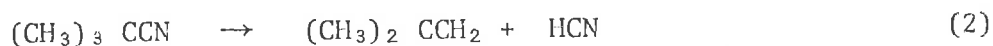
The α-cyanoisopropyl radical should decompose via H atom loss to form methyl vinyl cyanide

$$(CH_3)_2 \, \overset{\bullet}{C}CN \longrightarrow CH_3(CN)CCH_2 + H \tag{3}$$
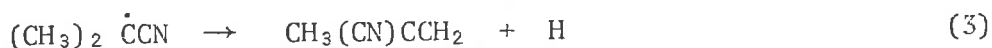
and, under VLPP conditions, this reaction should be more rapid than the escape of $(CH_3)_2\overset{\bullet}{C}CN$. RRK calculations* confirmed this. The product mass spectrum was in agreement with the occurrence of these reactions.

The disappearance of tert-butyl cyanide (t-BuCN) was monitored at peak m/e = 42amu (and also at m/e = 68 amu) using argon (at m/e = 40 amu) as an internal standard. The formation of methyl vinyl cyanide (MeVCN) was followed at m/e = 67 amu, while isobutene formation was followed at

---

* Using $\log k_3 = 14.4-48.1/\theta$, taken from that for the tert-butyl radical [31], but with A corrected for reaction path degeneracy, and E for stabilization by CN ($\sim$ 5 kcal/mole, [79,80]; see discussion), with the tables of Kassel integral [67] yielded: at 1200K, S = 19.6, B = 20.2 and D = 10.2 giving k_{uni} = 767 sec^{-1} compared to the fastest escape rate constant, k_{ea} (10 mm) = 54.2 sec^{-1}.

m/e = 56 amu. The mass spectrometer was calibrated for the relative sensitivities of products and reactant by preparing known mixtures on the vacuum line, and allowing them to effuse into the VLPP system.

The relationships obtained were

$$[MeVCN] / [t\text{-}BuCN] = (I_{67}/I_{68} - 0.367) / 0.6994$$

$$[Isobutene] / [t\text{-}BuCN] = (I_{56}/I_{68} - 0.021) / 1.2855$$

The unimolecular rate constants were calculated from the expression $k_{uni} = k_{ea}$ [product]/[reactant]. The results for the three aperture settings are presented in Tables 3.14 - 3.16. The experimental data and computer program used to calculate these results are included in the Appendix. Percentages of decomposition based on reactant disappearance and formation of products show good agreement. It can be seen from the tables that C-C bond fission was the major reaction, HCN elimination accounting for less than 5% of the overall decomposition. The unimolecular rate constants were found to be independent of the aperture settings and flow rates, thereby confirming the reactions to be unimolecular.

Details of the frequency assignment and molecular parameters for the molecule and transition-state are given in Table 3.17. Westrum and Ribner [81] and Durig, Craven and Bragin [82] have reported frequency assignments for the tert-butyl cyanide molecule, and these were used for the model. The moments of inertia, calculated by using the normal alkyl cyanide bond lengths and angles, agree with the results of Nugent, Mann and Lide [83], and the calculated molecular entropy of 79.6 cal K^{-1} mole^{-1} at 300K is in agreement with the work of Westrum and Ribner. The same transition state model as has been outlined for C_2-C_3 fission in isopropyl cyanide was applied to tert-butyl cyanide. The calculated A-factor at 1100K was $10^{15.4}$ sec^{-1} per reaction path or $10^{15.8}$ sec^{-1} overall. This

TABLE 3.14   VLPP Results for tert-Butyl Cyanide
(Z = 19,550,   flow rate = 2.6 x 10^{14} molecules/sec)

Run[a]	Temp K	% decomposition t-BuCN decay	Product formation MeVCN	Product formation i-C_4H_8[b]	k_{uni}, sec^{-1} MeVCN	k_{uni}, sec^{-1} i-C_4H_8
TB 12	1022.9	10.8	11.9		0.093	
40	1023.4	14.6	10.7		0.083	
85	1023.5	12.4	10.9		0.084	
4	1036.0	15.1	15.8		0.133	
41	1043.5	21.1	17.8		0.152	
86	1043.7	20.2	17.8		0.150	
13	1044.2	18.5	19.7		0.172	
5A	1056.0	24.4	24.7		0.233	
42	1057.8	27.6	23.7		0.221	
14	1062.2	28.0	28.1		0.277	
87	1073.3	34.1	31.7		0.33	
43	1075.5	36.9	33.2		0.36	
6	1077.9	36.9	36.0		0.41	
15	1084.0	40.8	39.3		0.47	
44	1095.0	48.2	43.5		0.56	
16	1103.6	52.6	49.8	2.2	0.73	0.032
88	1112.8	58.0	55.1	1.5	0.90	0.025
45	1114.4	58.1	55.8	2.2	0.94	0.037
17	1122.5	64.0	59.8	2.3	1.12	0.043
89	1133.3	67.9	65.3	1.6	1.41	0.034
46	1134.6	67.8	64.6	2.3	1.40	0.051
47	1147.5	73.1	71.1	2.5	1.93	0.067
48	1154.5	76.2	73.2	2.4	2.17	0.072
49	1166.5	79.7	77.7	2.3	2.82	0.083
50	1177.2	82.5	81.0	2.3	3.5	0.100
51	1177.1	83.4	81.1	2.3	3.6	0.100
52	1188.0	85.4	84.1	2.1	4.5	0.113

a
Flow rate = 3.8 x 10^{15} molecules/sec for Runs TB 4-6; 2.8 x 10^{15}
molecules/sec for Runs TB 12-17; 1.9 x 10^{15} molecules/sec for
Runs TB 51-2; 8 x 10^{14} molecules/sec for Runs TB 85-89.

b Isobutene formation at temps below 1100K was too small to be of
quantitative significance.

TABLE 3.15   VLPP Results for tert-Butyl Cyanide

(Z = 2,140,   flow rate = 3×10^{15} molecules/sec)

Run[a]	Temp K	t-BuCN decay	Product formation MeVCN	i-C$_4$H$_8$	k_{uni}, sec^{-1} MeVCN	i-C$_4$H$_8$
TB 65	1095.1	9.6	10.3		0.73	
22	1103.5	10.1	12.0		0.88	
66	1105.9	12.8	12.4		0.91	
67	1118.5	17.0	16.2		1.25	
18	1122.0	17.4	18.6		1.48	
24	1123.7	17.9	19.4		1.56	
68	1134.9	23.1	21.4		1.77	
25	1140.7	24.8	25.6		2.26	
53	1145.4	24.4	25.5		2.24	
54	1154.7	28.5	29.7		2.80	
26	1165.1	36.3	35.6		3.7	
69	1173.7	39.0	37.2	0.9	4.0	0.093
55	1175.3	37.4	38.4	1.2	4.2	0.126
56	1184.7	41.8	42.4	1.2	5.0	0.138
27	1188.0	46.7	45.4	1.2	5.7	0.176
70	1192.4	48.1	45.7	0.9	5.7	0.117
57	1196.9	48.0	47.7	1.3	6.2	0.167
28	1201.6	52.7	51.7	1.4	7.4	0.228
62	1213.0	55.7	54.3	1.5	8.2	0.221
71	1213.0	56.9	55.2	1.1	8.4	0.164
63	1213.4	58.3	54.7	1.4	8.3	0.214
58	1213.5	55.2	55.0	1.4	8.3	0.207
29	1225.4	62.5	61.3	1.6	11.2	0.32
59	1233.0	62.6	62.8	1.5	11.9	0.28
30	1245.6	69.3	68.5	1.8	15.6	0.40
60	1253.0	69.3	69.7	1.6	16.5	0.38
61	1253.0	70.3	69.0	1.7	16.0	0.39

a   Flow rate = 1.5×10^{15} molecules/sec for Runs TB 53-60; 6.2×10^{15} molecules/sec for Runs TB 61-2; 1.1×10^{16} molecules/sec for Run TB 63; 9.9×10^{14} molecules/sec for Runs TB 65-71.

TABLE 3.16   VLPP Results for tert-Butyl Cyanide

(Z = 246, flow rate = 1-2 x 10^{15} molecules/sec)

Run[a]	Temp K	% decomposition		k_{uni}[c], sec^{-1}
		t-BuCN decay	MeVCN formation	
TB 75	1173.7	7.6	9.7	4.6
80	1174.4	8.6	10.0	5.0
35	1185.7	8.1	12.2	5.5
76	1193.8	12.8	13.8	7.5
72	1194.8	14.4	14.4	8.2
36	1203.2	12.7	15.6	8.1
81	1215.1	17.3	19.0	10.9
37	1216.3	16.5	19.3	10.8
83	1217.0	17.1	18.4	10.8
73	1217.0	19.9	19.1	12.0
77	1217.2	18.0	19.8	11.6
84	1225.3	19.5	20.5	12.5
38	1232.5	21.5	23.3	14.4
78	1233.3	22.7	23.9	15.1
82	1240.5	24.2	26.4	16.9
74	1241.4	28.1	25.9	18.5
39[b]	1244.9	25.8	27.2	18.1
79[b]	1253.5	29.1	29.9	21.1

a   Flow rate = 5 x 10^{15} molecules/sec for Runs TB 75-79; 1.5 x 10^{16} molecules/sec for Runs TB 80-2; 4.9 x 10^{14} molecules/sec for Runs TB 83-4.

b   Isobutene was detected; $k_{uni} \simeq 0.50$ sec^{-1}.

c   Average.

TABLE 3.17   Molecular Parameters for tert-Butyl Cyanide Pyrolysis

	Molecule	Complex (C-C)	Complex (-HCN)
Frequencies (cm^{-1}) and degeneracies	2950 (9)	2950 (9)	2950 (8)
	2255 (1)	2255 (1)	2230 (2)
	1440 (9)	1440 (9)	1440 (9)
	1125 (3)	1120 (2)	1300 (1)
	935 (2)	935 (1)	1070 (2)
	869 (2)	869 (2)	935 (1)
	753 (2)	738 (1)	869 (2)
	561 (3)	579 (2)	787 (2)
	371 (3)	376 (2)	553 (2)
	255 (2)	299 (3)	463 (1)
	220 (2)	251 (3)	366 (4)
	175 (1)	158 (1)	260 (2)
		108 (1)	176 (1)
			140 (1)
$I_A \cdot I_B \cdot I_C$, $(g\ cm^2)^3$ x 10^{113}	1.70	3.55	3.77
I_r, $(g\ cm^2)$ x 10^{40}	-	5.42[a]	-
Sigma[b]	3.0	1.0	1.0
Collision diameter, Å	6.3[c]		
S^0_{300} cal K^{-1} mole^{-1}	79.6	89.7	82.7

a   Using internal symmetry $\equiv$ "foldness" of the rotor = 3

b   Sigma = σ/n, where σ is the symmetry number for external rotation and n is the number of optical isomers.

c   Assumed equal to that for n-butyl cyanide [66].

agrees with the values for isopropyl and n-propyl cyanide. The

elimination of hydrogen cyanide was assumed to be via a four-centre cyclic

transition-state, and application of the methods of O'Neal and Benson

[30, 45] yielded an A-factor of $10^{14 \cdot 1} sec^{-1}$ at 1100K or $10^{13 \cdot 9} sec^{-1}$ at

600K. This is similar to the observed and estimated values for the

elimination of hydrogen halide from alkyl halides [30, 73].

The experimental rate constants are compared with theory

(RRKM, RRK, RRK/2) in Figure 3.5. For the major pathway of C-C fission,

the three computed curves are similar, while interaction of the competitive

reaction paths causes the rate constants for the minor pathway to be

lower by a factor of ~5 than those predicted by RRK and RRKM theories.

The unimolecular rate data are found to be consistent with the high pressure

rate constants given by

$$\log k_1 \ (1100K) \ = \ (15.8 \pm 0.3) - (74.9 \pm 1.6)/\Theta$$
$$\log k_2 \ (1100K) \ = \ (14.1 \pm 0.3) - (74.1 \pm 1.6)/\Theta$$

where k is in sec^{-1}.
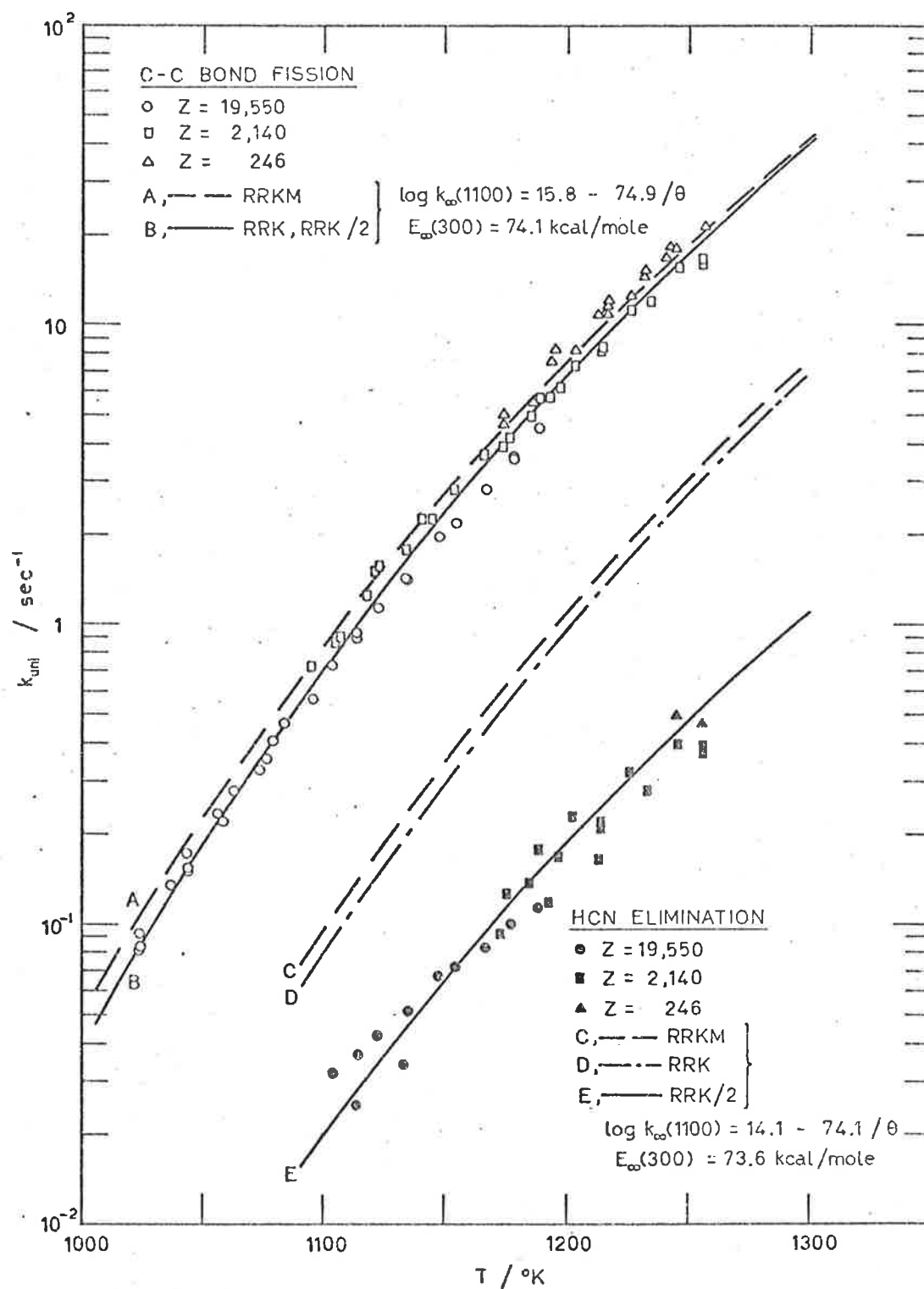
Figure 3.5 k_{uni} as a function of T for the decomposition
of tert-butyl cyanide.

3.6 Cyclopentyl Cyanide

To gain more information about the unimolecular elimination of hydrogen cyanide, the decomposition of a five or six membered cyclic cyanide was considered. Due to the increased strength of the ring bonds, it was .expected that the elimination reaction would play a greater role in the overall decomposition than it does for alkyl cyanide pyrolyses. Cyclopentyl cyanide was chosen as a suitable compound to study in the reactor systems available; its pyrolysis has not been reported in the literature.

The expected reactions are

$$(1)$$

$$+ \quad HCN \qquad (2)$$

The biradical may decompose to produce propylene and vinyl cyanide, and ethylene and cyanopropenes.

$$C_3H_6 \; + \; C_2H_3CN \qquad (3)$$

$$C_2H_4 \; + \; C_3H_5CN \qquad (4)$$
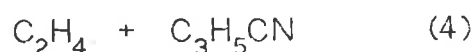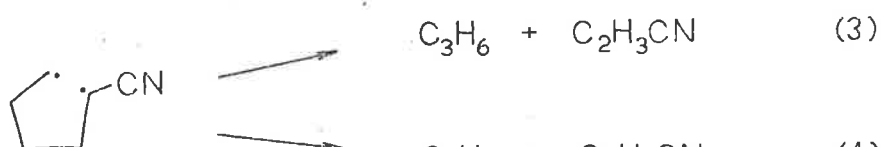
The cyanopropenes are taken to be a mixture of cis- and trans- crotonitrile and allyl cyanide.

An initial investigation was carried out in the batch reactor at temperatures of ca. 400, 450 and $500°C$. Very little decomposition of the cyclopentyl cyanide (c-PeCN) was observed. For a kinetic run carried out over 67 hours at ca. $500°C$ at an initial pressure of ca. 15 torr, the

rate constant for cyclopentene formation was found to be ca. 10^{-7} sec^{-1} assuming a first-order reaction; a RRK calculation* shows it not to be in the fall-off region. Products relating to the formation of vinyl cyanide and cyanopropenes were not observed.

The flow system provided more information. It was used to study the pyrolysis over the temperature range of 897-1056K, and the presence of toluene as a radical chain inhibitor could be introduced. Over this temperature range, the flow rates through the reactor were maintained above 20 mls/sec to satisfy good mixing requirements by forced convection and diffusion. Of the columns available for GC quantitative analysis (see Chapter 2), the squalane column, using temperature programming from 40^0C to 70^0C , was found to give good separation of the product peaks. The Porapak Q + R column was also used for a qualitative analysis of the low boilers. The expected products, i.e. ethylene, propylene, hydrogen cyanide, cyclopentene, vinyl cyanide, crotonitrile and allyl cyanide were detected as well as the observation of a dark brown residue deposited along the exit lines from the reactor. In addition, as the temperature was increased cyclopentene was found to decompose to cyclopentadiene.

$$\hspace{6cm} + \ H_2 \hspace{3cm} (5)$$
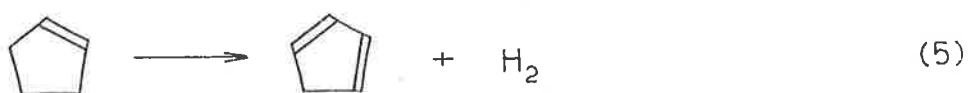
Rate parameters for the thermal decomposition of cyclopentene [84] suggest that over the temperature range of this investigation, almost all of the cyclopentene formed from cyclopentyl cyanide will subsequently decompose.

The GC flame ionization detector (FID) was calibrated by preparing known mixtures of products and reactant on the vacuum line; cyclopentene and cyclopentyl cyanide were calibrated against each other, whilst the other

* Assuming $k_{-2,\infty} \sim 10^{13-70/\theta}$ (from analogy of cyclopentyl halide eliminations [30], and the preceding studies of alkyl cyanide HCN eliminations), and using the Kassel integral tables [67]: at 773K, S = 23.2, B = 45.6, and D = 4.9 giving k_{uni}/k_∞ = 0.9999.

products were calibrated relative to cyclopentene. Decompositions via the assumed biradical mechanism were followed by the formation of vinyl cyanide (VCN) and of cyanopropene, C_3H_5CN. (It was found the crotonitrile and allyl cyanide had similar retention times on the squalane column and the same sensitivity of detection, and were therefore analysed together as C_3H_5CN). The HCN elimination was complicated by cyclopentene decomposing to cyclopentadiene plus some side products [84]. Thus it was decided to prepare some hydrogen cyanide (see Chapter 2) for calibration purposes, so its formation could be followed, as well as that of cyclopentene and cyclopentadiene. The calibration plots are shown in the Appendix, and the relationships obtained are

$$[VCN]/[c-PeCN] = 1.403 \text{ x peak area ratio, } VCN/c-PeCN$$

$$[C_3H_5CN]/[c-PeCN] = 1.463 \text{ x peak area ratio, } C_3H_5CN/c-PeCN$$

$$[C_5H_8]/[c-PeCN] = 1.240 \text{ x peak area ratio, } C_5H_8/c-PeCN$$

$$[C_5H_6]/[c-PeCN] = 1.240 \text{ x peak area ratio, } C_5H_6/c-PeCN$$

$$[HCN]/[c-PeCN] = 16.666 \text{ x peak area ratio, } HCN/c-PeCN$$

It should be noted that hydrogen cyanide was found to have a very low flame ionization sensitivity relative to the other species.

Toluene to reactant ratios of 0 - 36:1 and residence times of 3.5 - 10.3 seconds were used. The results of the study are presented in Table 3.18, from which it can be seen that the elimination of HCN is the major process of decomposition at lower temperatures, while vinyl cyanide formation dominates at the higher temperatures. The three pathways of decomposition have equivalent rates at ca. 980K. The rate of disappearance of cyclopentyl cyanide was not obtained for all runs. The combined rate of formation of cyclopentene and cyclopentadiene was found to be less than the formation of hydrogen cyanide. At temperatures to 950K, the discrepancy was small, but at ca. 1050K the combined rate was ca. 40% of

TABLE 3.18   Stirred-Flow Reactor Results for Cyclopentyl Cyanide

| Run | Temp K | U/V sec^{-1} | VCN | Rate constants, k x 10^2, sec^{-1} | | | |
				C_3H_5CN	HCN	$(C_5H_8+C_5H_6)$	c-PeCN
cPe 43	905.3	0.1134	0.062				
15	915.7	0.1180	0.070	0.054		0.16	
14	916.2	0.1186	0.087	0.060		0.15	
13	918.7	0.1033	0.086	0.054		0.18	
46	925.0	0.1147	0.132	0.109		0.16	
48	926.0	0.2186	0.119	0.071		-	
47	926.1	0.1651	0.142	0.101		0.21	
19	941.2	0.1032	0.33	0.28		0.43	
18	941.4	0.1025	0.30	0.28		0.43	
17	941.7	0.1247	0.26	0.30		0.46	
16	942.8	0.1233	0.28	0.13		0.46	
51	946.0	0.2198	0.31	0.19		-	
50	946.3	0.1665	0.38	0.18		0.30	
49	946.3	0.1188	0.44	0.20	0.32	0.31	1.1
20	954.8	0.1243	0.57	0.40	-	0.65	
21	956.0	0.1241	0.57	0.34	-	0.61	
22	956.1	0.1051	0.67	0.54	-	0.70	
2	966.2	0.0970	1.43	1.14	1.00	1.67	
54	966.5	0.2276	1.02	0.42	-	0.57	2.4
53	966.6	0.1709	0.84	0.50	-	0.67	2.6
52	966.6	0.1184	0.81	0.47	0.86	0.55	2.7
3	966.9	0.0934	1.31	0.93	1.06	1.64	
26	971.2	0.2246	0.97	0.49	-	0.84	
25	971.6	0.1728	1.26	0.75	-	1.11	
57	986.1	0.2302	2.13	1.09	1.67	1.06	
56	986.3	0.1851	2.29	0.89	1.81	0.99	7.2
55	986.8	0.1269	2.24	0.94	1.94	1.03	5.2
29	991.2	0.2299	2.81	1.15	2.00	1.47	
7	991.4	0.1257	3.36	2.23	2.68	3.22	
6	991.5	0.1247	2.98	2.07	2.50	2.93	
5	991.5	0.0964	2.93	1.99	2.13	2.76	

TABLE 3.18 Continued......

Run	Temp K	U/V sec^{-1}	VCN	C$_3$H$_5$CN	HCN	(C$_5$H$_8$+C$_5$H$_6$)	c-PeCN
cPe 4	991.6	0.0996	3.04	1.83	2.36	2.87	
28	991.6	0.1768	2.48	1.05	2.41	1.59	
58	1004.6	0.1317	4.5	1.71	3.5	1.45	12.2
60	1005.4	0.2358	4.6	2.35	4.0	1.44	9.4
61	1005.9	0.1777	4.4	1.82	3.9	1.67	13.3
30	1012.8	0.1786	4.9	1.66	3.9	1.66	18.8
32	1013.4	0.1269	4.8	2.2	4.0	1.69	14.8
31	1013.7	0.2391	5.2	2.1	4.7	2.1	17.0
11	1015.5	0.1435	7.3	4.0	5.5	4.9	
10	1015.5	0.1412	8.0	4.0	6.1	5.7	
9	1015.7	0.1280	7.6	3.8	5.6	5.3	
8	1015.7	0.1274	8.6	4.1	6.4	5.8	
84	1034.5	0.1841	13.9	4.8	7.7	3.4	4.7
35	1035.4	0.1301	12.1	3.9	6.9	2.7	3.7
34	1035.9	0.2415	12.2	4.6	8.1	3.1	32
36	1055.2	0.1915	26.1	9.9	15.2	5.5	69
38	1055.9	0.1331	30.0	9.3	16.2	5.5	84
37	1056.4	0.2482	28.2	11.0	17.6	5.6	72

Rate constants, k. x 10^2,sec^{-1}

that for HCN formation. The studies of Lewis and coworkers [84a], and Knecht [84b], on the decomposition of cyclopentene have shown that for ca. 50% conversion, side reactions account for 2-5% of the loss of reactant; but at larger extents of reaction, higher yields of ring fragmentation products were observed. The major side products were found to be ethylene, propylene, allene and 1,3-butadiene, and their formation has a strong temperature dependence [84a]. Swarc [85] has reported that the decomposition of cyclopentadiene yielded mainly hydrogen, methane, and C_2 hydrocarbons, but the work of Lewis and coworkers [84a] and Tanji and co-workers [84c] have shown that over the temperature ranges at which they studied cyclopentene decomposition, most side products were produced from the cyclopentene. A brief qualitative investigation of these two cyclo-alkenes in the flow system confirmed the product analyses of the previous studies. Since the residence times at temperatures above ~ 1000K allowed for complete decomposition of any cyclopentene formed, it is not surprising that the discrepancy between the formations of hydrogen cyanide and cyclopentene + cyclopentadiene becomes large at the higher temperatures.

Experiments carried out in the extended surface reactor (Chapter 2) over similar temperatures and flow rates of this study, showed that the rate constants for the formation of vinyl cyanide and of hydrogen cyanide are unaffected by a threefold increase in the S/V ratio of the reaction vessel.

Consider the consecutive reaction scheme for the formation of cyclopentene and cyclopentadiene from cyclopentyl cyanide

$$A \xrightarrow{2} B + C$$
$$\downarrow 5$$
$$D + E$$
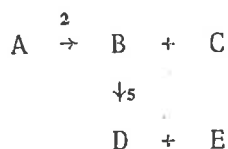
Then for a stirred-flow system

$$\frac{1}{t} = \frac{k_2 [A]}{[B] + [D]} = \frac{k_2 [A] - k_5 [B]}{[B]} = \frac{k_5 [B]}{[D]}$$

i.e. $\quad k_2 \; \alpha \quad \dfrac{[B] + [D]}{[A]}$

$\quad k_5 \; \alpha \quad \dfrac{[D]}{[B]}$

Hence the rate constants for the decomposition of cyclopentene to cyclopentadiene (i.e. B → D + E) can be obtained from the concentrations of these compounds in the effluent reaction mixture. The values obtained are compared in Table 3.19 with the rate constants given

Table 3.19 Comparison of Rate Constants for Cyclopentene
Decomposition

Temp K	% decomposition	$k_{exptl} \times 10^2$ sec^{-1}	$k_5 \times 10^2$ sec^{-1} [a]
867	11.9	1.4	1.7
886	21.8	3.1	3.5
897	30.4	5.0	5.4
905	47.1	10.1	7.2
917	50.0	11.5	11.2
936	69.8	26.2	21.8

[a] Lewis and coworkers [84a]

by the Arrhenius expression, $\log(k_5, sec^{-1}) = 13.35 - 60.0/\theta$, found by Lewis and coworkers [84a] from a shock tube study at $T_m \sim 1100K$. The agreement is good, considering that the previous studies only followed the

decomposition to 50% completion, and that the actual amounts of cyclopentene and cyclopentadiene present in the effluent stream are very small, the decomposition of cyclopentyl cyanide at these temperatures being below 10%.

The presence or absence of toluene had no effect on HCN elimination, except at the highest temperatures of the range, where its absence caused the rate to be slightly higher. This could be due to free radical processes caused by fragmentation of the ring. For the purpose of analysis of the elimination rate data, the values based on hydrogen cyanide, detectable at temperatures over 950K, were combined with the rates based on cyclopentene + cyclopentadiene at temperatures below 950K. This enables the temperature range of HCN elimination to be extended, and the Arrhenius plot is shown in Figure 3.6. A least-squares treatment carried out on the data gives the following first-order rate expression

$$\log k_2 = (12.75 \pm 0.3) - (65.3 \pm 1.3)/\theta$$

where the error limits are one standard deviation. These Arrhenius parameters are consistent with the proposed four-centre cyclic transition-state for HCN elimination.

It can be seen from Table 3.18 that the rates of formation of vinyl cyanide and of cyanopropene are approximately the same at the lower end of the temperature range, but at the higher temperatures the rate constants for cyanopropene are less than those for vinyl cyanide. It was expected that the energetics of reactions 3 and 4 should be similar since the strengths of the breaking C-C bonds in the biradical are not expected to be affected by cyano stabilization. Thus the overall activation energies of the two pathways should be the same, and the A-factors should be similar. Unfortunately, a check on the formation of propylene and of ethylene was complicated by the formation of these products due to ring fragmentation of cyclopentene. Since the investigation was carried out at high
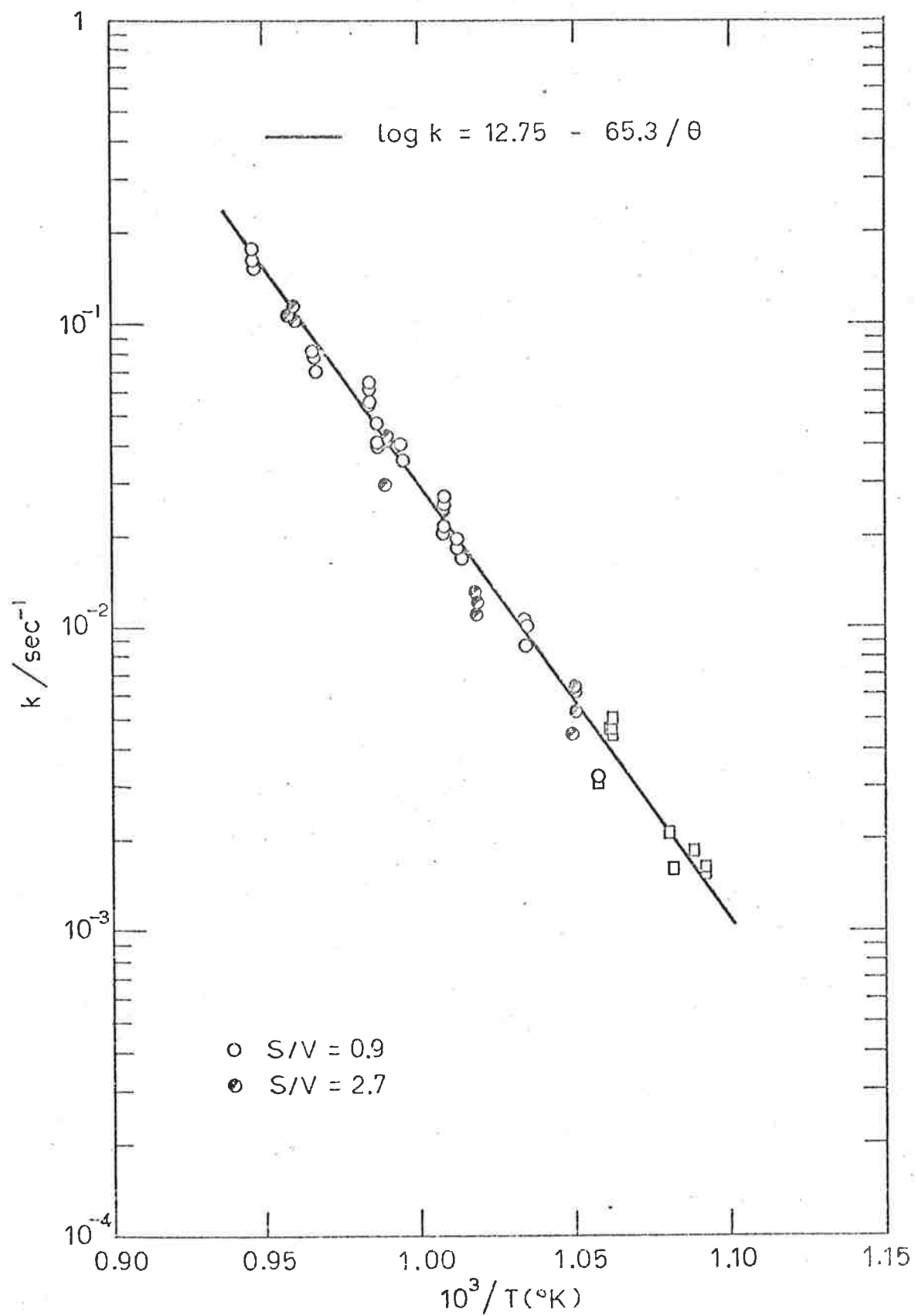
Figure 3.6 Arrhenius plot for HCN elimination from cyclopentyl cyanide. O and □ , formations of HCN and (C_5H_8 + C_5H_6) respectively.

temperatures it was decided to check whether there is any decomposition of crotonitrile or allyl cyanide, which would cause the lower rate constants relative to vinyl cyanide. A study was conducted over 940-1070K, with U/V ~ 0.13 sec^{-1}. Both the squalane and Porapak Q + R columns were used for product analysis. Allyl cyanide was found to decompose to mainly cis-trans crotonitrile before cracking to hydrogen, methane, ethylene, acetylene, propylene, vinyl cyanide and a dark brown residue. Smaller amounts of hydrogen cyanide and methyl cyanide were also observed. The extent of decomposition reached 70% at 1050K. Crotonitrile was found to decompose to a similar extent. Products were methane, ethylene, acetylene, vinyl cyanide and a brown residue, plus some hydrogen, propylene and hydrogen cyanide. Vinyl cyanide was also checked for decomposition, and was found to be fairly stable.

An Arrhenius plot for the formation of vinyl cyanide from cyclopentyl cyanide is shown in Figure 3.7, and the first-order rate expression obtained from a least-squares treatment is

$$\log k_3 = (16.05 \pm 0.25) - (80.0 \pm 1.1)/\theta$$

where the error limits are one standard deviation. From the limited study of crotonitrile and allyl cyanide decomposition, corrected rate constants can be estimated for the formation of cyanopropene. The results were found to be satisfied by the rate expression given by $\log k_4 \sim 16.1 - 81.0/\theta$; that is, having rates which are lower than those for vinyl cyanide by a factor of ~ 2.

When the rates of formation of hydrogen cyanide, vinyl cyanide, and the estimated cyanopropene (corrected for secondary decomposition), are compared with the data available for the disappearance of cyclopentyl cyanide, a discrepancy of 15-20% is evident. It is suspected that a large
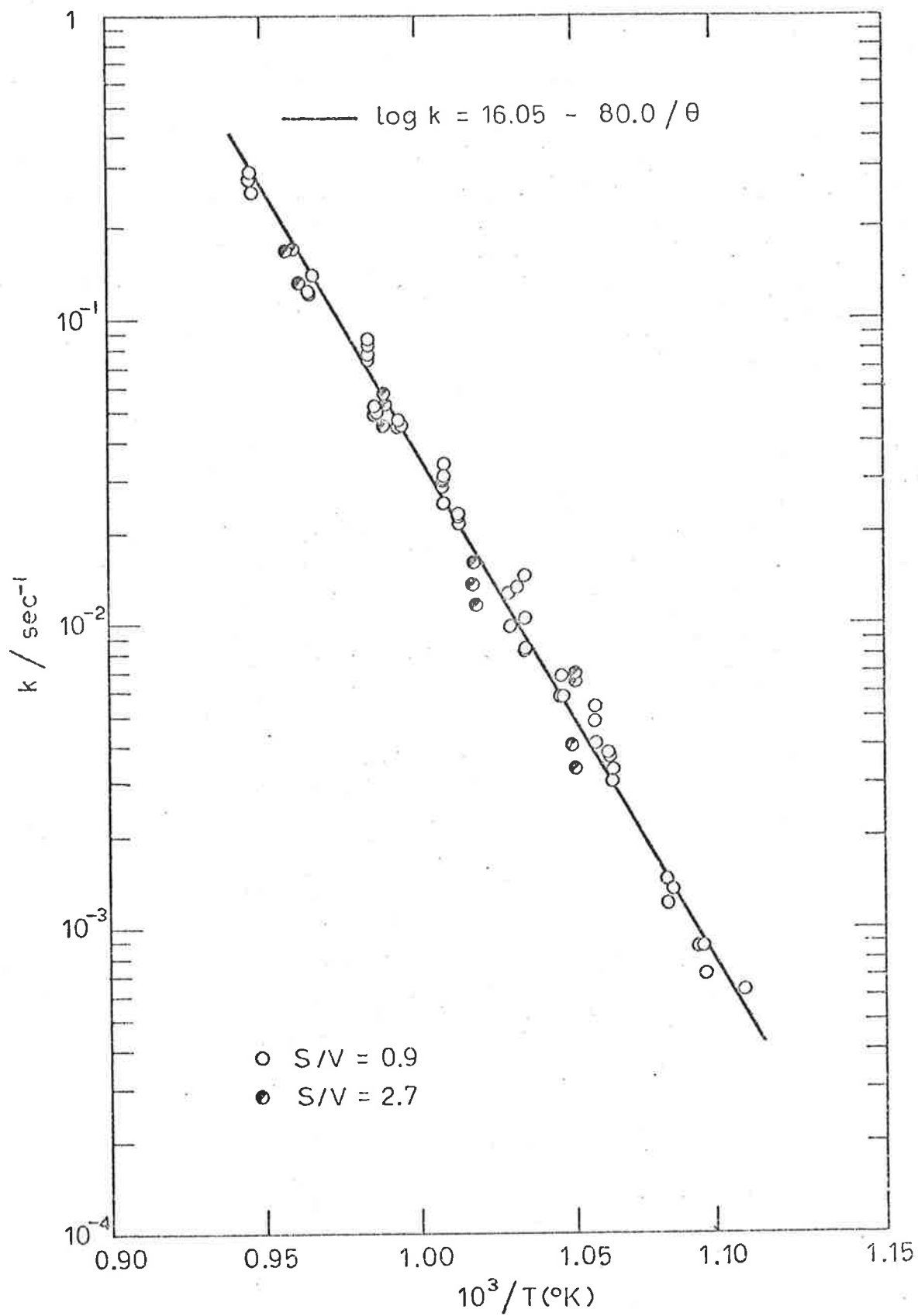
Figure 3.7   Arrhenius plot for vinyl cyanide formation
from cyclopentyl cyanide.

portion of this discrepancy is due to the formation of the brown residue observed along the exit lines. Analysis of it was attempted with the GC, and revealed some very high boilers. This observation brings to mind the dark, tarry, polymeric residues reported by many investigators [26, 27 39] of cyanide pyrolyses. An analysis by Asmus and Hauser [27] of the polymeric residue that they observed, showed it to be of a cyano-substituted ethylenic type.

A limited investigation of the decomposition by the VLPP technique was carried out to verify the results obtained in the high-pressure study. The disappearance of cyclopentyl cyanide was monitored by peak m/e = 54 amu, using argon (m/e = 20 amu) as an internal standard. The formation of vinyl cyanide, propylene and ethylene were monitored at peaks 53, 42 and 28 amu respectively. Hydrogen cyanide was followed at m/e = 27 amu, while cyclopentene and cyclopentadiene were followed at peaks 67 and 66 amu respectively. Peaks 42 and 53 were corrected for cyclopentene contribution, while peaks 27 and 28 amu were also corrected for cyclopentadiene, vinyl cyanide and propylene. The mass spectrometer calibration plots are shown in the Appendix, and the relationships obtained were

$$[VCN]/[c\text{-}PeCN] = (I_{53}/I_{54} - 0.043)/0.4430$$

$$[C_3H_6]/[c\text{-}PeCN] = (I_{42}/I_{54} - 0.944)/0.5079$$

$$[C_2H_4]/[c\text{-}PeCN] = (I_{28}/I_{54} - 0.22)/1.0453$$

$$[HCN]/[c\text{-}PeCN] = (I_{27}/I_{54} - 0.40)/1.1470$$

$$[C_5H_8]/[c\text{-}PeCN] = (I_{67}/I_{54} - 0.07)/0.7687$$

$$[C_5H_6]/[c\text{-}PeCN] = (I_{66}/I_{54} - 0.03)/0.7129$$

Use of these relationships with the experimental data tabulated in the Appendix, results in the rate constants and % decomposition shown in

Tables 3.20 and 3.21. Note that Table 3.20 shows the information for the disappearance of cyclopentyl cyanide, and formations of vinyl cyanide and hydrogen cyanide, while in Table 3.21 these formation rate constants are compared with the results for propylene, ethylene and cyclopentene plus cyclopentadiene. The same product distribution as found for the high-pressure study was observed in the VLPP investigation. Cyclopentene plus cyclopentadiene formation initially agree with the formation of hydrogen cyanide, but as the temperature is increased, a shortfall is evident. From Table 3.21 it can be seen that the rate constants for propylene and for ethylene formation approximate those for vinyl cyanide formation. It was found that there was a 10-15% discrepancy between the formations of vinyl cyanide, propylene, ethylene and hydrogen cyanide and the disappearance of cyclopentyl cyanide. Inspection of the reactor after this study revealed a substantial carbonaceous coating on the walls, which may be the source of the mass balance discrepancy.

To relate the rate constants obtained in the VLPP system to high-pressure parameters requires application of unimolecular rate theory, and from a given A_∞ value, E_∞ is obtained from a fit of k_{uni} versus T to a computed line. Rather than use the A-factors obtained in the high-pressure study, it was decided to estimate them from models of the reaction mechanism, constructed according to the procedures outlined earlier (see section on isopropyl cyanide). A complete vibrational assignment for cyclopentyl cyanide has not been reported in the literature, and estimates were made from the data on cyclopentane and the preceding cyanides. A structural model of cyclopentane was first developed, and the value obtained for its moment of inertia using normal bond lengths and angles [71], was found to agree with the value of Tanner and Weber [86], and Kruse and Scott [87]. Addition of the CN group to the model enabled the moment of inertia

TABLE 3.20   VLPP Results for Cyclopentyl Cyanide Pyrolysis
(flow rate = 8×10^{14} molecules/sec)

Run	Temp K	% decomposition			k_{uni}, sec^{-1}		
		c-PeCN decay	VCN	HCN	c-PeCN	VCN	HCN
Z = 19,550:							
CP 64	1032.6	7.5	3.7	-	0.052	0.025	
55	1043.0	12.5	4.1	-	0.092	0.029	
34	1043.4	16.1	4.8	-	0.123	0.034	
47	1049.2	12.7	5.4	-	0.094	0.039	
65	1051.9	14.2	4.7	-	0.106	0.033	
31	1054.2	17.1	6.5	(2.9)	0.133	0.049	
56	1064.0	18.7	6.3	(1.0)	0.149	0.049	
35	1064.3	17.9	7.7	(4.1)	0.142	0.058	
66	1073.0	24.5	7.3	(5.0)	0.211	0.055	
40	1073.5	24.4	9.6	-	0.211	0.079	
48A	1073.5	23.9	8.0	(1.1)	0.205	0.063	
48	1073.6	23.9	8.1	-	0.204	0.064	
32	1075.6	25.9	9.1	5.0	0.228	0.077	0.042
57	1083.6	28.9	8.3	4.2	0.27	0.071	0.035
36	1084.0	27.6	10.2	8.8	0.25	0.084	0.075
69	1092.3	31.3	10.4	7.3	0.30	0.087	0.063
49	1097.1	37.6	12.3	9.0	0.40	0.110	0.084
58	1103.5	40.0	12.6	9.8	0.44	0.121	0.099
70	1112.6	45.3	14.1	8.1	0.55	0.141	0.082
38	1123.2	51.4	18.0	16.4	0.71	0.207	0.209
50	1123.4	54.5	17.1	11.5	0.80	0.210	0.149
71	1132.0	57.2	17.8	9.2	0.90	0.23	0.120
39	1143.4	62.6	21.2	19.7	1.12	0.32	0.34
Z = 2,140:							
CP 42	1095.8	4.7	3.2	-	0.29	(0.22)	
43	1111.5	9.4	4.0	-	0.62	(0.28)	
74	1113.1	9.9	3.8	-	0.66	(0.25)	
75	1132.8	14.4	4.6	-	1.02	0.34	
44	1133.0	14.8	4.6	-	1.05	0.34	

TABLE 3.21 VLPP Results for Cyclopentyl Cyanide (Z = 19,550)

Comparison of Product Rate Constants

Run	Temp K	cPeCN decay	Rate Constants, k_{uni}, sec^{-1}				
			C-C Scission			HCN Elimination	
			VCN	C_3H_6	C_2H_4	HCN	$(C_5H_8+C_5H_6)$
CP 64	1032.6	0.052	0.025	0.049	0.008		0.011
55	1043.0	0.092	0.029	0.033	0.027		0.022
34	1043.4	0.0123	0.034	0.022	0.002		0.027
47	1049.2	0.094	0.039	0.059	0.015		0.024
65	1051.9	0.106	0.033	0.066	0.013		0.016
31	1054.2	0.133	0.049	0.053	0.031		0.035
56	1064.0	0.149	0.049	0.058	0.052		0.027
35	1064.3	0.142	0.058	0.057	0.016		0.036
66	1073.0	0.211	0.055	0.068	0.029		0.026
40	1073.5	0.211	0.079	0.144	0.064		0.033
48A	1073.5	0.205	0.063	0.102	0.038		0.031
48	1073.6	0.204	0.064	0.085	0.039		0.032
32	1075.6	0.228	0.077	0.081	0.063	0.042	0.047
57	1083.6	0.27	0.071	0.071	0.084	0.035	0.042
36	1084.0	0.25	0.084	0.072	0.043	0.075	0.046
69	1092.3	0.30	0.087	0.095	0.055	0.063	0.036
49	1097.1	0.40	0.110	0.126	0.074	0.084	0.047
58	1103.5	0.44	0.121	0.130	0.123	0.099	0.056
70	1112.6	0.55	0.141	0.138	0.137	0.082	0.059
38	1123.2	0.71	0.207	0.153	0.195	0.209	0.083
50	1123.4	0.80	0.210	0.27	0.27	0.149	0.084
71	1132.0	0.90	0.23	0.33	0.29	0.120	0.083
39	1143.4	1.12	0.32	0.22	0.39	0.34	0.113

for cyclopentyl cyanide to be determined. The vibrational assignment for cyclopentane was taken from Kilpatrick and coworkers [88], Kruse and Scott [87], and Durig and coworkers [89], and its pseudorotation moment of 11.0×10^{-40} g cm^2]90] had to be treated as an internal rotation to give a entropy contribution of ca. 5 cal K^{-1}mole^{-1} at 300K [30]. The resultant entropy data from 300-1300K were consistent with the results of Kilpatrick and coworkers [88]. The same model was applied for cyclopentyl cyanide with the addition of a C-CN stretch (738cm^{-1}), a C≡N stretch (2255cm^{-1}), two C-C-(CN) bends (500cm^{-1}), two C-C≡N bends (175,220cm^{-1}), and two H-C-(CN) bends (1150, 820 cm^{-1}); its pseudorotation moment was assumed to be similar to that for methylcyclopentane (18.0 $\times 10^{-40}$ g cm^2, [91]). The calculated entropy of the molecule, S^0_{300} = 84.8 ca. K^{-1}mole^{-1}, agrees with that obtained from group additivity tables [42]. Details of the molecular parameters used in the RRK(M) calculations are shown in Table 3.22.

The transition-state complex for propylene + vinyl cyanide was based on the structure
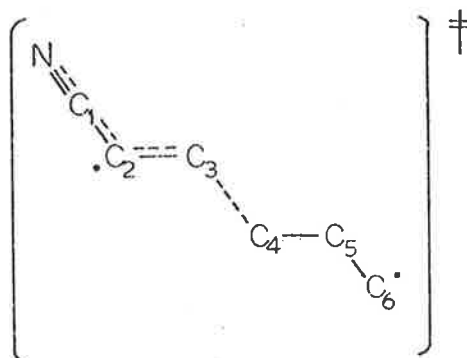
Calculation of the A-factor was made by application of the same procedure for C-C fission outlined in detail for isopropyl cyanide, with the additional assignments for ĊH$_2$, Ċ$_2$H$_4$ torsions and the Ċ$_3$H$_6$ free rotation about the breaking C$_3$-C$_4$ bond. The A-factor obtained is $10^{16.0}$ sec^{-1} at 1100K

TABLE 3.22   Molecular Parameters for Cyclopentyl Cyanide Pyrolysis.

	Molecule	Biradical complex	Complex (-HCN)
Frequencies (cm^{-1}) and degeneracies	2950 (9)	2950 (9)	2950 (8)
	2255 (1)	2255 (1)	2230 (2)
	1465 (4)	1465 (4)	1465 (3)
	1290 (4)	1290 (4)	1290 (4)
	1135 (7)	1135 (7)	1140 (5)
	950 (1)	950 (1)	1055 (1)
	890 (1)	820 (3)	925 (3)
	825 (6)	738 (1)	824 (7)
	738 (1)	500 (2)	530 (3)
	600 (1)	400 (1)	380 (2)
	500 (3)	300 (1)	154 (2)
	220 (1)	245 (3)	126 (1)
	162 (2)	180 (3)	
$I_A \cdot I_B \cdot I_C$, $(g\ cm^2)^3 \times 10^{113}$	1.45	10.9	2.65
I_r, $(g\ cm^2) \times 10^{40}$	18.0 a	29.9^b, 55.0^c	..
Sigma[d]	1.0	1.0	1.0
Collision diameter, Å	6.0		
S^0_{300}, cal K^{-1} mole^{-1}	84.8	93.2^b, 93.8^c	81.1

a   Pseudorotation of ring treated as an internal rotation.

b   For ethylene formation; moment of inertia of $\dot{C}_2H_4 \rightarrow \infty$.

c   For propylene formation; moment of inertia of $\dot{C}_3H_6 \rightarrow \infty$.

d   Sigma = σ/n, where σ is the symmetry number for external rotation, and n is the number of optical isomers.

which agrees with the experimental high-pressure value. The transition-state for ethylene plus cyanopropene formation has a similar structure to that above, except that it has a $\dot{C}_2H_4$ free rotation about the breaking C_4-C_5 bond. Due to its smaller size, it contributes less entropy than does the $\dot{C}_3H_6$ free rotation, thereby giving a slightly lower A-factor; the value is found to be $10^{15.9} \text{sec}^{-1}$. The HCN elimination transition-state was constructed as a four-centre cyclic structure, based on the procedures of O'Neal and Benson [30,45]. For the purposes of calculating the moments of inertia of the complex, a 1,2 elimination was assumed although the 1,4 elimination across the ring could also be considered. The frequencies of the modes involved in the elimination mechanism were reduced to 72% of their molecular values, and the pseudorotation mode was "frozen out" [30]. Calculations using this model give an A-factor of $10^{13.2} \text{sec}^{-1}$ at 1100K, or $10^{12.9} \text{sec}^{-1}$ at 600K which is close to the value obtained from the stirred-flow study. It also agrees with the estimated value for HX elimination from cyclopentyl halides [30].

Before fitting the experimental rate constants for these reaction pathways to the computed curves given by unimolecular rate theory, an examination was made on the rates obtained for cyclopentene decomposition in the VLPP system. As described earlier, the rate of formation of cyclopentadiene can be obtained from the product concentrations of the exit stream from a stirred-flow system. Correcting the escape rate constant, $k_{ea} \propto \sqrt{T/M}$, for the molecular weight of cyclopentene, the results are shown in Table 3.23. Note that the actual yields of cyclopentene from cyclopentyl cyanide were quite small (see Table 3.21). RRKM calculations were carried out. Bond lengths and angles for the molecule were taken from Davis and Mueke [92], and the frequency assignments of Harris and Longshore [93], and Wertz and coworkers [94] were used. The calculated molecular

TABLE 3.23   VLPP Results for Cyclopentene Pyrolysis[a]

Run	Temp K	% formation C_5H_6	k_{uni} sec^{-1}
Z = 19,550:			
CP 28	992.5	41.4	0.52
45	998.0	47.9	0.68
53	1003.9	53.3	0.85
29	1014.1	53.1	0.85
33	1021.5	60.3	1.14
54	1022.9	58.7	1.07
46A	1024.0	60.2	1.14
30	1033.0	61.6	1.21
55	1043.0	67.6	1.58
34	1043.4	65.1	1.41
47	1049.2	72.1	1.97
65	1051.9	75.1	2.29
31	1054.2	69.5	1.74
56	1064.0	73.5	2.13
35	1064.3	68.7	1.68
66	1073.0	77.7	2.7
40	1073.5	79.4	3.0
48A	1073.5	74.9	2.3
48	1073.6	76.0	2.4
32	1075.6	75.4	2.4
57	1083.6	74.1	2.2
36	1084.0	72.4	2.0
69	1092.3	78.1	2.8
49	1097.1	79.1	2.9
58	1103.5	76.6	2.6
70	1112.6	77.3	2.7
38	1123.2	74.9	2.4
50	1123.4	78.0	2.8
71	1132.0	77.4	2.7
39	1143.4	79.0	3.0
Z = 2,140:			
CP 67	1073.0	36.7	4.0
41	1076.5	28.4	2.8
72	1083.7	46.4	6.0
68	1092.3	47.4	6.3
73	1092.4	46.6	6.1
42	1095.8	41.5	5.0
43	1111.5	46.2	6.1
74	1113.1	54.6	8.5
75	1132.8	57.0	9.5
44	1133.0	52.9	8.0

[a] Determined from the VLPP of cyclopentyl cyanide.

entropy of 69.3 cal K^{-1}mole^{-1} at 300K is in agreement with the value reported by Furuyama, Golden and Benson [95]. The transition-state was devised by following the methods already outlined, and the calculated A-factor was found to be $10^{13.0}$sec^{-1} at 600K, and $10^{13.4}$sec^{-1} at 1100K. This is in accord with the experimental values [84]. In Figure 3.8 the unimolecular rate constants over the range 993-1143K are compared with E_∞ (600K) = 58.1 kcal/mole, or E_∞(1100K) = 59.5 kcal/mole. The rate constants found using the 1.1mm aperture up to ca. 1080K, and the 3.3 mm aperture values can be seen to delineate the degree of fall-off. However, the 1.1mm aperture results found at temperatures above 1080K, corresponding to high % decompositions, were found to fall away from the 3.3 aperture values. The mass balance between the sum of the cycloalkenes and hydrogen cyanide is found to also deviate at these temperatures (see Table 3.21). The ring fragmentation of cyclopentene via C-C rupture to form the biradical alkene [84a]

will
account for some of the discrepancy, however, it appears that there is some time dependent mechanism operating at these high temperatures.

Since there are three competitive pathways operating in the decomposition of cyclopentyl cyanide, the RRK/3 method was used (see page 214, Appendix for derivation). In Figures 3.9, 3.10 and 3.11 the experimental rate constants for scission products VCN, and ethylene, and for HCN elimination, are compared with the RRK/3 computed curves. The assumption of equivalent activation energies has been made for the two bond fission pathways, since the strengths of the breaking bonds in the molecule and the biradical should be the same in each case. It was found that the computed curves (see Figures 3.9 and 3.10) give very similar values since their estimated A-factors differ by only $10^{0.13}$sec^{-1}. Fitting the vinyl cyanide
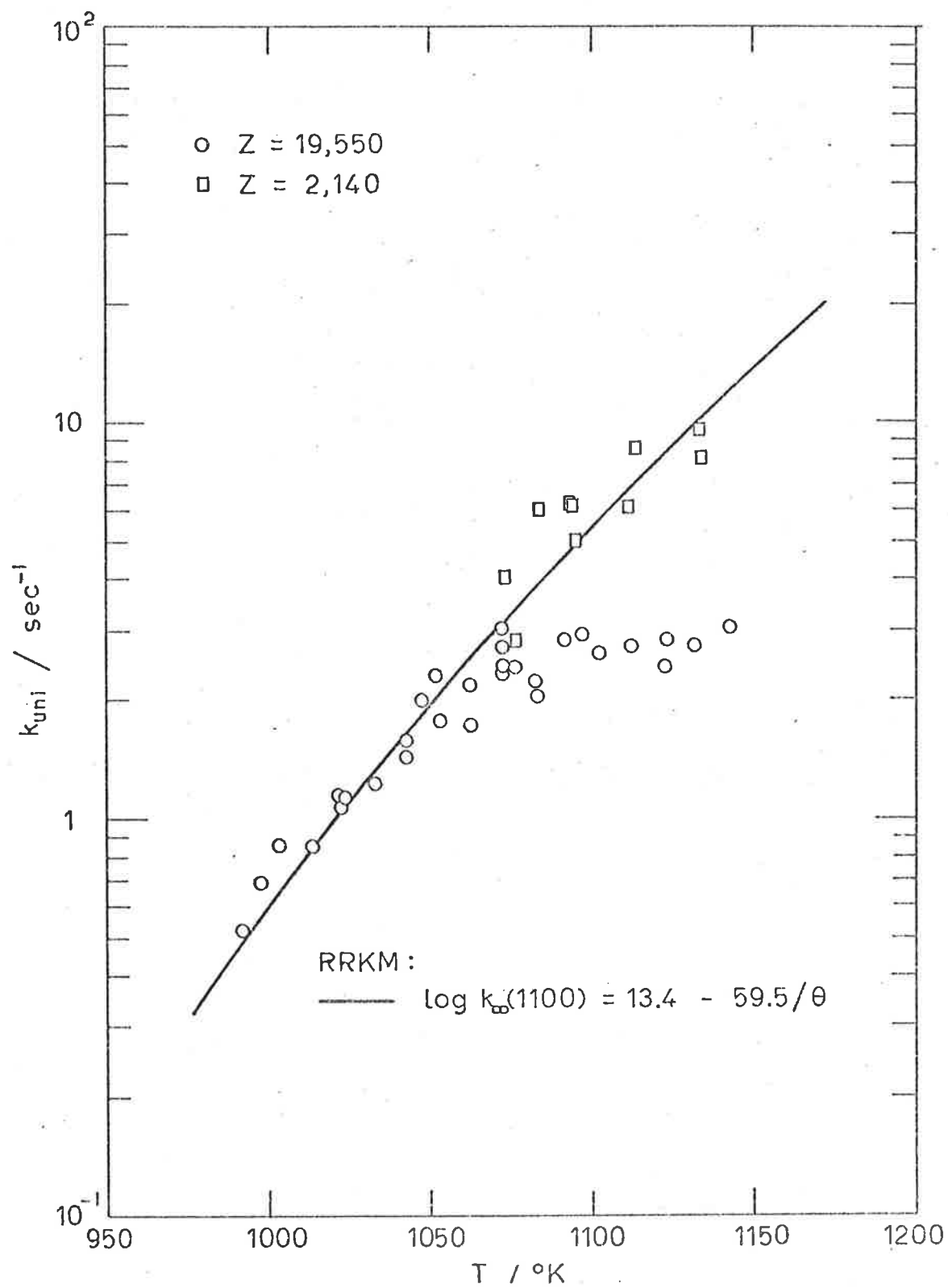
Figure 3.8 k_{uni} as a function of T for the formation of
cyclopentadiene from cyclopentene.
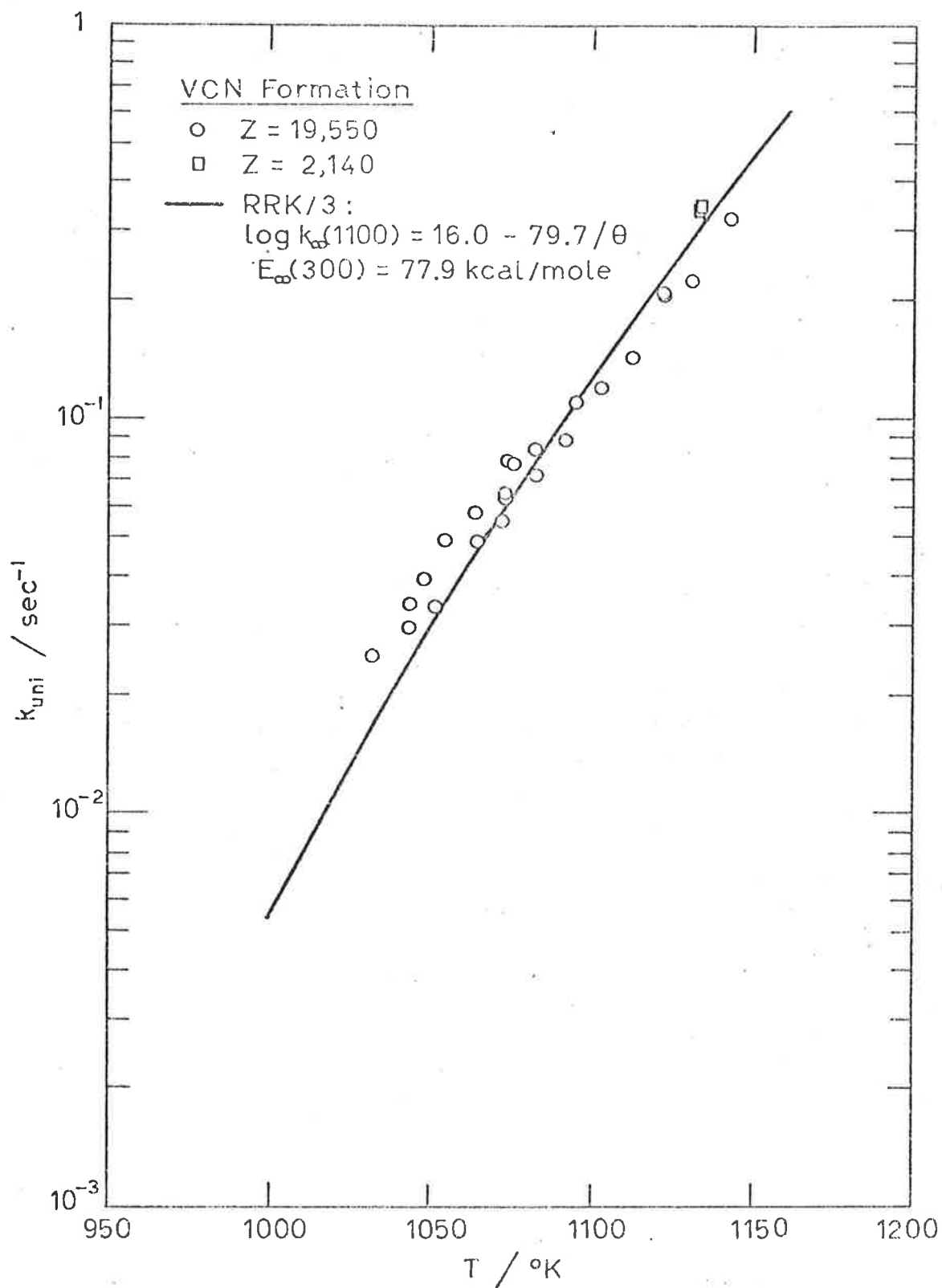
Figure 3.9 k_{uni} as a function of T for the formation of vinyl cyanide from cyclopentyl cyanide. Complementary RRK/3 curves are shown in Figures 3.10 and 3.11.
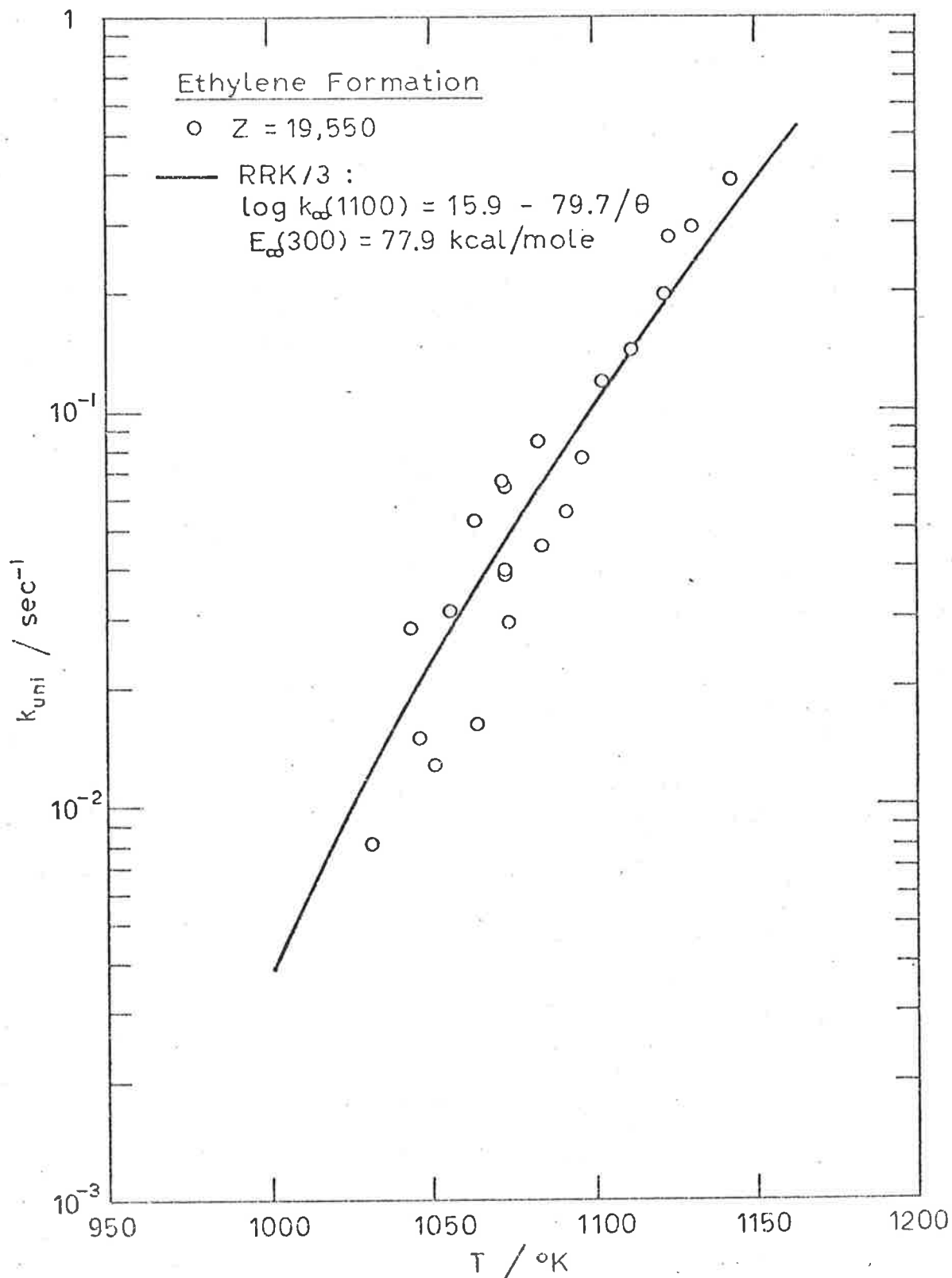
Figure 3.10. k_{uni} as a function of T for the formation of
ethylene from cyclopentyl cyanide. Complementary
RRK/3 curves are shown in Figures 3.9 and 3.11.
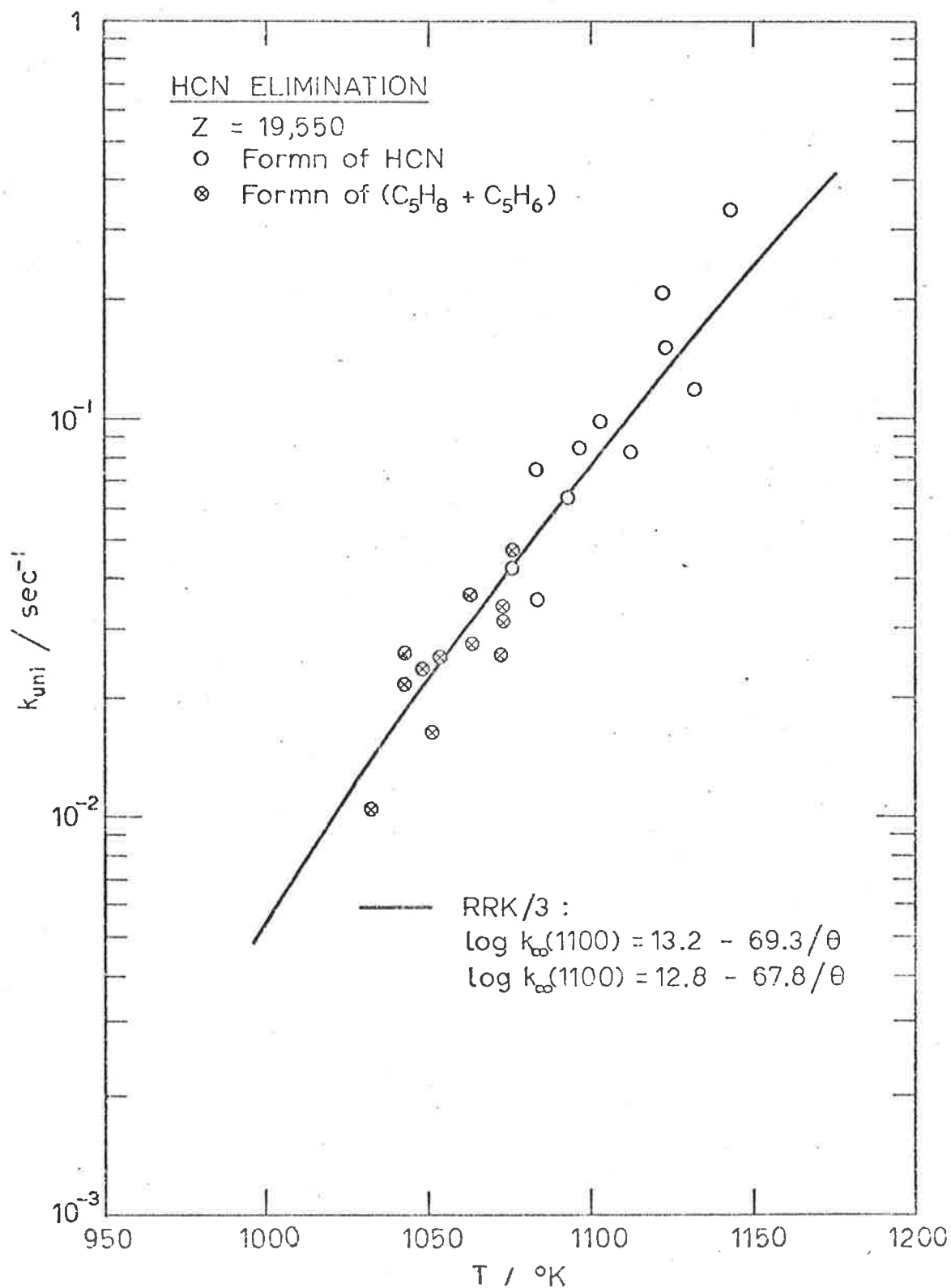
Figure 3.11. k_{uni} as a function of T for HCN elimination from cyclopentyl cyanide. Complementary RRK/3 curves are shown in Figures 3.9 and 3.10.

rate data gives the following high-pressure rate expression

$$\log k_{3,\infty} (1100K) = 16.0 - 79.7/\theta$$

which is virtually identical with the result obtained in the high-pressure study. Although there is some scatter attached to the ethylene rate constants they are consistent with the rate expression

$$\log k_{4,\infty} (1100K) = 15.9 - 79.7/\theta$$

The VLPP study shows the rates of ethylene and cyanopropene formation to be a factor of ca. 1.4 less than the rates for vinyl cyanide formation, which is in good agreement with the results of the high-pressure study where the factor was estimated to be ~ 2. In Figure 3.11 the RRK/3 computed curve for HCN elimination is compared with the unimolecular rate constants for hydrogen cyanide and the summed values for cyclopentene and cyclopentadiene (at temperatures less than 1080K). The data are found to be reasonably consistent with the Arrhenius expression

$$\log k_{2,\infty} (1100K) \simeq 13.2 - 69.3/\theta$$

The high-pressure study of this reaction, however, gives a lower A-factor ($10^{12.75} \sec^{-1}$ at $T_m \sim 1000K$); and if the A_{∞} is now adjusted to this value, the RRK/3 computed curve is found to be refitted by

$$\log k_{2,\infty} (1100K) \simeq 12.8 - 67.8/\theta$$

An uncertainty of ca. ± 2 kcal/mole in the activation energy obtained, shows the VLPP and high-pressure studies of HCN elimination to be in agreement within experimental errors.

3.7   Ethyl Cyanide

From the preceding studies it was anticipated that C-C bond fission should be the major pathway for the pyrolysis

$$C_2H_5CN \rightarrow \dot{C}H_3 + \dot{C}H_2CN \qquad (1)$$

An initial investigation showed the decomposition to be too slow under VLPP conditions.   Therefore the stirred-flow reactor was used for this study over a temperature range of ca. 890-1075K.   It has been shown (see section on isopropyl cyanide) that the previous studies by Hunt and coworkers [28], and Dastoor and Emovon [32], suffered from the complications of secondary chain processes even in the presence of a chain inhibitor.   At the temperatures required for the pyrolyses of alkyl cyanides, it has been shown earlier that very large amounts of inhibitor are required to decrease the effect of chain processes.   Thus, a few preliminary experiments were carried out using large volumes of toluene added to the ethyl cyanide in the saturator.   Using a diethylene glycol adiapate column, GLC analysis indicated the products hydrogen cyanide, vinyl cyanide and methyl cyanide, while analysis of the low boilers using a Porapak Q + R column, revealed hydrogen, methane and ethylene.   Thus the suspected free radical chain formation of hydrogen and vinyl cyanide, observed by Hunt and coworkers [28] is still a substantial pathway of decomposition even with large amounts of inhibitor.   Almost all the hydrogen cyanide and ethylene result from the chain reactions; the molecular elimination of HCN

$$C_2H_5CN \rightarrow C_2H_4 + HCN \qquad (2)$$

should, from the n-propyl cyanide study [80], be practically not observable.

The gas chromatograph was calibrated for the products hydrogen cyanide, methyl cyanide (MeCN), and vinyl cyanide, against ethyl cyanide (EtCN).   The relationships obtained from the calibration plots are

[MeCN]/[EtCN] = 1.4695 x peak area ratio, MeCN/EtCN

[VCN]/[EtCN] = 0.9625 x peak area ratio, VCN/EtCN

[HCN]/[EtCN] = 5.28 x peak area ratio, HCN/EtCN

Before considering the results when a chain inhibitor is present, it was decided to follow the reactions that occur without the inhibitor to gather information on the free-radical chain reactions. The experimental data obtained over the temperature range 896-1020K are included in the Appendix, and the results are summarized in Table 3.24. Over residence times of 3.8-7.7 seconds, mainly hydrogen, ethylene, hydrogen cyanide and vinyl cyanide were found, with only a small amount of methyl cyanide being observed at the higher temperatures. The chain reactions were also observed in the reaction vessel containing a threefold increase in the S/V ratio. The results are shown in Figure 3.12. The rate constants obtained are unaffected by the increase in surface-to-volume ratio, and indicate that application of the steady-state treatment to the differential equations of the probable chain steps could give parameters to satisfy the observed values, and yield a plausible free radical mechanism (see Chapter 4). The experimental rate data were found to satisfy a first-order relationship, and the Arrhenius parameters found from a least-squares procedure are

$$\log k = 14.3 - 67.8/\theta \quad \text{for the formation of HCN}$$
$$\log k = 12.1 - 59.1/\theta \quad \text{for the formation of VCN}$$

Comparison with the VLPP results indicate that the observed activation energy for hydrogen cyanide formation is too low to be explained in terms of a four-centre molecular elimination. The rate constants are approximately a thousand times larger than predicted from analogy with n-propyl cyanide (see Chapter 4). The formation of vinyl cyanide with accompanying liberation of hydrogen most certainly is not a molecular elimination reaction, and this pathway was not observed for the other cyanides.
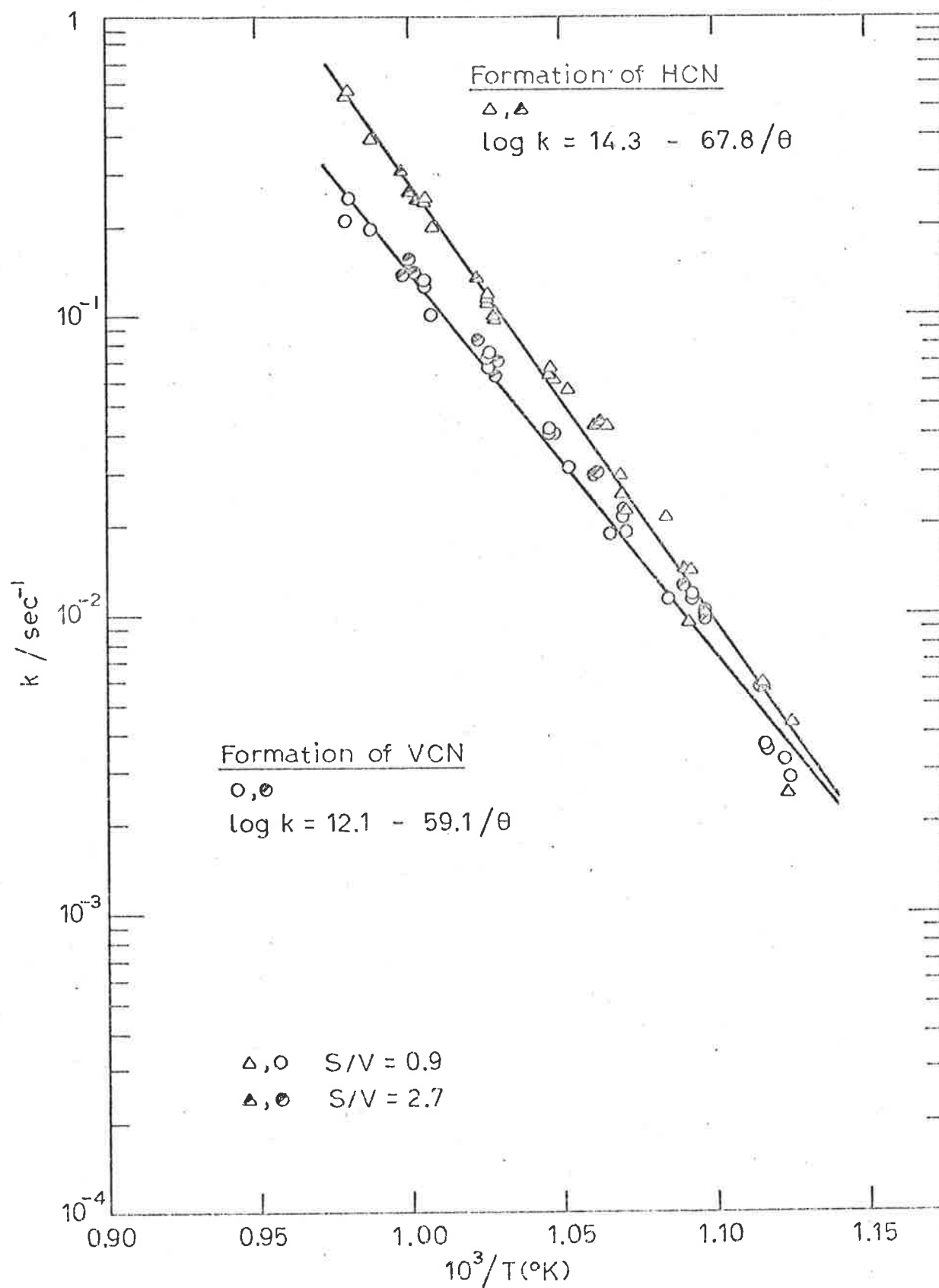
Figure 3.12.   Arrhenius plot for free-radical formations of hydrogen cyanide and of vinyl cyanide from ethyl cyanide.

TABLE 3.24   Stirred-flow Reactor Results for Ethyl Cyanide
(in the absence of a chain inhibitor)

Run	Temp K	Flow rate U, mls/sec	U/V	$k \times 10^2$, sec^{-1} HCN	VCN
ET 7	888.6	21.84	0.1218	0.43	0.28
8	890.3	30.67	0.1710	0.25	0.32
21	895.2	26.47	0.1476	0.56	0.35
20	895.5	32.74	0.1826	0.58	0.36
19	895.7	23.33	0.1301	0.59	0.58
23	914.4	33.93	0.1893	1.40	1.13
22	915.6	24.18	0.1349	0.93	1.12
9	921.5	22.24	0.1240	2.10	1.10
24	932.4	25.45	0.1419	2.21	1.86
25	934.0	34.61	0.1930	2.5	2.09
26	934.2	42.46	0.2368	2.9	2.25
11	938.2	32.42	0.1808	4.3	1.80
10	950.2	23.28	0.1298	5.6	3.0
29	954.2	44.04	0.2456	6.1	3.9
28	954.7	34.93	0.1948	6.7	4.1
27	954.8	26.08	0.1454	6.2	3.9
32	974.1	45.54	0.2540	11.7	7.4
31	974.5	35.99	0.2007	11.2	7.2
30	974.6	25.98	0.1449	10.7	6.6
33	991.7	26.08	0.1455	19.5	10.0
34	994.1	36.76	0.2050	24.6	12.4
35	994.1	46.06	0.2569	24.1	12.7
38	1011.6	46.93	0.2617	37.9	19.1
37	1019.7	37.83	0.2110	56.4	24.5
36	1020.2	27.30	0.1523	55.0	20.6

Free-radical processes are the likely cause.

The effect of the presence of a chain inhibitor, namely aniline, was examined. Product analysis was by flame ionization using the diethylene glycol adiapate column. With an aniline/ethyl cyanide ratio of ~ 4, the rates of formation of hydrogen cyanide and vinyl cyanide decrease by a factor of ~20 from the values obtained in the absence of inhibitor. The results are found to be in close agreement with the values for hydrogen and HCN formation obtained by Hunt and coworkers [28], and with Dastoor and Emovon's work [32] on HCN formation. However, on increasing the ratio of inhibitor to reactant, the rates of formation continued to decrease. This was monitored until the dominating presence of aniline began to interfere with the chromatographic measurements of the reaction products.

The formation of methyl cyanide was also observed in the above experiments, and the rate constants obtained are plotted in Figure 3.13. When the aniline/reactant ratio is ~ 4, the rate constants obtained are similar to those reported by Hunt and coworkers [28], but as the ratio is increased to 6 and 8:1 the rate of formation of methyl cyanide decreases and steadies with values that are 2-3 times less than those at 4:1. This is probably a result of competition between the reactions

$$\dot{C}H_2CN + RH \rightarrow CH_3CN + \dot{R} \tag{3}$$

$$\dot{C}H_2CN + C_2H_5CN \rightarrow CH_3CN + \dot{C}_2H_4CN \tag{4}$$
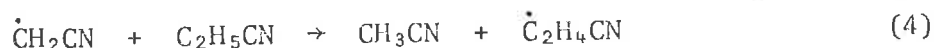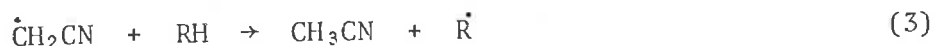
If insufficient inhibitor (RH) is present then the cyanomethyl radical can attack the ethyl cyanide and thereby reduce its concentration. The rate constants for C-C fission thereby obtained from [MeCN]/[Et-CN] are observed to decrease to a limit as reaction (3) becomes the dominant pathway for cyanomethyl radicals. At the highest temperatures of the range, the rate constants fall away probably due to the decomposition of

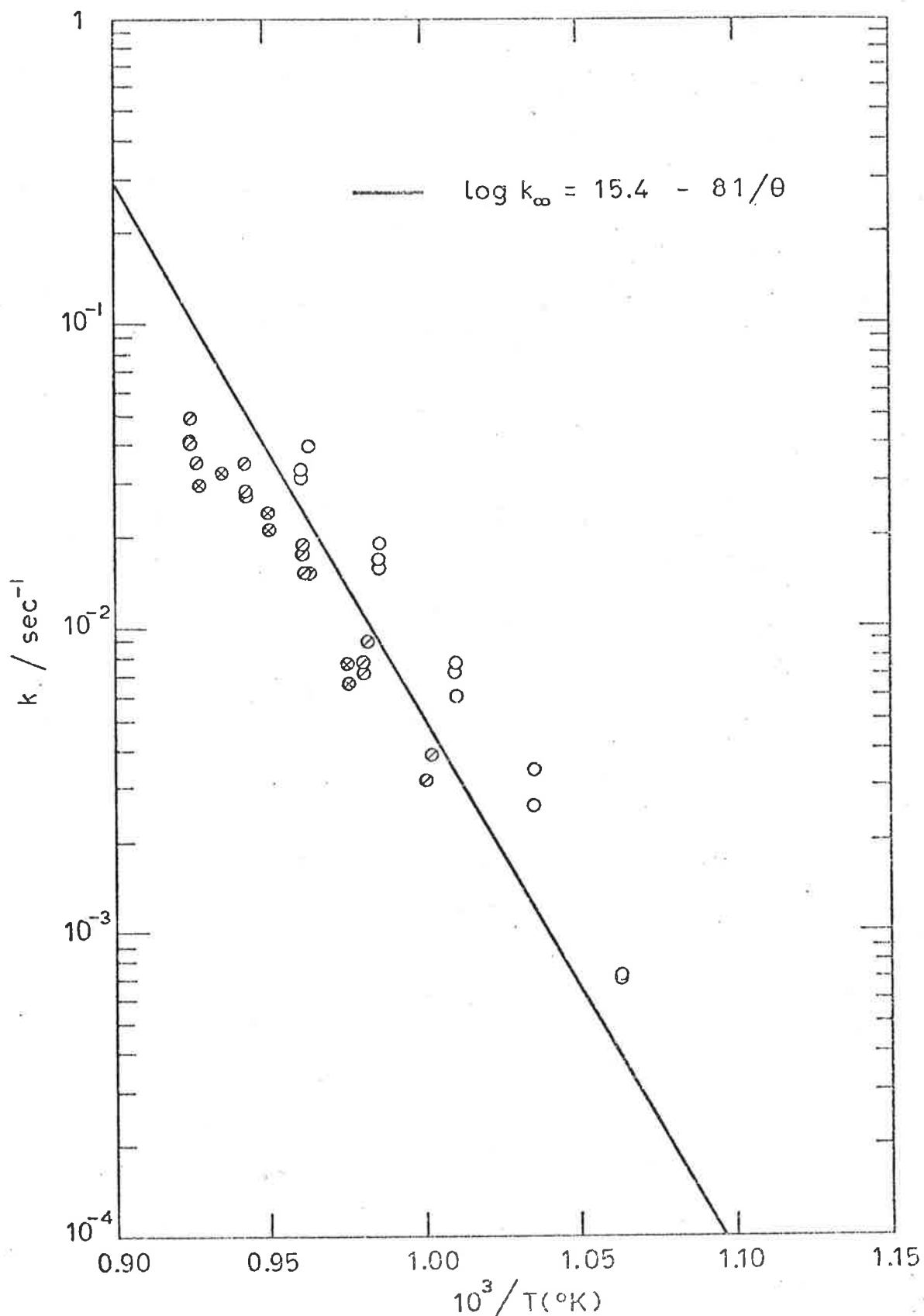Figure 3.13.   Arrhenius plot for methyl cyanide formation
from ethyl cyanide.

o   ,   aniline/ethyl cyanide ~ 4,

⊘   ,   aniline/ethyl cyanide ~ 6,

⊗   ,   aniline/ethyl cyanide ~ 8.

———   ,   prediction based on the VLPP of

n-propyl cyanide.

methyl cyanide [27]. The line corresponding to the predicted rate expression,*

$$\log \; k \; (1100K) \; \simeq \; 15.4 \; - \; 81/\theta$$

for C-C fission in ethyl cyanide has also been included in Figure 3.13. Although the data obtained from this brief investigation are insufficient to determine rate parameters, they support the parameters predicted from the VLPP of n-propyl cyanide.

An aniline/ethyl cyanide ratio of ten or more was found to interfere with product analysis, and thus it was decided to investigate the effect of toluene as the chain inhibitor, in an attempt to obtain the limiting unimolecular rate constants for HCN elimination. Due to similar retention times of ethyl cyanide and toluene on the diethylene glycol adiapate column, a squalane column was used, which allowed the formation of hydrogen cyanide to be followed, but not of methyl cyanide or vinyl cyanide due to their similar retention periods on this column. A series of experiments were carried out at temperatures of 900, 941 and 990K, with toluene/reactant ratios of up to ~ 60; the two lower temperatures are within Dastoor and Emovon's range [32]. The results are shown with predicted rate constants (see discussion, Chapter 4) in Table 3.25. A low boilers analysis using the Porapak Q + R column showed a rapid disappearance of hydrogen and ethylene with increasing inhibitor concentration. Over this range of inhibitor to ethyl cyanide, the rate of formation of hydrogen cyanide declined by a factor of ~ 300, and a limiting value was not obtained due to the chromatograph's insensitivity to HCN in the effluent

---

* The results of the VLPP of n-propyl cyanide yield the heat of formation of the cyanomethyl radical, from which the activation energy for ethyl cyanide fission can be estimated (see Chapter 4, pg 152) The A-factor is found by following the procedures outlined for the other alkyl cyanides.

TABLE 3.25   Rate of Formation of HCN with the Addition of Toluene as a Chain Inhibitor.

T = 900K		T = 941K		T = 990K	
$\dfrac{PhCH_3}{EtCN}$	$k,\ sec^{-1}$	$\dfrac{PhCH_3}{EtCN}$	$k,\ sec^{-1}$	$\dfrac{PhCH_3}{EtCN}$	$k,\ sec^{-1}$
0	9.7×10^{-3}	0	3.3×10^{-2}	0	2.9×10^{-1}
1.4	2.3×10^{-3}	1.0	1.4×10^{-2}	1.2	8.5×10^{-2}
5.5	4.0×10^{-4}	1.2	3.2×10^{-3}	3.5	3.5×10^{-2}
20	$\sim 1 \times 10^{-4}$	2.2	8.6×10^{-4}	8.5	1.1×10^{-2}
>20	HCN not detectable	8	4.7×10^{-4}	35	3.2×10^{-3}
		19	$\sim 1 \times 10^{-4}$	60	$\sim 1 \times 10^{-3}$
		>20	HCN not detectable	>60	HCN not detectable
molecular elimination[a]	5×10^{-7}	molecular elimination[a]	4×10^{-6}	molecular elimination[a]	5×10^{-5}

[a]   Predicted from $\log k \simeq 13.6 - 82/\theta$ (see Chapter 4, page 152)

samples. As mentioned earlier when similar results were found from the isopropyl cyanide investigation in the flow system, it is surprising that Dastoor and Emovon did not observe any change in HCN formation in the presence or absence of toluene.

CHAPTER 4.

DISCUSSION AND CONCLUSIONS

Before examining in detail the effect of the cyano group on the pyrolyses, reviews of the kinetic parameters obtained in Chapter 3 are made, and reaction mechanisms proposed. The results are compared with the previous studies on the thermal decomposition of organic cyanides. This is followed by a study of bond dissociation energies and heats of formation of cyano radicals obtained from C-C fission of the alkyl cyanides. The parameters for HCN elimination are compared with HX elimination from alkyl halides, and the semi-ion pair theories are tested for their applicability. The postulated four-centre transition-state for elimination is examined in the light of these results. The chapter closes with implications and conclusions of this research program.

4.1   Discussion

The resultant experimental Arrhenius parameters obtained and
reported in Chapter 3 for each cyanide in this research investigation are
repeated below and reviewed in relation to each other and with the results
of other researchers.   To assist the discussion, the compounds are
examined under the categories of cyclic cyanides and alkyl cyanides.

4.1.1   Review of Cyclic Cyanides

The VLPP technique was applied to the pyrolysis of cyclobutyl
cyanide over the temperature range 833 – 1023 K, and the decomposition was
found to yield ethylene and vinyl cyanide.   Basing the value of A_∞ on
the high–pressure work of Sarner and coworkers [35], the unimolecular
rate constants are given by the high–pressure rate expression

$$\log k = 15.0 - (57.0 \pm 1.0) / \theta$$

However, if A_∞ is adjusted relative to the VLPP results for cyclobutane
[49], then an A–factor of $10^{15.9}$ sec^{-1} is obtained (see Chapter 3, page 65).
The experimental rate constants are then found to be fitted by a
unimolecular rate theory computed curve having E_∞ = 59.1 $\pm$ 1.0 kcal/mole.

The above experimental Arrhenius parameters obtained for cyclobutyl
cyanide are shown in Table 4.1 and compared with the rate constants
reported by Sarner and coworkers in Tables I and II of their study [35].
There is good agreement with the data of Table II, but their Table I data
suggests that a heterogeneous process could be present.   A similar
observation is also made for their trans – 1,2 – dicyanocyclobutane results
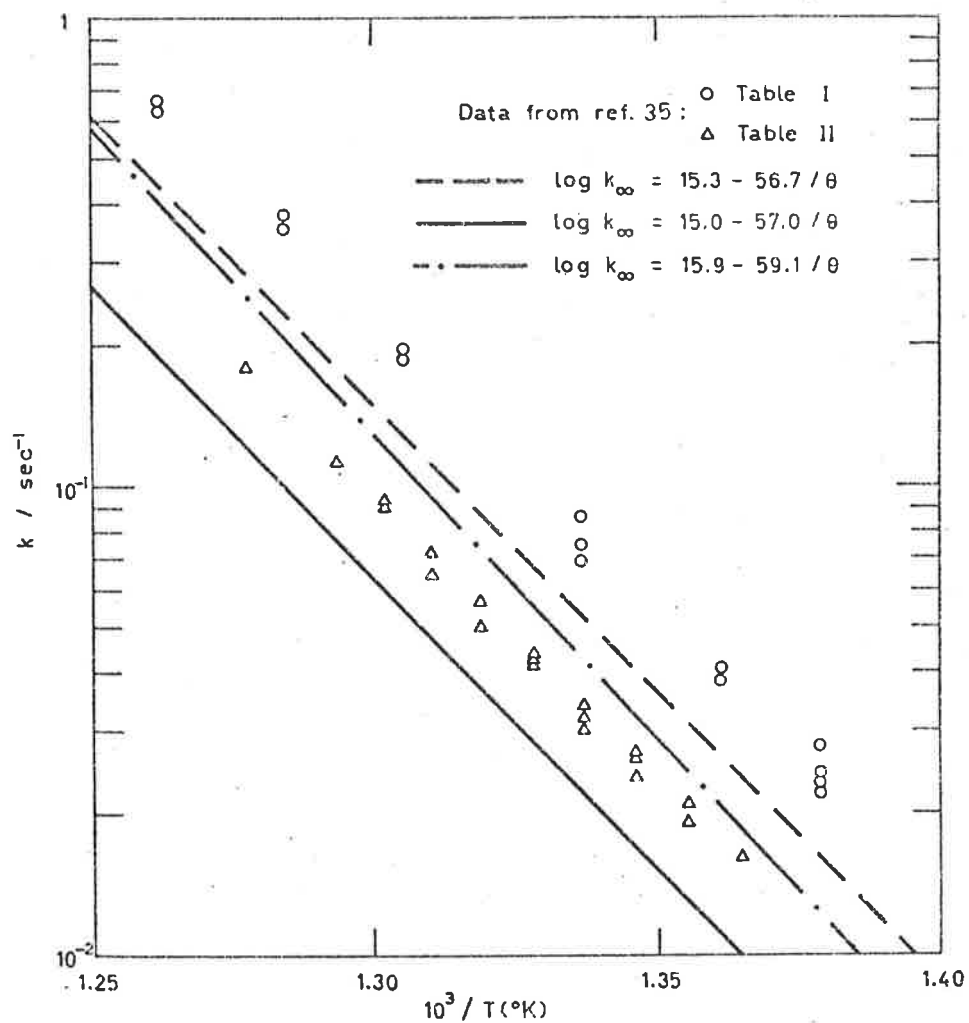(see later discussion, page 145).

Figure 4.1 Arrhenius plot for the decomposition of cyclobutyl cyanide. — — — —, parameters from [35]; ————— and —— · —— parameters from this work.

The high-pressure pyrolysis of <u>trans - 1,2 - dicyanocyclobutane</u> yielded vinyl cyanide as the only product over the temperature range 571–661 K. A least-squares treatment of the observed rate constants gives log k = (16.0 ± 0.3) - (52.9 ± 0.8) / θ where the error limits are one standard deviation. On the basis of the cyano group reducing the cyclobutane A-factor by $10^{0.3}$ sec^{-1} per reaction path [79], the A-factor for trans - 1, 2 - dicyanocyclobutane is predicted to be $10^{1.2}$ sec^{-1} less than that for cyclobutane. If this is the case then taking the results of Walters and coworkers [96] for cyclobutane (log k = 15.6 - 62.5 / θ), anc A = $10^{14.4}$ sec^{-1} is obtained, while the recent VLPP study on cyclobutane [49] (log k = 16.5 - 65.5 / θ) gives A = $10^{15.3}$ sec^{-1} .

To qualify this descrepancy between the experimental A-factors and values predicted from the parent ring compound, it was decided to develop a transition-state model for the decomposition of four-membered ring compounds based on the known molecular parameters for cyclobutane and using the methods outlined in Chapter 3. This procedure would be used to yield estimated A-factors for the series cyclobutane, cyclobutyl cyanide, and trans - 1,2 - dicyanocyclobutane. A planar ring structure using normal bond lengths and angles was used in the calculation of the moments of inertia products. The value of the moments of inertia products obtained for cyclobutane is in good agreement with the puckered ring value of 0.952 x 10^{-114} $(g\ cm^2)^3$ reported by Beadle and coworkers [49]. The values obtained when cyano groups are added to the ring structure were for cyclobutyl cyanide and trans - 1,2 - dicyanocyclobutane. The moments of inertia products for the respective transition-states were calculated for the structure
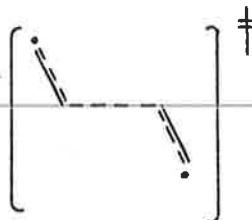
with the breaking bond lengthened by 1Å. The frequency assignments for

the cyclobutane molecule were taken from reference 49, and from Rathjens and coworkers [63]. Using this as a foundation for cyclobutyl cyanide and the dicyanide, the additional assignments for the cyano group contributions were taken from Klaboe [64a], and Durig and coworkers [64b, 65] as outlined for the isopropyl cyanide study in Chapter 3. The calculated entropies were adjusted to agree with the group additivity estimations by lowering the ring vibration frequencies slightly. (It was expected that these vibrations would be progressively lower than those of cyclobutane due to the heavy cyano group). Applying the procedures outlined in Chapter 3 for the frequency assignment of the transition-state, the C-C stretch at 930 cm^{-1} was taken as the reaction co-ordinate, the frequencies of two methylene rocks (890 cm^{-1}) and two methylene wags (1150 cm^{-1}) were lowered to 30% of their molecular values, and the C-C-(CN) bend (450 cm^{-1}) and the two C-C≡N bends (165, 200 cm^{-1}) were increased to 140% of their molecular values, to account for resonance stabilization. Table 4.1 lists the frequencies and parameters used to calculate the A-factors. (the frequencies have been averaged and rounded).

From these proposed models, the estimated values of log (A, sec^{-1}) for cyclobutane, cyclobutyl cyanide, and trans-1,2-dicyanocyclobutane are 16.0, 15.4 and 14.9 respectively, all quoted at 700K. The differences between the A-factors for the series is in agreement with the cyano group lowering the cyclobutane A-factor by $10^{0.3}$ sec^{-1} per reaction path [79]. Although the A-factor for cyclobutane is higher than the estimate of O'Neal and Benson [61], their value should be revised using more recent group additivity data [42]; the calculated value is $10^{16.0}$ sec^{-1}.

This development of reaction models using a consistent treatment gives Arrhenius A-factors that lie between the values predicted from the

TABLE 4.1   MOLECULAR PARAMETERS FOR CYANOCYCLOBUTANE PYROLYSIS

	Cyclobutane		Cyclobutyl Cyanide		Trans-1,2-dicyanocyclobutane	
	Molecule	Complex	Molecule	Complex	Molecule	Complex
Frequencies and degeneracies (cm^{-1})	2900 (8)	2900 (8)	2900 (7)	2900 (7)	2900 (6)	2900 (6)
	1450 (4)	1450 (4)	2250 (1)	2250 (1)	2250 (2)	2250 (2)
	1300 (4)	1300 (6)	1450 (3)	1450 (3)	1450 (2)	1450 (2)
	1150 (4)	1150 (2)	1300 (5)	1300 (7)	1300 (6)	1300 (8)
	1000 (1)	890 (2)	1150 (3)	1100 (2)	1150 (2)	1050 (2)
	930 (2)	400 (2)	950 (3)	890 (1)	950 (3)	630 (2)
	890 (4)	350 (2)	890 (3)	630 (1)	890 (2)	350 (2)
	750 (1)	270 (2)	695 (2)	370 (1)	740 (2)	320 (2)
	625 (1)	200 (1)	500 (2)	320 (1)	550 (1)	275 (4)
	95 (1)		320 (1)	275 (3)	450 (3)	215 (4)
			200 (1)	215 (2)	320 (2)	100 (1)
			165 (1)	100 (1)	200 (2)	
			80 (1)		165 (2)	
					60 (1)	
$I_A \cdot I_B \cdot I_C$, $(g\ cm^2)^3$ $\times 10^{114}$	0.978	4.00	6.71	40.4	31.8	203.6
Sigma	8	1	1	1	1	1
S^0_{300}, cal K^{-1} mole^{-1}	63.3	72.1	77.9	84.5	88.0	93.1
log A_∞ (300K)		15.2		14.7		14.3
log A_∞ (700K)		16.0		15.4		14.9

experimental work of Walters and coworkers [96], and Beadle and coworkers [49] using VLPP.

If the A-factor of $10^{14.9}$ sec^{-1} predicted above for trans $-$ 1,2 $-$ dicyanocyclobutane is combined with the rate constant at the mid-temperature of this work, then the activation energy obtained is 49.8 kcal/mole.   Similarly, if the prediction for A $(10^{15.3}$ sec$^{-1})$ based on VLPP study of cyclobutane [49] is used, then we find an activation energy of 50.9 kcal/mole.   The line corresponding to these latter parameters has been plotted in Figure 4.2 as a comparison with the experimental rate constants. It is found that the postulated line passes within the error limits of the data points, and that the A-factor is just over two standard deviations and within the 95% confidence limits of the least-means-squares parameter.*

The high-pressure data obtained by Sarner and coworkers [35] have also been plotted in Figure 4.2.   Their rate constants are much higher than the present study although the discrepancy diminishes with increasing temperature.   This suggests that the results of Sarner and coworkers may contain a heterogeneous component although no evidence for such effects was found in this study.

The formation of vinyl cyanide and propylene, and cyanopropene and ethylene (in similar concentrations), from the decomposition of cyclopentyl cyanide, is consistent with a biradical mechanism.   Over the temperature range 905–1143 K, the two pathways for decomposition of the ring are found to be competitive, and the high-pressure and VLPP studies give excellent agreement for the reaction kinetics.   The Arrhenius expression for vinyl cyanide formation is log k = $(16.0 \pm 0.3) - (80 \pm 1.5)$ /θ, while that for the products cyanopropene and ethylene is log k = 15.9 $-$ 80 /θ .   The A-factors are consistent with the biradical mechanism [61].   HCN elimination is found to be the only other reaction pathway over the range, accounting for

---

* It should be noted that there might be some experimental complexities which bias the data toward a high A-factor.   As discussed in Chapter 3, page 69, during sampling there existed the possibility of condensation of the dicyanide due to its low volatility resulting in rate constants larger than the true value.
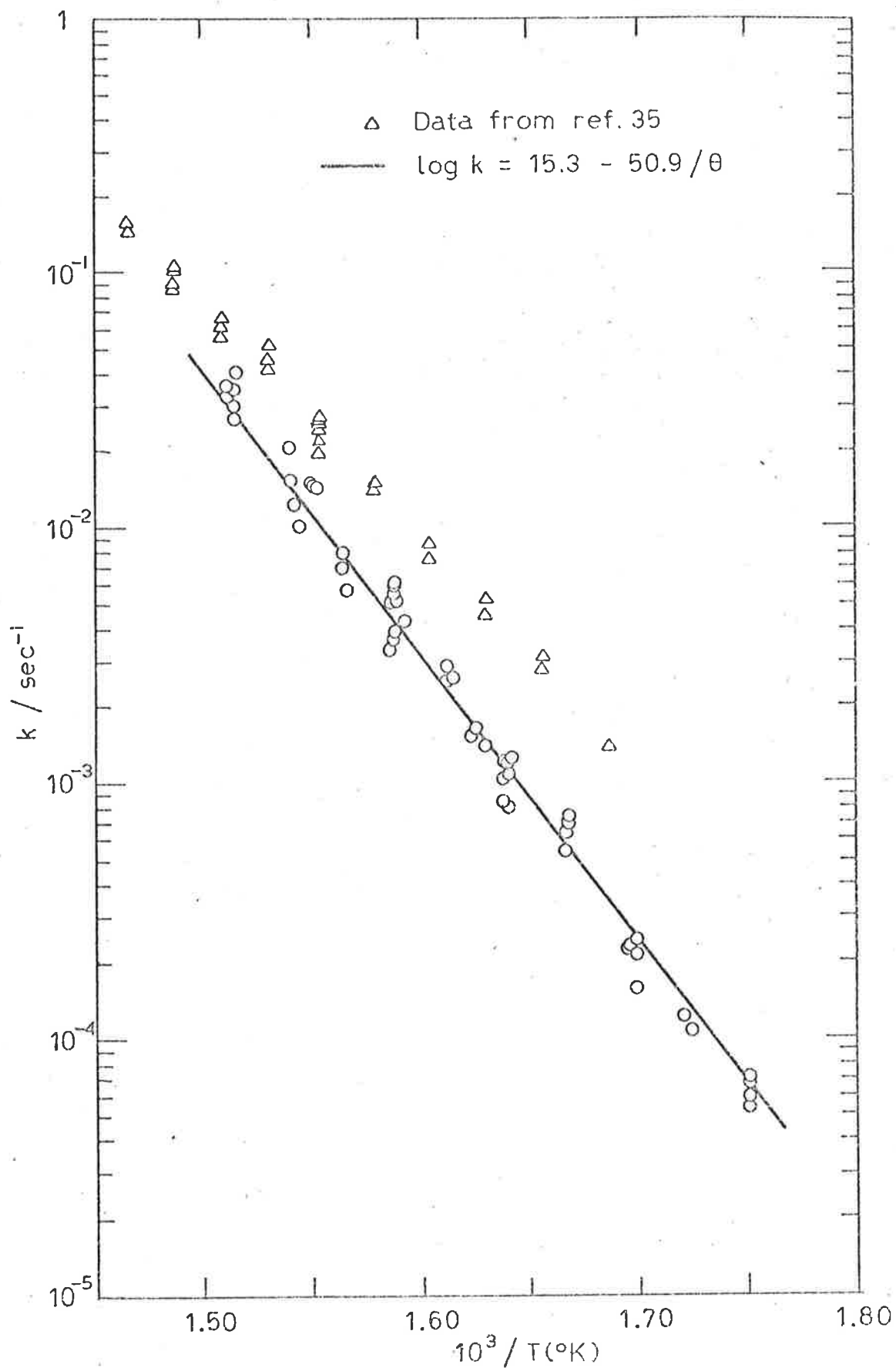
Figure 4.2   Arrhenius plot for the decomposition of trans-
1,2-dicyanocyclobutane.   △ , data points
from [35]; ———— , parameters from this work.

ca. 25% of the overall decomposition. VLPP data reveals the reaction
to be in accord with log k = (13.2 ± 0.3) - (69.3 ± 2)/Θ, while a least-
squares treatment of the high-pressure study yields log k = (12.8 ± 0.3) -
(65.3 ± 1.3)/Θ. If the predicted A_∞ in the VLPP study is adjusted to
$10^{12.8}sec^{-1}$, then it is found that E_∞= 67.8 kcal/ mole. From a comparison
of the activation energies for hydrogen halide elimination from
cyclopentyl halide [30], it was expected that the activation energy for
HCN elimination should be of a similar magnitude to the elimination from
tert-butyl cyanide (74.1 kcal/mole, [97]). The experimental result is
much less than this prediction based on analogy; it will be discussed
further in this chapter.

4.1.2 Effect of CN Group on Ring Bond Strengths

From the kinetic parameters for unimolecular reaction pathways in the pyrolysis of organic cyanides, information is obtained about the effect of the cyano group on C-C and C-H bond dissociation energies and on reactivity. This in turn enables the stabilization energies of the cyano-substituted radicals to be determined.

Values of 6-7.3 kcal/mole for the radical stabilization energy of the CN group have been previously reported from the kinetics of the pyrolysis of cyano-substituted small-ring compounds [34, 35, 37]. It should be realized, however, that these values all refer to the stabilization energy relative to a hydrogen atom; that is, the activation energy for decomposition of the substituted compound was compared with that of the parent hydrocarbon. To obtain the stabilization energy as originally defined by Benson [98], it is more correct to make the comparison with respect to the corresponding alkyl substituent. On this basis, using activation energies of 63.0 and 62.1 kcal/mole for methylcyclopropane and methylcyclobutane respectively [61], and 31.0 kcal/mole for 1,4-dimethyl-bicyclo[2.2.0] hexane [99], the corrected values are 5.0 kcal/mole from the pyrolysis of cyclopropyl cyanide [34], 5.4 kcal/mole from the pyrolysis of cyclobutyl cyanide [35], and 4.7 kcal/mole from the pyrolysis of 1,4-dicyanobicyclo [2.2.0] hexane [37]. On the basis of a biradical mechanism, comparison of $E_\infty = 57.0 \pm 1$ kcal/mole obtained from this investigation of the VLPP of cyclobutyl cyanide with that for methylcyclobutane yields a value of 5.1 ± 1 kcal/mole for the cyano stabilization energy. This is in excellent agreement with the above values.

For the high-pressure pyrolysis of trans-1,2-dicyanocyclobutane, the activation energy obtained by a least-squares treatment of the data is 52.9 kcal/mole, which compared with the activation energy for trans-1,2-

dimethylcyclobutane (61.4 ± 1.5 kcal/mole, [61]) yields a

stabilization energy of 4.3 ± 1.7 kcal/mole per cyano group.

Thus the effect of two cyano groups at opposite ends of the

tetramethylene biradical is approximately additive.   This is in

agreement with the results reported for allyl stabilization in the

decomposition of 1,2 –divinylcyclobutane [50].

There is very little information published on the kinetics of

decomposition of five membered ring compounds.   This lack of knowledge

has prevented a cyano stabilization energy to be obtained from a

comparison of cyclopentyl cyanide with analogous hydrocarbons.

A research program to investigate ring fission reactions in five

membered ring compounds in a suitable high–temperature reactor system is

recommended.

4.1.3   Review of Alkyl Cyanides

For primary alkyl cyanides, HCN elimination was found to be practically unobservable compared to C-C bond fissions. The VLPP of n-propyl cyanide over 1090-1251K was found to yield ethylene as a major product. Vinyl cyanide was also formed accounting for ca. 10% of the overall decomposition. Considering C_2-C_3 fission as the major pathway for decomposition, application of unimolecular rate theory shows that the experimental rate constants are consistent with the high-pressure parameters

$$\log k_{\infty} = (15.4 \pm 0.3) - (76.7 \pm 1.7)/\Theta$$

The rate constant for vinyl cyanide formation have been shown to be consistent with

$$\log k_{\infty} = 16.2 - 82.3/\Theta$$

which is in good agreement with the parameters for methyl rupture from n-butane (corrected for reaction path degeneracy) [69c]. Both Arrhenius expressions are quoted at $T_m \simeq 1100K$.

Taking E_{∞} (298K) = 76.3 kcal/mole (see text and Figure 3.4 of Chapter 3) and assuming that the activation energy of the reverse radical combination reaction is zero at 298K, when the rate constant is measured in molar concentration units [44], then $\Delta H^0_{298} = E_{\infty}(298K) + RT = 76.9 \pm 1.7$ kcal/mole. This is equivalent to the C-C bond dissociation energy. Combining this with the known heats of formation of n-propyl cyanide (7.5 kcal/mole, [42]) and the ethyl radical (25.9 kcal/mole, [44]) yields $\Delta H^0_{f,298}$ (CH_2CN,g) = 58.5 $\pm$ 2.2 kcal/mole. This value should be able to be used for the prediction of the activation energies for C_2-C_3 fission in primary alkyl cyanides. King [80] has confirmed this by a study of the VLPP of isobutyl cyanide over the temperature range 1011-1123K. The decomposition reactions

paralleled those of n-propyl cyanide, and the experimental rate data for C_2-C_3 fission are in accord with

$$\log k_\infty = (15.4 \pm 0.3) - (73.1 \pm 1.7)/\Theta$$

Combining the value of $\Delta H^0_f(\dot{C}H_2CN)$ with the heats of formation of isobutyl cyanide (1.2 kcal/mole; estimated from group additivity [42]) and the isopropyl radical (18.2 kcal/mole, [44]) leads to the prediction that $E_\infty(298K) = 74.9$ kcal/mole, with an uncertainty of ca. $\pm$ 3 kcal/mole, due to the error limits in the thermochemical quantities.

The activation energy for the pyrolysis of ethyl cyanide via C-C fission should also be predictable; from the heats of formation of ethyl cyanide (12.3 kcal/mole, [43]) and the methyl radical (34.1 kcal/mole, [44]) combined with $\Delta H^0_f(\dot{C}H_2CN)$, $E_\infty(298K) \simeq 80$ kcal/mole. Hence the high-pressure Arrhenius expression should be

$$\log k \simeq 15.4 - 81/\Theta$$

the equation being quoted at 1100K[*] in line with the other alkyl cyanides. In addition, if the activation energy for HCN addition to ethylene is approximately equal to that for the anti-Markovnikov addition to propylene (comparing HX addition to olefins [22]) then the predicted rate constants for HCN elimination from ethyl cyanide are given by

$$\log k \simeq 13.6 - 82/\Theta$$

where the A-factor was estimated according to the methods of Benson and O'Neal [30, 45]. Thus C-C fission should be the dominant pathway of uni-molecular decomposition. High-pressure experiments in the stirred-flow system, carried out with aniline to reactant ratios of up to 8:1, were found

---

* Heat capacity data from 298K to 1100K reveal an increase in the enthalpy change of the reaction resulting in an increase in activation energy of ca. 1 kcal/mole. See footnote, page 136, for A-factor.

to support the predicted parameters for C-C fission (see Figure 3.13). Although a limiting value for HCN elimination was not found in experiments with toluene to reactant ratios of up to 60:1, the results revealed that HCN elimination is not an observable pathway for decomposition relative to C-C fission, over the range 900-1080K.

The Arrhenius parameters differ markedly from the work of Hunt and coworkers [28], who observed both C-C fission (with log k = 14.1 - 72.7/Θ) as well as the elimination of hydrogen cyanide (with log k = 15.0 - 77.3/Θ) and of hydrogen (with log k = 12.4 - 64.6/Θ). The rate constants for the elimination reactions showed a reasonable amount of scatter, and were found to be in approximate agreement with the results obtained for the aniline inhibited runs of the present study when the aniline to reactant ratio was ca. 4. The aniline-carrier technique employed by Hunt and coworkers is expected to have had ratios of this order. However, it has been shown that with increasing concentration of inhibitor the rate of formation of hydrogen cyanide and of vinyl cyanide decrease much further. Dastoor and Emovon [32] reported an observation of HCN elimination only (with log k = 13.11 - 69.48/Θ), and their data are plotted with that of Hunt and coworkers, and the lines of the predicted parameters in Figure 4.3. It can be seen that the C-C fission data of Hunt and coworkers are in reasonable agreement with the predicted rates, and if their mid-temperature rate constant is combined with A = $10^{15.4} sec^{-1}$, then E = 78.6 kcal/mole. It is not surprising that Dastoor and Emovon did not observe C-C fission, if hydrogen cyanide and ethylene are products of a radical chain reaction initiated by C-C fission. This was suggested by O'Neal and Benson [30] when analysing Hunt and coworkers observation of the formation of hydrogen and of hydrogen cyanide.
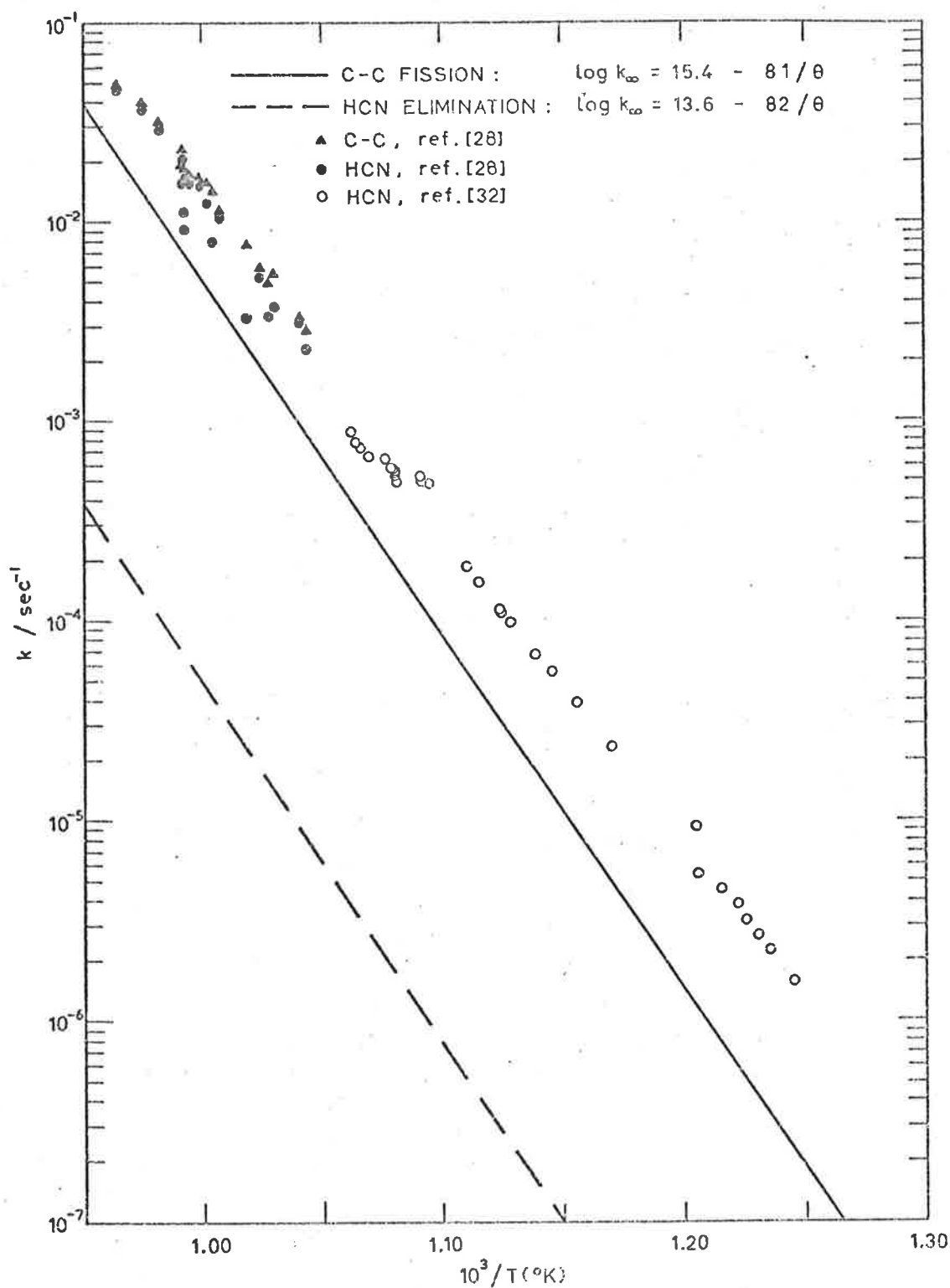
Figure 4.3   Arrhenius plot for the decomposition of ethyl
cyanide. ——————— and — — — —
predictions based on the VLPP of alkyl cyanides;
the data points are from [28] and [32].

To gain more accurate parameters for the unimolecular decomposition of ethyl cyanide, a high-temperature shock tube study would be helpful. Only the primary products of decomposition would be observed, the chain processes being terminated by the very short period of reaction.

Over the temperature range 1074-1253K, the unimolecular decomposition of isopropyl cyanide under VLPP conditions was found to yield products relating mainly to C-C fission of the bond adjacent to the cyano group. The formation of propylene resulting from HCN elimination was found to account for only ca. 10% of the overall decomposition. Taking into account the interaction of the two pathways, RRK/2 calculations show that the experimental rate constants are given by

$$\log k_\infty = (15.7 \pm 0.3) - (79.0 \pm 2.0)/\Theta \quad \text{for C-C fission,} \quad \text{and}$$
$$\log k_\infty = (13.9 \pm 0.3) - (76.2 \pm 2.0)/\Theta \quad \text{for HCN elimination, where } k$$

is in sec^{-1}, and quoted at 1100K.

The data of Dastoor and Emovon [32] for the elimination of HCN are plotted in Figure 4.4 with the lines corresponding to the parameters obtained from this investigation. Dastoor and Emovon found $\log k = 12.2 - 64.14/\Theta$, but as mentioned earlier, their A-factor is too low for a four-centre molecular elimination. However, if the rate constant at the mid-temperature of their study is combined with the predicted $A_\infty = 10^{13.9} \text{sec}^{-1}$, then E = 70.9 kcal/mole which is closer to the VLPP estimate. From Figure 4.4 it can be seen that HCN elimination cannot compete with C-C fission over the temperature range of their study, and free radical chain processes must be suspected. Dastoor and Emovon considered that chain processes required the CN radical being involved in the reaction scheme, and concluded that since DH^0 (C-CN) is exceptionally large, then HCN must be formed molecularly. However H atoms have been shown [100] to react rapidly with methyl and ethyl cyanides to form mainly HCN with little H abstraction. Thus, the following chain propagation

Figure 4.4 Arrhenius plot for the decomposition of
isopropyl cyanide. ———— and — — —
parameters from this work; the data points
are from [32].

steps are proposed for Dastoor and Emovon's results

$$H + CH_3CH (CN) CH_3 \rightarrow HCN + CH_3\overset{\bullet}{C}HCH_3$$

$$CH_3\overset{\bullet}{C}HCH_3 \rightarrow C_3H_6 + H$$
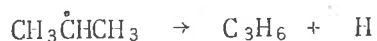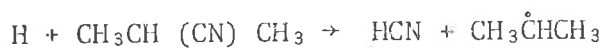
In support of their proposal for a molecular elimination, they reported that HCN formation was unaffected by the presence of a chain inhibitor, namely toluene. However, this has been refuted by the present work carried out with the stirred-flow system, which revealed that toluene had a marked effect on the formation of propylene. It was found that excessive amounts of inhibitor are required to substantially reduce the chain processes.

In the case of the VLPP of tert-butyl cyanide, the formation of methyl vinyl cyanide was found to account for over 95% of the disappearance of reactant over the temperature range 1023-1254K. Isobutene accounted for the remainder. RRK(M) calculations show that the rate constants are consistent with the high-pressure Arrhenius expressions

$\log k_\infty = (15.8 \pm 0.3) - (74.9 \pm 1.6)/\Theta$ for C-C fission, and

$\log k_\infty = (14.1 \pm 0.3) - (74.1 \pm 1.6)/\Theta$ for HCN elimination, quoted at

1100K. Hunt, Kerr and Trotman-Dickenson [28] reported $\log k - 15.2-70.2/\Theta$ for C-C fission, but as discussed earlier their parameters appear to be too low. If the rate constant at the mid-temperature of their study is combined with the predicted A-factor of $10^{15.8} sec^{-1}$, then E = 72.6 kcal/mole, which is close to the activation energy obtained in the present study. In Figure 4.5 the experimental data of Hunt and coworkers are compared with the lines corresponding to the parameters from this work. Dastoor and Emovon's reported experimental data [32] for HCN elimination are included also; the Arrhenius expression found from a least-squares treatment being $\log k = 12.2 - 64.69/\Theta$. Their A-factor is too low for a four-centre elimination [30], and combination of the mid-temperature rate constant with the predicted $A_\infty = 10^{14.1} sec^{-1}$ yields E = 72.4 kcal/mole which is more
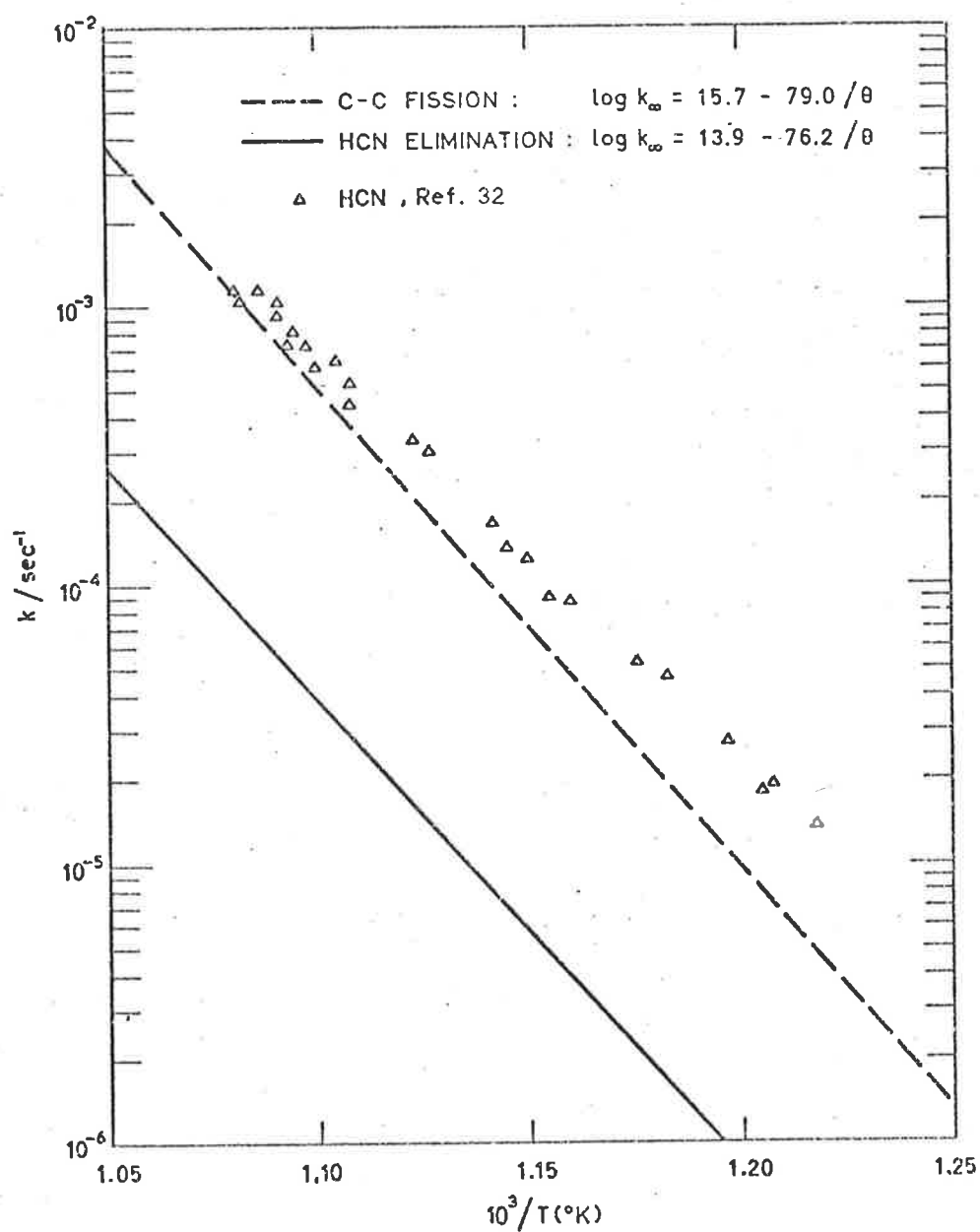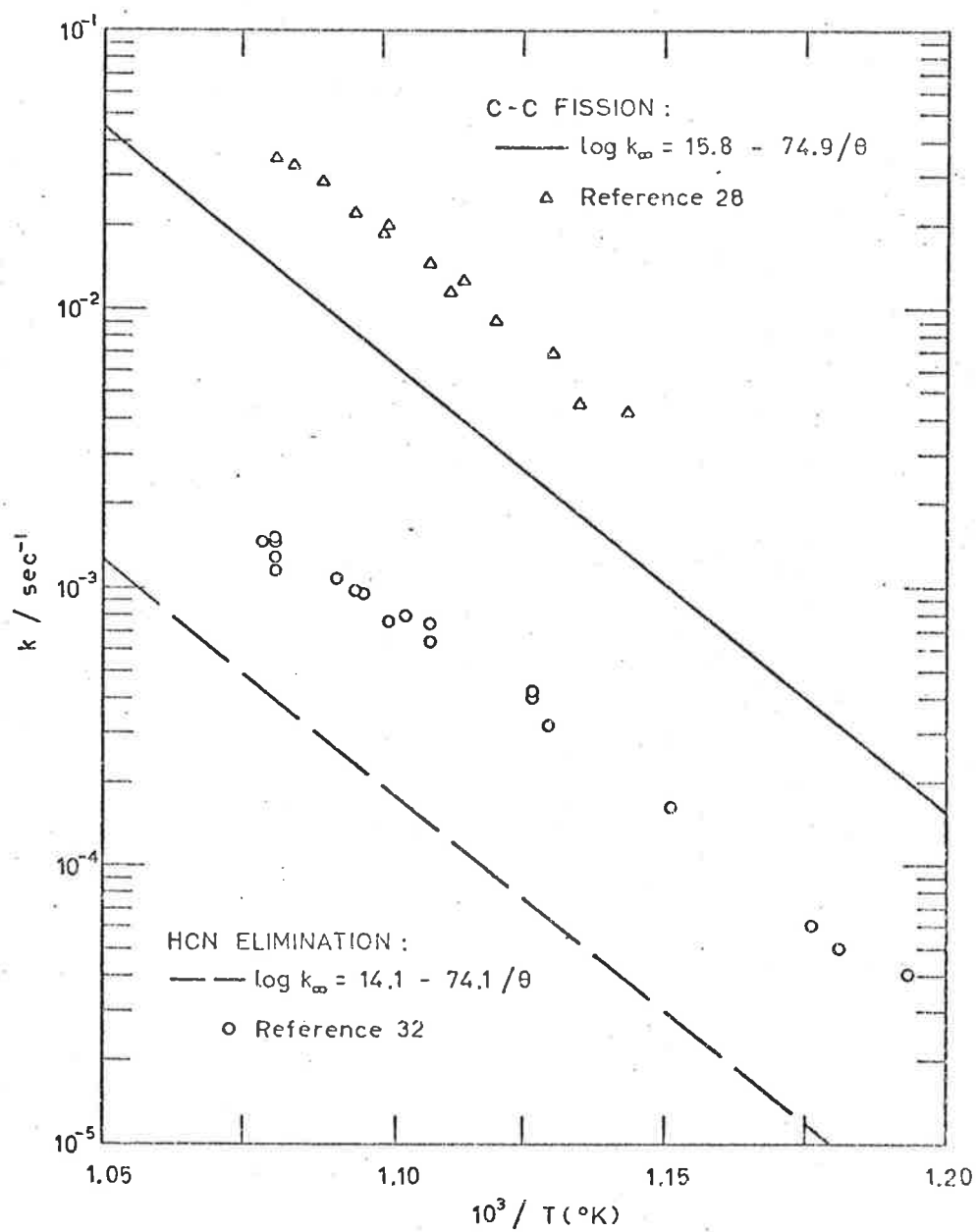
Figure 4.5   Arrhenius plot for the decomposition of
tert-butyl cyanide. ———— and — — —
parameters from this work; the data points
are from [28] and [32].

reasonable. Both the present study and the fission data of Hunt and coworkers indicate that the elimination of hydrogen cyanide cannot compete with C-C fission over the temperature range of Dastoor and Emovon's study. The isopropyl cyanide investigation confirmed that chain processes make a significant contribution to HCN formation in high-pressure studies, and thus a chain contribution in the pyrolysis of tert-butyl cyanide under the experimental conditions of Dastoor and Emovon seems very probable.

It is of interest to note that Dastoor and Emovon's adjusted E, corresponding to the predicted A_∞, for tert-butyl cyanide gives better agreement with the VLPP results, than does their adjusted E for isopropyl cyanide, and in turn than for ethyl cyanide. There appears to be a decrease in chain contribution along the series ethyl, isopropyl and tert-butyl cyanide.

In order to gain a further understanding of the chain processes that can occur in high-pressure studies of alkyl cyanides, an investigation was carried out in the stirred-flow system using ethyl cyanide. As detailed in Chapter 3, no inhibitor was present and the experiments were conducted over the range 890 - 1020K. The study revealed that the rates of formation of hydrogen cyanide and of vinyl cyanide are homogeneous, of the first-order and given by the Arrhenius expressions

$\log k = 14.3 - 67.8/\Theta$ for hydrogen cyanide formation, and

$\log k = 12.1 - 59.1/\Theta$ for vinyl cyanide formation.

To account for these parameters, a free radical mechanism was sought. The probable chain steps for decomposition are

initiation: $C_2H_5CN \rightarrow \dot{C}H_3 + \dot{C}H_2CN$ (1)

chain transfer: $\dot{C}H_3 + C_2H_5CN \rightarrow CH_4 + CH_3\dot{C}HCN$ (3)

$\dot{C}H_2CN + C_2H_5CN \rightarrow CH_3CN + CH_3\dot{C}HCN$ (4)

propagation: $CH_3\dot{C}HCN \rightleftharpoons CH_2CHCN + H$ (5,5')

$H + C_2H_5CN \rightarrow HCN + CH_3\dot{C}H_2$ (6)

$CH_3\dot{C}H_2 \rightleftharpoons CH_2CH_2 + H$ (7,7')

$H + C_2H_5CN \rightarrow H_2 + CH_3\dot{C}HCN$ (8)
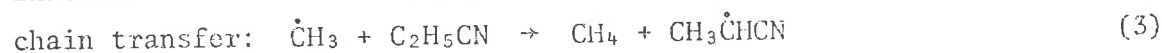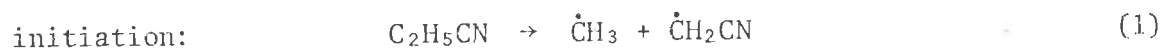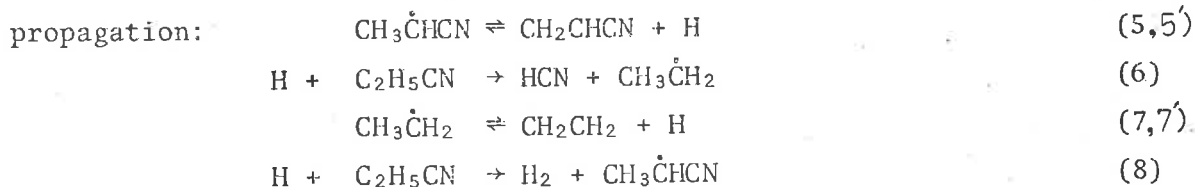
From a steady-state treatment of the propagation steps

$$\frac{[CH_3\dot{C}HCN]}{[H]} = \frac{k_8[C_2H_5CN] + k_{5'}[CH_2CHCN]}{k_5}$$

and

$$\frac{[CH_3\dot{C}H_2]}{[H]} = \frac{k_6[C_2H_5CN] + k_{7'}[CH_2CH_2]}{k_7}$$

RRK calculations[*] for the initiation step show that a second-order initiation is unlikely, and a first-order initiation should be considered. From the table of overall orders, for a general kinetic scheme of simple chain mechanisms [9] (Table 1.1, Chapter 1), the observation of first-order kinetics suggests that the termination step is either H atom combination with the cyanoethyl or the ethyl radical ($\beta\mu$), or ter-molecular H atom recombination ($\beta\beta M$).

At the mid-temperature of the study (950K), the decomposition of ethyl cyanide was ca. 50%, and the formations of ethylene and vinyl cyanide were similar. Thus the approximation $[VCN] \simeq [C_2H_4] \simeq [EtCN]/2$ can be applied to the concentration relationships above, to give

$$\frac{[CH_3\dot{C}HCN]}{[H]} \simeq \frac{2k_8 + k_{5'}}{2k_5}[C_2H_5CN]$$

$$\frac{[CH_3\dot{C}H_2]}{[H]} \simeq \frac{2k_6 + k_{7'}}{2k_7}[C_2H_5CN]$$

---

[*] Using $k_1 \simeq 10^{15.4} - 81/\theta$ with the Kassel tables [67]: at 1000K, S = 14.2, B = 40.8 and D = 5.7 giving $k/k_\infty = 0.95$

The Arrhenius parameters for reactions (5)-(8) were taken from the shown references, or estimated from analogous reactions and thermochemistry

$$\log k_5 \simeq 14.0 - 46.6/\Theta \qquad [31]$$
$$\log k_{5'} \simeq 10.0 - 1.2/\Theta \qquad [101]$$
$$\log k_6 \simeq 9.3 - 5.0/\Theta \qquad [100b,102]$$

$$\log k_7 \simeq 13.5 - 40.7/\Theta \qquad [31]$$
$$\log k_{7'} \simeq 11.0 - 2.8/\Theta \qquad [101]$$
$$\log k_8 \simeq 10.0 - 7.5/\theta \qquad [102]$$

The concentration of ethyl cyanide through the reactor was estimated to be 10^{-3} M, which when combined with the rate parameters shows the concentration of cyanoethyl radicals to be approximately twice that of ethyl radicals, and both species to be much more abundant than H atoms. This suggests that $\beta\mu$ terminations are more probable than H atom recombination. Taking $k \simeq A = 10^{10.0} \sec^{-1}$ for the termination step of H atom with cyanoethyl radical, calculations on the steady-state equations reveal an overall first-order rate of formation of hydrogen cyanide equalling $10^{14.15-67.7}/\Theta$ [EtCN], and an overall first-order rate of formation of vinyl cyanide equalling $10^{14.85-70.2}/\Theta$ [EtCN]. The parameters for HCN formation are in close agreement with experiment, while the vinyl cyanide formation parameters are higher than found experimentally; however comparison of predicted rate constants at 950K show them to be in reasonable agreement with experiment. If the termination step of ethyl radicals with H atoms is considered, then $k = 10^{13.4-64.0}/\Theta$ for HCN formation, and $k = 10^{14.1-66.5}/\Theta$ for VCN formation. Predicted and experimental rate constants at 950K are within experimental error. Thus steady-state treatment of the postulated mechanism supports it as a possible mode for free-radical chain decomposition, and it is probable that the two termination steps considered are competitive.

4.1.4 Kinetics and Thermochemistry of C-C Fission

From E_∞ (298K) = 78.2 kcal/mole for C-C fission in isopropyl cyanide,

$$\Delta H^0_{298} = E_\infty (298K) + RT = 78.8 \pm 2.0 \text{ kcal/mole}$$

if it is assumed that the activation energy of the reverse radical combination reaction is zero at 298K when the rate constant is measured in molar concentration units [44]. Thus knowing the heats of formation of isopropyl cyanide and the methyl radical (see Table 4.2), the heat of formation of the α-cyanoethyl radical can be determined; the result (incorporating error limits) being

$$\Delta H^0_f (CH_3\dot{C}HCN,g) = 50.1 \pm 2.3 \text{ kcal/mole}$$

The formation of a radical centre adjacent to a π-bond can be accompanied by resonance stabilization due to delocalization of the unpaired electron. The stabilization energy, SE^0, of a delocalized radical has been defined [103] as $\Delta H_a - \Delta H_b$, where

$$R_S H \xrightarrow{a} R_S^\cdot + H$$

$$R_\pi H \xrightarrow{b} R_\pi^\cdot + H$$

and $R_S^\cdot$ represents the hydrogen-saturated radical, and $R_\pi^\cdot$ the analogous π-delocalized radical. Thus the stabilization energy of the α-cyanoethyl radical may be determined by comparing $DH^0_{298}[CH_3CH(CN) - H]$ with $DH^0_{298}[CH_3CH(CH_3) - H]$. Combining the value for the heat of formation of the α-cyanoethyl radical with those of the H atom and ethyl cyanide (Table 4.2) we can calculate

$$DH^0_{298}[CH_3CH(CN) - H] = 89.9 \pm 2.3 \text{ kcal/mole.}$$

Comparing this value with the secondary C-H bond strength in propane (95 ± 1 kcal/mole, [104]) yields $SE^0 (CH_3\dot{C}HCN) = 5.1 \pm 2.5$ kcal/mole. This is in excellent agreement with the previous determinations based on small ring compound reactions.

TABLE 4.2　　　　THERMOCHEMICAL DATA

Species	ΔH_f^0 (298K) kcal/mole	S_{298}^0 cal K^{-1} mole^{-1}	C_p^0 , cal K^{-1} mole^{-1}			
			300	500	800	1000
C_2H_5CN[a]	12.3[b]	68.7	17.3	24.9	32.7	36.1
$i\text{-}C_3H_7CN$[a]	5.4[b]	76.2	23.4	32.9	43.3	48.1
$n\text{-}C_3H_7CN$[a]	7.5	77.8	22.8	33.2	43.8	48.4
$t\text{-}C_4H_9CN$[c]	-0.8[b]	79.6	28.2	40.0	54.0	60.0
$\dot{C}H_3$[d]	34.1	46.4	8.3	10.1	12.6	14.0
$CH_3\dot{C}H_2$[d]	25.9	59.5	11.1	16.8	22.9	25.8
$\dot{C}H_2CN$[d]	e	58.5	10.7	14.5	18.1	19.8
$CH_3\dot{C}HCN$[d]	e	68.8	15.3	22.2	29.0	31.9
$(CH_3)_2\dot{C}CN$[d]	e	75.8	21.2	29.1	39.0	43.5
C_3H_6[a]	4.9	63.8	15.2	22.6	30.7	34.5
$i\text{-}C_4H_8$[a]	-4.0	70.3	21.4	31.2	41.9	46.9
HCN[f]	32.3	48.2	8.6	10.0	11.3	12.2
H[f]	52.1	27.4	5.0	5.0	5.0	5.0

a
　Reference　[42]

b
　Reference　[43]

c
　Reference　[81]

d
　Reference　[44]

e
　See text.

f
　JANAF Thermochemical Tables, Natl. Stand. Ref. Data　Ser.,
　Natl. Bur. Stand., No. 37　(1970).

Similar calculations can be made for the other alkyl cyanides. The bond fission activation energy of 74.9 kcal/mole observed for the pyrolysis of tert-butyl cyanide leads to $\Delta H^0_{298} = 74.7 \pm 1.6$ kcal/mole, which is equivalent to $DH^0_{298}[(CH_3)_2 C(CN) - CH_3]$. From the thermochemical data in Table 4.2, the heat of formation of the α-cyano-isopropyl radical can be determined.

$$\Delta H^0_f [(CH_3)_2\overset{\bullet}{C}CN, \text{ g}] = 39.8 \pm 2.0 \text{ kcal/mole}$$

Thus, $DH^0_{298}[(CH_3)_2C(CN) - H] = 86.5 \pm 2.0$ kcal/mole. Comparing this bond strength with the tertiary C-H bond strength in 2-methylpropane (92 ± 1 kcal/mole. [104] yields $SE^0 [(CH_3)_2 \overset{\bullet}{C}CN] = 5.5 \pm 2.2$ kcal/mole.

The pyrolysis of n-propyl cyanide yields

$$\Delta H^0_{298} = 76.9 \pm 1.7 \text{ kcal/mole} \equiv DH^0_{298}[C_2H_5 - CH_2CN]$$

from which the heat of formation of the cyanomethyl radical is determined to be 58.5 ± 2.2 kcal/mole. Since the error limits on the heat of formation of methyl cyanide are significant, a comparison of C-H bond strengths in methyl cyanide and ethane to yield a value for the stabilization energy is not accurate. However, Rodgers, Wu, and Kuitu [103] have shown that stabilization is a property of the radical and does not depend on the bond that is broken. Thus a comparison of the bond strengths of $C_2H_5 - CH_2CN$ and $C_2H_5 - C_2H_5$ (82 ± 1.5 kcal/mole, [45]) gives $SE^0 (\overset{\bullet}{C}H_2CN) = 5.1 \pm 2.3$ kcal/mole. This is in excellent agreement with the values for the α-cyanoethyl and α-cyanoisopropyl radicals, as well as the small ring cyanide determinations. Combining the value with $DH^0_{298} [C_2H_5 - H] = 98 \pm 1$ kcal/mole [104] and from the definition of stabilization energy, we obtain $DH^0_{298} [CH_2(CN) - H] \sim 93$ kcal/mole. This bond strength yields $\Delta H^0_f(CH_3CN) \sim 17.6$ kcal/mole, which is between the value of 19.1 kcal/mole reported by Evans and Skinner [105], and the calorimetry value of 15.7 ± 1.7 kcal/mole found by Hall and Baldt [43].

The above data show that the effect of replacing a methyl group in an alkyl radical by a cyano group increases the heat of formation by ~ 32 kcal/mole (see Table 4.3). The thermochemical properties of free radicals are able to be estimated by group additivity methods, but the heat of formation group contributions of $[\dot{C}- (H)_2(CN)]$, $[\dot{C}-(H)(C)(CN)]$, and $[\dot{C}-(C)_2(CN)]$ listed by O'Neal and Benson [44] were based on radical stabilization energies of 10.8 - 12.6 kcal/mole [31]. These values clearly need revising, and using the heats of formation of the cyanoalkyl radicals listed in Table 4.3 the group additivity values derived from this work are

$$[\dot{C} - (H)_2(CN)] \ = \ 58.5 \ \text{kcal/mole}$$

$$[\dot{C} - (H)(C)(CN)] \ = \ 60.2 \ \text{kcal/mole}$$

$$[\dot{C} - (C)_2(CN)] \ = \ 60.0 \ \text{kcal/mole}$$
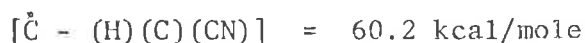
In addition, the heats of formation of cyanide molecules recently reported by Hall and Baldt [43] enable the group contributions of $C - (H)_2(C)(CN)$, $C - (H)(C)_2(CN)$, and $C - (C)_3(CN)$ listed by Benson and coworkers [42] to be updated. (In fact a value for $C - (C)_3(CN)$ was not given). The molecular heat of formation group additivity values are

$$C - (H)_2(C)(CN) \ = \ 22.4 \ \text{kcal/mole}$$

$$C - (H)(C)_2(CN) \ = \ 25.6 \ \text{kcal/mole}$$

$$C - (C)_3(CN) \ = \ 29.4 \ \text{kcal/mole}$$
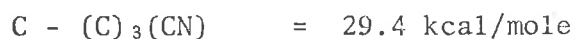
In Table 4.4, the C-H and C-C bond dissociation energies for corresponding alkanes and alkyl cyanides are compared. It can be seen that the cyano group decreases the adjacent bond dissociation energy consistently by an average of 5.1 ± 1.8 kcal/mole. This is a consequence of the cyano stabilization energy, and confirms the findings of Rodgers, Wu, and Kuitu [103] regarding stabilization being a property of the radical and not of the bond. The stabilization energy of the allyl radical has been shown to

TABLE 4.3 <u>EFFECT OF CN SUBSTITUTION ON FREE RADICAL HEAT OF</u>
<u>FORMATION</u>[a]

Radical	R=	CH_3[b]		CN[c]		Δ[d]		
$\overset{\bullet}{C}H_2R$		25.9	± 1.3	58.5 ± 2.2		32.6	±	2.6
$CH_3\overset{\bullet}{C}HR$		18.2	± 1.5	50.1 ± 2.3		31.9	±	2.7
$(CH_3)_2\overset{\bullet}{C}R$		7.6	± 1.2	39.8 ± 2.0		32.2	±	2.3

a
  All values in kcal/ mole

b
  Reference [104]

c
  This work

d
  Difference.

TABLE 4.4 <u>EFFECT OF CN SUBSTITUTION ON BOND DISSOCIATION ENERGIES</u>[a]

Bond	R =	CH_3[b]		CN[c]	Δ[d]
$H-CH_2R$		98	± 1	~ 93	~ 5
CH_3-CH_2R		85	± 1.5	80.3 ± 2.5	4.5 ± 2.9
$C_2H_5-CH_2R$		82	± 1.5	76.9 ± 1.7	5.1 ± 2.3
$H-CH(CH_3)R$		95	± 1	89.9 ± 2.3	5.1 ± 2.5
$CH_3-CH(CH_3)R$		84	± 1.5	78.8 ± 2.0	5.2 ± 2.5
$H-C(CH_3)_2R$		92	± 1	86.5 ± 2.0	5.5 ± 2.2
$CH_3-C(CH_3)_2R$		80	± 1.5	74.7 ± 1.6	5.3 ± 2.2

a
  All values in kcal/mole

b
  References [45] and [104]

c
  This work

d
  Difference.

increase by ~ 3 kcal/mole [106] with methyl substitution. A similar effect has been found for the acetonyl radical [107]. It has been suggested that this is due to an inductive effect [104, 107]. No significant variation in the cyano stabilization energy for α-methyl substitution was observed, although the error limits could mask any small effect.

The heat of formation of an α-cyanoalkyl radical can be used to find the change in enthalpy of the decomposition of the radical to a cyano-alkene and a H atom. Combining ΔH_f^0 ($CH_3\dot{C}HCN$) with ΔH_f^0 (VCN) = 43 kcal/mole [43] yields ΔH^0 = 45 kcal/mole. This value is also the difference between DH^0 [βC-H] in the radical and the C=C π-bond energy in vinyl cyanide. Assuming that DH^0 [βC-H] is equivalent to DH^0 [C_2H_5-H] = 98 kcal/mole [45], then DH_π^0 [CH_2= CHCN] = 53 kcal/mole. This π-bond is 6.1 kcal/mole less than DH_π^0 [CH_2= CHCH$_3$] [108]. A similar calculation, using the α - cyano - isopropyl heat of formation, shows DH_π^0 [CH_2= C(CH$_3$)CN] to be 6.3 kcal/mole less than DH_π^0 [CH_2= C(CH$_3$)$_2$]. This suggests that the cyano group has a similar effect on π-bond energies as it does on σ-bond energies, in agreement with the work of Egger and Cocks [108] on the effect of substituents on π-bond energies. The π-bond energies obtained for vinyl cyanide and methyl vinyl cyanide suggest that the activation energies for the cis-trans isomerizations of crotonitrile (51.3 kcal/mole, [39], and β-cyanostyrene (46 kcal/mole, [38]) are too low. Marley and Jeffers' [40] recently reported activation energy (58.0 ±2 kcal/mole) for the isomerization of crotonitrile is a more acceptable result.

4.1.5 Kinetics of HCN Elimination

This investigation has shown that the unimolecular elimination of hydrogen cyanide is a minor pathway only. Activation energies for the reaction have been determined for the alkyl cyanides and cyclopentyl cyanide. As discussed in Chapter 1, HCN elimination activation energies may be calculated theoretically by using the Benson-Haugen semi-ion pair theory [22], or its modification developed by Tschuikow-Roux, Maltman, and Jung [23]. The activation energies for the four-centre addition of HCN across a double bond is calculated, and then the endothermicity of the elimination reaction added.

As a first approximation in using the Benson-Haugen model, the HCN molecule was treated as a pseudo-diatomic with a bond length equal to the H-N distance in the molecule (2.226Å, [71]). Using $\alpha_{mean}(CN^-)/\alpha_{mean}(HCN) = 1.29$ the effective longitudinal polarizability of HCN, $\alpha_1^{\ddagger}(HCN)$ was calculated to be $4.20Å^3$. This reveals the polarization energy of the HCN bond to be 68.1 kcal/mole. The equilibrium distance between the dipole centres in the reacting bonds was calculated to be 2.193Å, resulting in a value of 21.7 kcal/mole for the equilibrium electrostatic interaction energy of the dipoles. From the polarizabilities of HCN ($\alpha_{mean}^0 = 2.59Å^3$, $\alpha_1 = 3.92Å^3$, [109]) and its dipole moment ($\mu = 3.00D$, [110]), the ground state polarization energy was calculated to be 16.4 kcal/mole. Combining these values with the polarization energy of the olefin double bond [22], results in a value for the addition activation energy at 0 K. The elimination activation energies for 298K are obtained after inclusion of the thermal energy change and the endothermicity of the reaction. The model of HCN addition to $s - C_4H_8$ was assumed to represent the addition to cyclopentene (calculations carried out for HX eliminations from cyclopentyl halides support this treatment).

The model of Tschuikow-Roux and coworkers [23] requires a standard

reaction whose activation energy is known with some degree of certainty to fix a value for the partial formal charge separation to be used in a homologous series of compounds. For the reaction, olefin + HX → RX, they proposed the following relationship between the p-factors and the value of δ

$$\delta_X^{ol} = \delta_X^e - \beta (p_X^{ol} - p_X^e)$$

where δ_X^{ol} is the partial formal charge separation, and p_X^{ol} is the value of the p-factor for the C-C bond. δ_X^e and p_X^e are the corresponding values for the ethylene + HX reaction. Tschuikow-Roux and coworkers determined δ_X^e by trial and error fitting for the ethylene + HX reaction, while the constant β was found by trial and error fitting for the anti-Markovnikov addition of HCl to propylene. They adopted the procedure for calculating the C-C bond energy in species with a X group in the primary position, of increasing the energy of the adjacent C-C bond by S(X) relative to its strength in the species in which the X was replaced by a CH_3

$$DH^0 [R-CH_2X] = DH^0 [R - CH_2CH_3] + S(X)$$

From S(Cl) = 3.7 kcal/mole [23], and $DH^0 [C_2H_5 - C_2H_5]$ = 87 kcal/mole, taken from Kerr [111], they used $DH^0 [C_2H_5 - CH_2Cl]$ = 90.7 kcal/mole to find the βvalue which gave the known activation energy of 55.0 kcal/mole [31] for HCl elimination from n-propyl chloride. The value of β obtained is 0.415. From the tables of Kerr [111] they noted that $DH^0 [(CH_3)_2CH - CH_3] < DH^0 [C_2H_5 - C_2H_5]$, leading them to the procedure for species with X in the secondary position of replacing X by H and subtracting S(X). However, the C-C bond strength in n-butane reported by Kerr is incorrect (being ca. 5 kcal/mole too high), and the C-C bond strength in isobutane is larger than in n-butane. From heats of formation data [42, 112], the C-C bond strength in n-propyl chloride is 85.2 kcal/mole which implies β = 5.9 to satisfy the activation energy. (This large deviation in β is due to $p_{Cl}^{C_3H_6}$ and p_{Cl}^e being almost equal, requiring β to be substantial in order to alter δ).

Fortunately, for the cyanides investigated it was found that p_{CN}^e and p_{CN}^{ol} are almost equal and therefore the value of β is not critical. The model requires the dissociation energies of the participating bonds and their single bond lengths. The bond dissociation energy of HCN (123.8 kcal/mole) and the C-CN bond energies were calculated from thermochemical data [42, 43, 113], the C-H bond energies were taken from reference [104], and the experimental bond energies found from this research were used for the carbon-carbon bonds. The bond strength of the C-C bond in cyclopentyl cyanide adjacent to the cyano group was estimated from thermochemistry [43] and group additivity [44] using $[\dot{C} - (H)(C)(CN)] = 60.2$ kcal/mole. Single bond lengths were taken from the tables of Sutton [71]. Of the cyanides investigated, HCN elimination was followed most accurately from the VLPP of tert-butyl cyanide, being able to be monitored over the three apertures. Using the reaction, isobutene + HCN → tert-butyl cyanide as the standard for this homologous series, the value of δ_{CN} was found to be 0.1862. The interior angle ϕ_1 of the convex quadrilateral representing the geometry of the four-centre transition state [23] was found to be 69^0, and the energy contributions to the activation process were computed.[*]

The results of the calculations for the Benson-Haugen semi-ion pair model, and the modified model of Tschuikow-Roux are compared with experiment in Table 4.5. The agreement is good except in the Benson-Haugen calculation for tert-butyl cyanide. However their model has been found to be sensitive to the choice of transition state parameters; if the H-C bond is considered to be the reacting part of the HCN molecule then the calculated activation energies are ~13.5 kcal/mole [97] lower than those shown in Table 4.5. The treatment of HCN as a pseudo-diatomic may be an oversimplification, but treatment of it as a triatomic raises the question of the transition-state

---

[*] A copy of the computer program for the modified semi-ion pair theory was kindly supplied by Professor E. Tschuikow-Roux of the University of Calgary.

TABLE 4.5   COMPARISON OF THEORETICAL AND EXPERIMENTAL
ACTIVATION ENERGIES FOR HCN ELIMINATION

COMPOUND	E (298K), kcal/mole		
	BH [a]	TMJ [b]	Experimental
C_2H_5CN	78.4	79.0	~ 82 [c]
$i-C_3H_7CN$	73.1	78.6	75.3
$n-C_3H_7CN$	76.0	74.8	> 75.7
$t-C_4H_9CN$	63.0	73.6	73.6
$c-C_5H_9CN$	69.8	67.8	65.3 [d] , 67.5 [e]

[a]
  Semi-ion pair model of Benson and Haugen [22] .

[b]
  Modified semi-ion pair model of Tschuikow-Roux, Maltman,
  and Jung [23].

[c]
  Estimated from the VLPP of n-propyl cyanide.

[d]
  Obtained from the stirred-flow system at T_m ~ 1000K.

[e]
  Obtained from VLPP.

structure.[*] Although the predicted values for the addition of 'bent' molecules such as H_2O and H_2S [22] agree with experiment, the addition of the linear HCN molecule implies some bending is necessary in the transition state. That is, in the transition from reactant to products, extra re-organizational energy may be involved, either about the $C-C\equiv N$ angle (HCN linear) or the $H-C\equiv N$ angle (HCN bent), and this may require a modification to the Benson-Haugen calculation. Since the model of Tschuikow-Roux and coworkers requires known kinetic parameters to fix values for δ_x and β, and the data is limited, the apparent success of the model in this case may only be artificial.

In Table 4.6, the Arrhenius parameters for HCN elimination are compared with those for HX elimination from the corresponding alkyl halides. From the table it can be seen that hydrogen cyanide elimination is a very much slower reaction that hydrogen halide eliminations, and that α-methyl substitution does not have as significant an effect. Treatment of cyanides as pseudohalides in order to predict kinetic parameters can lead to discrepancies if used as a rule, as if found in the case of cyclopentyl cyanide. Although the heterolytic bond dissociation energies $D(R^+CN^-)$ [97] are similar to $D(E^+F^-)$, the activation energies for elimination differ by ~ 20 kcal/mole. This suggests that the degree of heterolysis of the R-CN bond is very small [20].

---

[*] The question of bending in the transition-state was proposed by Dr S.W. Benson of Stanford Research Institute in a private communication to Dr K.D. King.

TABLE 4.6   ARRHENIUS PARAMETERS[a] FOR HX ELIMINATION FROM
HALIDES[b] AND CYANIDES

Compound	log A[c]	E				
		I	Br	Cl	F[d]	CN[e]
C_2H_5X	13.3	50.6	53.5	56.5	59.9	~ 82[f]
$i\text{-}C_3H_7X$	13.7	45.0	47.8	51.2	53.9	75.7
$n\text{-}C_3H_7X$	13.2	48.4[g]	51.5	54.2	58.3	⩾ 76.5
$t\text{-}C_4H_9X$	13.8	38.4	41.8	45.2	51.5	73.8
$c\text{-}C_5H_9X$	12.8	-	43.7	46.5	-	69[h]

[a]
A in sec^{-1}, and E in kcal/mole, quoted at 600K.

[b]
Values from O'Neal and Benson [30].

[c]
Estimation following the method of O'Neal and Benson [30].

[d]
Reference [114].

[e]
This work, quoted at 600K.

[f]
Estimated from the VLPP of n-propyl cyanide.

[g]
Reference [53].

[h]
VLPP .

4.2   Conclusions and Implications

The dominant feature of all the decompositions of the cyanides investigated was the fission of the carbon-carbon bond adjacent to the cyano group. Hydrogen cyanide elimination was found to be a minor reaction, accounting for less than 10% of the overall decomposition of alkyl cyanides. Most of the previous studies of the kinetics of organic cyanides have been shown to have had serious secondary reaction complications, resulting in dubious thermochemical data on cyanoalkyl radicals. High-pressure stirred-flow studies have revealed that free radical chain processes markedly contribute to the elimination of hydrogen cyanide, and were extremely difficult to inhibit at the high temperatures at which the kinetics were investigated. The usual procedures for checking for secondary reactions, valid for decompositions at temperatures of up to 800K, are found to be ineffective when extended to 1000 - 1100K. Extremely large concentrations of inhibitors are required to prevent chain processes. In virtually eliminating these secondary reactions, the VLPP technique proved to be a very successful procedure to follow cyanide unimolecular decompositions.

From the kinetic parameters of the carbon-carbon fissions, fundamental knowledge has been obtained on bond energies, and the thermochemistry of cyano-substituted molecules and radicals. For the cyanomethyl, α-cyanoethyl, and α-cyanoisopropyl radicals,

$$\Delta H_f^0 \; (\dot{C}H_2CN) \; = \; 58.5 \pm 2.2$$

$$\Delta H_f^0 \; (CH_3\dot{C}HCN) \; = \; 50.1 \pm 2.3$$

$$\Delta H_f^0 \; ((CH_3)_2\dot{C}CN) \; = \; 39.8 \pm 2.0, \; \text{all in kcal/mole.}$$

The replacement of a methyl group by a cyano group in the alkyl radical increases the heat of formation by ~32 kcal/mole. These radical heats of formation enable revised values of the free radical group additivity contributions to be calculated; they are

$$[\dot{C} - (H)_2(CN)] \; = \; 58.5$$

$$[\dot{C} - (H)(C)(CN)] \; = \; 60.2$$

$$[\dot{C} - (C)_2(CN)] \; = \; 60.0, \quad \text{all in kcal/mole.}$$

Comparison of the heats of formation of the cyanoalkanes and cyano-cycloalkanes with the analogous hydrogen saturated alkanes show that the effect of the cyano group is to increase the heats of formation by ~ 37.5 kcal/mole per group. The difference between the effects of a cyano group on cyanoalkyl radicals and on cyanoalkanes, compared with the analogous hydrogen saturated species, in effect defines the stabilization energy of the delocalized radical [103]. This was shown in another way when the C-H and C-C bond dissociation energies for alkanes and alkyl cyanides were compared; the cyano group consistently decreased the adjacent bond strength by an average of 5.1 ± 1.8 kcal/mole. Being a property of the radical and not the bond, it was found that the cyano resonance stabilization has a similar effect on π-bond energies as it does on single bond energies.

By applying the Benson-Haugen or Tschuikow-Roux and coworkers theoretical semi-ion pair models, it was found that the predicted addition activation energies of hydrogen cyanide to the appropriate olefin, resulted in elimination activation energies in good agreement with experimentally observed values. However the models were originally devised with hydrogen halides and similar species in mind, and when extended to a linear triatomic molecule such as HCN, the treatment of it as pseudo-diatomic may be an over simplification. Possibly some modification may be required to allow for extra reorganizational energy due to the bending involved in going from the reactants to products.

Some of the conclusions resulting from this work have been reported in articles published during the course of the research program. They were co-authored with Dr K.D. King, and reprints of these have been included in the Appendix. We anticipate publication of the work on trans-1,2-dicyano-cyclobutane, cyclopentyl cyanide, and ethyl cyanide in the near future.

The data obtained from this investigation of the kinetics and thermo-chemistry of the unimolecular decomposition of short chain and small ring organic cyanides, has filled a substantial gap that existed in the fundamental knowledge of one of our most important substituent groups. Knowledge gained on the effects of triple bond resonance on reactivity, may help with a study of alkynes on which there is presently limited information.* A sound foundation of these basics should enable accurate estimations to be made on the thermochemistry of longer chain cyanides. Future developments in the polymer chemistry of new cyanide reactive monomers, and the production of light-weight, high strength building materials incorporating poly-crystalline carbon fibres, produced from polyacrylonitrile, were discussed in the introduction of Chapter 1. It is hoped that this research will enable the chemistry of production of these materials to be understood more clearly, making technical refinements and their future marketing much closer.

---

* Studies of alkyne decompositions are currently being undertaken by Dr K.D. King of the University of Adelaide.

A P P E N D I X

A.1 Experimental Data

The data obtained from experimental runs conducted in the VLPP system and in the stirred-flow reactor system are presented in Tables A.1-A.9. They contain the information used to calculate the rate constants presented in Chapter 3. The pyrolyses of cyclobutyl cyanide, isopropyl cyanide, n-propyl cyanide, tertbutyl cyanide, and cyclopentyl cyanide using the VLPP technique are shown in Tables A.1, A.3 and A.4, A.5, A.6 and A.8 respectively. Tabulated are the run number, aperture, reactor temperature in $^\circ$C, relative mass spectral peak intensities, reactant to argon ratio, and the molecular flow rate. The flow system studies on trans-1,2-dicyanocyclobutane, cyclopentyl cyanide, and ethyl cyanide (in the absence of a chain inhibitor) are shown in Tables A.2, A.7 and A.9 respectively. Presented are the run number, reactor temperature in $^\circ$C, the ambient temperature flow rate (U'), the reactor temperature flow rate (U), U/V (where V = reactor volume), and the chromatograph peak areas (measured in integrator counts).

TABLE A.1   VLPP RAW EXPERIMENTAL DATA
                PYRØLYSIS ØF CYCLØBUTYL CYANILE

RUN	APERTURE MM	TEMP. °C	PEAK INTENSITIES			CN/AR (54/40)°	FLØW RATE MØLEC/SEC
			I 40	I 53	I 54		
CB 8	10.0	689.2	74.8	7.25	46.9	0.70	5.7E+14
9	10.0	709.5	74.2	8.05	44.7	0.70	5.7E+14
10	10.0	728.8	73.7	9.5	42.3	0.70	5.7E+14
11	10.0	748.7	73.4	10.2	36.9	0.70	5.7E+14
12	10.0	769.5	73.8	12.1	33.9	0.70	5.7E+14
13	10.0	789.8	72.6	13.0	29.1	0.70	5.7E+14
14	10.0	808.2	72.4	14.7	25.9	0.70	5.7E+14
16	10.0	786.7	100.8	15.6	36.1	0.63	1.2E+15
17	10.0	808.2	99.7	18.0	31.5	0.63	1.2E+15
18	10.0	830.2	77.4	15.85	21.1	0.63	1.2E+15
19	10.0	848.7	78.8	17.3	18.5	0.63	1.2E+15
20	10.0	869.9	100.6	23.6	19.05	0.63	1.2E+15
21	10.0	890.2	99.6	24.4	15.5	0.63	1.2E+15
22	10.0	910.7	98.4	25.2	12.5	0.63	1.2E+15
23	10.0	929.7	99.6	26.7	10.6	0.63	1.2E+15
31A	3.3	649.7	74.8	8.2	39.2	0.635	8.9E+14
32	3.3	659.9	74.4	8.2	37.9	0.635	8.9E+14
33	3.3	679.4	70.4	9.0	31.8	0.635	8.9E+14
34	3.3	697.4	74.2	11.9	27.6	0.635	8.9E+14
35	3.3	720.4	70.6	12.8	20.7	0.635	8.9E+14
36	3.3	739.4	70.6	14.3	16.9	0.635	8.9E+14
37	3.3	759.4	70.0	15.1	12.8	0.635	8.9E+14
38	3.3	779.8	70.2	16.1	9.9	0.635	8.9E+14
39	3.3	799.9	70.4	16.9	7.5	0.635	8.9E+14
40	3.3	820.0	70.2	17.4	5.7	0.635	8.9E+14
45	3.3	629.6	37.8	5.05	32.0	0.94	8.3E+14
46	3.3	650.4	37.1	5.9	29.0	0.94	8.3E+14
47	3.3	668.9	36.5	7.05	26.4	0.94	8.3E+14
48	3.3	689.7	34.4	8.05	21.7	0.94	8.3E+14
54	3.3	699.1	30.75	7.3	17.4	0.945	3.3E+14
55	3.3	710.8	76.2	19.8	39.0	0.945	3.3E+14
56	3.3	729.3	30.2	8.7	12.5	0.945	3.3E+14
57	3.3	751.3	73.25	22.2	22.2	0.945	3.3E+14
58	3.3	770.3	76.0	24.1	17.7	0.945	3.3E+14

TABLE A.1   VLPP RAW EXPERIMENTAL DATA
     contd   PYRØLYSIS ØF CYCLØBUTYL CYANILE

RUN	APERTURE MM	TEMP. °C	PEAK INTENSITIES			CN/AR (54/40)°	FLØW RATE MØLEC/SEC
			I 40	I 53	I 54		
CB 81	1.1	559.6	54.1	3.35	22.1	0.43	3.0E+15
82	1.1	571.0	51.8	3.5	20.1	0.464	3.0E+15
83	1.1	581.0	51.8	3.9	19.2	0.464	3.0E+15
84	1.1	590.5	51.0	4.3	18.0	0.464	3.0E+15
85	1.1	600.1	50.7	4.75	16.45	0.464	3.0E+15
87	1.1	609.5	49.7	5.1	14.8	0.464	3.0E+15
88	1.1	619.8	48.6	5.5	12.9	0.464	3.0E+15
89	1.1	630.9	48.5	6.05	11.6	0.464	3.0E+15
92	1.1	590.5	69.3	5.1	20.7	0.40	5.6E+14
93	1.1	629.6	67.7	7.2	13.25	0.40	5.6E+14
94	1.1	639.7	66.8	7.7	11.25	0.40	5.6E+14
95	1.1	650.1	127.5	15.4	18.7	0.40	5.6E+14
96	1.1	660.0	131.2	17.2	16.8	0.40	5.6E+14
97	1.1	668.3	130.2	17.6	14.7	0.40	5.6E+14
98	1.1	680.1	126.7	18.0	11.7	0.40	5.6E+14
99	1.1	691.0	125.5	18.4	9.7	0.40	5.6E+14
100	1.1	699.7	125.9	18.7	8.3	0.40	5.6E+14
101	1.1	710.6	127.1	19.1	6.9	0.40	5.6E+14
103A	3.3	709.2	125.9	13.7	23.0	0.40	4.7E+14
104	3.3	718.7	125.5	13.8	21.8	0.40	4.7E+14
105	3.3	730.3	125.1	14.6	18.8	0.40	4.7E+14
106	3.3	740.9	124.6	15.0	16.4	0.40	4.7E+14
107	3.3	764.3	121.4	16.2	12.1	0.40	4.7E+14
108	3.3	785.8	125.1	17.7	9.7	0.40	4.7E+14

TABLE A.2   STIRRED-FLØW REACTØR EXPERIMENTAL DATA
PYRØLYSIS ØF TRANS-1,2-DICYANØCYCLØBUTANE

RUN	TEMP. °C	U' ML/SEC	T(AMB) °C	U ML/SEC	U/V SEC^{-1}	PEAK AREA, CØUNTS	
						VCN	DICN
DI 6	340.6	7.43	29.0	15.09	0.0842	55	1195
7	342.4	7.46	28.9	15.20	0.0848	55	1160
8	342.0	10.53	28.9	21.44	0.1196	45	1220
9	356.7	7.49	28.4	15.64	0.0872	125	1140
10	356.5	7.46	28.2	15.59	0.0869	125	1125
11	356.0	10.58	28.2	22.09	0.1232	98	1185
12	370.4	7.48	27.7	16.00	0.0892	300	720
13	371.6	7.46	27.7	15.99	0.0892	325	750
14	372.4	10.53	27.4	22.62	0.1261	250	770
15	387.3	7.42	26.7	16.34	0.0911	715	680
16	387.1	10.58	26.6	23.30	0.1300	560	850
17	386.5	13.11	26.3	28.88	0.1611	450	1020
27	297.5	7.33	25.2	14.02	0.0782	4	2120
28	297.6	7.35	26.0	14.02	0.0782	5	2460
29	306.4	7.38	26.4	14.23	0.0796	9	2520
30	307.6	7.34	27.0	14.20	0.0792	9	2120
31	316.2	7.42	28.5	14.50	0.0808	20	3360
32	317.5	7.39	28.7	14.46	0.0806	23	3100
33	317.1	7.38	29.2	14.41	0.0803	25	3280
34	326.5	7.45	31.1	14.68	0.0819	45	1840
35	327.6	7.50	31.9	14.77	0.0824	51	2420
36	327.2	7.49	31.9	14.74	0.0822	54	3080
37	327.1	7.50	32.0	14.75	0.0823	47	2100
38	335.9	7.58	33.3	15.06	0.0840	67	1640
39	337.1	7.53	33.4	14.99	0.0836	67	1660
40	337.1	10.70	33.4	21.30	0.1188	49	2620
41	336.5	13.56	33.3	26.97	0.1504	36	2420
42	336.8	7.81	34.0	15.51	0.0865	69	1780

TABLE A.2   STIRRED-FLØW REACTØR EXPERIMENTAL DATA
contd   PYRØLYSIS ØF TRANS-1,2-DICYANØCYCLØBUTANE

RUN	TEMP. °C	U' ML/SEC	T(AMB) °C	U ML/SEC	U/V SEC^{-1}	PEAK AREA, CØUNTS VCN	DICN
DI 43	345.4	7.94	34.3	15.97	0.0891	70	940
44	346.4	10.84	35.0	21.79	0.1215	58	1080
45	346.9	13.65	35.0	27.46	0.1532	51	1015
47	355.1	7.78	35.2	15.85	0.0884	113	715
48	355.7	10.84	35.2	22.11	0.1233	101	780
49	356.3	13.70	35.0	27.98	0.1561	79	745
51	297.5	7.46	28.6	14.11	0.0787	5	2080
52	297.6	7.42	28.4	14.04	0.0783	4	1940
53	297.6	7.38	28.2	13.98	0.0780	4	1670
54	315.7	7.48	28.1	14.62	0.0815	13	1580
55	315.8	7.38	28.1	14.43	0.0805	13	1740
56	317.4	7.45	28.0	14.61	0.0815	14	2000
57	335.4	7.33	28.1	14.91	0.0831	27	1075
58	336.4	7.37	28.3	14.90	0.0831	33	950
59	337.7	7.41	28.4	15.01	0.0837	36	1075
60	354.7	7.45	28.5	15.51	0.0865	90	700
61	356.2	7.50	28.6	15.64	0.0872	110	640
62	357.7	10.50	28.7	21.94	0.1224	80	1100
63	357.4	13.20	28.7	27.57	0.1538	68	1135
64	356.8	6.91	29.0	14.41	0.0803	110	670
65	365.4	11.02	30.8	23.15	0.1291	157	1340
66	366.0	8.03	30.5	16.90	0.0943	197	880
67	366.4	13.75	31.3	28.83	0.1611	142	1250
68	375.0	14.76	32.2	31.33	0.1747	220	1460
69	375.7	12.38	32.0	26.32	0.1468	250	1030
70	376.4	10.42	32.0	22.13	0.1237	295	890
71	376.7	8.35	32.0	17.78	0.0992	350	620
72	386.1	10.44	30.9	22.63	0.1262	460	540
73	386.6	7.16	31.0	15.53	0.0866	550	600
74	386.5	13.07	30.3	28.41	0.1584	400	680

TABLE A.3   VLPP RAW EXPERIMENTAL LATA
           PYRØLYSIS ØF ISØPRØPYL CYANILE

RUN	APERTURE MM	TEMP. °C	PEAK INTENSITIES				CN/AR (42/40)°	FLØW RATE MØLEC/SEC
			I26	I39	I40	I42		
IP128A	1.1	838.3	58.8	37.2	243.1	173.9	0.817	9.1E+14
129	1.1	859.2	67.9	35.6	243.1	161.5	0.817	9.1E+14
130	1.1	882.3	80.9	33.8	243.4	144.3	0.817	9.1E+14
131	1.1	899.1	92.6	31.7	243.6	130.3	0.817	9.1E+14
132	1.1	918.4	104.0	29.1	243.6	113.6	0.817	9.1E+14
133	1.1	937.7	117.5	25.5	243.4	93.6	0.817	9.1E+14
134	1.1	959.0	129.5	22.9	242.8	76.4	0.817	9.1E+14
135	1.1	977.8	139.4	20.3	244.7	62.7	0.817	9.1E+14
140	3.3	929.5	44.7	30.95	201.5	149.8	0.81	1.2E+15
141	3.3	948.5	48.4	30.4	202.3	145.3	0.81	1.2E+15
142	3.3	968.3	51.5	29.1	198.1	135.7	0.81	1.2E+15
143	3.3	980.2	55.9	29.1	201.8	130.5	0.81	1.2L+15
144	3.3	979.3	125.0	53.0	452.6	287.7	0.81	5.4E+15
145	3.3	947.3	42.6	23.15	180.8	126.3	0.81	5.4E+15
146	3.3	925.5	39.6	23.4	179.0	131.0	0.81	5.4E+15
151	1.1	850.1	64.6	33.15	252.4	175.5	0.814	5.2E+14
152	1.1	872.2	75.2	35.25	250.9	157.9	0.814	5.2E+14
153	1.1	890.8	87.1	33.4	253.6	144.3	0.814	5.2E+14
154	1.1	912.5	99.0	30.35	252.6	123.8	0.814	5.2E+14
155	1.1	930.5	109.7	27.1	248.7	105.2	0.814	5.2E+14
156	1.1	951.3	118.3	23.15	242.3	83.6	0.814	5.2E+14
157	1.1	969.8	133.9	22.15	253.2	73.2	0.814	5.2E+14
161	1.1	828.5	44.7	30.75	202.1	147.4	0.80	7.5E+14
162	1.1	844.2	46.3	27.7	195.4	135.9	0.80	7.5E+14
166	3.3	933.2	41.0	30.75	207.1	150.7	0.80	7.1E+14
167	3.3	949.5	48.3	30.75	208.1	147.2	0.80	7.1E+14
168	3.3	978.1	56.8	30.55	211.6	139.2	0.80	7.1E+14
179	1.1	801.1	42.55	32.5	171.9	156.5	0.95	1.0E+15
180	1.1	831.6	46.55	30.95	171.9	146.1	0.95	1.0E+15
181	1.1	875.5	60.6	23.35	171.1	124.8	0.94	1.0E+15
188	1.1	833.7	64.2	39.8	266.5	183.6	0.80	1.0E+15
189	1.1	809.6	59.65	43.85	265.7	203.4	0.80	1.0E+15
190	1.1	820.3	61.3	43.25	254.2	193.1	0.80	1.0E+15

TABLE A.4   VLPP RAW EXPERIMENTAL DATA
PYRØLYSIS ØF ISØPRØPYL CYANILE

RUN	APERTURE MM	TEMP. °C	PEAK INTENSITIES				CN/AR (68/20)°	FLØW RATE MØLEC/SEC
			I 20	I 41	I 53	I 63		
IP128A	1.1	838.3	27.1	55.9	21.0	40.45	1.70	9.1E+14
129	1.1	859.2	27.5	53.05	25.0	37.85	1.70	9.1E+14
130	1.1	882.3	27.6	43.9	30.3	33.4	1.70	9.1E+14
131	1.1	899.1	28.1	45.5	35.1	30.4	1.70	9.1E+14
132	1.1	918.4	28.05	40.8	40.1	26.3	1.70	9.1E+14
133	1.1	937.7	28.05	35.35	45.65	21.8	1.70	9.1E+14
134	1.1	959.0	28.1	30.15	50.9	17.55	1.70	9.1E+14
135	1.1	977.8	28.4	26.8	55.0	14.75	1.70	9.1E+14
140	3.3	929.5	22.95	46.3	15.85	34.9	1.70	1.2E+15
141	3.3	943.5	23.0	45.5	17.55	33.85	1.70	1.2E+15
142	3.3	963.3	22.8	42.9	19.25	31.8	1.70	1.2E+15
143	3.3	980.2	23.0	42.1	20.6	31.0	1.70	1.2E+15
144	3.3	979.3	52.5	98.2	44.1	64.8	1.60	5.4E+15
145	3.3	947.3	21.4	41.2	15.0	29.5	1.60	5.4E+15
146	3.3	925.5	21.1	41.4	13.5	30.3	1.60	5.4E+15
151	1.1	850.1	28.2	55.75	23.7	41.2	1.74	5.2E+14
152	1.1	872.2	28.05	51.45	28.45	37.1	1.74	5.2E+14
153	1.1	890.8	28.75	48.0	34.0	34.05	1.74	5.2E+14
154	1.1	912.5	28.8	42.85	39.95	29.4	1.74	5.2E+14
155	1.1	930.5	28.7	37.5	43.7	24.7	1.74	5.2E+14
156	1.1	951.3	27.95	31.55	48.05	19.85	1.74	5.2E+14
157	1.1	969.8	29.35	29.3	54.3	17.2	1.74	5.2E+14
161	1.1	828.5	22.35	44.9	15.9	34.5	1.71	7.5E+14
162	1.1	844.2	21.7	41.6	16.3	31.7	1.70	7.5E+14
166	3.3	933.2	23.25	46.35	16.15	35.6	1.70	7.1E+14
167	3.3	949.5	23.9	45.7	18.65	34.8	1.70	7.1E+14
168	3.3	978.1	24.05	43.7	21.1	32.9	1.70	7.1E+14
179	1.1	801.1	19.4	48.1	14.0	34.75	1.89	1.0E+15
180	1.1	831.6	19.35	46.0	15.9	32.8	1.90	1.0E+15
181	1.1	875.5	19.5	41.35	21.85	27.9	1.90	1.0E+15
188	1.1	833.7	31.75	58.2	21.0	40.1	1.41	1.0E+15
189	1.1	809.6	32.05	64.8	19.4	44.3	1.5	1.0E+15
190	1.1	820.3	31.75	63.75	20.65	42.7	1.5	1.0E+15

TABLE A.5   VLPP RAW EXPERIMENTAL DATA
              PYRØLYSIS ØF N-PRØPYL CYANILE

| RUN | APERTURE MM | TEMP. °C | PEAK INTENSITIES | | | | | | CN/AR (29/20)° | FLØW RATE MØLEC/SEC |
			I 14	I 20	I 26	I 29	I 42	I 53		
NP 66	1.1	829.3	8.1	23.4	33.3	116.7	6.8	–	5.81	2.4E+15
67	1.1	851.6	9.55	23.5	38.7	108.2	6.2	–	5.84	2.4E+15
68	1.1	869.8	10.7	23.7	42.4	99.1	5.7	–	5.86	2.4E+15
69	1.1	837.3	10.9	23.3	45.8	91.5	5.2	–	5.86	1.6E+15
70	1.1	910.8	12.9	24.05	54.1	75.9	4.4	–	5.86	1.6E+15
71	1.1	930.1	13.4	23.5	59.8	62.9	4.2	–	5.86	1.6E+15
72	1.1	950.0	16.3	24.9	68.1	54.1	3.4	–	5.86	1.6E+15
73	1.1	957.8	16.6	24.7	68.1	48.4	2.9	–	5.86	1.6E+15
74	1.1	969.4	17.7	24.7	72.5	42.9	2.9	–	5.86	1.6E+15
82	3.3	917.3	12.7	39.0	50.6	202.5	10.8	–	5.80	1.7E+15
83	3.3	940.6	14.3	39.7	55.1	195.6	10.8	–	5.80	1.7E+15
84	3.3	959.5	16.1	39.95	60.5	188.9	10.3	–	5.80	1.7E+15
85	3.3	974.4	16.7	39.0	62.4	171.7	9.8	–	5.80	1.7E+15
87	3.3	897.9	5.9	24.0	24.4	109.2	5.7	1.1	4.83	3.2E+15
88	3.3	917.7	6.9	24.45	26.3	109.2	5.2	1.2	4.83	3.2E+15
89	3.3	938.2	7.45	24.6	28.9	104.5	5.5	1.35	4.83	3.2E+15
90	3.3	937.9	10.8	41.1	44.5	159.5	8.6	2.6	4.83	8.4E+15
91	3.3	938.5	21.75	61.15	89.4	321.4	18.2	5.0	6.21	5.2E+15

TABLE A.5   VLPP RAW EXPERIMENTAL DATA
contd   PYRØLYSIS ØF N-PRØPYL CYANIDE

RUN	APERTURE MM	TEMP. °C	PEAK INTENSITIES						CN/AR (29/20)°	FLØW RATE MØLEC/SEC
			I 14	I 20	I 26	I 29	I 42	I 53		
NP 98	1.1	316.6	7.65	24.0	30.7	136.5	7.3	1.6	6.26	2.0E+15
99	1.1	838.2	8.9	24.1	35.9	129.5	6.8	2.1	6.29	2.0E+15
100	1.1	857.8	10.2	24.35	40.6	123.2	6.5	2.7	6.32	2.0E+15
101	1.1	873.5	23.55	49.2	93.1	219.6	12.4	6.55	6.35	2.0E+15
102	1.1	897.5	26.4	49.5	105.2	201.3	10.8	7.4	6.35	2.0E+15
103	1.1	920.5	30.45	50.05	121.4	168.7	9.3	7.9	6.35	2.0E+15
104	1.1	937.5	33.8	50.1	134.3	145.8	8.8	8.45	6.35	2.0E+15
105	1.1	958.6	38.1	51.4	149.4	119.1	7.7	8.4	6.35	2.0E+15
106	1.1	977.5	40.4	51.9	158.7	97.0	6.3	7.7	6.35	2.0E+15
109	1.1	819.5	14.45	39.9	65.3	272.7	14.2	3.1	7.57	7.1E+14
110	1.1	858.8	21.25	40.9	80.6	246.0	13.1	4.1	7.57	7.1E+14
111	1.1	898.9	26.65	42.8	105.8	203.1	10.0	5.3	7.57	7.1E+14
113	3.3	899.3	16.1	41.4	65.0	298.5	15.8	2.8	7.60	6.1E+14
114	3.3	919.2	18.8	42.8	63.1	295.4	15.3	2.9	7.60	6.1E+14
115	3.3	939.5	19.9	41.4	71.0	275.6	13.7	3.0	7.60	6.1E+14
116	3.3	962.4	22.5	41.4	77.0	259.0	13.1	3.1	7.60	6.1E+14
117	3.3	975.5	24.8	43.3	85.5	259.0	13.7	3.4	7.60	6.1E+14

TABLE A.6   VLPP RAW EXPERIMENTAL DATA
                 PYROLYSIS OF T-BUTYL CYANIDE

RUN	APERTURE MM	TEMP. °C	PEAK INTENSITIES					CN/AR (42/40)°	FLOW RATE MOLEC/SEC
			I 40	I 42	I 56	I 67	I 68		
TB 4	1.1	762.8	226.7	186.7	1.96	16.2	32.85	0.97	3.8E+15
5A	1.1	782.8	227.0	166.4	1.61	17.3	29.6	0.97	3.8E+15
6	1.1	804.7	227.8	139.4	1.61	18.5	25.05	0.97	3.8E+15
12	1.1	749.7	342.2	305.2	2.10	24.8	54.4	1.00	2.8E+15
13	1.1	771.0	345.8	281.8	2.39	27.6	52.1	1.00	2.8E+15
14	1.1	789.0	343.7	247.5	2.22	28.7	45.95	1.00	2.8E+15
15	1.1	810.8	347.9	205.9	2.37	30.4	38.4	1.00	2.8E+15
16	1.1	830.4	351.0	166.4	2.24	31.1	30.9	1.00	2.8E+15
17	1.1	849.3	352.0	131.8	2.15	32.2	24.7	1.04	2.8E+15
18	3.3	848.8	343.7	299.5	1.66	28.8	55.8	1.04	2.8E+15
22	3.3	830.3	259.2	237.6	1.22	19.8	43.4	1.02	3.1E+15
24	3.3	850.5	260.3	217.9	1.27	21.0	40.05	1.02	3.1E+15
25	3.3	867.5	262.3	201.2	1.37	21.9	36.95	1.02	3.1E+15
26	3.3	891.9	265.5	172.6	1.39	23.2	31.95	1.02	3.1E+15
27	3.3	914.8	269.9	146.6	1.41	24.6	27.3	1.02	3.1E+15
28	3.3	928.4	547.1	264.1	2.95	51.75	49.45	1.02	3.0E+15
29	3.3	952.2	551.3	211.1	2.9	54.0	40.0	1.02	3.0E+15
30	3.3	972.4	556.5	174.3	2.7	55.1	33.0	1.02	3.0E+15
35	10.0	912.5	226.2	205.9	0.98	17.4	38.0	0.99	2.2E+15
36	10.0	930.0	227.8	196.8	0.98	17.8	36.5	0.99	2.2E+15
37	10.0	943.1	229.6	189.8	0.98	18.4	35.2	0.99	2.2E+15
38	10.0	959.3	230.9	179.4	1.00	19.1	33.8	0.99	2.2E+15
39	10.0	971.7	234.3	172.1	1.07	19.95	32.7	0.99	2.2E+15

TABLE A.6   VLPP RAW EXPERIMENTAL LATA
    contd   PYRØLYSIS ØF T-BUTYL CYANILE

RUN	APERTURE MM	TEMP. °C	PEAK INTENSITIES					CN/AR (42/40)°	FLØW RATE MØLEC/SEC
			I 40	I 42	I 56	I 67	I 68		
TB40	1.1	750.2	265.7	218.9	1.61	17.65	39.6	0.965	2.6E+14
41	1.1	770.3	265.2	201.8	1.66	18.85	36.9	0.965	2.6E+14
42	1.1	784.6	269.1	188.0	1.76	19.75	34.45	0.965	2.6E+14
43	1.1	802.3	270.4	164.6	1.85	21.4	30.8	0.965	2.6E+14
44	1.1	321.8	275.1	137.5	1.86	22.7	26.1	0.965	2.6E+14
45	1.1	841.2	275.9	109.7	1.66	24.55	21.0	0.95	2.6E+14
46	1.1	861.4	562.8	172.2	3.25	50.3	33.5	0.95	2.6E+14
47	1.1	874.3	553.1	142.3	3.2	51.1	27.6	0.95	2.6E+14
43	1.1	331.3	584.3	132.3	3.2	53.3	26.7	0.95	2.6E+14
49	1.1	893.3	593.3	114.5	3.0	55.2	23.4	0.95	2.6E+14
50	1.1	904.0	609.0	101.3	3.0	57.5	21.1	0.95	2.6E+14
51	1.1	903.?	465.7	74.6	2.15	41.1	15.05	0.965	1.9E+15
52	1.1	914.8	441.0	62.0	1.9	39.95	12.75	0.965	1.9E+15
53	3.3	872.2	309.2	226.8	1.41	23.55	39.9	0.97	1.5E+15
54	3.3	881.5	317.1	220.0	1.49	25.35	39.45	0.97	1.5E+15
55	3.3	902.1	320.8	194.8	1.53	27.25	35.35	0.97	1.5E+15
56	3.3	911.5	322.9	182.2	1.53	28.5	33.9	0.97	1.5E+15
57	3.3	923.7	327.6	165.4	1.57	30.0	31.65	0.97	1.5E+15
58	3.3	940.3	333.4	144.9	1.53	31.35	27.7	0.97	1.5E+15
59	3.3	959.8	326.4	118.3	1.51	32.35	23.1	0.97	1.5E+15
60	3.3	979.8	326.6	97.1	1.47	32.75	18.9	0.97	1.5E+15
61	3.3	979.7	797.0	229.4	3.49	73.7	43.4	0.97	6.2E+15
62	3.3	939.8	800.6	343.9	3.69	71.3	63.9	0.97	6.2E+15
63	3.3	940.2	883.6	357.0	3.57	71.1	63.2	0.97	1.1E+16
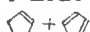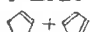
TABLE A.6 contd   VLPP RAW EXPERIMENTAL DATA
PYRØLYSIS ØF T-BUTYL CYANILE

RUN	APERTURE MM	TEMP. °C	PEAK INTENSITIES					CN/AR (42/40)°	FLØW RATE MØLEC/SEC
			I 40	I 42	I 56	I 67	I 68		
TB65	3.3	821.9	224.7	207.1	0.96	17.45	39.55	1.02	9.9E+14
66	3.3	832.7	220.8	196.4	0.94	17.0	37.0	1.02	9.9E+14
67	3.3	845.3	225.5	190.9	0.93	17.95	36.4	1.02	9.9E+14
68	3.3	861.7	229.6	180.2	1.00	18.9	34.7	1.02	9.9E+14
69	3.3	900.5	233.1	145.1	1.04	20.9	27.9	1.02	9.7E+14
70	3.3	919.2	228.0	120.7	0.96	21.2	23.5	1.02	9.7E+14
71	3.3	939.8	237.2	104.3	0.96	22.8	20.1	1.02	9.7E+14
72	10.0	921.6	230.2	201.1	0.98	18.7	39.2	1.02	1.1E+15
73	10.0	943.8	233.1	190.4	0.98	19.5	37.4	1.02	1.1E+15
74	10.0	963.2	231.0	169.3	1.00	19.85	33.4	1.02	1.1E+15
75	10.0	900.5	299.0	208.5	0.76	16.2	37.1	0.755	5.3E+15
76	10.0	920.6	301.6	193.6	0.78	16.9	35.9	0.755	5.3E+15
77	10.0	944.0	293.7	184.9	0.83	17.7	33.5	0.755	4.9E+15
78	10.0	960.1	301.1	175.8	0.90	18.2	31.85	0.755	4.9E+15
79	10.0	980.3	302.9	162.2	0.95	19.2	29.8	0.755	4.9E+15
80	10.0	901.2	255.8	201.5	0.59	12.95	29.5	0.86	1.5E+16
81	10.0	941.9	248.0	176.3	0.61	14.0	26.95	0.86	1.5E+16
82	10.0	967.3	242.8	153.6	0.59	15.05	25.1	0.86	1.5E+16
83	10.0	943.8	219.2	179.7	1.34	17.9	34.7	0.99	4.9E+14
84	10.0	952.1	221.5	176.3	1.32	18.4	34.3	0.99	4.9E+14
85	1.1	750.3	130.8	178.1	0.86	14.25	31.9	1.125	7.9E+14
86	1.1	770.5	134.1	164.2	0.93	15.25	29.95	1.115	7.9E+14
87	1.1	800.1	132.5	133.5	1.00	16.15	24.1	1.11	7.9E+14
88	1.1	839.6	195.2	90.4	1.02	19.4	17.05	1.10	8.3E+14
89	1.1	860.1	198.0	69.5	0.94	20.2	13.4	1.095	8.3E+14

TABLE A.7 STIRRED-FLØW REACTØR EXPERIMENTAL DATA PYRØLYSIS ØF CYCLØPENTYL CYANIDE

RUN	TEMP. $^\circ$C	U' ML/SEC	T(AMB) $^\circ$C	U ML/SEC	U/V SEC^{-1}	HCN	$\bigcirc$+$\bigcirc$	VCN	C3H5CN	CPCN
CPE 2	693.0	5.35	24.0	17.39	0.0970	20	450	340	260	3240
3	693.7	5.15	24.0	16.75	0.0934	22	455	323	220	3220
4	718.4	5.35	23.8	17.86	0.0996	34	555	520	300	2390
5	718.3	5.18	23.8	17.29	0.0964	32	557	522	340	2410
6	718.3	6.70	23.8	22.37	0.1247	36	567	510	340	2990
7	718.2	6.76	24.2	22.53	0.1257	36	580	535	340	2310
8	742.5	6.71	25.2	22.84	0.1274	49	595	780	360	1630
9	742.5	6.74	25.1	22.95	0.1280	50	635	810	390	1920
10	742.3	7.46	26.0	25.32	0.1412	51	650	805	385	1935
11	742.3	7.56	25.2	25.73	0.1435	51	615	812	425	2230
13	645.5	5.98	23.3	18.53	0.1033	5	95	40	20	6720
14	643.0	6.88	23.3	21.26	0.1186	5	60	30	20	5760
15	642.5	6.85	23.3	21.16	0.1180	3	70	27	20	6410
16	669.6	6.95	23.1	22.11	0.1233	7	170	90	40	5640
17	668.5	7.04	23.2	22.37	0.1247	5	200	100	110	6760
18	668.2	5.79	23.3	18.38	0.1025	5	220	133	120	6440
19	668.0	5.83	23.3	18.51	0.1032	10	245	145	120	6390
20	681.6	6.94	24.1	22.29	0.1243	10	275	215	145	6530
21	682.8	6.94	24.9	22.26	0.1241	10	265	220	125	6720
22	682.9	5.88	25.0	18.85	0.1051	15	335	285	220	6240
25	693.4	9.46	23.5	30.98	0.1728	10	155	175	100	3365
26	698.0	12.30	23.5	40.26	0.2246	10	105	108	52	3500
28	713.4	9.50	24.0	31.70	0.1768	22	195	305	120	2695
29	718.0	12.35	23.8	41.22	0.2299	35	345	515	210	6700

TABLE A.7 contd   STIRRED-FLØW REACTØR EXPERIMENTAL DATA
PYRØLYSIS ØF CYCLØPENTYL CYANIDE
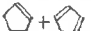
RUN	TEMP. °C	U' ML/SEC	T(AMB) °C	U ML/SEC	U/V SEC^{-1}	HCN	⬠+⬠	VCN	C3H5CN	CPCN	CPCN°
CPE30	739.6	9.38	23.5	32.02	0.1786	57	330	860	230	4410	9050
31	740.5	12.55	23.6	42.86	0.2391	60	355	795	310	5140	8300
32	740.2	6.65	23.1	22.74	0.1269	75	425	1060	475	3950	8550
33	761.3	9.46	23.3	33.01	0.1841	29	175	626	205	1160	4150
34	762.7	12.40	23.5	43.29	0.2415	35	180	628	225	1740	4025
35	762.2	6.67	22.9	23.32	0.1301	32	170	670	205	1010	3900
36	732.0	9.65	23.3	34.34	0.1915	39	190	797	290	820	3775
37	733.2	12.50	23.5	44.51	0.2482	40	170	760	235	940	3650
38	732.7	6.70	23.3	23.86	0.1331	35	160	770	230	430	3525
43	632.1	6.65	23.0	20.32	0.1134	-	170	70	-	18000	
46	651.8	6.57	22.4	20.56	0.1147	5	232	170	135	20700	
47	652.9	9.46	22.8	29.60	0.1651	3	185	110	75	17940	
48	652.8	12.54	23.1	39.19	0.2186	2	135	70	40	18060	
49	673.1	6.67	23.1	21.30	0.1188	28	360	460	195	17380	19000
50	673.1	9.35	23.1	29.36	0.1665	17	280	315	140	19200	
51	672.8	12.35	23.2	39.42	0.2193	10	192	132	110	18400	
52	693.4	6.50	22.7	21.33	0.1184	35	300	390	215	8000	9300
53	693.4	9.39	23.0	30.64	0.1709	22	270	300	170	8520	9300
54	693.3	12.50	22.9	40.30	0.2276	30	340	535	210	16800	18600
55	713.6	6.85	23.9	22.75	0.1269	56	400	770	310	6120	8640
56	713.1	10.00	24.0	33.19	0.1851	41	300	615	230	6970	9700
57	712.9	12.42	23.5	41.28	0.2302	35	300	530	260	8050	
58	731.4	6.98	23.7	23.62	0.1317	38	210	580	210	2360	4550
59	732.7	9.40	23.5	31.87	0.1777	35	200	470	185	2640	4620
60	732.2	12.50	24.0	42.29	0.2358	30	145	410	200	2940	4110

TABLE A.8   VLPP RAW EXPERIMENTAL DATA
                 PYRØLYSIS ØF CYCLØPENTYL CYANIDE
                 (FLØW RATE = 8 E+14 MØLECULES/SEC)

RUN	APERTURE MM	TEMP. °C	PEAK INTENSITIES								CN/AR (54/20)°
			I 20	I 27	I 28	I 42	I 53	I 54	I 66	I 67	
CP 31	1.1	781.0	10.25	32.9	3.55	59.05	4.85	59.9	3.4	4.95	7.05
32	1.1	802.4	10.3	34.7	6.1	54.2	5.35	53.3	3.7	4.5	7.05
34	1.1	770.2	10.1	28.05	0.5	54.45	3.95	56.6	2.8	4.6	6.68
35	1.1	791.1	10.2	31.9	2.0	56.85	5.0	57.5	3.3	4.8	6.87
36	1.1	810.8	10.2	35.7	4.3	52.55	5.5	52.55	3.45	4.45	7.12
38	1.1	850.0	10.6	45.4	13.0	41.7	7.4	39.3	3.8	3.7	7.63
39	1.1	870.2	10.8	51.0	20.0	34.3	8.05	30.85	3.85	3.0	7.63
40	1.1	800.3	10.5	41.45	8.0	71.65	6.75	67.85	4.0	5.3	8.55
42	3.3	822.6	10.7	40.8	7.7	84.8	5.6	87.2	3.5	7.45	8.55
43	3.3	838.3	10.4	40.05	9.0	73.8	5.6	80.6	3.5	7.0	8.55
44	3.3	859.8	10.5	42.6	12.0	76.1	5.7	76.5	3.35	6.85	8.55
47	1.1	776.0	10.7	26.9	1.8	54.7	4.0	55.2	2.7	4.3	5.91
48	1.1	800.4	10.6	25.5	3.55	48.7	4.3	48.2	2.7	3.8	5.97
48A	1.1	800.3	10.7	27.55	3.55	49.75	4.3	48.6	2.7	3.85	5.97
49	1.1	823.9	10.7	30.6	5.35	41.55	4.8	39.9	2.8	3.25	5.97
50	1.1	850.2	10.5	34.05	12.75	32.65	5.4	28.5	2.85	2.6	5.97
55	1.1	769.8	9.9	23.3	3.05	58.8	4.0	60.6	2.8	4.75	7.00
56	1.1	790.8	9.95	31.0	5.35	57.4	4.6	58.0	3.0	4.55	7.17
57	1.1	810.4	10.1	33.9	7.65	52.55	5.0	52.6	3.35	4.35	7.33
58	1.1	830.3	10.15	37.85	9.45	46.55	5.75	44.6	3.4	3.8	7.33
64	1.1	759.4	8.6	25.0	1.0	54.55	3.4	55.5	2.15	4.05	6.98
65	1.1	778.7	8.6	26.8	1.55	53.4	3.6	53.6	2.3	4.0	7.26
66	1.1	799.8	8.9	29.05	2.8	49.45	4.1	49.6	2.55	3.8	7.38
69	1.1	819.1	8.8	31.35	4.6	46.8	4.8	46.0	2.8	3.65	7.61
70	1.1	839.4	9.0	32.15	8.95	39.9	5.4	38.0	3.0	3.25	7.72
71	1.1	858.8	9.0	36.6	14.8	35.95	6.0	30.1	2.95	2.75	7.82
74	3.3	839.9	8.8	32.65	3.85	66.55	4.3	66.7	2.65	5.25	8.41
75	3.3	859.6	8.3	34.8	9.7	64.4	4.6	64.3	2.85	5.25	8.54

TABLE A.9 STIRRED-FLØW REACTØR EXPERIMENTAL DATA
PYRØLYSIS ØF ETHYL CYANIDE
(ABSENCE ØF INHIBITØR)

RUN	TEMP. °C	U' ML/SEC	T(AMB) °C	U ML/SEC	U/V SEC	PEAK AREA , CØUNTS		
						HCN	VCN	ETCN
ET 7	615.4	7.30	23.8	21.84	0.1213	62	220	9330
8	617.1	10.23	23.8	30.67	0.1710	25	130	9180
9	648.3	7.17	23.9	22.24	0.1240	260	760	8200
10	677.0	7.23	24.0	23.23	0.1298	225	655	2735
11	665.0	10.27	24.0	32.42	0.1808	150	350	3300
19	622.5	8.01	34.3	23.33	0.1301	60	325	7040
20	622.3	11.27	35.1	32.74	0.1826	43	145	7070
21	622.0	9.09	34.2	26.47	0.1476	50	170	7000
22	642.4	8.14	35.0	24.18	0.1349	85	560	6485
23	641.2	11.40	34.0	33.93	0.1893	95	420	6775
24	659.2	8.40	34.6	25.45	0.1419	165	760	5585
25	660.8	11.39	34.2	34.61	0.1930	150	690	6130
26	661.0	13.97	34.2	42.46	0.2363	150	640	6470
27	681.6	8.39	34.0	26.03	0.1454	370	1270	4565
28	681.5	11.24	34.0	34.93	0.1948	340	1145	5250
29	681.0	14.16	33.6	44.04	0.2456	255	905	5470
30	701.4	8.15	32.5	25.98	0.1449	440	1500	3150
31	701.3	11.29	32.5	35.99	0.2007	390	1365	3690
32	700.9	14.25	31.6	45.54	0.2540	370	1280	4245
33	713.5	8.00	31.0	26.03	0.1455	585	1650	2310
34	720.9	11.24	30.8	36.76	0.2050	510	1415	2245
35	720.9	14.08	30.7	46.06	0.2569	540	1565	3040
36	747.0	8.13	30.6	27.30	0.1523	780	1605	1140
37	746.5	11.26	30.3	37.83	0.2110	790	1830	1560
38	738.4	14.08	30.3	46.93	0.2617	600	1660	2185

A.2 Calibration Plots for the Concentration Ratio

The concentration ratio [product] / [reactant] is required to calculate the rate constants for the reaction paths. This was obtained by determining the calibration factor found by measuring the mass spectral peak intensity ratio for known mixtures of product and reactant in the VLPP system, or for the flow system, by measuring the peak area ratio for known product to reactant mixtures.

The mass spectrometer calibration plots for the VLPP of cyclobutyl cyanide, isopropyl cyanide, n-propyl cyanide, tert-butyl cyanide, and cyclopentyl cyanide are shown in Figures A.1, A.3 - A.4, A.5 -A.7, A.8 -A.9, and A.15 - A.20. Gas chromatograph calibration plots for the pyrolyses of trans - 1,2-dicyanocyclobutane, cyclopentyl cyanide, and ethyl cyanide are shown in Figures A.2, A.10 - A.14, and A.21 - A.23.
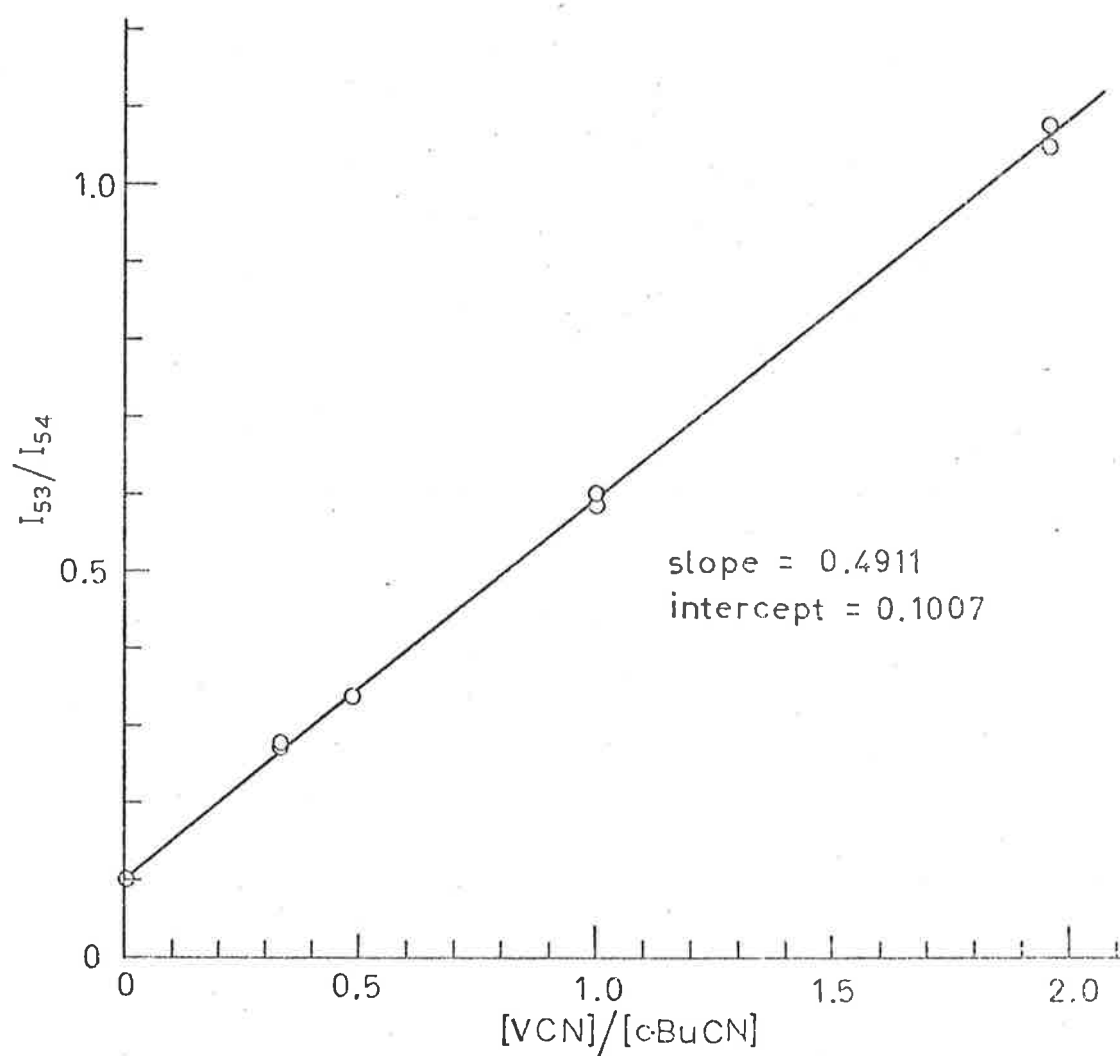
Figure A.1   Mass spectrometer calibration plot of the
ratio [vinyl cyanide]/[cyclobutyl cyanide]
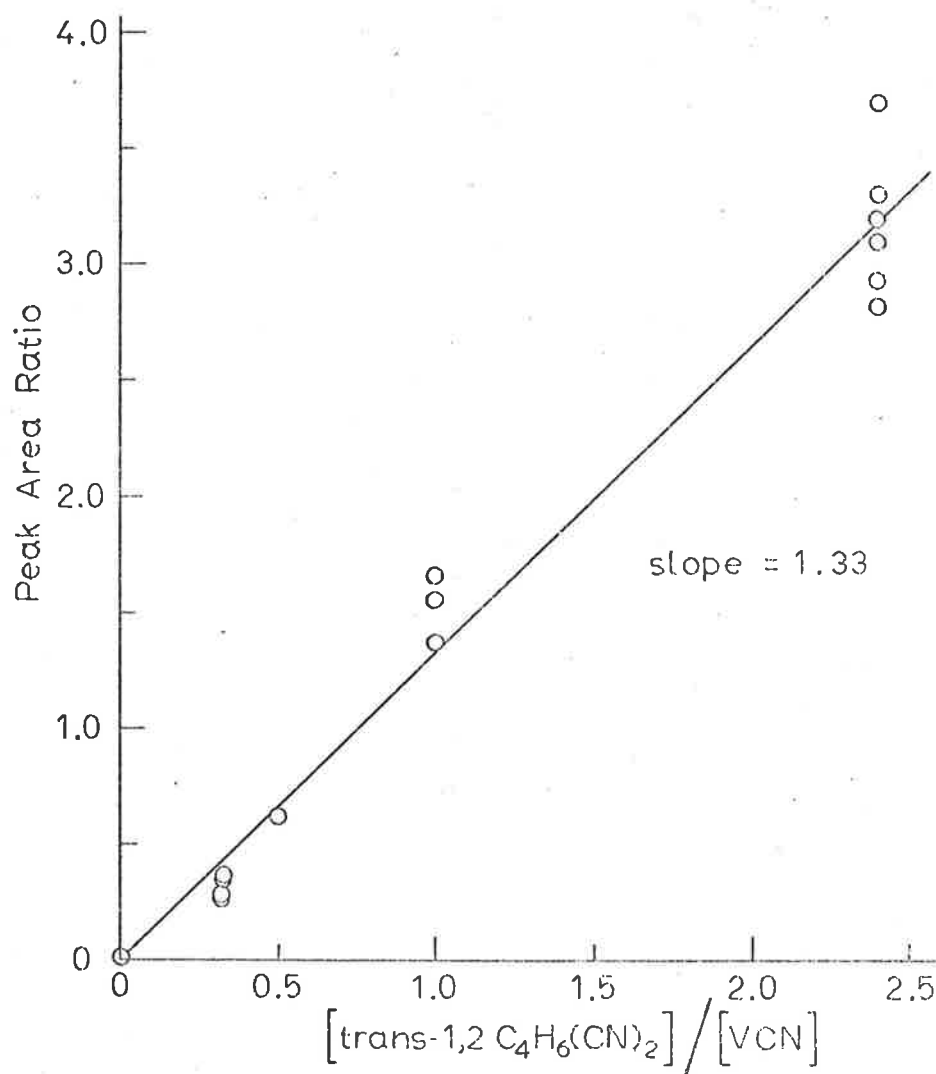
Figure A.2   Gas chromatograph calibration plot of the ratio
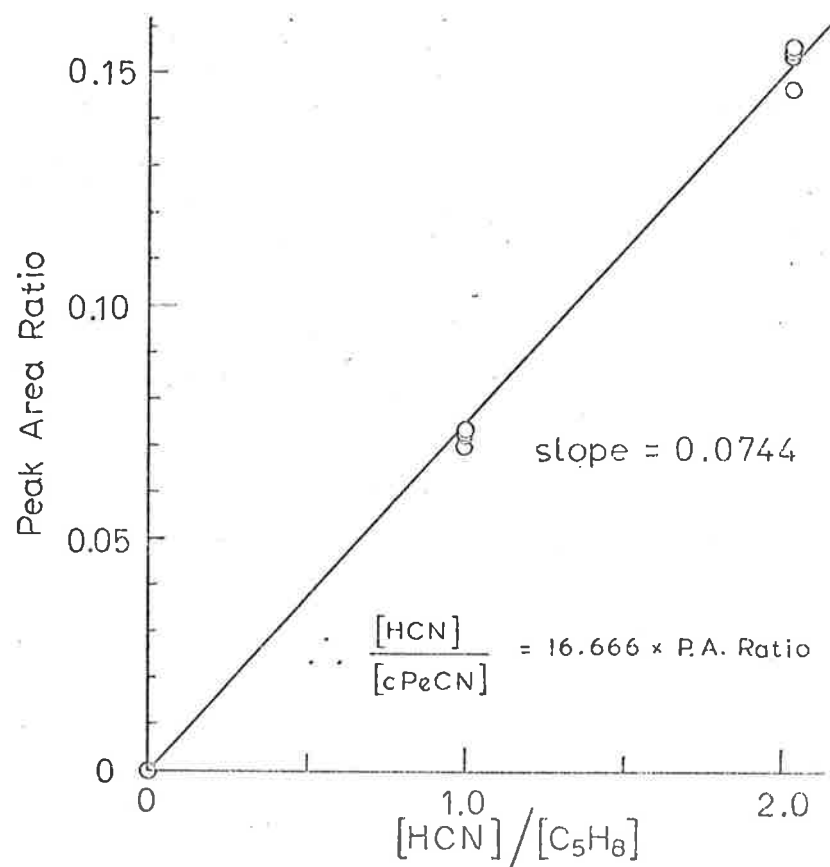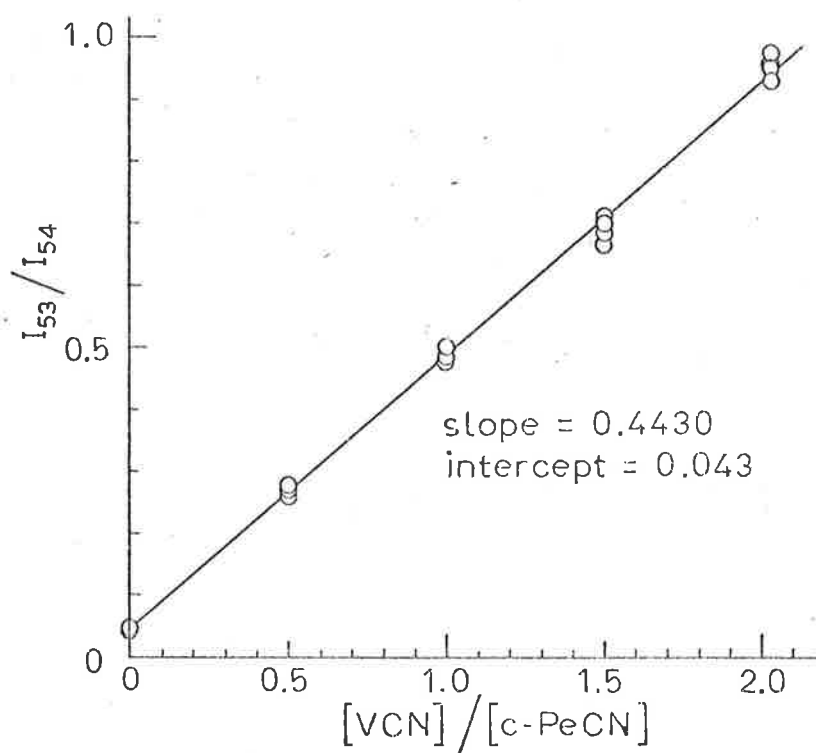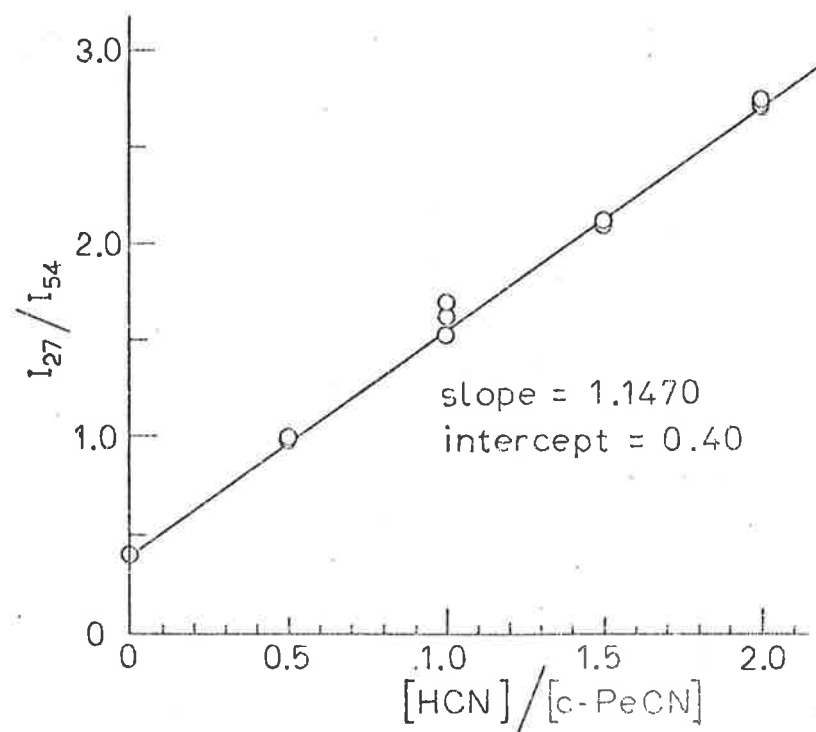   [trans-1,2-dicyanocyclobutane]/[vinyl cyanide]
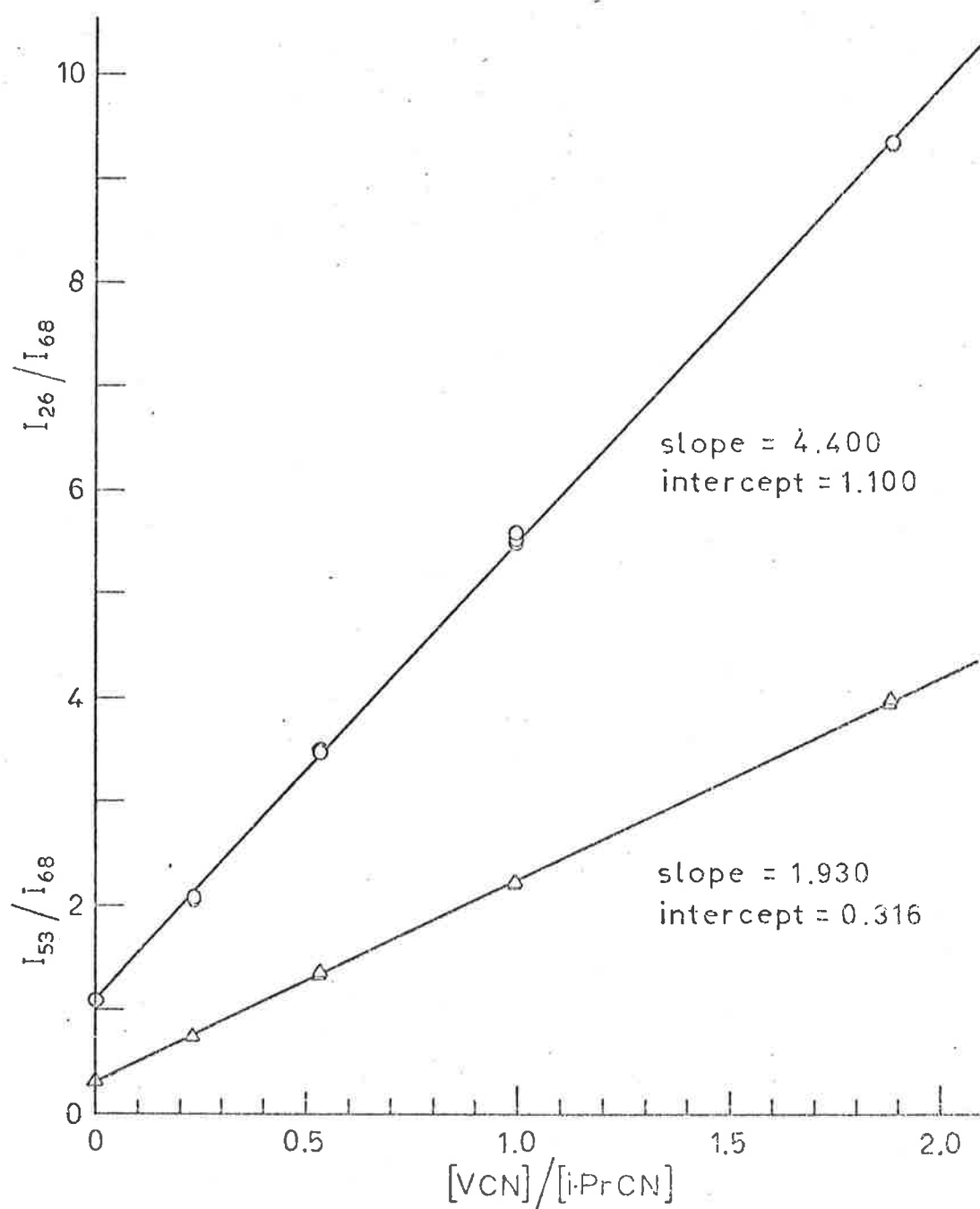
Figure A.3   Mass spectrometer calibration plot of the
            ratio [vinyl cyanide]/[isopropyl cyanide]
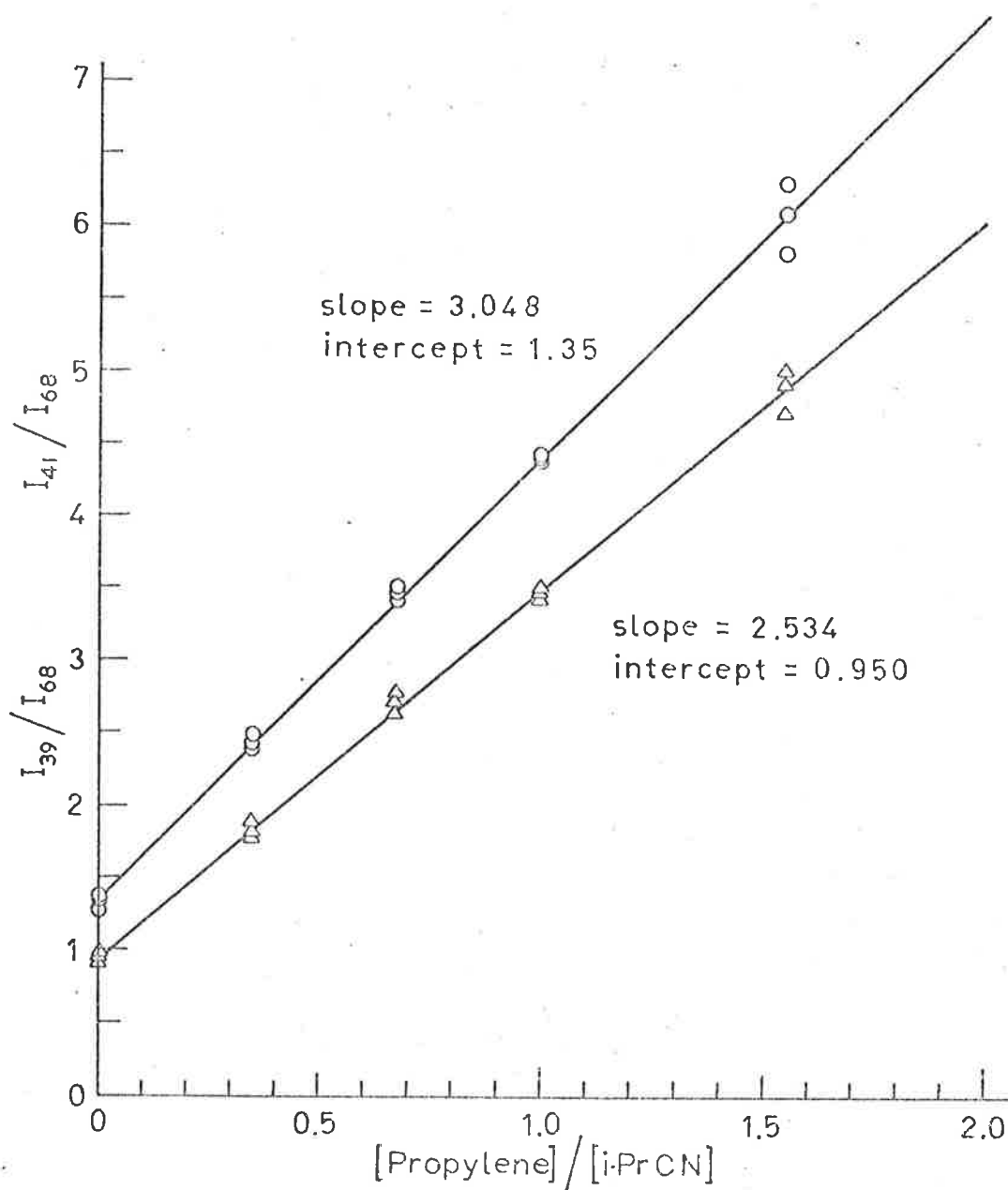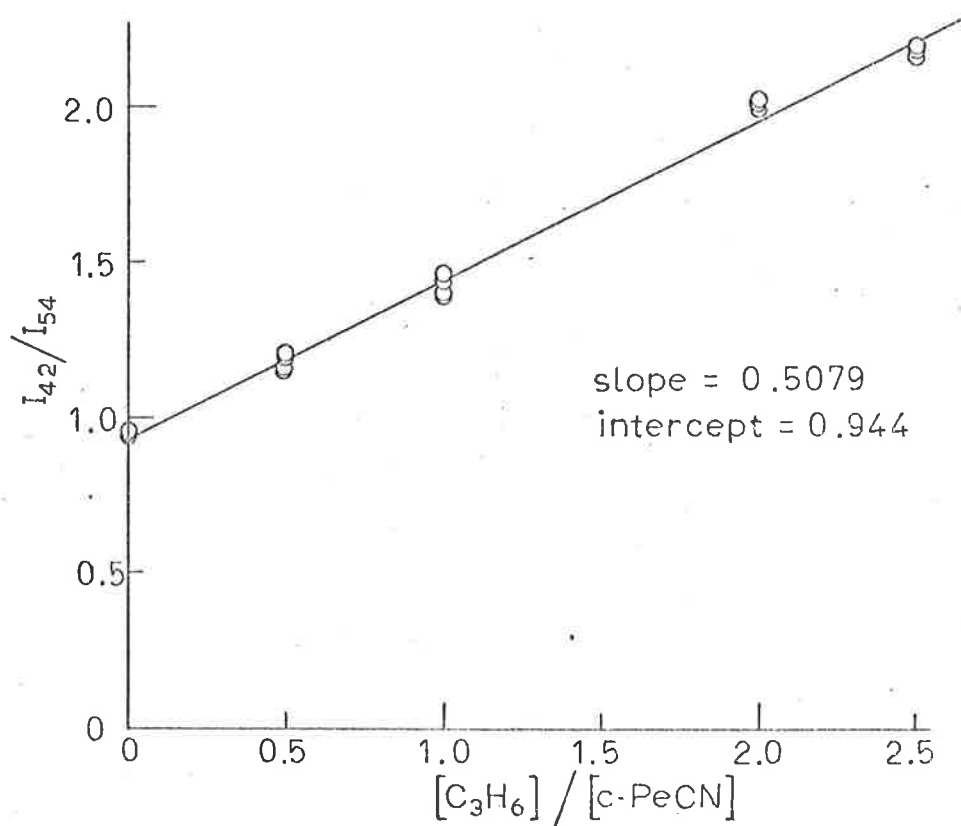
Figure A.4   Mass spectrometer calibration plot of the
ratio [propylene]/[isopropyl cyanide]
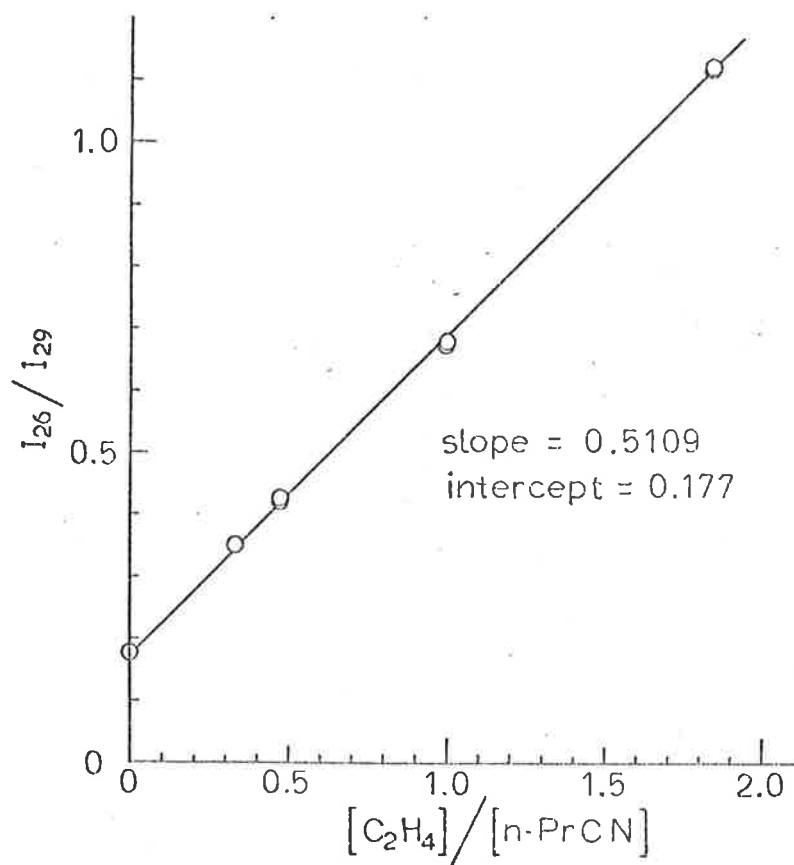
Figure A.5   Mass spectrometer calibration plot of the
ratio [ethylene]/[n-propyl cyanide]
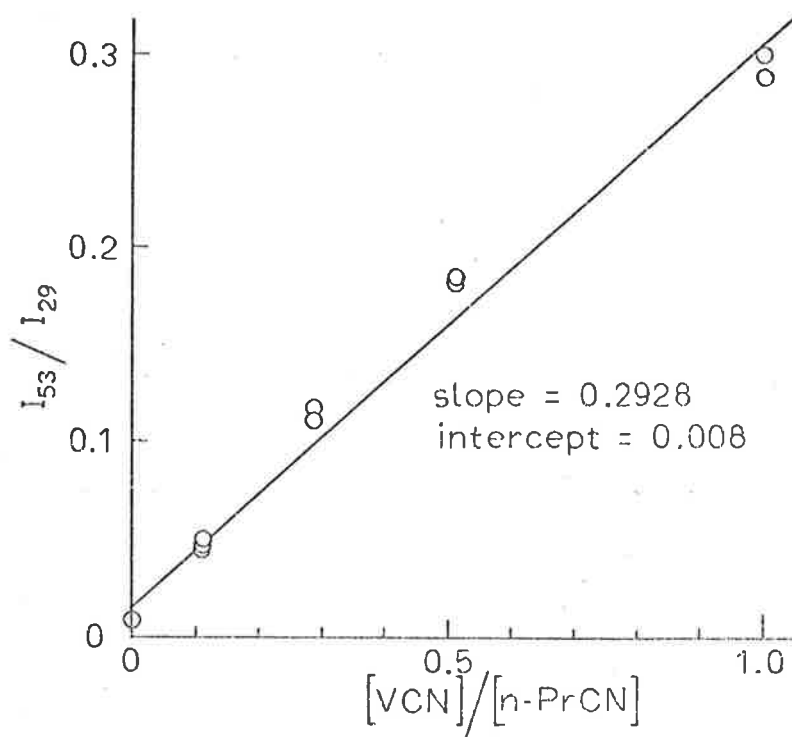
Figure A.6   Mass spectrometer calibration plot of the
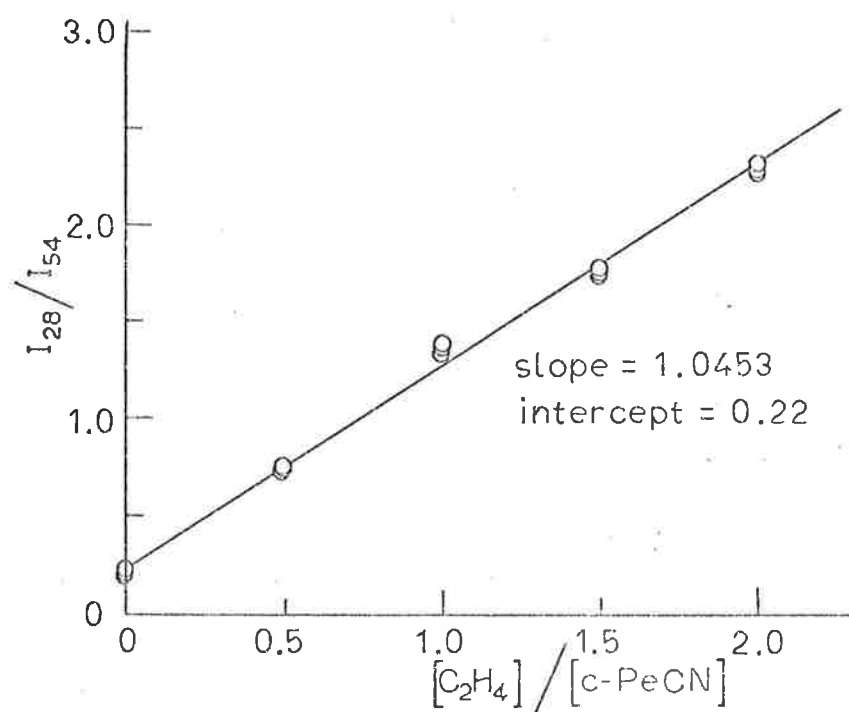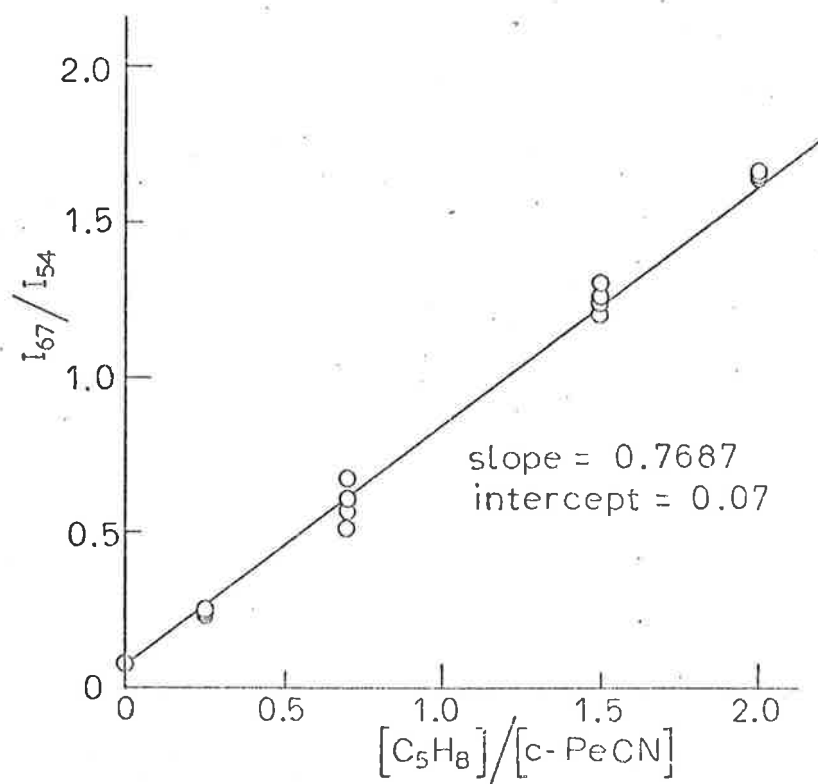ratio [vinyl cyanide]/[n-propyl cyanide]
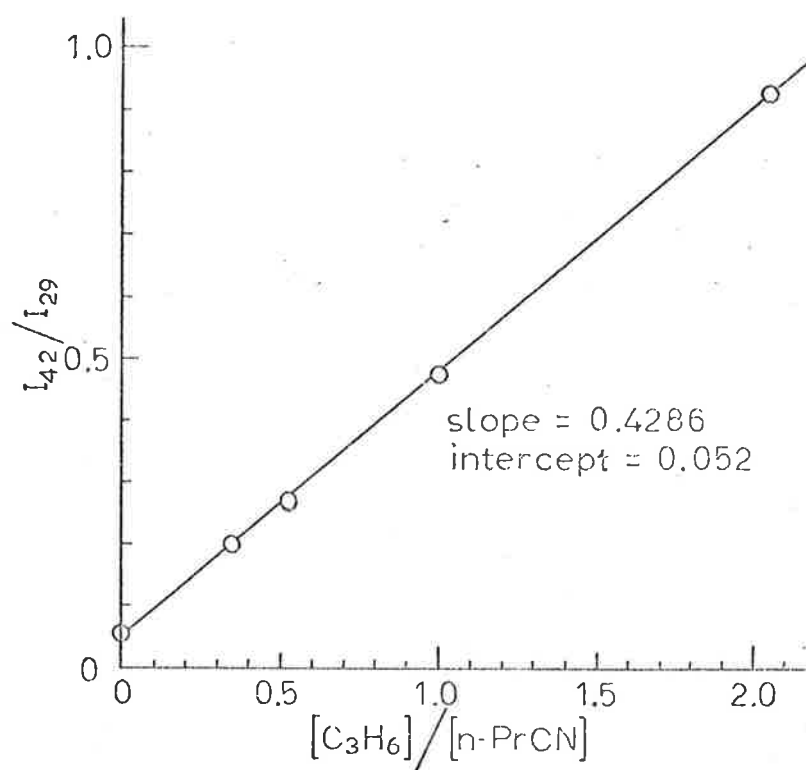
Figure A.7   Mass spectrometer calibration plot of the
ratio [propylene]/[n-propyl cyanide]
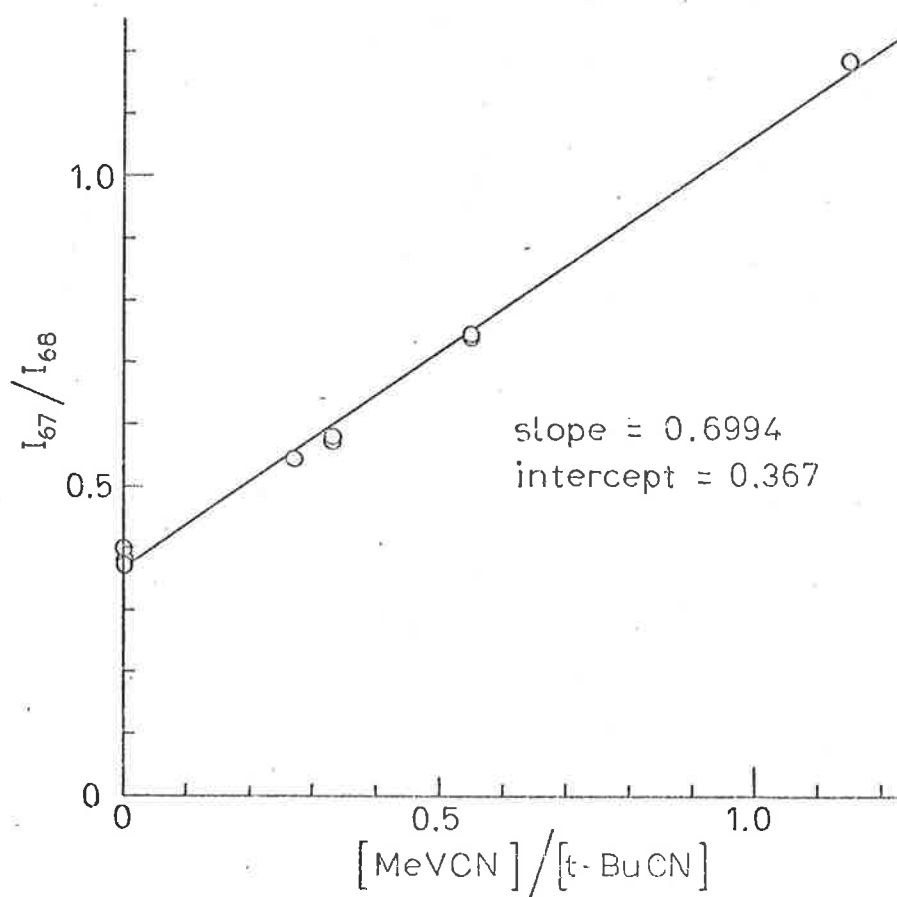
Figure A.8   Mass spectrometer calibration plot of the
             ratio [methyl vinyl cyanide]/[tert-butyl cyanide]
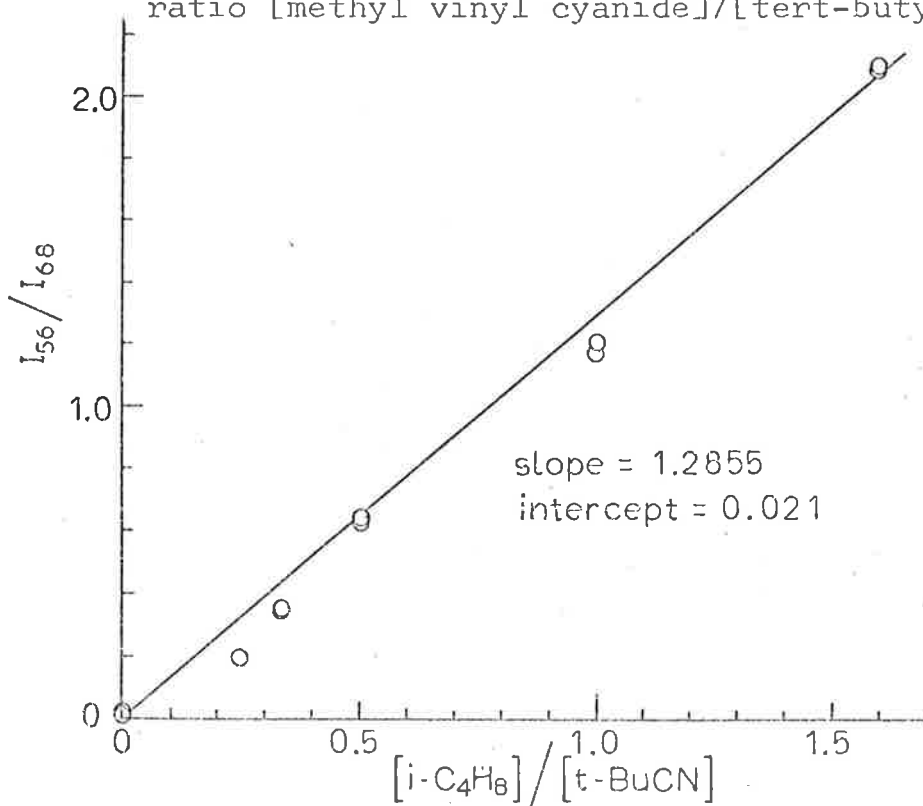
Figure A.9   Mass spectrometer calibration plot of the
             ratio [isobutene]/[tert-butyl cyanide]
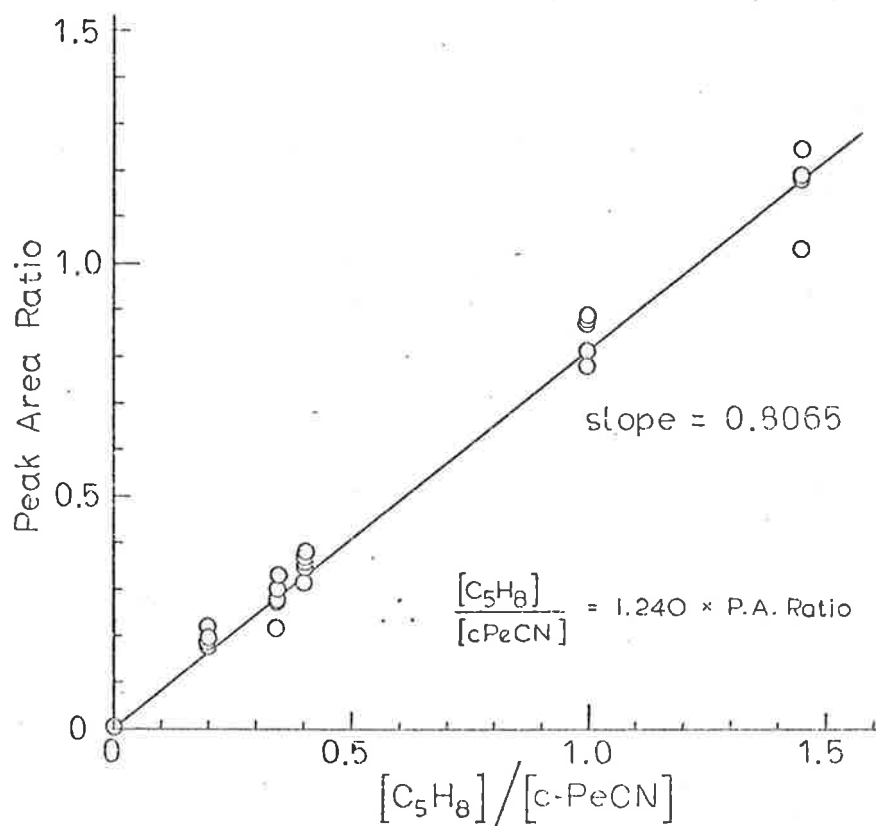
Figure A.10   Gas chromatograph calibration plot of the
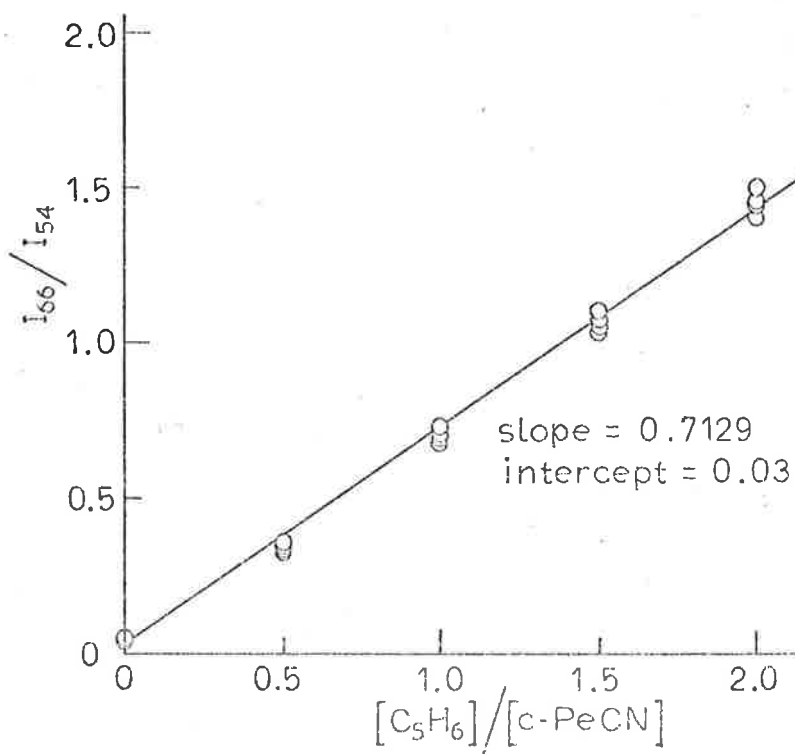   ratio [cyclopentene]/[cyclopentyl cyanide]
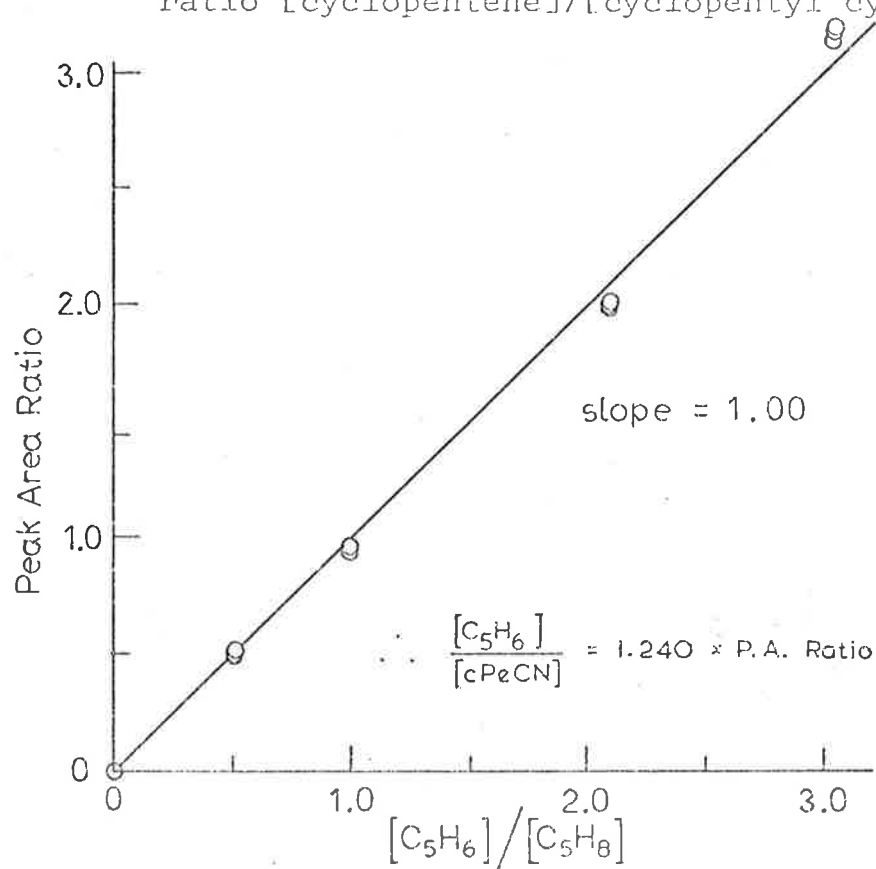
Figure A.11   Gas chromatograph calibration plot of the
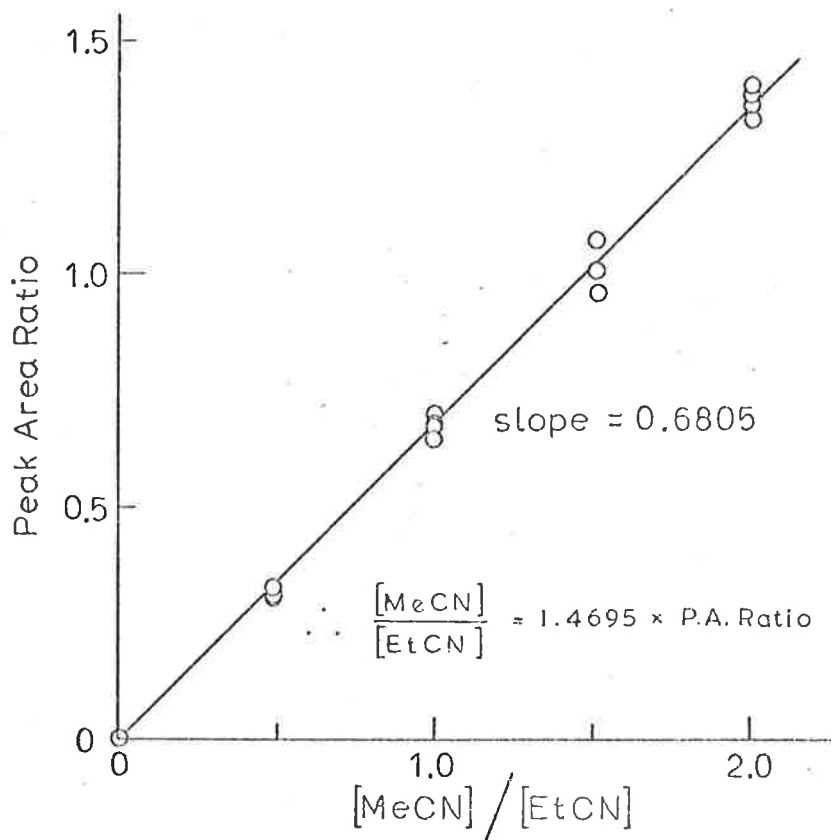   ratio [cyclopentadiene]/[cyclopentyl cyanide]
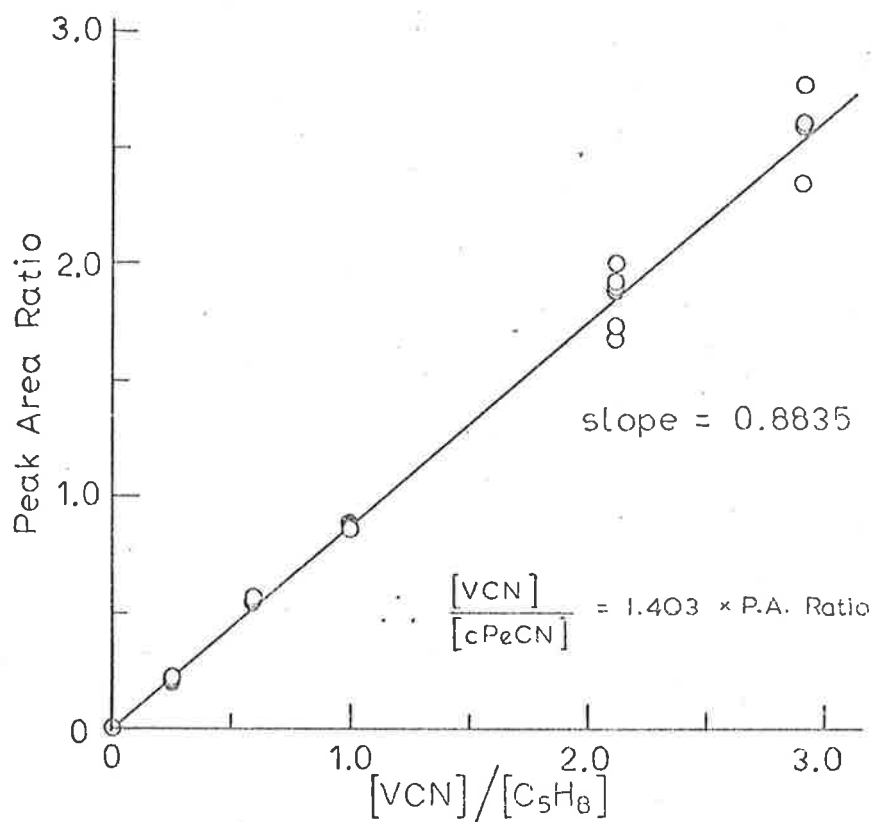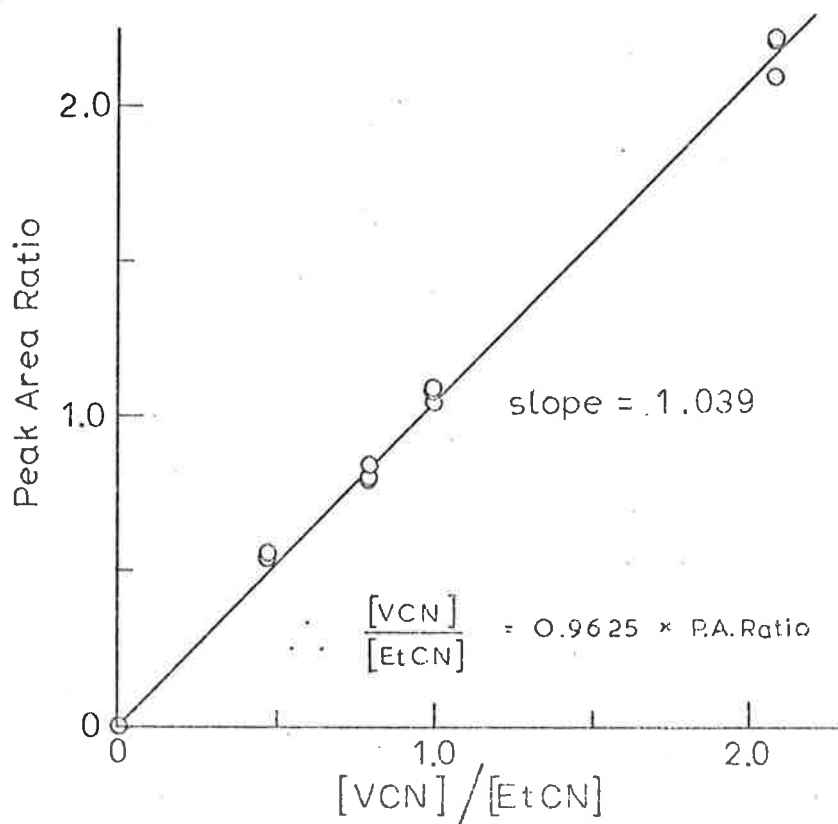
Figure A.12   Gas chromatograph calibration plot of the
                ratio [vinyl cyanide]/[cyclopentyl cyanide]
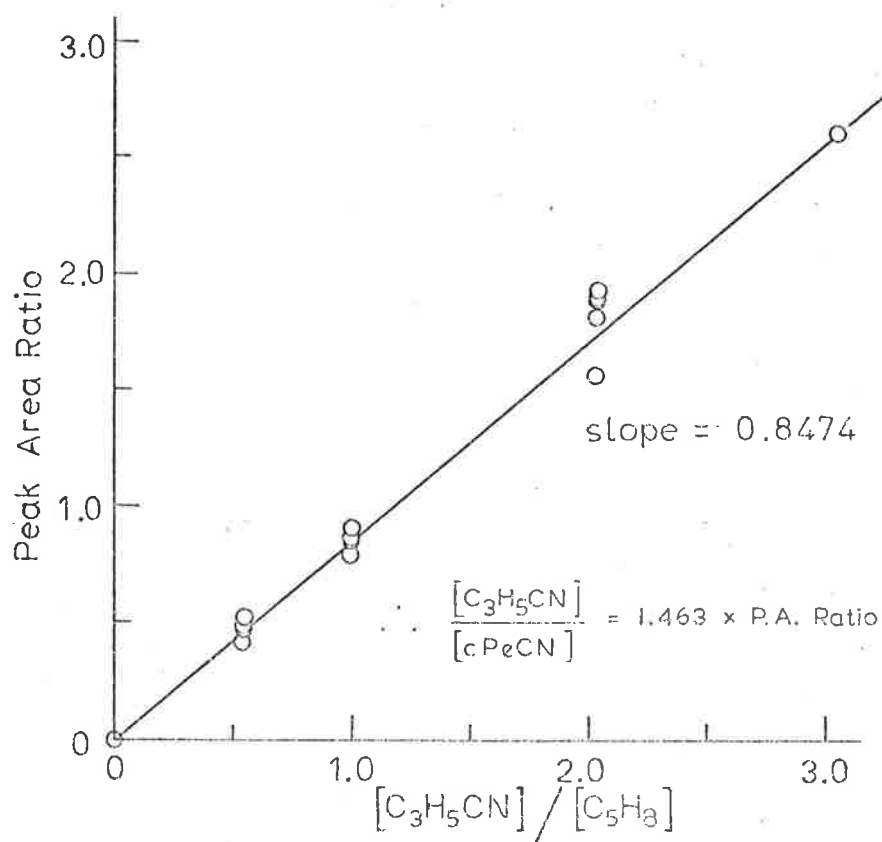
Figure A.13   Gas chromatograph calibration plot of the
                ratio [cyanopropene]/[cyclopentyl cyanide]

Figure A.14   Gas chromatograph calibration plot of the ratio
[hydrogen cyanide]/[cyclopentyl cyanide]

Figure A.15   Mass spectrometer calibration plot of the
ratio [vinyl cyanide]/[cyclopentyl cyanide]

Figure A.16   Mass spectrometer calibration plot of the
ratio [hydrogen cyanide]/[cyclopentyl cyanide]

Figure A.17   Mass spectrometer calibration plot of the
ratio [propylene]/[cyclopentyl cyanide]

Figure A.18   Mass spectrometer calibration plot of the
ratio [ethylene]/[cyclopentyl cyanide]

Figure A.19   Mass spectrometer calibration plot of the
ratio [cyclopentene]/[cyclopentyl cyanide]

Figure A.20   Mass spectrometer calibration plot of the
ratio [cyclopentadiene]/[cyclopentyl cyanide]

Figure A.21   Gas chromatograph calibration plot of the ratio [methyl cyanide]/[ethyl cyanide]

Figure A.22   Gas chromatograph calibration plot of the ratio [vinyl cyanide]/[ethyl cyanide]
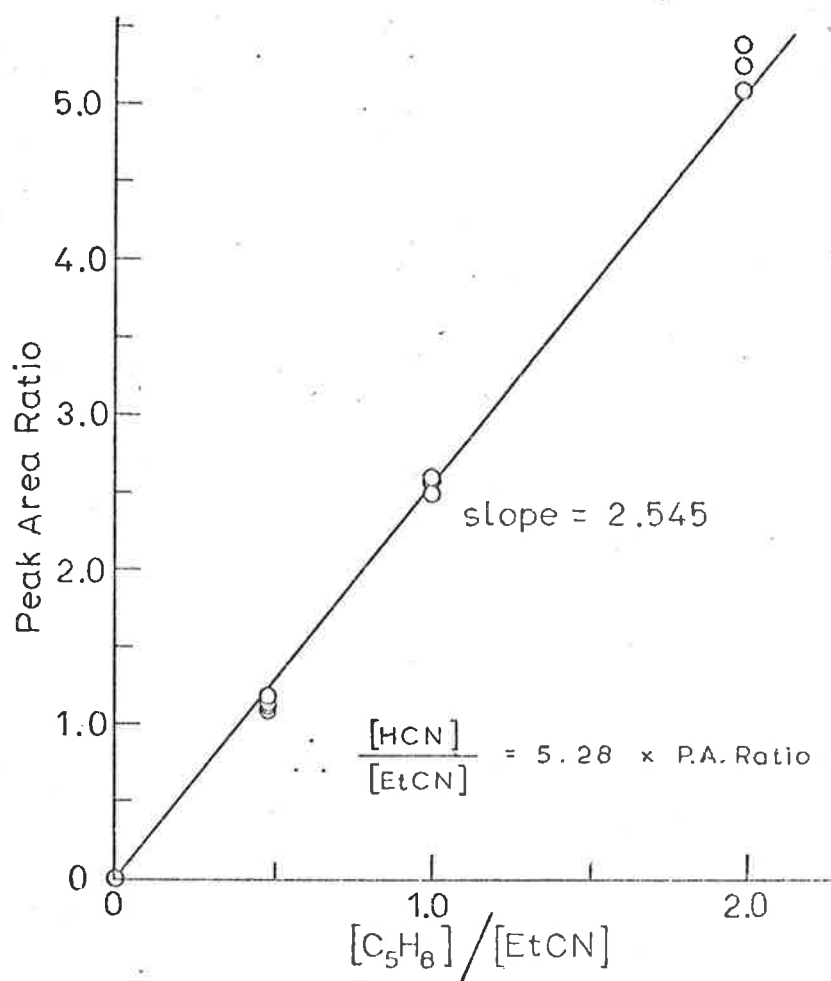
Figure A.23   Gas chromatograph calibration plot of the
ratio [hydrogen cyanide]/[ethyl cyanide]

A.3 Computer Program for Calculation of k_{uni}

For the VLPP studies, computer programs were written to calculate the unimolecular rate constants from the experimental data tabulated in Section A.1, using the mass spectrometer calibration factors obtained from the plots shown in Section A.2. The format of the programs was similar, and an example for the VLPP of tert-butyl cyanide is listed on the following page. A sample print-out for the experimental runs TB13-18, TB24-28, TB36-39 has also been included.

Computer program for the calculation of k_{uni} values
for the VLPP of tert-butyl cyanide

```
700 DIM K1(50),T1(50),A(50),C(50),D(50),E(50),F(50),G(50),H(50)
705 DIM T2(50),K2(50),Y(50),Z(50),P(50),I(50),Q(50),U(50),W(50)
710 DIM R(50),S(50),T(50),V(50),M(50),N(50),O(50),J(50),K(50),L(50)
715 INPUT N
725 FØR I=1 TØ N
730 READ K1(I),T1(I),C(I),D(I),E(I),F(I),G(I)
735 NEXT I
737 FØR I=1 TØ N
738 READ A(I)
740 NEXT I
745 FØR I=1 TØ N
750 T2(I)=T1(I)+273.2
755 K2(I)=K1(I)*SQR(T2(I)/83.13)
760 Y(I)=1-(D(I)/C(I))/A(I)
765 Z(I)=A(I)*(C(I)/D(I))-1
770 P(I)=K2(I)*Z(I)
772 X=F(I)-0.33*G(I)
773 G(I)=G(I)-0.115*X
775 R(I)=(F(I)/G(I)-0.3668)/0.6994
780 T(I)=K2(I)*R(I)
800 M(I)=(E(I)/G(I)-0.021)/1.2855
805 N(I)=M(I)/(1+M(I)+R(I))
810 O(I)=K2(I)*M(I)
821 S(I)=R(I)/(1+R(I)+M(I))
822 NEXT I
825 PRINT "TEMP","DECØMP","F/(1-F)","KEA","KTB(UNI)"
830 PRINT
835 FØR I=1 TØ N
840 PRINT T2(I),Y(I),Z(I),K2(I),P(I)
845 NEXT I
850 PRINT
855 PRINT
860 PRINT "TEMP","MVCN/TBCN","FØRMN","K67(UNI)"
865 PRINT
870 FØR I=1 TØ N
875 PRINT T2(I),R(I),S(I),T(I)
880 NEXT I
885 PRINT
890 PRINT
930 PRINT "TEMP","I-BUTENE/TBCN","FØRMN","K56(UNI)"
935 PRINT
940 FØR I=1 TØ N
945 PRINT T2(I),M(I),N(I),O(I)
950 NEXT I
955 PRINT
960 PRINT
990 END
```

where   N is the number of runs

I is the ith run

K1 is the physical constant in the escape rate constant for each aperature.

K2 is the escape rate constant, $k_{ea} = K1 \sqrt{T/M}$

T1 is the reactor temperature, $^{\circ}C$

T2 is the reactor temperature, K

A is the relative intensity of reactant to internal standard at zero decomposition, $(I_{42}/I_{40})^{\circ}$

C is the intensity of peak 40, i.e. argon

D is the intensity of peak 42, i.e. tert-butyl cyanide

E is the intensity of peak 56, i.e. isobutene

F is the intensity of peak 67, i.e. methyl vinyl cyanide

G is the intensity of peak 68, i.e. tert-butyl cyanide

Y is the fraction of decomposition, f

Z is the steady-state ratio of product to reactant, (f/1-f).

P is the unimolecular rate constant for decomposition, k_{uni} (t-Bu CN).

X is the methyl vinyl cyanide contribution to peak 67, corrected for tert-butyl cyanide contribution.

G is then corrected for the contribution of methyl vinyl cyanide to peak 68

R is the concentration ratio of [MeVCN]/[t-Bu CN]

S is the fraction of formation of methyl vinyl cyanide.

T is the unimolecular rate constant for formation, k_{uni} (MeVCN)

M is the concentration ratio of [Isobutene]/ [t-Bu CN]

N is the fraction of formation of isobutene

O is the unimolecular rate constant for formation, k_{uni} (Isobutene)

Computer print-out for tert-butyl cyanide experimental
runs TB13-18,TB24-28,TB36-39.

TEMP	DECØMP	F/(1-F)	KEA	KTB(UNI)
1044.2	.185078	.227111	.687566	.156154
1062.2	.279895	.388687	.693467	.269542
1084.	.408163	.689655	.700547	.483136
1103.6	.525926	1.10938	.706852	.784164
1122.5	.639969	1.77754	.712879	1.26717
1122.	.17413	.210845	6.42918	1.35556
1123.7	.179303	.218476	6.43405	1.40569
1140.7	.24798	.329751	6.43254	2.13763
1165.1	.362653	.569003	6.5515	3.72783
1188.	.467486	.877885	6.61557	5.80771
1201.6	.526738	1.113	6.65333	7.40512
1203.2	.127358	.145945	49.0772	7.16258
1216.3	.164995	.197597	49.3436	9.75018
1232.5	.215192	.274197	49.6712	13.6197
1244.9	.258052	.347804	49.9204	17.3625

TEMP	MVCN/TBCN	FØRMN	K67(UNI)
1044.2	.250794	.197323	.172438
1062.2	.399906	.281134	.277321
1084.	.670938	.393442	.470024
1103.6	1.036	.497881	.732296
1122.5	1.57452	.597668	1.12244
1122.	.229652	.185658	1.47647
1123.7	.242395	.193716	1.55958
1140.7	.349379	.256371	2.26486
1165.1	.56333	.355985	3.69066
1188.	.854504	.454241	5.65303
1201.6	1.10621	.516813	7.36001
1203.2	.185698	.155966	9.11353
1216.3	.239885	.192571	11.8368
1232.5	.305963	.232976	15.1975
1244.9	.37689	.271759	18.8145

TEMP	I-BUTENE/TBCN	FØRMN	K56(UNI)
1044.2	2.01831E-2	1.58839E-2	1.38807E-2
1062.2	2.25652E-2	1.58634E-2	1.56482E-2
1084.	3.43673E-2	2.01532E-2	.024076
1103.6	.044813	2.15363E-2	3.16762E-2
1122.5	5.99142E-2	2.27428E-2	4.27116E-2
1122.	7.31218E-3	5.91139E-3	4.70113E-2
1123.7	8.89559E-3	7.10913E-3	5.72346E-2
1140.7	.013405	9.83647E-3	8.68983E-2
1165.1	1.91225E-2	1.20841E-2	.125281
1188.	2.66658E-2	1.41751E-2	.176409
1201.6	3.42382E-2	1.59958E-2	.227798
1203.2	4.93593E-3	4.14564E-3	.242242
1216.3	5.81249E-3	4.66605E-3	.286809
1232.5	7.31846E-3	5.57265E-3	.363516
1244.9	9.96560E-3	7.18575E-3	.497487

A.4 Competitive Unimolecular Reactions at Low Pressures

When a reactant decomposes by competiting unimolecular paths in the fall-off region, energized molecules are depleted by all reaction paths and each path feels the effect of the drain on energized molecules of other paths. The usual unimolecular rate theory expression for k_{uni} has to be modified to take into account this interaction among reaction paths. This has been done previously for the system of two competitive reaction paths [53]; the modification being applied to RRK theory and the procedure was called the RRK/2 method. It has been shown that RRK (using $s \equiv C_{vib}(T)/R$) and RRKM theory give substantially the same result for fall-off calculations for thermally activated systems [53,74]

The derivation of the RRK/3 method for a system of three competitive reaction paths is as follows:

Consider the reaction scheme

$$A + M \underset{-1}{\overset{1}{\rightleftharpoons}} A^* + M$$

$$
A^*
\begin{array}{l}
\overset{2}{\longrightarrow} B + C \qquad\qquad \text{(i)} \\
\overset{3}{\longrightarrow} D + E \qquad\qquad \text{(ii)} \\
\overset{4}{\longrightarrow} F + G \qquad\qquad \text{(iii)}
\end{array}
$$
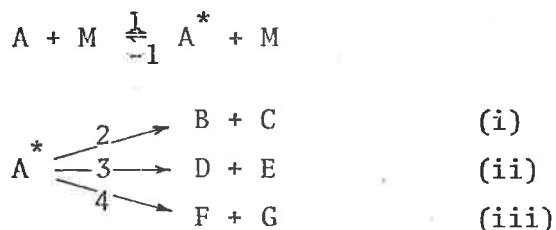
In the steady state

$$\frac{d[A^*]}{dt} = k_1[A][M] - k_{-1}[A^*][M] - k_2[A^*] - k_3[A^*] - k_4[A^*] = 0$$

$$\therefore [A^*] = \frac{k_1[A][M]}{[M]k_{-1} + k_2 + k_3 + k_4} \tag{1}$$

$$\therefore \text{Rate} = (k_2 + k_3 + k_4)[A^*] = \frac{k_1(k_2 + k_3 + k_4)[A][M]}{[M]k_{-1} + k_2 + k_3 + k_4}$$

$$= \frac{\left(\dfrac{k_1(k_2 + k_3 + k_4)}{k_{-1}}\right)[A]}{1 + \dfrac{k_2 + k_3 + k_4}{k_{-1}[M]}} \tag{2}$$

The pseudo first-order rate constant for the total disappearance of A is then

$$k_{uni} = \frac{1}{[A]} \left[-\frac{d[A]}{dt} \right] = \frac{\left(\dfrac{k_1 (k_2 + k_3 + k_4)}{k_{-1}} \right)}{1 + \dfrac{k_2 + k_3 + k_4}{k_{-1} [M]}} \qquad (3)$$

At high pressures, $k_{-1} [M] \gg k_2 + k_3 + k_4$

$$\therefore \quad R_\infty = \frac{k_1 (k_2 + k_3 + k_4)}{k_{-1}} [A] \equiv k_\infty [A] \qquad (4)$$

$$\therefore \quad k_{uni} \text{ (total)} = \frac{k_\infty \text{(total)}}{1 + \dfrac{k_\infty \text{(total)}}{k_{-1}[M]}} \qquad (5)$$

Now, for the formation of B or C

$$\frac{d[B]}{dt} = k_{uni}^{(i)} [A] \qquad (6)$$

$$\therefore \quad k_{uni}^{(i)} = \frac{1}{[A]} \frac{dB}{dt} = \frac{1}{[A]} \frac{k_1 k_2 [A] [M]}{k_{-1}[M] + k_2 + k_3 + k_4}$$

$$= \frac{k_1 k_2 / k_{-1}}{1 + \dfrac{k_1 (k_2 + k_3 + k_4)}{k_1 k_{-1}[M]}} \qquad (7)$$

$$\therefore \quad k_{uni}^{(i)} = \frac{k_\infty^{(i)}}{1 + \dfrac{k_\infty \text{(total)}}{k_1 [M]}} \qquad (8)$$

similarly $\quad k_{uni}^{(ii)} = \dfrac{k_\infty^{(ii)}}{1 + \dfrac{k_\infty \text{(total)}}{k_1 [M]}} \qquad (9)$

$$k_{uni}^{(iii)} = \frac{k_\infty^{(iii)}}{1 + \dfrac{k_\infty \text{(total)}}{k_1 [M]}} \qquad (10)$$

where k_1, k_2, k_3, k_4 are energy dependent, and k_{-1} is independent of energy.

Application of RRK theory to equation (7) for reaction (i) gives

$$k_{uni}^{(i)} = \int \frac{P(E)\ k_2(E)\ dE}{1 + \dfrac{k_2(E) + k_3(E) + k_4(E)}{\omega}} \tag{11}$$

where $P(E)$ is the energy distribution function $\equiv k_1/k_{-1}$

$$P(E) = \frac{1}{\Gamma(s)}\ \left(\frac{E}{RT}\right)^{s-1}\ \frac{e^{-E/RT}}{RT} \qquad \text{on a per mole basis}$$

and $k_{-1}[M] = \omega$, the collision frequency for de-energization.

Now, the energy range for integration covers E_i^* to ∞, and if $E_i^* < E_{ii}^* < E_{iii}^*$

then over the energy range $E_{(i)}^*$ to E_{ii}^*

$$k_3(E) = A_{ii}\left(\frac{E - E_{ii}^*}{E}\right)^{s-1} = 0$$

and similarly over E_{ii}^* to E_{iii}^*, $k_4(E) = 0$

i.e. the A^* species are not sufficiently energized for reactions (ii) and (iii)

to occur. Reaction (ii) is not of importance until the energy is at least

E_{ii}^*, the critical energy for the reaction. Reaction (iii) is not of

importance until the energy is at least E_{iii}^*.

Hence we may divide the integral into three portions,

$$k_{uni}^{(i)} = \int_{E_i^*}^{E_{ii}^*} \frac{P(E)\ k_2(E)\ dE}{1 + k_2(E)/\omega} + \int_{E_{ii}^*}^{E_{iii}^*} \frac{P(E)\ k_2(E)\ dE}{1 + \{k_2(E) + k_3(E)\}/\omega}$$

$$+ \int_{E_{iii}^*}^{\infty} \frac{P(E)\ k_2(E)\ dE}{1 + \{(k_2(E) + k_3(E) + k_4(E))/\omega\}} \tag{12}$$

For reaction (ii), integration is from E_{ii}^* to ∞, and since $E_{ii}^* > E_i^*$,

$k_2(E)$ is always appropriate,

$$\therefore k_{uni}^{(ii)} = \int_{E_{ii}^*}^{E_{iii}^*} \frac{P(E)\ k_3(E)\ dE}{1 + \{(k_2(E) + k_3(E))/\omega\}} + \int_{E_{iii}^*}^{\infty} \frac{P(E)\ k_3(E)\ dE}{1 + \{(k_2(E) + k_3(E) + k_4(E))/\omega\}}$$

$$\tag{13}$$

For reaction (iii), integration is from E_{iii}^* to ∞, and since $E_{iii}^* > E_{ii}^* > E_i^*$,

$k_2(E)$ and $k_3(E)$ are always appropriate,

$$\text{(iii)} \quad k_{uni} = \int_{E_{iii}^*}^{\infty} \frac{P(E)\, k_4(E)\, dE}{1 + \{\, (k_2(E) + k_3(E) + k_4(E)\,)/\omega\}} \tag{14}$$

The above expressions reflect that, each reaction path feels the effect of the other paths on the drain of energized species. These expressions may be written, using RRK theory, as follows:

$$\frac{k_{uni}^{(i)}}{k_{\infty}^{(i)}} = \frac{1}{\Gamma(s)} \left[\int_0^{\alpha} \frac{x^{s-1} e^{-x}\, dx}{1 + 10^D \left[\frac{x}{x+B}\right]^{s-1}} + \int_{\alpha}^{\beta} \frac{x^{s-1} e^{-x}\, dx}{1 + 10^D \{ \frac{x^{s-1} + \gamma(x-\alpha)^{s-1}}{(x+B)^{s-1}} \}} \right.$$

$$\left. + \int_{\beta}^{\infty} \frac{x^{s-1} e^{-x}\, dx}{1 + 10^D \frac{\{ x^{s-1} + \gamma(x-\alpha)^{s-1} + \delta(x-\beta)^{s-1} \}}{(x+B)^{s-1}}} \right] \tag{15}$$

$$k_{uni}^{(ii)} = \frac{e^{\alpha}}{\Gamma(s)} \left[\int_{\alpha}^{\beta} \frac{(x-\alpha)^{s-1} e^{-x}\, dx}{1 + 10^D \frac{\{ x^{s-1} + \gamma(x-\alpha)^{s-1} \}}{(x+B)^{s-1}}} \right.$$

$$\left. + \int_{\beta}^{\infty} \frac{(x-\alpha)^{s-1} e^{-x}\, dx}{1 + 10^D \frac{\{ x^{s-1} + \gamma(x-\alpha)^{s-1} + \delta(x-\beta)^{s-1} \}}{(x+B)^{s-1}}} \right] \tag{16}$$

$$\frac{k_{uni}^{(iii)}}{k_{\beta}^{(iii)}} = \frac{e^{\beta}}{\Gamma(s)} \int_{\beta}^{\infty} \frac{(x-\beta)^{s-1} e^{-x}\, dx}{1 + 10^D \frac{\{ x^{s-1} + \gamma(x-\alpha)^{s-1} + \delta(x-\beta)^{s-1} \}}{(x+B)^{s-1}}} \tag{17}$$

where $P(E) = \frac{1}{\Gamma(s)} \left(\frac{E}{RT} \right)^{s-1} \frac{e^{-E/RT}}{RT}$

$$\Gamma(s) = (s-1)!$$

$$k_2(E) = A_i \left(\frac{E - E_i^*}{E} \right)^{s-1} \quad \text{for } E > E_i^*$$

$$k_3(E) = A_{ii} \left(\frac{E - E_{ii}^*}{E} \right)^{s-1} \quad \text{for } E > E_{ii}^*$$

$$k_4(E) = A_{iii} \left(\frac{E - E_{iii}^*}{E} \right)^{s-1} \quad \text{for } E > E_{iii}^*$$

$s = C_{vib} (T) / R =$ "effective number of oscillators"

$x = (E - E_i^*)/RT$

$B = E_i^* /RT$

$\alpha = (E_{ii}^* - E_i^*)/RT$

$\beta = (E_{iii}^* - E_i^*) /RT$

$\gamma = A_{ii}/A_i$

$\delta = A_{iii}/A_i$

$D = \log A_i - \log \omega$

The computer program written for the RRK/2 method [51] was extended to numerically evaluate the integrals in the above expressions and compute values of $k_{uni}^{(i)}$, $k_{uni}^{(ii)}$ and $k_{uni}^{(iii)}$ for comparison with experiment. The procedure was appropriately called the RRK/3 method.

A.5   Reprints of Publications from this Research

The following reprints were published during the course of the
research program. They were co-authored with Dr K.D. King. We anticipate
publication of the work on trans-1,2-dicyanocyclobutane, cyclopentyl
cyanide, and ethyl cyanide in the near future.

"Very Low-Pressure Pyrolysis of Cyclobutyl Cyanide.   The Cyano
Stabilization." by K.D. King and R.D. Goddard.

(Reprinted from Int. J. Chem. Kinet., Vol. 7, pp. 109-123 (1975).)

"Very Low-Pressure Pyrolysis (VLPP) of Alkyl Cyanides.   I.   The
Thermal Unimolecular Reactions of Isopropyl Cyanide." by K.D. King
and R.D. Goddard.

(Reprinted from J. Am. Chem. Soc., Vol. 97 pp 4504-4509 (1975).)

"Very Low-Pressure Pyrolysis (VLPP) of Alkyl Cyanides.   II.   n-Propyl
Cyanide and Isobutyl Cyanide.   The Heat of Formation and Stabilization
Energy of the Cyanomethyl Radical." by K.D. King and R.D. Goddard.

(Reprinted from Int. J. Chem. Kinet., Vol. 7, pp. 837-855 (1975).)

"Very Low-Pressure Pyrolysis (VLPP) of Alkyl Cyanides.   III. tert-
Butyl Cyanide.   The Effect of the Cyano Group on Bond Dissociation
Energies and Reactivity." by K.D. King and R.D. Goddard.

(Reprinted from J. Phys. Chem, Vol. 80, pp 546-552 (1976).)

King, K. D. & Goddard, R. D. (1975). Very low-pressure pyrolysis of cyclobutyl cyanide. The cyano stabilization energy. *International Journal of Chemical Kinetics, 7*(1), 109-123.

King, K. D. & Goddard, R. D. (1975). Very low-pressure pyrolysis (VLPP) of alkyl cyanides. I. The thermal unimolecular reactions of isopropyl cyanide.
Journal of the American Chemical Society, 97(16), 4504-4509.

King, K. D. & Goddard, R. D. (1975). Very low-pressure pyrolysis (VLPP) of alkyl cyanides. II. n-propyl cyanide and isobutyl cyanide. The heat of formation and stabilization energy of the cyanomethyl radical. *International Journal of Chemical Kinetics, 7*(6), 837-855.

King, K. D. & Goddard, R. D. (1976). Very low-pressure pyrolysis of alkyl cyanides. III. tert-Butyl cyanide. Effect of the cyano group on bond dissociation energies and reactivity. *Journal of Physical Chemistry, 80*(5), 546-552.

REFERENCES

[1] A Shindo, Rpt. Govt. Ind. Res. Inst., Osaka, 317, 50 (1961);
     W. Watt, L.N. Phillips and W. Johnson, The Engineer, 815 (1966).

[2] E. Epremian, Appl. Polymer Symp., 15, 139 (1970).

[3] C.H. Vervalin, Hydroc. Process., 54 (4), 19 (1975).

[4] H.K. Hall, E.P. Blanchard, S.C. Cherkofsky, J.B. Sieja, and
     W.A. Sheppard, J. Am Chem. Soc., 93, 110 (1971);
     H.K. Hall, C.D. Smith, E.P. Blanchard, S.C. Cherkofsky, and
     J.B. Sieja. ibid, 93, 121 (1971).

[5] K.J. Laidler, "Reaction Kinetics", Vol I, Pergamon Press,
     London, 1963.

[6] S. Arrhenius, Z. Physik Chem, 4, 226 (1889).

[7] F.O. Rice and K.F. Herzfeld. J. Am. Chem. Soc., 56, 285, (1934).

[8] D. Edelson and D.L. Allara, A. I. Ch. E Journal, 19, 638 (1973);
     L.F. Albright, ibid 19, 640 (1973).

[9] P. Goldfinger, M. Letort and M. Niclause. "Contribution a l'Etude de
     la Structure Moleculaire," Victor Henri Commemorative Volume,
     Desoer, Liège, 1948.

[10] W.C. McC. Lewis. J. Chem. Soc., 113, 471 (1918)

[11] H. Eyring, J. Chem. Phys., 3, 107, (1935); M.G. Evans and M. Polanyi,
     Trans. Faraday Soc., 31, 875 (1935); ibid, 33, 448 (1937);
     M. Polanyi, J. Chem. Soc., 629 (1937).

[12] S. Glasstone, K.J. Laidler and H. Eyring, "The Theory of Rate
     Processes," McGraw-Hill, New York, 1941.

[13] F.A. Lindemann, Trans. Faraday Soc., 17, 598, (1922).

[14] C.N. Hinshelwood, Proc. Roy. Soc. A113, 230, (1927)

[15] O.K. Rice and H.C. Ramsperger. J. Am. Chem. Soc., 49, 1617 (1927);
     ibid., 50, 617 (1928); L.S. Kassel "Kinetics of Homogeneous Gas
     Reactions", Chemical Catalog Co., New York. 1932; L.S. Kassel. J.
     Phys. Chem., 32, 225 (1928); ibid., 32, 1065 (1928).

[16] R.A. Marcus, J. Chem. Phys., 20, 359, (1952); G.M. Weider and
     R.A. Marcus, ibid., 37, 1835, (1962).

[17] P.J. Robinson and K.A. Holbrook, "Unimolecular Reactions", Wiley,
     London, 1972.

[18] K.J. Laidler and J.C. Polanyi, Progr. Reac. Kinetics. 3, 1, (1966).

[19]   W. Forst, "Theory of Unimolecular Reactions", Academic Press, New York, 1973.

[20]   (a) J.H.S. Green, G.D. Harden, A. Maccoll and P.J. Thomas, J. Chem. Phys., 21, 178, (1953); A. Maccoll and P.J. Thomas, Nature, 176, 392, (1955); (b) A. Maccoll and P.J. Thomas, Progr. Reac. Kinetics. 4, 119 (1967).

[21]   S.W. Benson and A.N. Bose, J. Chem. Phys., 39, 3463, (1963).

[22]   S.W. Benson and G.R. Haugen, J. Am. Chem. Soc. 87, 4036, (1965); J. Phys. Chem., 70, 3336 (1966); ibid., 74, 1607, (1970); Int. J. Chem. Kinet., 2, 235, (1970).

[23]   K.R. Maltman, E. Tschuikow-Roux and K.H. Jung, J. Phys. Chem., 78, 1035, (1974); E. Tschuikow-Roux and K.R. Maltman, Int. J. Chem. Kinet., 7, 363, (1975).

[24]   H.S. Johnston, "Gas Phase Reaction Rate Theory", Ronald Press, New York, 1966.

[25]   A.W. Ralston. H.J. Harwood and W.O. Pool, J. Am. Chem. Soc., 59, 986, (1937).

[26]   B.S. Rabinovitch and C.A. Winkler, Can. J. Res. B, 20, 69, (1942).

[27]   T.W. Asmus and T.J. Houser, J. Phys. Chem., 73, 2555, (1969).

[28]   M. Hunt, J.A. Kerr and A.F. Trotman-Dickenson, J. Chem. Soc., 5074, (1965).

[29]   M. Swarc, J. Chem. Phys., 17, 431 (1949).

[30]   H.E. O'Neal and S.W. Benson. J. Phys. Chem., 71, 2903, (1967).

[31]   S.W. Benson and H.E. O'Neal, Natl. Stand. Ref. Data Ser., Natl. Bur. Stand., No. 21 (1970).

[32]   P.N. Dastoor and E.U. Emovon, Can. J. Chem., 51, 366, (1973); extract of experimental data sent in private communication to Dr. K.D. King.

[33]   P.N. Dastoor and E.U. Emovan, J. Chem. Soc., Faraday Trans. I, 68, 2098, (1972).

[34]   D.A. Luckraft and P.J. Robinson, Int. J. Chem. Kinet., 5, 137, (1973).

[35]   S.F. Sarner, D.M. Gale, H.K. Hall and A.B. Richmond, J. Phys. Chem. 76, 2817, (1972) ; rate data reported in microfilm edition only.

[36]   H. Kwart, S.F. Sarner and J.H. Olson, J. Phys. Chem., 73, 4056, (1969).

[37]   D. Bellus and G. Rist, Helv. Chim. Acta. 57, 194, (1974).

[38]   G.B. Kistiakowsky and W.R. Smith, J. Am. Chem. Soc. 58, 2428, (1936).

[39] J.N. Butler and R.D. McAlpine, Can. J. Chem., 41, 2487, (1963).

[40] W.M. Marley and P.M. Jeffers , J. Phys. Chem., 79, 2085, (1975).

[41] K.D. King, private communication.

[42] S.W. Benson , F.R. Cruikshank, D.M. Golden, G.R. Haugen.,
      H.E. O'Neal , A.S. Rodgers, R. Shaw and R. Walsh, Chem. Rev.
      69, 279, (1969).

[43] H.K. Hall and J.H. Baldt. J. Am. Chem. Soc., 93, 140, (1971)

[44] H.E. O'Neal and S.W .Benson, Int. J. Chem. Kinet., 1, 221, (1969);
      H.E. O'Neal and S.W. Benson, "Free Radicals", Vol II,   J.K. Kochi,
      Ed., Wiley, New York, 1973,   Chapter 17.

[45] S.W. Benson, "Thermochemical Kinetics", Wiley, New York, 1968.

[46] D.M. Golden, Fourteenth Symposium (Intl) on Combustion, The
      Combustion Institute, 121 (1973).

[47] D.M. Golden, G.N. Spokes and S.W. Benson. Angew. Chem., Int. Ed.
      Engl., 12, 534, (1973).

[48] K.D. King and R.D. Goddard, Int. J. Chem. Kinet. 7, 109, (1975).

[49] P.C. Beadle, D.M. Golden, K.D. King and S.W. Benson. J. Am. Chem.
      Soc., 94, 2943, (1972).

[50] S.W. Benson, J. Chem. Phys., 46, 4920, (1967); G.S. Hammond and
      C.D. DeBoer, J. Am. Chem. Soc., 86, 899, (1964); D.J. Trecker and
      J.P .Henry, ibid., 86, 902, (1964).

[51] Knapsack-Griesheim A.-G., Chemical Abstracts, 63, 6885c (1965);
      H. Mueller and D. Mangold, ibid., 71, 101402d, (1969).

[52] S.W .Benson and G.N. Spokes, J. Am. Chem. Soc., 89, 2525, (1967).

[53] K.D. King, D.M. Golden, G.N. Spokes and S.W. Benson, Int. J.
      Chem. Kinet., 3, 411, (1971).

[54] M.J. Perona and D.M. Golden. Int. J. Chem. Kinet. 5, 55, (1973).

[55] B. Stead, F.M. Page and K.G. Denbigh. Disc. Faraday. Soc., 2, 263,
      (1947).

[56] W.C. Herndon, M.B. Henley and J.M. Sullivan, J. Phys. Chem., 67,
      2842 (1963); ibid., 68, 2016, (1964).

[57] M.F.R. Mulcahy and D.J. Williams, Austral. J. Chem., 14, 535, (1961).

[58] K.D. King, private communication.

[59] A. Maccoll, "Technique of Organic Chemistry, Vol VII, Rates
      and Mechanisms of Reactions - Part I", Chapter X.

[60] E.S. Swinbourne, Austral. J. Chem. 11, 314, (1958).

[61]   H.E. O'Neal and S.W. Benson. J. Phys. Chem., 72, 1866, (1968).

[62]   C.S. Blackwell, L.A. Carriera, J.R. Durig., J.M. Karriker and
        R.C. Lord. J. Chem. Phys. 56, 1706, (1972).

[63]   A.W. Rathjens, N.K. Freeman, W.D. Gwinn and K.S. Pitzer. J. Am.
        Chem. Soc. 75, 5634, (1953).

[64]   (a) P. Klaboe, Spectrochim. Acta. 26A, 87, (1970);
        (b) J.R. Durig, C.M. Plager, Y.S. Li, J. Bragin and C.W. Hawley.
        J. Chem. Phys., 57, 4544, (1972).

[65]   J.R. Durig, L.A. Carriera and W.J. Lafferty, J. Mol. Spectr.
        46, 187, (1973).

[66]   S.C. Chan, J.T. Bryant, L.D. Spicer and B.S. Rabinovitch,
        J. Phys. Chem, 74, 2058, (1970).

[67]   G. Emanuel, Int. J. Chem. Kinet., 4, 591, (1972).

[68]   (a) W. Tsang, J. Chem. Phys., 46, 2817, (1967);

        (b) W. Tsang, J. Phys. Chem. 76, 143, (1972).

[69]   (a) B.S. Rabinovitch and D.W. Setser. Adv. Photochem., 3, 1, (1964);
        (b) R.L. Johnson, W.L. Hase and J.W. Simons. J. Phys. Chem., 69,
        4348, (1965); Int. J. Chem. Kinet., 5, 77, (1973);
        F.B. Growcock, W.L. Hase and J.W. Simons. J. Phys. Chem., 76,
        607, (1972).
        (c) R.L. Johnson, W.L. Hase and J.W. Simons, Int. J. Chem.
        Kinet, 4, 1 (1972).

[70]   W. Tsang, Int. J. Chem. Kinet., 2, 23, (1970).

[71]   L.E. Sutton, Chem. Soc. Spec. Publ., No. 11, (1958); No. 18 (1965).

[72]   J.R. Durig and Y.S. Li, J. Mol Struc., 21, 289, (1974).

[73]   A. Maccoll, Chem. Rev., 69, 33, (1969).

[74]   D.M. Golden, R.K. Solly and S.W. Benson, J. Phys. Chem., 75,
        1333, (1971).

[75]   T. Fujiyama, Bull. Chem. Soc. Japan, 44, 3317, (1971).

[76]   N.E. Duncan and G.J. Janz, J. Chem. Phys. 23, 434, (1955);
        T. Shimanouchi, Natl. Stand. Ref. Data Ser., Natl. Bur. Stand.,
        No. 39, (1972).

[77]   S.H. Schachtschneider and R.G. Synder, Spectrochim. Acta, 19,
        117, (1963); ibid., 21, 169, (1965).

[78]   E. Hirota, J. Chem. Phys., 37, 2918, (1962).

[79]   K.D. King and R.D. Goddard, J. Am. Chem. Soc. 97, 4504, (1975).

[80]   K.D. King and R.D. Goddard, Int. J. Chem. Kinet., 7, 837, (1975).

[81]   E.F. Westrum and A. Ribner, J. Phys. Chem., 71, 1216, (1967).

[82]   J.R. Durig, S.M. Craven and J. Bragin, J. Chem. Phys. 53, 38, (1970)

[83]   L.J. Nugent, D.E. Mann and D.R. Lide, J. Chem. Phys., 36, 965, (196

[84]   (a) D.K. Lewis, M. Sarr and M. Keil, J. Phys. Chem., 78, 436, (1974)
        (b) D.A. Knecht, J. Am. Chem. Soc., 95, 7933, (1973).
        (c) D.W. Vanas and W.D. Walters, J. Am. Chem. Soc., 70, 4035,
        (1948); H. Tanji, M. Uchiyama, A. Amana and H. Tokuhisa, Int.
        Chem. Eng., 7, 32, (1967); G.I. Mackay and R.E. Marsh, Can. J. Chem.
        48, 913, (1970).

[85]   M. Swarc, Chem. Rev. 47, pp 135-6, (1950).

[86]   K. Tanner and A. Weber, J. Mol. Spectr., 10, 381, (1963).

[87]   F.H. Kruse and D.W. Scott, J. Mol. Spectr., 20, 276, (1966).

[88]   J.E. Kilpatrick, K.S. Pitzer and R. Spitzer. J. Am. Chem. Soc.
        69, 2483, (1947).

[89]   J.R. Durig, K.L. Kiser and J.M. Karriker. J. Raman Spectr. 1,
        17, (1973).

[90]   J.R. Durig and D.W. Wertz, J. Chem. Phys., 49, 2118, (1968).

[91]   D.W. Scott, W.T. Berg and J.P. McCullough, J. Phys. Chem., 64,
        906, (1960).

[92]   M.I. Davis and T.W. Muecke, J. Phys. Chem., 74, 1104, (1970).

[93]   W.C. Harris and C.T. Longshore. J. Mol. Structure, 16, 187, (1973).

[94]   D.W. Wertz, D.F. Bocian and M.J. Hazouri, Spectrochim. Acta,
        29A, 1439, (1973).

[95]   S. Furuyama, D.M. Golden and S.W. Benson, J. Chem. Thermodynamics
        2, 161, (1970).

[96]   C.T. Genaux, F. Kern and W.D. Walters, J. Am. Chem. Soc. 75,
        6196, (1953); R.W. Carr, Jr., and W.D. Walters, J. Phys. Chem.,
        67, 1370, (1963).

[97]   K.D. King and R.D. Goddard, J. Phys. Chem., 80, 546, (1976).

[98]   S.W. Benson, J. Chem. Educ. 42, 502, (1965).

[99]   R. Scrinivasan, Int. J. Chem. Kinet., 1, 133, (1969).

[100]   (a) W. Forst and C.A. Winkier. Can. J. Chem. 33, 1814, (1955);
        D.E. McElcheran, M.H.J. Wijen and E.W.R. Steacie, ibid., 36,
        321, (1958);
        (b) J.W.S. Jamieson, G.R. Brown and J.S. Tanner. Can. J. Chem.
        48, 3619, (1970).

[101]   J.A. Kerr and M.J. Parsonage, "Evaluated Kinetic Data on Gas Phase
        Addition Reactions", Butterworths, London, 1972.

[102]   I. Draganic, Z. Draganic, Lj. Petkovic and A. Nikolic, J. Am. Chem. Soc., 95, 7193, (1973).

[103]   A.S. Rodgers, M.C.R. Wu and L. Kuitu. J. Phys. Chem., 76, 918, (1972).

[104]   D.M. Golden and S.W. Benson, Chem. Rev., 69, 125, (1969).

[105]   F.W. Evans and H.A. Skinner, Trans. Faraday Soc., 95, 255, (1959).

[106]   A.S. Rodgers and M.C.R. Wu, J. Am. Chem. Soc., 95, 6913, (1973).

[107]   R.K. Solly, D.M. Golden and S.W. Benson, Int. J. Chem. Kinet. 2, 381, (1970).

[108]   K.W. Egger and A.T. Cocks, Helv. Chim. Acta. 56, 1516, (1973).

[109]   Landolt-Bornstein, "Zahlenwertie und Funktionen", Band I, Teil 3, Springer Verlag, Berlin, 1951.

[110]   B.N. Bhattacharya and W. Gordy, Phys. Rev., 119, 144, (1960).

[111]   J.A. Kerr, Chem. Rev., 66, 465. (1966).

[112]   S. Furuyama, D.M. Golden and S.W. Benson, J. Am. Chem. Soc., 91, 7564, (1969).

[113]   JANAF Thermochemical Tables, Natl. Stand. Ref. Data Ser., Natl. Bur. Stand., No. 37 (1970).

[114]   P. Cadman, M. Day and A.F. Trotman-Dickenson, J. Chem. Soc. (A), 2498 (1970); ibid., 248, (1971).